CONFÉRENCE NANOQUÉBEC 2012

Santé

Micro-nanosystèmes

Foresterie

Nouveaux matériaux

Environnement-Santé-Sécurité

Affiches présentées les 20-21 Mars 2012

HYATT REGENCY, MONTRÉAL

www.nanoquébec.ca

Santé

HYATT REGENCY, MONTRÉAL

www.nanoquébec.ca

Investigation of the static properties of DNA under complex nanoconfinement

A. Klotz [*1], *H. Brandao*[1], *W. Reisner*[1]

[1]McGill University, Department of Physics

Mots clés : nanofluidics, biophysics, polymer physics, DNA

We investigated the static properties of DNA under complex nanoconfinement. Experiments in nanofluidics, used as a platform to make precise measurements in polymer physics, have typically relied on simple systems. This work studies DNA in a system with spatially varying confinement: a nanofluidic slit embedded with a lattice of square pits, which forces the molecule into discrete conformational states. By observing how the molecule's conformational state changes with the parameters of confinement and comparing to theory, we can use this system as a probe of polymer physics. Measured free energy parameters show two distinct regimes with respect to the height of the slit, corresponding to the transition between the Odijk and deGennes confinement regimes. Furthermore, we can use this system to make a direct measurement of the effective width of a single molecule and potentially observe its variation with changing ionic conditions. This research demonstrates that complex nanotopography can be used as a powerful probe of polymer physics.

Références
[1] W. Reisner et al. Directed self-organization of single DNA molecules in a nanoslit via embedded nanopit arraysPNAS 2009 106 (1) 79-84

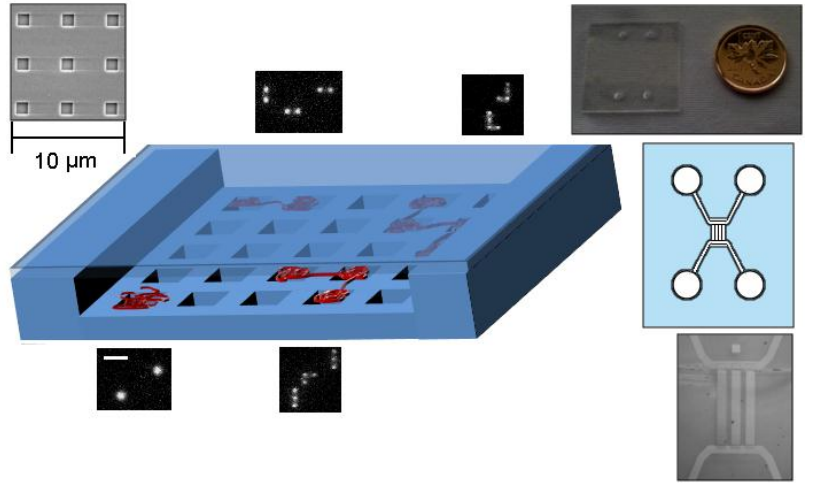

Figure 1 –Outline of the system under study and the behaviour of DNA molecules within it.

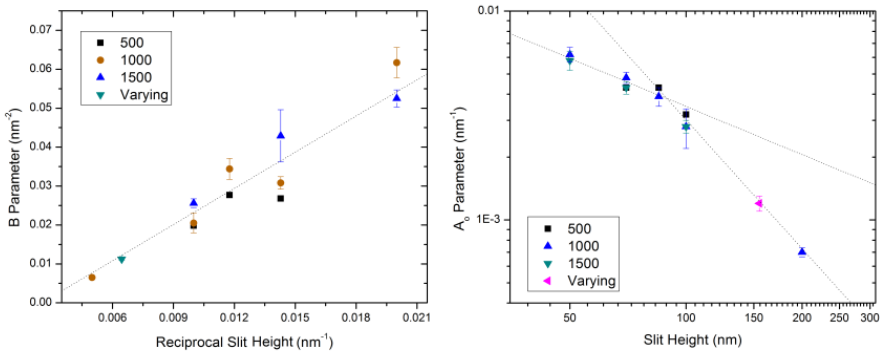

Figure 2 : Plots of measured free energy parameters with respect to slit height, showing the transition between two regimes and a measurement of the effective width of a molecule.

The effect of synthetic vertices and DNA-vertex connectivity on the stability of self-assembled DNA nanostructures

A. A. Greschner[*1], H. F. Sleiman*

[1]McGill University, 801 Sherbrooke St. Ouest, Bureau 1515, Montréal, Canada, H3C 3X6

Mots clés : DNA, nanostructures, stability, cooperativity, vertex

DNA is rapidly emerging as a powerful building block in bottom-up self assembly. Recent advances demonstrate its potential range of applications through such constructs as DNA networks[1], geometric shapes[2], and DNA-based nanotubes[3]. As the complexity of these nanostructures increases, it becomes increasingly essential to understand the various methods used to link multiple DNA strands. Currently, qualitative assumptions are being applied to interstrand junctions – such as using a rigid synthetic organic vertex molecule to provide preorganization, or a single-stranded polythymine chain to impart flexibility. In addition, the directionality of the DNA where it is connected to these vertices (via the 3' end or the 5' end) is largely ignored. At this stage in the development of DNA nanotechnology, a quantitative analysis of the effects of vertices and connectivities would greatly aid the DNA nanostructure community, allowing for the selection of vertices and vertex-to-DNA connectivities that complement the desired structure.

Three vertices are studied: a rigid synthetic organic vertex, a flexible organic vertex, and a DNA-based linker. In addition, the directionality of the DNA-to-vertex connectivity is examined to determine its influence on self-assembly. Variations in stability are mapped using thermal denaturation, and reveal a strong link between choice of vertex and DNA duplex cooperativity – a factor that results in significant changes in the predicted melting temperatures of the DNA assemblies. The disparity in melting temperature would disrupt larger structures that rely on stepwise assembly if not accounted for in the overall design.

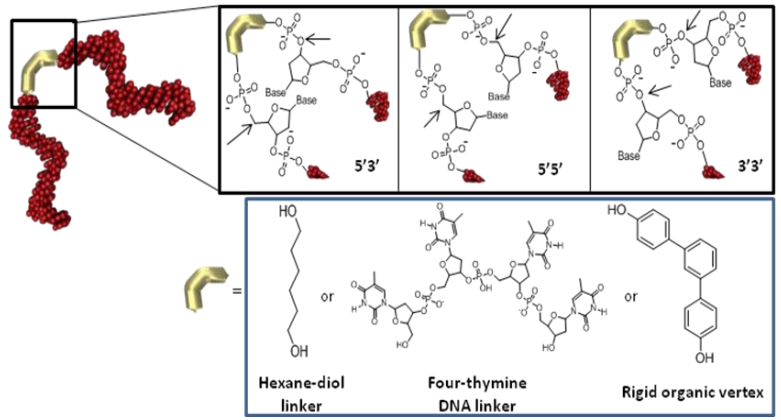

Figure 1 – The possible DNA-to-vertex connectivities and vertices studied

Références

[1] Seeman, N. C. *Journal of Theoretical Biology* **1982**, *99*, 237.
[2] Aldaye, F. A.; Sleiman, H. F. *J Am Chem Soc* **2007**, *129*, 13376.
[3] Aldaye, F. A.; Lo, P. K.; Karam, P.; McLaughlin, C. K.; Cosa, G.; Sleiman, H. F. *Nat Nanotechnol* **2009**, *4*, 349.

Detecting methylation of single molecules of DNA using a methyl binding domain GFP fusion protein

Jaan Altosaar[1], Walter Reisner[1]

[1] McGill University, Montreal, QC

Mots clés : nanochannels, methylation, DNA, molecular combing

Measuring DNA methylation is important for cancer diagnostics. Alteration of a single nucleotide by methylation may cause faulty gene expression of a key trait and prompt cell proliferation inappropriate for normal cell development. To assess such alterations at the DNA level, single molecules of methylated DNA were stretched out on silanized coverslips via molecular combing. Methyl binding domain green fluorescent protein (MBD-GFP) was prepared by recombinant fusion protein expression systems and the engineered protein was used as a marker to indicate the position of the methylated cytosine nucleotides along the molecule. The GFP was imaged and processed to generate 'barcodes' corresponding to methylation patterns of single molecules of DNA.

Références

[1] W. Reisner, N. Larsen, A. Silahtaroglu, A. Kristensen, N. Tommerup, J. Tegenfeldt, and H. Flyvbjerg. Single-molecule denaturation mapping of DNA in nanofluidic channels. Proc. Natl. Acad. Sci. USA 107, 13294 (2010).

L’agrégation de la nanoparticule du PapMV est nécessaire à son effet adjuvant

G. Rioux, C. Mathieu, D. Leclerc

Département de Microbiologie-Infectiologie et Immunologie, Centre de Recherche en Infectiologie, Université Laval, 2705 boul. Laurier, Québec, PQ, Canada G1V 4G2

Mots clés : PapMV, nanoparticule, adjuvant, vaccin

Les nanoparticules du virus de la mosaïque de la papaye (PapMV) sont des particules virales filamenteuses formées de la nucléocapside du PapMV produite en bactérie et d’un ARN simple brin. Ces particules sont bien connues pour leurs propriétés d’adjuvant et sont ainsi utilisées en vaccination pour augmenter la réponse immunitaire contre un antigène donné [1]. Le mécanisme d’action de l’adjuvant PapMV est cependant peu connu jusqu’à maintenant. Il a récemment été démontré que les particules virales ont une capacité intrinsèque de coller à un antigène lorsqu’elles sont exposées à une température d’environ 37°C, c’est-à-dire la température corporelle d’un mammifère. En effet, des mutations précises à la surface du PapMV ont améliorée sa thermostabilité et diminuer la capacité de ces particules à agréger avec l’antigène. Ces nanoparticules mutantes pouvaient supporter de plus importantes températures et ne formaient pas d’agrégats à 37°C. La perte de ce pouvoir d’agrégation a eu comme conséquence de diminuer fortement la capacité d’adjuvant du PapMV mutant. Cette capacité d’agrégation des nanoparticules du PapMV permet ainsi d’élucider une partie du mécanisme d’action de l’adjuvant PapMV consistant en le ciblage de l’adjuvant à un antigène de façon non-spécifique.

Références

[1] Savard, C., A. Guérin, et al. (2011). "Improvement of the Trivalent Inactivated Flu Vaccine Using PapMV Nanoparticles." PLoS ONE 6(6): e21522.

Ultra low-cost massively parallel nanopatterning of proteins as digital nanodot gradients for cell biological studies

S. G. Ricoult[*1,2], *M. Pla-Roca*[1], *R. Safavieh*[1], *Monserratt Lopez-Ayon*[3], *P. Grütter*[3], *T. E. Kennedy*[2] *and D. Juncker*[1]

[1]Department of Biomedical Engineering, McGill University and Génome Québec Innovation Centre, 740 Dr. Penfield Avenue, Montréal, Québec H3A 1A4, Canada
[2]Department of Neuroscience, McGill University, 3801 University Avenue, Montréal, Québec H3A 1A4, Canada
[3]Center for the Physics of Materials and the Department of Physics, McGill University, Montréal, Québec H3A 2T8, CANADA

Mots clés : cell recognition, digital nanodot gradient, microcontact printing, nanopatterning, proteins

Cells navigate by integrating signals derived from discrete binding of signaling proteins to individual receptors. There is thus a great interest in creating deterministic *in vitro* patterns to address how the density and distribution of proteins control intracellular signaling and cell navigation. Investigation of these issues *in vitro* has been limited by the lack of available and affordable methods. Here, we present a novel microcontact printing process that we developed. We introduce a double nanoreplication method that allows for the creation of multiple copies of a single e-beam patterned Si master into photopolymerized polymers. These photopolymer masters were subsequently used as lift-off stamps for microcontact printing of proteins by placing them in contact with a flat PDMS stamp inked with protein, the contacted proteins are then lifted-off by removing the stamp. The flat PDMS stamp is then printed onto the target substrate and the remaining proteins are transferred. We patterned 100 million 200-nm-wide spots of fibronectin on an area of 1 cm^2 and showed that it could be recognized by an antibody as well as by cells which formed focal adhesions on these spots. Next, we formed digital gradients of fluorescent antibodies patterned as 200 nm spots over a distance of 400 µm with a variable spacing between 0 nm and 10 µm, thus spanning 4.4 orders of magnitude in density compared to only 2 in previous studies. This method will be useful for rapid and low cost nanopatterning of proteins for a wide range of applications, such as for the study of axonal migration in response to digital gradients.

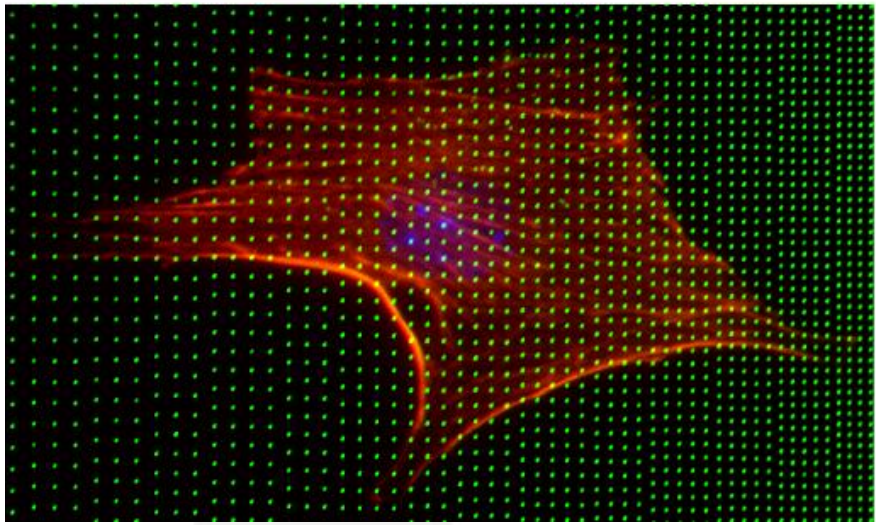

Figure 1 – C2C12 myoblast cell on a DNG of RGD peptides. (a) Fluorescent micrograph of a DNG or RGD peptides mixed with fluorescent IgG (green dots) and a C2C12 cell grown for 18 h, fixed and stained to reveal actin filaments (red) and the cell nucleus (blue). (b) Close-up of the frame in (a) showing that actin filaments align with the nanodot patterns. Arrows indicate areas where cell shape or structures strikingly coincide with the nanodot pattern.

Stimuli-responsive organization of block copolymers on DNA nanotubes

Karina M. M. Carneiro[1], Graham D. Hamblin[1], Kevin D. Hänni[1], Johans Fakhoury[1], Manoj K. Nayak[2], Georgios Rizis[1], Christopher K. McLaughlin[1], Hassan F. Bazzi[2] and Hanadi F. Sleiman[1]*

[1]McGill University, 801 Sherbrooke St. West, Otto Maass, Room 400, Montréal, Canada, H3A 2K6
[2]Texas A&M University at Qatar, Doha, Qatar

DNA nanotubes are an attractive class of materials that can be assembled with precise control over their size, shape, length and porosity, and can encapsulate and release cargo in response to specific added molecules.[1] In parallel, block copolymer assemblies can provide biocompatibility, stability, nuclease resistance, the ability to encapsulate small molecules, long-range assembly and numerous additional functionalities that can be tuned with subtle chemical modifications. Herein, we describe a new class of hybrid materials, in which block copolymer assemblies are sequence specifically and longitudinally positioned on robust DNA nanotubes constructed using rolling circle amplification. These materials are dynamic, allowing the polymer structures to be cleanly removed from the DNA nanotubes only when a specific DNA sequence is added, creating a single stranded form of these nanotubes. Specifically, we first describe the use of rolling circle amplification to create a long DNA strand containing a repeat sequence. This is used as a guide strand in a new method to construct robust nanotubes with a non-nicked backbone.[2] We then synthesize polymer-DNA conjugates using the ring-opening metathesis polymerization, followed by on-column functionalization with a DNA strand. These polymers self-assemble into spherical aggregates, which then position themselves onto the DNA nanotubes using sequence specific hybridization, creating a 'striped' structure. The polymer aggregates can be cleanly lifted off the nanotubes using a strand displacement strategy, thus uncapping these DNA nanotubes. We also show that this longitudinal alignment of polymer aggregates on DNA nanotubes is general for a variety of DNA-block copolymers.

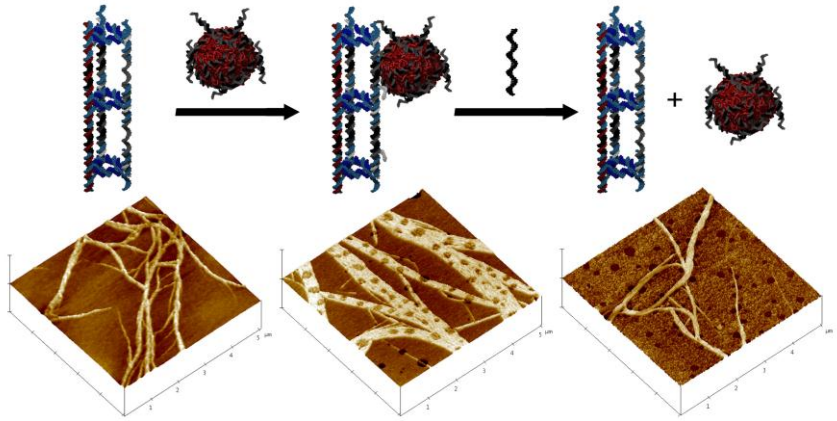

Figure 1 – Scheme of the write-erase of polymer micelles from DNA nanotubes (top) with representative AFM data (bottom).

Références
[1] P. Lo, P. Karam, F. Aldaye, G. Hamblin, G. Cosa, H. F. Sleiman, Nature Chem. 2010.
[2] G. Hamblin, K. Carneiro, J. Fakhoury, K. Bujold, H. Sleiman, J. Am. Chem. Soc., 2012, 134, (accepted).

Biodegradable and Thiol-Responsive Block Copolymer Micelles as Drug-Delivery Carriers

A. Cunningham[1], B. Khorsand[1], J. K. Oh[1]

[1]Department of Chemistry and Biochemistry, Concordia University, 7141 rue Sherbrooke Ouest, Montréal, Quebec, Canada, H4B 1R6

Mots clés : Copolymerization, Polylactide, Poly Oligo(ethylene glycol) monomethyl ether methacrylate, Atom-Transfer Radical Polymerization, Drug-Delivery System.

Amphiphilic block copolymers (ABP) have been materials of choice in constructing multifunctional biomedical devices for a variety of biological applications ranging from biodegradable implants and sutures to drug delivery systems. In order to obtain successful biological application for drug-delivery systems, the nanostructured material needs to be biocompatible and possess good release kinetics. Towards this goal, the present strategy employs a biodegradable and stimuli-responsive Polylactide(PLA)-based ABP with hydrophilic polymethacrylate coronas being shed in response to reductive reactions. Thiol-responsive amphiphilic block copolymer micelles were prepared by aqueous micellization of a disulfide-linked copolymer containing a biodegradable PLA core. In this presentation, the synthesis, characterization, and degradation of the block copolymers in response to thiols are presented. The polymerization employs a new double-head initiator allowing for the combination of atom-transfer radical polymerization (ATRP) and ring-opening polymerization (ROP) via the bromine and hydroxyl functionality, respectively. Well-defined copolymers were synthesized with the thiol-responsive disulfide functionality at the block junctions. Aqueous micellization of the resulting copolymer and its thiol-responsive character are presented. In the presence of water soluble thiols, the hydrophilic coronas are shed in response to the cleavage of the disulfide bond causing the PLA cores to precipitate. This method allows the construction of biocompatible micelles for future use in the biomedical field.

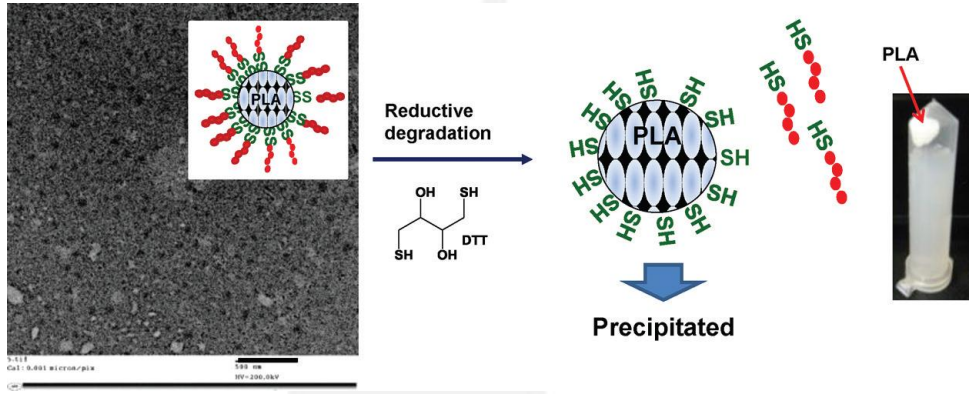

Figure 1. Illustration of reductive degradation of sheddable micelles of biodegradable PLA-based ABPs (PLA-SS-POEOMA) with hydrophilic POEOMA coronas being shed in the presence of water-soluble thiols. Also, TEM image shows ABP micelles.

Design, synthesis, characterization and application of peptide-based artificial ion channels

F. Otis[*1], E. Biron[1], J.-C. Meillon[1], M. Arseneault[1], C. Racine-Berthiaume[1], N. Voyer[1]*

[1]PROTÉO et Département de Chimie, Université Laval, 1245 avenue de la Médecine, Québec, Canada, G1V 0A6

Keywords : peptide nanostructures; ion channels; membrane transport

Channel proteins are essential for ion transport through cell membranes in physiological fonctions and have the potential to be used in many fields as therapeutics, antibacterials or component in biosensors. Therefore, developing functional artificial ion channels is attractive, because it allows easy molecular engineering and the modulation of channel proprieties such as ion selectivity and molecular recognition. Our group has developed an approach that uses hydrophobic α-helical 21mer peptides as framework to orient macrocyclic neutral ligands (crown ethers) of different diameters that can be used to obtain ion selective transport.[1] We will describe our results on the synthesis, characterization and understanding of the mechanism of action of these artificial ion channels. We will also present our work towards exploiting such channels for sensing.

Références

[1] E. Biron, F. Otis, J.-C. Meillon, M. Robitaille, J, Lamothe, P. Van Hove, M.-E. Cormier, N. Voyer, *Bioorg. Med. Chem.* **2004**, *12*, 1279-1290.

Etude structurale et thermodynamique de la formation oligomérique de l'Amylin humain en utilisant des simulations de dynamique moléculaire avec échange de répliques

S. Bouzakraoui, N. Mousseau

Département de Physique, Groupe de Recherche sur les Protéines Membranaires et Calcul Québec, Université de Montréal, C.P. 6128, succursale centre-ville, Montréal (Québec), Canada

Mots clés : Amylin, Structure, Propriétés thermodynamiques, Dynamique moléculaire

La formation de structures amyloïdes joue un rôle important dans plusieurs maladies comme la maladie d'Alzheimer, du Parkinson et de Huntington [1]. L'amylin (IAPP) est un peptide de 37 résidus qui constitue la composante majeure de l'amylin pancréatique associé au diabète type 2. Il est aussi l'un des polypeptides amyloidogéniques les plus connus [2]. Le fait que l'IAPP humain forme des fibrilles riche en feuillets β ordonnés alors que l'IAPP du rat n'en forme pas [3] permet une comparaison utile pour comprendre la dépendance de la séquence sur le processus d'agrégation relié aux maladies. Dans cette étude, et suivant nos travaux antérieurs sur les structures complètes des monomères et des dimères de l'IAPP [4], nous caractérisons la structure atomique et les propriétés thermodynamiques de la partie contenant les résidus 14-37 de l'IAPP humain en apportant des mutations sur quelques résidus pouvant affecter le processus d'agrégation. Plusieurs structures oligomériques ont été étudiées dans l'objectif de comprendre le rôle des interactions entre les résidus clés. L'étude théorique a été faite en utilisant des méthodes de dynamique moléculaire avec échange de répliques et le champ de force à gros grains OPEP [5].

Références

[1] Sipe, J. D. Crit. Rev. Clin. Lab. Sci. 1994, 31, 325-354
[2] Höppener, J. W; Lips, C.J. Int. J. Biochem. Cell Biol. 2006, 38, 726-736
[3] Sipe, J.D. Amyloid Proteins: The β-Sheet Conformation And Disease; Wiley-VCH: Weinheim, 2005
[4] Laghaei R.; Mousseau N.; Wei G. J. Phys. Chem. B, 2011, 115, 3146-3154
[5] Maupetit, J.; Tuffery, P.; Derreumaux, P. 2007, 69, 394-408B. Balmana. Documents internes, NanoQuébec, 2011.

Stimulation de l'immunité mucosale par les nanoparticules du PapMV

C. Mathieu, G. Rioux, D. Leclerc

Département de Microbiologie-Infectiologie et Immunologie, Centre de Recherche en Infectiologie, Université Laval, 2705 boul. Laurier, Québec, PQ, Canada G1V 4G2

Mots clés : PapMV, nanoparticule, adjuvant, vaccin

Les nanoparticules du virus de la mosaïque de la papaye (PapMV) sont composées de la nucléocapside du PapMV enroulée autour d'un ARN simple brin non-codant. Il a été démontré que ces particules ont des propriétés adjuvantes, c'est-à-dire qu'elles permettent d'augmenter la réponse immunitaire spécifique envers un antigène peu immunogène [1]. Il est essentiel pour un vaccin de stimuler l'immunité innée, qui entraîne l'apparition d'une réaction inflammatoire. Cette réaction constitue aussi la première ligne de défense contre l'invasion de pathogènes. Pour vérifier que les nanoparticules du PapMV stimulent l'immunité innée *in vivo*, un modèle murin de stimulation pulmonaire a été utilisé. Cette méthode a permis de mesurer des médiateurs de l'inflammation dans les poumons des souris, et d'observer une protection complète contre une infection virale des voies respiratoires suite à une stimulation avec les nanoparticules du PapMV. Puisque les nanoparticules du PapMV ont des propriétés adjuvantes et qu'elles stimulent efficacement l'immunité innée mucosale, elles ont aussi été utilisées comme adjuvant dans un vaccin grippal saisonnier administré par voie mucosale. Cette formulation a permis de protéger les animaux vaccinés contre une infection avec une souche hétéro-soustypique du virus influenza.

Références

[1] Savard, C., et al., Improvement of the Trivalent Inactivated Flu Vaccine Using PapMV Nanoparticles. PLoS ONE, 2011. **6**(6): p. e21522.

Synthesis of Novel Silver Nanostructures for Plasmonic Applications

H. Liang, F. Rosei, D. Ma

Institut National de la Recherche Scientifique, 1650 Boulevard Lionel-Boulet Varennes, Québec J3X 1S2, Canada

Keywords : Flower-like silver mesoparticle dimers, polarization dependent Raman spectroscopy, silver nanorice structures, oriented attachment, multipolar plasmonic resonances

Silver nanostructures have attracted much attention due to their broad applications in catalysis, biological labeling, and plasmonics. Particularly, many studies have focused on the controleld synthesis of silver nanostructures of different size and shape and therefore different localized surface plasmon resonances. Herein, we present the synthesis of two novel silver structures, flower-like silver mesoparticles and silver nanorice structures and their application in plasmonics.Flower-like silver mesoparticles, which could generate high electromagnetic (EM) field enhancement, were first obtained by reducing $AgNO_3$ with ascorbic acid in aqueous solution. We then used micro-manipulation method to create flower-like silver mesoparticle dimers, and found that the surface-enhanced Raman scattering (SERS) enhancement on the dimers were further enhanced 10~100 times more than on individal particles.[1] The strong SERS dependence of the dimers on the incident polarization reveals that the significant additional SERS enhancement is caused by the surface plasmon coupling effect in the dimers. We have also synthesized silver nanorice structures by reducing $AgNO_3$ with polyethylene glycol 600 and further investigated the anisotropic growth.[2] It was found that their growth is kinetically controlled and both oriented attachment and Ostwald ripening are involved. Interestingly, the longitudinal surface plasmon resonance of the nanorice structures is highly sensitive to the refractive index of surrounding dielectric media,[2] which predicts their promising applications as chemical or biological sensors. Moreover, the multipolar plasmonic resonances in these individual nanorice structures are for the first time visualized in real space by using high resolution electron energy-loss spectroscopy.[2]

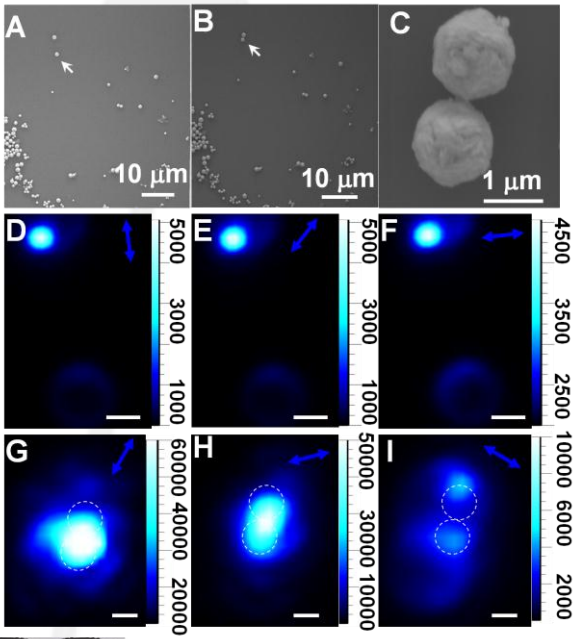

Figure 1 (A) SEM image of two isolated particles marked by an arrow. Corresponding Raman images at parallel (D), 45° angle (E) and perpendicular (F) incident polarization with respect to the symmetric axis of detected particles. (B) SEM and, (C) high magnification SEM image of the dimer formed by manipulating two individual particles in (A). Corresponding Raman images at parallel (G), 45° angle (H) and perpendicular (I) incident polarization with respect to the dimer axis. The white circles represent the location of the particles. The blue arrows show the polarization of incident laser light. All scale bars in (D ~ I) are 1 μm.

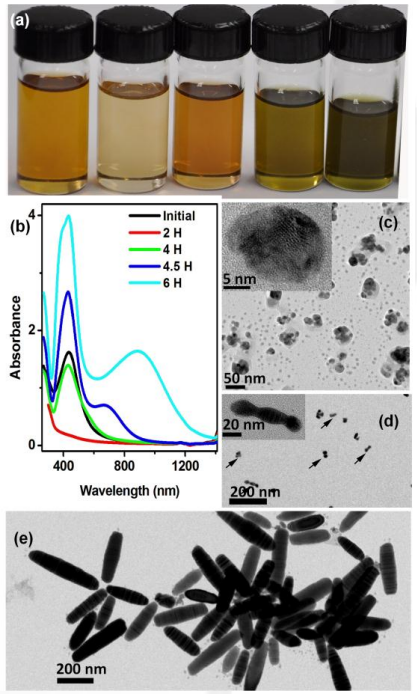

Figure 2 (a) Photographs of the reaction solution at 0 h, 2 h, 4 h, 4.5 h and 6 h (from left to right), respectively, following typical synthesis procedures. The stage II was set at 100°C. (b) Corresponding UV-Vis-NIR spectra. (c) – (e) TEM images of the products at different reaction time: (c) 0 h; (d) 4.5 h; and (e) 6h. Inset of (d) is a high resolution TEM image.

Reference
[1] H. Y. Liang, Z. P. Li, Z. X. Wang, W. Z. Wang, F. Rosei, D. L. Ma, H. X. Xu, Small, submitted.
[2] H. Y. Liang, H. G. Zhao, D. Rossouw, W. Z. Wang, H. X. Xu, G. A. Bottom, D. L. Ma. Acs Nano, to be submitted.

Structure-dependent Lysosomal Transit of Chitosan-pDNA Polyplexes

Marc Thibault, Mélina Astolfi, Michael D. Buschmann

Department of Chemical Engineering, École Polytechnique, Montréal, Québec, Canada.

Keywords : nanotechnology, chitosan, lysosomes, polyplexes, structure-dependence

The lysosomal degradation or sequestration of DNA cargo is considered a major obstacle to non-viral gene delivery. A better understanding of this obstacle is paramount to the rational design of efficient vectors. Chitosan-based polyplexes are known to traffic in lysosomes for relatively long time [1, 2], independently of both of their main structural parameters, namely the degree of deacetylation and molecular weight of chitosan, both of which have profound effect on the polyplexes stability and transfection efficiency [1-5]. The aim of this study was to investigate how modifying lysosomal transit affects polyplexes of different stabilities. Towards this end, we tested the effect of chloroquine and bafylomycin A1, two agents that modify the endosome/lysosome transit and their acidification process by distinct mechanisms, on the transfection efficiency of polyplexes prepared with chitosans of different structural parameters, hence of different stability, known to be either too stable or too unstable for efficient transfection, together with a formulation that is efficient both in vitro and in vivo [1-4]. The analysis of the effects of these intracellular trafficking modifying-agents on transfection efficiency and vesicular trafficking revealed novel and important chitosan structure-dependent consequences for lysosomal transit. Inhibiting lysosomal transit with chloroquine significantly increased the efficiency of unstable polyplexes and decreased the efficiency of highly stable polyplexes, while having minimal effects on efficient polyplexes. These results suggest that lysosomes are a site of DNA destruction for unstable polyplexes and, alternatively, for more stable polyplexes, a site of partial degradation of enzyme-labile chitosan, facilitating downstream DNA dissociation, hence transfection.

Références

1. Thibault, M., et al. Biomaterials, 2011. 32(20): p. 4639-4646.
2. Thibault, M., et al. Molecular Therapy, 2010. 18(10): p. 1787-1795.
3. Jean, M., et al. Gene Therapy, 2009. 16(9): p. 1097-1110.
4. Lavertu, M., et al. Biomaterials, 2006. 27(27): p. 4815-4824.
5. Ma, P.L., et al. Biomacromolecules, 2009. 10(6): p. 1490-1499.

Modeling, Fabrication and Testing of A Nanoilsands Integrated Biosensor for the Plasmonic Detection of Bovine somatotropin

Jayan Ozhikandathil, Simona Badilescu and Muthukumaran Packirisamy

Optical Bio-Microsystems Laboratory, Dept. of Mechanical and Industrial Engineering, Concordia University, Montreal Quebec Canada H3G 1M8.

Keywords : Gold nanoislands, Biosensor, Bovine somatotropin, FDTD

With the emergence of the recombinant DNA technology, large amounts of recombinant bovine somatotropin (rbST) are produced and used in the diary industry to increase the milk and meat production [1-3]. The use of bST for the food production raised the concern of the public and a rapid screening method became necessary. In this work, a novel method of fabrication and modeling of nano-biosensor for the label-free detection of bST is reported. The gold having a nanoisland morphology is fabricated on a glass substrate by convective assembly and post-deposition annealing. The LSPR band corresponding to nanoisland has been found to have a narrow absorbance peak in the modeling and experimental as well. The sensitivity of the gold nanoisland morphology to the local refractive index was analyzed by Finite-difference time-domain (FDTD) modeling and the theoretical results are validated with experimental observations. The sensing mechanism, that is, the shift of LSPR band on the local refractive index is found to be highly enhanced, compared to the gold aggregates in both the modeling and experiments. The increased surface area to volume ratio of the nanoislands is found to be suitable for the sensing of the antigen-antibody interaction of bST. The mechanism of shift of the LSPR band upon the change of local refractive index is analyzed using the FDTD.

References:
[1] F. H. Buttel, "The recombinant BGH controversy in the United States: toward a new consumption politics of food?" *Agriculture and Human Values*, **17**(1), 5-20 (2000).
[2] J. Burkhardt, "On the ethics of technical change: The case of bST," *Technology in Society*, **14**(2), 221-243 (1992).
[3] J. J. Molnar, K. A. Cummins and P. F. Nowak, "Bovine Somatotropin: Biotechnology Product and Social Issue in the United States Dairy Industry," *J. Dairy Sci.*,**73**(11),3084-3093(1990).
.

Structure-Activity Studies on a Model Antimicrobial

Pierre-Alexandre Paquet-Côté[1], Marie-Ève Provencher[1], Sébastien Cardinal[1], Laurie Bédard[1], Élise Caron[1], Aurélien Lorin[1], Mathieu Noël[1], Michèle Auger[1], and Normand Voyer[1]*

[1]Département de Chimie et PROTEO, Université Laval, 1045 avenue de la Médecine, Québec, Canada, G1V 0A6

Mots clés : Antimicrobial, conformation, hemolytic, crown ether, peptide

In the recent years, we have seen an important increase in antibiotic resistant bacteria. Such threat requires the development of new antimicrobial agents using a different mechanism of action minimizing the development of resistance. One family of compounds having such antimicrobial activity is the family of amphiphilic cationic peptides found widely in nature. Unfortunately, natural cationic peptides also target eukaryotic cells leading to undesirable side effects. To get a better understanding of the molecular determinants governing the biological activity of cationic peptides, analogs of a model compound **1,** identified in our group, were synthesized by parallel solid-phase synthesis. These analogs incorporate lysines, arginines or histidine substituting one or two leucines at several different positions. The antimicrobial activity and the hemolytic activity of the different analogs will be described, as well as our biophysical studies aiming at understanding the mode of action of these crown ether modified peptides.

References:

H-Leu-EC-Leu-Leu-Leu-EC-Leu-Leu-EC-Leu-Leu-Leu-EC-Leu-OH **1**

EC = (21-crown-7)-L-Phenylalanine

.

Accurate detection of pathogenic *Escherichia coli* bacteria employing Long period fiber gratings

S. M. Tripathi[*1], W. J. Bock[1], P. Mikulic[1], R. Chinnappan[2], A. Ng[2], M. Tolba[2], M. Zourob[2]*

[1]Centre de recherche en photonique, Département d'informatique et d'ingénierie, Université du Québec en Outaouais, Gatineau, Québec, Canada, J8Y 3G5
[2]Institut National de la Recherche Scientifique - Énergie, Matériaux et Télécommunications, Varennes, QC, J3X 1S2, Canada

Mots clés : nanotechnologies, bactérie

Pathogenic *Escherichia coli* (*E. coli*) is one of the most dangerous agents of food-borne disease. Consumption of contaminated food or water can be deadly, especially for children and the elderly [1]. We report a compact, stable, label-free, bacteriophage-based detection of pathogenic *E. coli* bacteria using ultra sensitive long-period fiber gratings (LPFGs). In our experiments we used the bacteriophage T4 as the recognition agent, covalently immobilized on optical fiber by forming a mono (multi) layer poly silane film on the surface of the fiber with the amino functional groups on the top of the film. The typical thickness of the film ranges between 10 – 20 nm. Blocking the non specific sites on the LPFG surface through Bovine Serum Albumin various concentrations of the *E. coli* are introduced to the sensor. Using highly accurate spectral interrogation mechanism, with a resolution of 0.02 nm, we measure the resonance wavelength shift as a function of *E. coli* concentrations. It has been plotted in Fig.1, where we demonstrate that our detection mechanism is capable of reliable detection of *E. coli* concentrations as low as 10^3 cfu/ml with an exceptional experimental accuracy (> 99%).
Finally, we also produce the SEM images of the LPFG surface confirming an excellent binding of different concentrations *E. coli* on it (see Fig.2). We observe that even a smaller concentration of the bacteria (10^3 cfu/ml) is well stuck to the fiber surface. Our study, thus, opens a possibility of an excellent real-time, experimental monitoring of bacteria growth/decay in the biological samples.

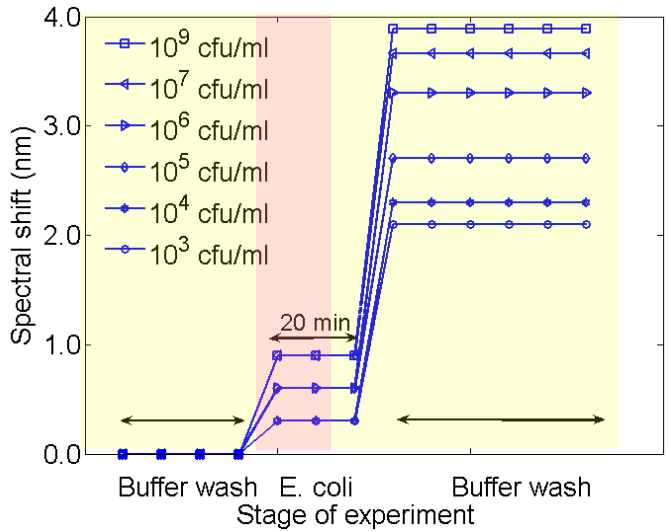

Figure 1 – Variation of the spectral shift of the resonance wavelength prior to and after the *E. coli* incubation on the LPFG.

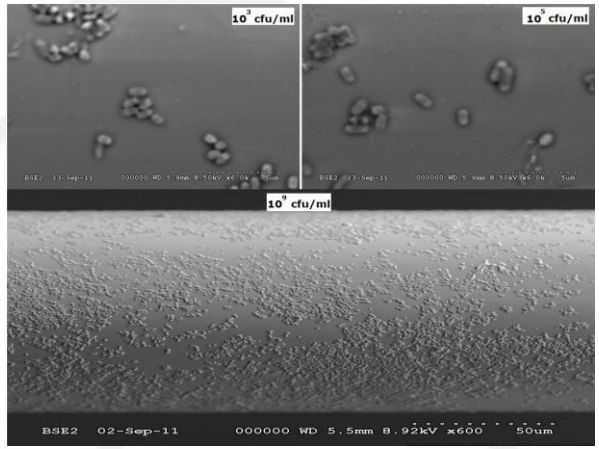

Figure 2 – SEM micrograph of the *E. coli* immobilized on the surface of the LPFG (a) 10^3 cfu/ml of *E. coli*, (b) 10^5 cfu/ml of *E. coli* and (c) 10^9 cfu/ml of *E. coli* concentration in PBS buffer.

Références
[1] WHO, 2008, http://www.cdc.gov/ecoli/2011/ecolio104/
[2] Homola, J., Ed., 2006, Surface Plasmon Resonance Based Sensors, Springer

Laser fragmentation of drugs in water : a novel particle size reduction tool for pharmaceutical R&D

Weimeng Ding[*1], Jean-Philippe Sylvestre[1], Emanuelle Bouvier[1], Grégoire Leclair[2] and Michel Meunier[1]*

[1]Canada Research Chair in Laser Micro/Nano-engineering of materials, Laser Processing and Plasmonics Laboratory, Department of Engineering Physics, École Polytechnique de Montréal, P.O. Box 6079, Downtown Station, Montréal, Québec, H3C 3A7, Canada
[2]Faculty of Pharmacy, Université de Montréal, P.O. Box 6128, Downtown Station, Montréal, Québec, H3C 3J7, Canada

Mots clés : laser fragmentation, drug discovery, naproxen, fenofibrate, beclomethasone dipropionate

Reducing the particle size of drugs is a simple method, which is used to improve their absorption in the body. However, current micro/nanonization techniques are not well adapted to the drug discovery stage, where the availability of the candidate substances is scarce (~10-100 mg). We propose a novel approach, laser fragmentation, to perform micro/nanonisation of drugs using small quantities. This study investigates the production of drug micro/nanocrystals by laser fragmentation and evaluates the effects of the process on their physicochemical properties. Three drug models are investigated: fenofibrate, naproxen and beclomethasone dipropionate, all oral or pulmonary anti-inflammatory drugs. Drugs' micro/nanocrystals were obtained by focusing a femto- or nanosecond laser radiation into a magnetically agitated drug suspension. The drugs' particle size was characterized by dynamic light scattering, laser diffraction and scanning electron microscopy. The degradation was evaluated by high performance liquid chromatography. The physicochemical properties of the lyophilized micro/nanocrystals were evaluated by Fourier transform infrared spectroscopy, x-ray diffraction, elemental analysis and differential scanning calorimetry. All laser-treated drugs were compared with those milled by conventional techniques.
Both micro- and nanocrystals of drugs were successfully produced by laser fragmentation. The particle size could be controlled by adjusting the fabrication parameters. Nanonization was accompanied by more chemical degradation than micronization, due to possible oxidation and loss in cristallinity. Laser fragmentation enables the micro/nanonization of small quantities of drugs with limited degradation and polymorphic transformation. The process therefore represents a simple and suitable micro/nanonization technique for the pharmaceutical R&D during the drug discovery phase.

Graphene-based label-free voltammetric immunosensor for the Sensitive detection of multiple food allergens.

S. Eissa[1], C. Tlili[1], M. Zourob[1]*

[1]Institut national de la recherche scientifique, Centre – Energie Matériaux Télécommunication, 1650, Boul. Lionel Boulet, Varennes (Québec) J3X 1S2, Canada

Keywords : Allergens, immunosensor, graphene

Food allergy has become one of the major health concerns nowadays. It is considered the fourth most important health problems in the world according to the world health organization [1], affecting about 1 to 3% of adults and 4 to 6% of infants. Here, we report a novel, simple, label-free, highly sensitive, and low cost electrochemical biosensing array platform based on disposable graphene-modified screen printed carbon electrodes for the monitoring of allergens present in food samples. The derivatization of the graphene electrode surface was achieved by electrochemical reduction of in situ generated 4-nitrophenyl diazonium cation in aqueous acidic solution, followed by electrochemical reduction of the terminal nitro groups to amines. Next, the amine groups on the graphene surface were activated using glutaraldehyde and used for the covalent immobilisation of the antibodies. Cyclic and differential pulse voltammetry carried out in an aqueous solution containing $[Fe(CN)_6]^{3-/4-}$ redox pair have been used for the immunosensor characterisation. The results demonstrated that the DPV reduction peak current of $[Fe(CN)_6]^{3-/4-}$ decreased linearly with increasing the concentration of the allergenic proteins due to the formation of antibody–antigen complex on the modified electrode surface. The proposed graphene immunosensors platform exhibited detection limit as low as 1.0 pg ml^{-1} of the two common allergens; Ovalbumin and lactogobulin. The novel electrochemical immunosensor presented herein is expected to have potential role in food safety and consumer protection.

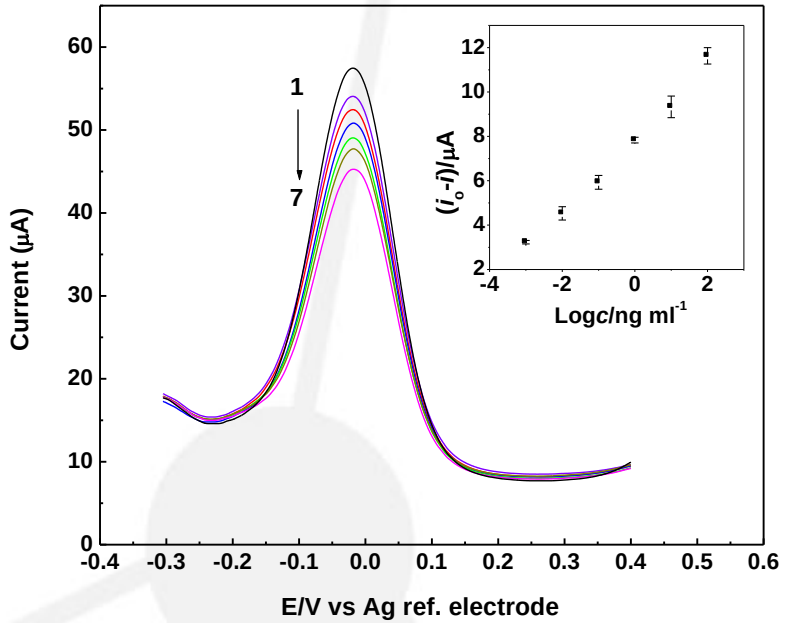

Figure 1 – DPVs of the immunosensor incubated with different concentrations of β-lactoglobulin (1–7): the concentrations of β- LG are 0.000, 0.001, 0.01, 0.1, 1.0, 10 and 100 ng mL^{-1}. The inset is the calibration curve based on the change of the DPV peak currents versus the logarithm of the concentrations.

References

[1] Vervloet D.et al. Consensus et perspectives de l'immunothérapie spécifique dans les maladies allergiques. La Lettre (Supplement to the Revue Française d'Allergologie et d'Immunologie Clinique) 1997; 37 (2): 4-5.

Array of nano-electrods for muliple Cancer bio-marker detection

I.Stateikina[1], R. Elshafey[1], C. Tlili[1], M. Zourob[1]*

[1]Institut national de la recherche scientifique, Centre – Energie Matériaux Télécommunication, 1650, Boul. Lionel Boulet, Varennes (Québec) J3X 1S2, Canada

Mots clés : Nanowires, sensor, gold, multiple cancer markers

In the field of bio-sensing, there is the increasing need for biomarker detection with high sensitivity, ultra-small volumes of reagents' consumptions, and robust disposable sensing platforms, which may be mass fabricated using available technologies. Multiple biomarkers are considered to be more confirmative in the diagnosis of complex diseases like cancer [1], for which the detection of a single maker is found to be inadequate for the screening of cancer disease. So, patterns of multiple cancer markers might provide the information necessary for diagnosis of cancer disease and determine the progression stage and monitor the effectiveness of the treatment. Nanowires are excellent bio-sensing components in terms of increased sensitivity and low reagents consumption. Many reports exist of nanowire-based sensing platforms fabricated from different materials and using different techniques. Unfortunately, up to date these processes showed notable complications in multi-steps fabrication of nanowires and micron-size contacting points. Recent studies reported to overcome this problem using micron-scaled chips and nanowires from various materials which were aligned and deposited using dielectrophoresis (DEP) [2]-[3]**.** This was followed by various methods for gluing the nanowires to the fabricated micron-sized contacts which is time consuming and lacks reproducibility, [4]-[6]. In this work, a simple method to combine macro-sized connectors with pre-fabricated nanowire array chips is proposed. The nanowires, 100 nm wide, were fabricated on Si wafer using available nano-fabrication techniques. The test socket, designed for this specific purpose, incorporates custom contact pads and the alignment features which allows precision positioning of these nanowire chips ensuring the connection, Figure 1. This complex (test socket/array of nanowires chip) was tested with a number of brain cancer markers. Recently, the design was improved by introducing nanowire based interdiginated electrode arrays (nIDE). This geometry allows more flexibility and higher accuracy in the sensing of the markers. The array arrangement provides the opportunity of testing number of markers simultaneously.

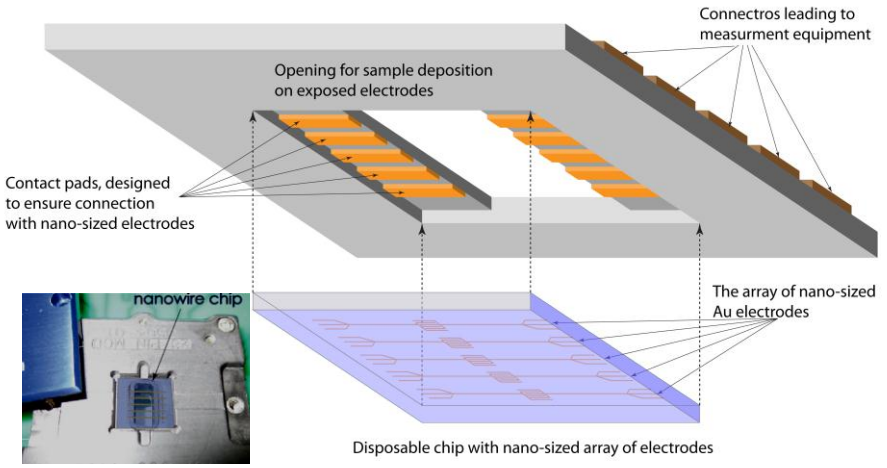

Figure 1: Schematic illustration of the test socket principle. Inlet is the optical image of actual test socket with the outline of the nanowire array chip placement

References:
[1] J. D. Wulfkuhle, L. A. Liotta, E. F. Petricoin, Nat. Rev. Cancer 3, 267–275, 2003
[2] J. J. Boote and S. D. Evans, Nanotechnology 16, 1500–1505, 2005
[3] Erik M. Freer, Oleg Grachev, Xiangfeng Duan, Samuel Martin, David P. Stumbo, Nature Nanotechnology 5, 525-530, 2010
[4] C. Tlili, L. N. Cella, N. V. Myung, V. Shetty, A. Mulchandani, Analyst, 135, 2637-2642, 2010
[5] Y. Xiang, A. Keilbach, L. M. Codinachs, K. Nielsch, G. Abstreiter, A. F. i Morral, T. Bein, Nano Letters, 10, 1341-1346, 2010
[6] J. Jorritsma, M. A. M. Gijs, C. Schönenberger, J. G. H. Stienen, Applied Physics Letter, 10, 1489-1491, 1995.

Real time microfluidic analysis system for small animal molecular imaging

L. Convert[*1,4], *F. Girard-Baril*[1], *V. Boiselle*[1], *V. Chabot*[1], *P.-J. Zermatten*[1], *R. Hamel*[1], *J.F. Pratte*[2], *R. Fontaine*[2], *J.-P. Cloarec*[3], *R. Lecomte*[4], *P. Charette*[1], *V. Aimez*[1]

[1]CRN2, Université de Sherbrooke, 2500 Bd Université, Sherbrooke, QC, Canada, J1K2R1
[2]GRAMS, Université Sherbrooke, 2500 Bd Université, Sherbrooke, QC, Canada, J1K2R1
[3]INL, École Centrale de Lyon, 36 avenue Guy de Collongue, 69134 Ecully Cedex, France
[4]CIMS, Université de Sherbrooke, 3001 12th Ave. North, Sherbrooke, QC, Canada, J1H5N4

Mots clés : Beta detector, microfluidic, small animal PET, Metal Clad Waveguides, Bovine Serum Albumin

Molecular imaging using positron emission tomography (PET) or single-photon emission computed tomography (SPECT) is one of the leading tools for diagnostic and therapeutic follow up studies in oncology and cardiology [1]. This work aims to develop an integrated blood analysis microfluidic chip to characterize new radiotracers for PET and SPECT in small animals before their use in humans. In the initial implementation, whole blood radioactivity is monitored in real time in a surface modified microchannel fabricated over unpackaged detectors (Figure 1).
A flat rectangular channel was microfabricated using an epoxy photoresist, KMPR, over a die containing *p-i-n* photodiodes (Excelitas Technologies). Gold traces were added before laying out the microchannel wall to connect the detector anodes. The chip was wire-bonded to a custom-made PCB and connected to preamplifier and amplifier modules. Measured absolute sensitivity to the most common PET tracers is 4 to 8 times better than typical non-microfluidic beta detectors [2] and allows the detection of ^{99m}Tc-SPECT tracers. Microchannel biocompatibility was enhanced using Bovine Serum Albumin (BSA) before assays with whole blood. Metal clad waveguides (MCWG) [3] were used in a new configuration to monitor KMPR surface biofouling without the need for additional labeling (Figure 2). MCWG was first compared to surface plasmon resonance (SPR) and long-range-SPR. Then, it was used to measure a drastic decrease in Fibronogen adsorption on BSA-treated KMPR [4] indicating an increased hemocompatibility. Further work will add microfluidic functionalities on-chip to provide full characterization of new radiotracers: plasma separation and plasma sampling for metabolites analysis.

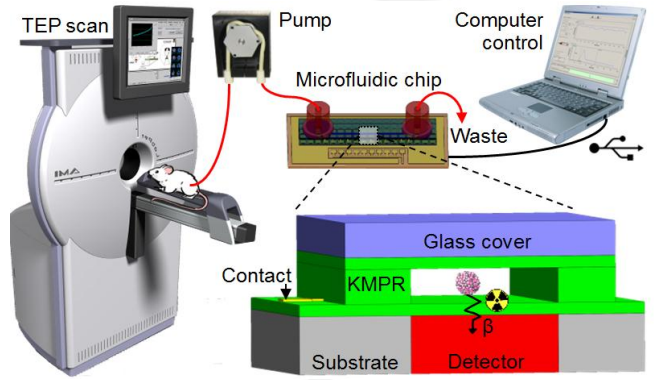

Figure 1 – Microfluidic blood counter connected to an animal for PET pharmacokinetic studies.

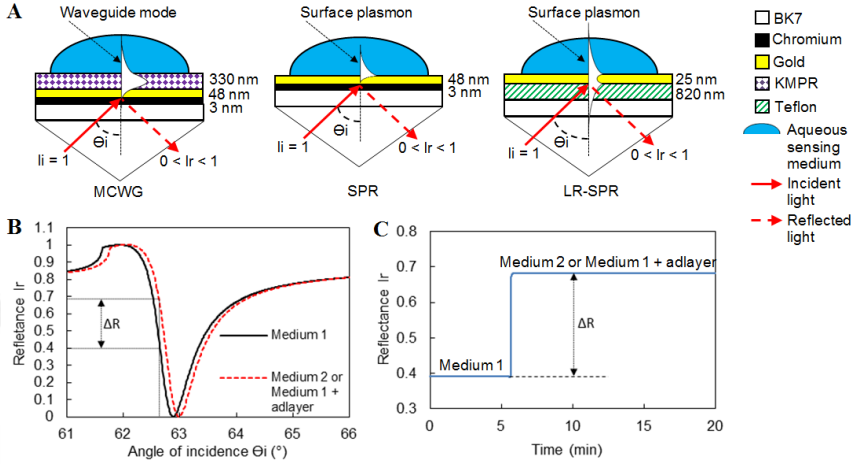

Figure 2 – A. Comparison between MCWG, SPR and long-range-SPR (LR-SPR) structures. B. Example of angular scans with the MCWG structure for two aqueous sensing medium with different RI or the same medium but with/without a thin adlayer on the surface. C. Corresponding reflectance monitoring over time at 62.1°. Fluid change at t = 6 min.

Références
[1] S.R. Cherry, S.S. Gambhir, ILAR J., 42:219, 2001
[2] L. Convert et al., J. of Nucl. Med., 48:1197, 2007
[3] P. Tien, Rev. Mod. Phys., 49(20):361-419, 1977
[4] Y. L. Jeyachandran et al., Langmuir, 25(19) :11614-20, 2009

Magnétites encapsulées dans les microsphères de polysaccharide comme porteur de molécules thérapeutiques : caractérisation et analyse cytotoxique.

D. A. Mbeh[1], R. França[1], T. Djavanbakht[1], Y. Merhi[3], T. Veres[4], M. A. Mateescu[5], E. Sacher[2], L'H. Yahia[1].

[1]Laboratoire d'Analyse et d'Innovation de Bioperformance (LIAB), Ecole Polytechnique, succursale Centre-Ville Montréal, Québec H3C 3A7 Canada; [2] Département de Génie Physique, CP 6079, succursale Centre-Ville Montréal, Québec H3C 3A7 Canada;
[3] Institut de cardiologie, 5000 rue Belanger Montréal, Québec, Canada, H1T 1C8 ;
[4] Institut Matériaux Industriels, 75 de Mortagne Boucherville, Québec, Canada, J4B6Y4 ;
[5] Département de Chimie UQAM, C.P. 8888, Montréal, Québec H3C 3P8 Canada.

Mots clés: nanoparticules; magnétite; chitosane; cytotoxicité; caractérisation de surface.

Les nanotechnologies appliquées à la nanomédecine passent particulièrement par l'utilisation des nanoparticules. C'est un nouveau domaine très prometteur en ce qui concerne le diagnostic et le traitement de pathologies d'origine infectieuse, génétique ou cancéreuse. Notre projet consiste à développer un nano-vecteur constitué de nanoparticules magnétiques (Fe_3O_4) considérées comme biocompatibles[1,2] encapsulées dans les microsphères de polysaccharide y compris le chitosane et l'amidon et leurs dérivés et capables de mener des substances thérapeutiques jusqu'à la paroi alvéolaire. Pour assurer le coté sécuritaire de ce nano-vecteur, il est crucial de connaitre leur caractéristiques physico-chimiques et leur biocompatibilité à chaque étape de leur fonctionnalisation. L'interaction entre la magnétite et les polysaccharides a été étudiée pour les différents protocoles. Les techniques de la spectrométrie photoélectronique X (XPS) (figure 1), la spectroscopie *infrarouge* à transformée de Fourier (FTIR) et la microscopie électronique à balayage (SEM) ont été utilisées afin de déterminer les propriétés physico-chimiques des échantillons. Les tests de cytotoxicité ont été réalisés par un contact direct des particules de chitosane avec les cellules épithéliales alvéolaires humaines (A549) en utilisant les essais MTT et LDH. Les résultats obtenus par SEM[3] ont montré que les tailles des nanoparticules de magnétite encapsulées dans les microsphères de carboxyéthylchitosane ont été de 20 à 70 nm. La caractérisation de la surface des échantillons effectuée par XPS a montré que l'identité de surface de quelques échantillons a été différente de celle de leur volume. L'épaulement du pic d'oxygène observé dans le spectre de XPS a indiqué la liaison entre les polysaccharides et les nanoparticules de magnétite. Les résultats montrent que les types de chitosane utilisés sont biocompatibles comme l'illustre la figure 2.

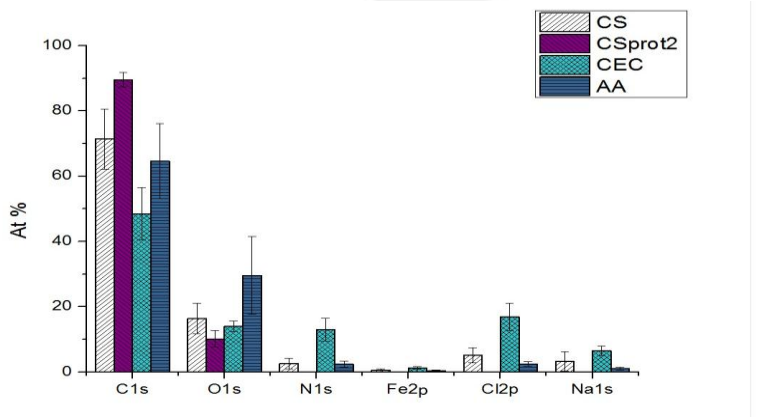

Figure 1- Le diagramme de XPS des nanoparticules de magnétite encapsulées dans le chitosan (CS) (2 protocoles), le carboxyéthyl chitosane (CEC) et l'acétate d'amidon (AA) représente le pourcentage atomique des atomes qui se trouvent à la surface des échantillons.

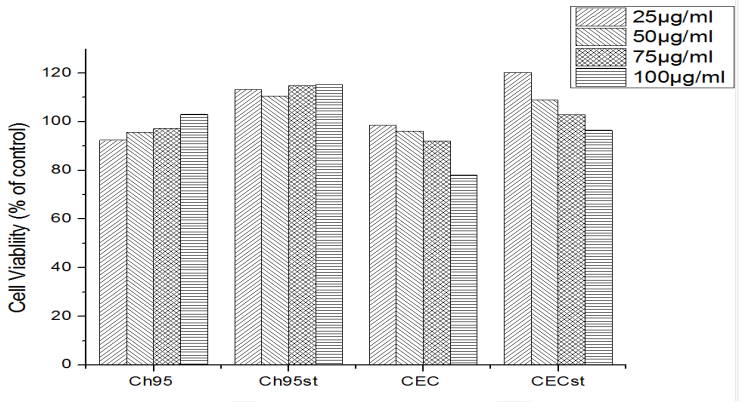

Figure 2: Effects of chitosan particles on A 549 cell viability (direct contact).

Références

[1] F. Y. Cheng, C. H. Su, Y. S. Yang, C. S. Yeh, C. Y. Tsai, C. L. Wu, M. T. Wu, Shieh DB. Aqueous dispersion of monodisperse magnetic iron oxide nanocrystals through phase transfer. Biomaterials 2005;26:729–38

[2] S. M. Hussain, K. L. Hess, J. M. Gearhart, K. T. Geiss, Schlager JJ. In vitro toxicity of nanoparticles in BRL 3A rat liver cells. Toxicol. In Vitro 2005;19:975–83.

[3] Franca R, Mbeh D, Le Tien C, Mateescu M, Yahia LH, Sacher E. In Vitro Biocompatibility and Surface Analysis of Chitosans: Effect of Ethylene Oxide Sterilization. Soumit à Biomacromolecules 2011.

Synthèse de nanostructures peptidiques hélicoïdales pour la reconnaissance moléculaire de protéines d'intérêt

C. Racine-Berthiaume, R. Barattin, N. Voyer

Département de chimie, Université Laval, 1045 ave de la Médecine, Québec, Canada, G1V0A6 et PROTEO

Mots clés : nanotechnologies, AFM, détection monomoléculaire, peptides, chimie click

La microscopie à force atomique(AFM) est reconnue comme une technique de choix dans l'étude de processus biologiques et événements de reconnaissance moléculaire dû à sa capacité à opérer en conditions aqueuses et/ou physiologiques, permettant l'imagerie et la mesure de propriétés mécaniques entre la pointe et le substrat(1). Pour ce faire, la modification des pointes d'AFM à l'aide de transducteurs constitue une étape-clé. Notre laboratoire vise à développer une approche pour la modifications de pointes d'AFM par des monocouches auto-assemblées (SAM) mixtes contenant une faible concentration de structures peptidiques hélicoïdales de dimensions nanométriques facilement modifiables aux C et N terminal pour introduire un système d'ancrage dithiol et un ligand biologique d'intérêt. Nous rapporterons nos résultats sur le design et la synthèse de peptides nanotransducteurs de différentes longueurs contenant l'espèce dithiol au C-terminal et une biotine au N-terminal pour les études préliminaires sur le système biotine-avidine déjà bien caractérisé(2). Nous rapporterons également nos résultats sur l'utilisation de la chimie click pour étendre le spectre des ligands biologiques à l'étude, spécifiquement un ligand mannose ancré au N-terminal pour l'étude de phénomènes de reconnaissance avec la concanavaline A.

Références

[1] A. Noy, D. V. Vezenov and C. M. Lieber, Annu. Rev. Mater. Sci.,1997, 27, 381–421
[2] E.-L. Florin, V. T. Moy and H. E. Gaub, Science, 1994, 264,415–417

Plasmonic enhanced laser nanosurgery and application to cancer cell transfection

B. St-Louis[1], J. Baumgart, E. Boulais[1], R. Lachaine[1] , J.J. LeBrun[2], M. Meunier[1]

[1]Polytechnique Montréal, 2500 chemin de Polytechnique, Montréal, Québec, H3T 1J4, Canada
[2]Royal Victoria Hospital, Department of Medecine, Montreal, Québec, H3A 1A1, Canada

Mots clés : transfection, nanoparticules d'or, plasmonique, laser, cellule cancéreuse

La transfection cellulaire est une technologie permettant de modifier le comportement d'une cellule en lui faisant exprimer du matériel génétique exogène. Cette technologie a attiré beaucoup d'attention au cours des dernières années, trouvant des applications dans de nombreux domaines scientifiques allant de la biologie fondamentale à certains traitements thérapeutiques. De nombreuses méthodes de transfection sont actuellement disponibles, mais toutes se rivent à de nombreux problèmes. Afin d'effectuer la transfection de façon sélective tout en conservant un rendement intéressant, nous proposons l'utilisation d'un laser infrarouge pulsé localement amplifié par des nanoparticules plasmoniques hors-résonance. L'irradiation de ces particules crée en effet des nanobulles de vapeur autour des particules et génère d'importantes ondes de pressions qu'on croit responsables de la perméabilisation des cellules. L'affiche présente divers travaux qui ont été réaliser afin de comprendre et caractériser les mécanismes responsables de la transfection. Des simulations théoriques de l'interaction entre laser ultra rapide (femtoseconde) et nanostructures plasmoniques sont présentées. Du coté expérimental, un montage de type pump-probe permet la détection de nanobulles en milieux liquide lorsqu'une solution de nanoparticules est irradier par un laser pulsé. Finalement une méthode de transfection optique à haut rendement a été testé sur des cellules cancéreuses (mélanomes). La membrane cellulaire a été perméabilisée avec succès à l'aide d'un laser femtoseconde ainsi qu'avec un laser nanoseconde. Un colorant fluorescent, un SiRNA (small interfering RNA) ou un plasmide a été incorporer à l'intérieure des mélanomes avec des taux d'efficacité différent pour les deux laser.

Bacteriophage-Nanoparticle Complexes for Pathogen Detection

N. Tawil[1,2,4], D. Rioux[1], E. Sacher[2], W.Chan[3], R. Mandeville[4], M. Meunier[1]

[1] Laser Processing and Plasmonics Laboratory, Department of Engineering Physics, École Polytechnique, C.P. 6079, Succ. centre-ville, Montréal, Québec, Canada, H3C 3A7
[2] Regroupement Québecois des Matériaux de Pointe, Department of Engineering Physics, École Polytechnique, C.P. 6079, Succ. centre-ville, Montréal, Quebec, Canada, H3C 3A7
[3] Cytodiagnostics, University of Toronto, 160 College St.,Toronto, Ontario, Canada, M5S 3E1
[4] Biophage Pharma, 6100 Royalmount, Montréal, Québec, Canada, H4P 2R2

Keywords : Nanoparticle, Bacteriophage, Biosensor, Surface Plasmon Resonance, MRSA

Nosocomial infection is the leading cause of death for hospitalized patients, affecting more than 2 million such patients per year, and leading to approximately 90,000 deaths annually [1]. Methicillin-resistant staphylococcus aureus (MRSA) is the leading cause of nosocomial and community-acquired infections. Reducing the time of diagnosis is directly related to reducing morbidity and mortality rates [2]. Bacteriophages are viruses that specifically interact with their host bacteria. Phages are also able to distinguish between live and dead cells, they are robust, easy to produce, and cost-effective. In this report, we describe the first application of bacteriophages bioconjugated to gold nanoparticles (NP) for the detection of MRSA. Multiple strategies were used to improve the immobilization of bacteriophages on nanoparticles, including the physisorption of phages and the covalent immobilization of phages via L-cysteine, glutaraldehyde, self-assembled monolayers, and Traut's reageant. An optical conjugation method that did not interfere with the viability and activity of the bacteriophages was selected. MRSA recognition by NP-phage complexes has been demonstrated. This system, coupled with the use of surface plasmon resonance (SPR) biosensors, promises to become a diagnostic tool for bacteria causing major public concern for food safety, bioterrorism, and nosocomial infections.

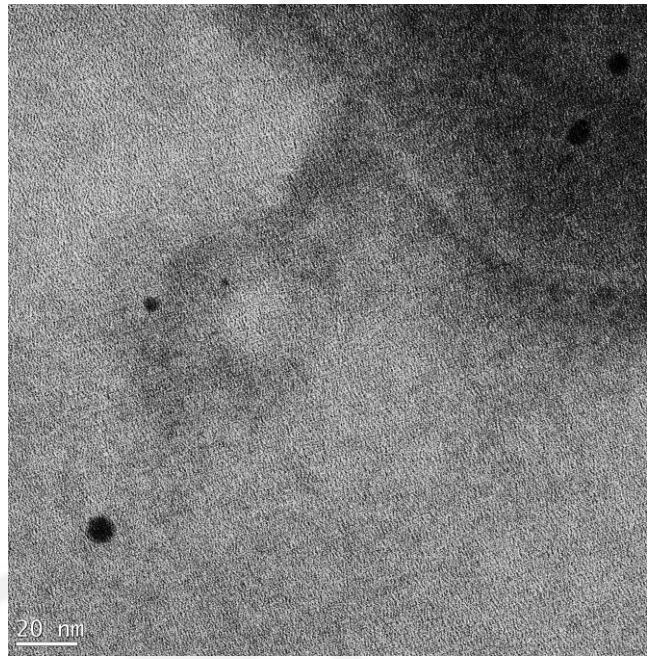

Figure 1 – TEM image of bacteriophage-nanoparticle complex interacting specifically with Methicillin-resistant *Staphylococcus aureus*

References
[1] Burke, J. P., Infection control - A problem for patient safety. *New England Journal of Medicine* **2003,** *348* (7), 651-656.
[2] Lindsey, W. C.; Woodruff, E. S.; Weed, D.; Ward, D. C.; Jenison, R. D., Development of a rapid diagnostic assay for methicillin-resistant Staphylococcus aureus and methicillin-resistant coagulase-negative Staphylococcus. *Diagnostic Microbiology and Infectious Disease* **2008,** *61* (3), 273-279.

Nanoparticules de silice mésoporeuse, une plateforme pour l'imagerie multimodale.

J.-L. Bridot[1,2,3,4], R. Guillet-Nicolas[1,3,4], M. Laprise Pelletier[1,2,3,4], M.-A. Fortin[1,2,3,4] et F. Kleitz[3,4].

[1]Centre Hospitalier Universitaire de Québec, Axe métabolisme, santé vasculaire et rénale (CRCHUQ-MSVR), Québec, Canada, G3L 1L5
[2]Département de génie des mines, de la métallurgie et des matériaux, Université Laval, Québec, Canada, G1V 0A6
[3]Département de chimie et Centre de recherche sur les matériaux avancés, Université Laval, Québec, Canada, G1V 0A6
[4]Centre de recherche sur les matériaux avancés (CERMA)

Mots clés : nanoparticules, silice mésoporeuse, multimodalité, imagerie biomédicale.

Depuis leur découverte, les silices mésoporeuses ont suscité un véritable engouement du fait de leurs propriétés uniques, notamment dans les domaines de la catalyse et de l'environnement. Ces structures originales présentent des surfaces spécifiques pouvant dépasser 1000 m^2/g et des volumes poreux de l'ordre de 1 cm^3/g. Depuis 2001, avec la réduction de la taille des domaines mésostructurés à des dimensions comprises entre 50 et 200 nm, ces nanoparticules ont ouvert de nouvelles opportunités dans le domaine biomédical. Notre objectif est d'exploiter les propriétés de ces plateformes pour les imageries par résonance magnétique (IRM) et nucléaire.Les nanoparticules sont synthétisées par un procédé d'auto-assemblage coopératif dynamique entre un système micellaire et un précurseur de silice. La synthèse achevée, la porosité du matériau est libérée en éliminant l'empreinte organique par calcination ou par extraction chimique. Afin de rendre ces particules efficaces en IRM, du gadolinium leur a été associé sous forme de silicate[1] ou chélaté par un polyaminocarboxylate. La voie des chélates permet également de piéger d'autres cations métalliques d'intérêt comme le ^{64}Cu, un radio-isotope dont la demi-vie (12.7 heures) est idéale pour des études longitudinales in vivo.Les matériaux synthétisés ont été caractérisés par physisorption d'azote à 77 K, analyse thermogravimétrique et spectroscopie des photoélectrons-X. La stabilité de ces particules dans des milieux physiologiques a été démontrée par diffusion dynamique de la lumière. Les mesures relaxométriques réalisées sur des solutions contenant les nanoparticules de silice mésoporeuse chargées avec du gadolinium prouvent leur intérêt comme agents de contraste en IRM.

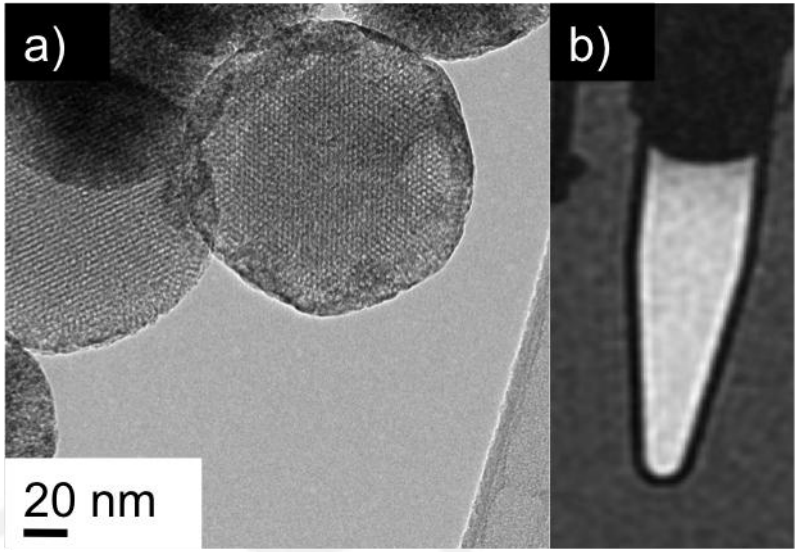

Figure 1 – a) Cliché MET de nanoparticules de silice mésoporeuse de type MCM48 *chargée en Gd et b) cliché IRM d'une solution aqueuse de nanoparticules de Gd-MCM-48.*

Références
[1] R. Guillet-Nicolas, J.-L. Bridot, Y. Seo, M.-A. Fortin, F. Kleitz, *Advanced Functional Materials* **2011**, *21*, 4653-4662.

Evanescent field biosensor for label-free and real-time in situ monitoring of multiple analytes ex vivo and in vivo

P.- J. Zermatten[1], A. Duval[1], A. Jaouad[1], D. Fillion[2], E. Wieczerzak[2], M.-J. Colbert[2], M.-R. Lefebvre[2], H. Traboulsi[2], M. Grandbois[2], C. Allen[3], E. Marsault[2], E. Escher[2], V. Aimez[1], P. G. Charette[1]

[1]Département de génie électrique et génie informatique, 2500 boul. Université, Sherbrooke, Canada, J1K 2R1.
[2]Institut de Pharmacologie de Sherbrooke, 12e Av. Nord, Sherbrooke, Canada, J1H 5N4.
[3]Université de Laval, 2325 rue de l'Université, Québec, Canada, G1V 0A6.

Mots clés : planar waveguide, biosensors, fluorescence

Drug discovery and healthcare have been greatly influenced by technological advances. In both fields, the capacity to monitor selected analytes (drugs, biomarkers, metabolites) in biological fluids directly impacts the decision making process and the development of diagnostics. In collaboration with the Institut de Pharmacologie de Sherbrooke, we are developing a biosensor for in situ, real-time and label-free detection of multiple analytes in biological fluids, ex vivo and in vivo.
The biosensor, shown Figure 1, is composed of PEG chain molecular tethers bound to a planar waveguide surface. The tether links a Q-dot/discriminator complex that folds back onto the sensor surface during a recognition event with a surface-bound analyte. In this way, the fluorophore is excited by the evanescent field at the surface and emits light which is collected by the waveguide. The intensity of the light captured monitors the number of recognition events which occurs.The strong evanescent field, which is necessary to excite the Qdots, is created at the waveguide-analyte interface by the deposition of a thin silicon nitride film on top of a planar silicon dioxide waveguide [1]. Consequently the intensity of the light is locally concentrated at the waveguide surface (see simulation Figure 2). The PECVD silicon nitride layers have been optimized in order to exhibit very low absorption in the visible range [2]. The light emitted by Qdots attached to the surface of the waveguide is observed by a fluorescence camera (see Figure 2). Our current work is focused on collection of the fluorescence emission by the waveguide.

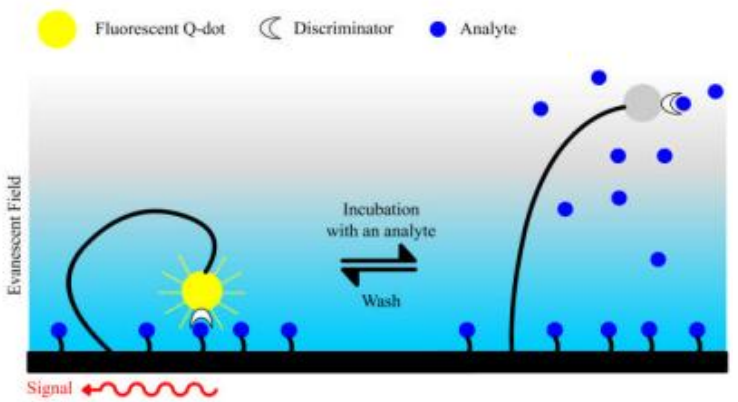

Figure 1 – Schematic representation of the chemical recognition part of the biosensor.

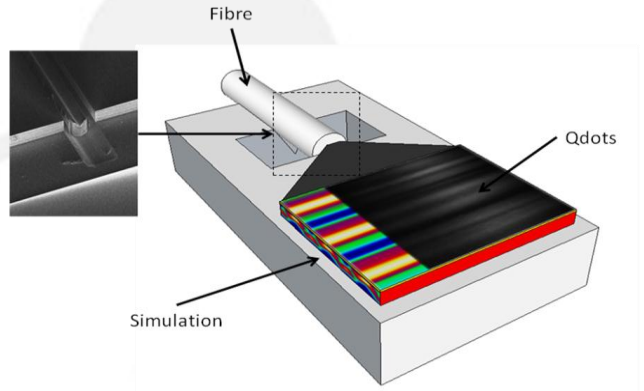

Figure 2 – Schematic representation of the optical part of the biosensors. An optical image of the light emitted by the Qdots (λ=560 nm) excited by a λ=470 nm light coming from the fiber, is superimposed on the schematic, as well as the corresponding simulation. An SEM image of the V-groove fabricated on the Si substrate and needed to clamp the fiber is also represented.

Références
[1] T. Tamir. Integrated Optics, Springer, Volume 7.
[2] A. Gorin, A. Jaouad, E. Grondin, V. Aimez, and P. Charette, Optics Express **16,** 13509 (2008).

Adsorption et réactivité des biomolécules en présence de nanomatériaux inorganiques

Meryem Bouchoucha[1,2], Maguy Jaber[1], Jean-François Lambert[1]

[1] Laboratoire de Réactivité de Surface – Université Pierre et Marie Curie, Paris, France
[2] Laboratoire de Matériaux fonctionnels nanoporeux – Université Laval, Québec, Canada

Mots clés : nanomatériaux inorganiques, adsorption et encapsulation, acides aminés, chimie de surface.

Nous avons étudiées l'adsorption et la réactivité de deux acides aminés : L-DOPA et acide glutamique (Glu) en présence de différents nanomatériaux inorganiques pour des applications potentielles en vectorisation des médicaments, en synthèse de nouveaux biomatériaux nanocomposites et en catalyse des synthèses organiques. En combinant les informations des caractérisations macroscopiques (HPLC, DRX, ATG, Physisorption d'azote, DLS et Rhéométrie) avec les observations microscopiques et spectroscopiques (UV-Visible, IR, Raman, RMN, RPE), nous avons mis en évidence que la réactivé de ces biomolécules dépend des propriétés du nanomatériau utilisé. En présence d'aluminosilicates (Zéolithes BEA, FAU), la DOPA a tendance à s'oxyder en Dopaquinone et DopaChrome. Ces réactions d'oxydation dépendent des cations compensateurs de la zéolithe qui sont responsable de l'interaction DOPA-Zéolithe et de l'activation catalytique de ces réactions oxydantes. En présence de phyllosilicates (Laponite), la DOPA a tendance à se polymériser en Mélanine. Cette polymérisation favorise la structuration des suspensions de Laponite (gélification), résultat intéressant pour la synthèse de nouveaux nanocomposites et le contrôle de leurs propriétés mécaniques[1]. En présence de la silice amorphe, l'adsorption et la réactivité thermique de l'acide glutamique dépend de la spécificité de la chimie de surface de la silice (nature et abondance des sites à la surface) qui active sélectivement les réactions de condensation du Glu adsorbé. Avec les nanoparticules MCM-41, une seule étape significative de condensation interne du Glu a eu lieu (formation du PyroGlu). Alors que sur l'Aerosil, deux étapes de condensation successives (intra et intermoléculaires) sont observées (formation du PyroGlu qui se condense par la suite en PyroGluDKP)[2].

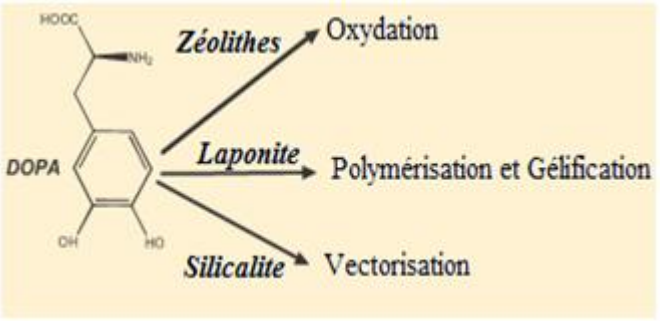

Figure 1 : Réactivité de la L-Dopa [1]

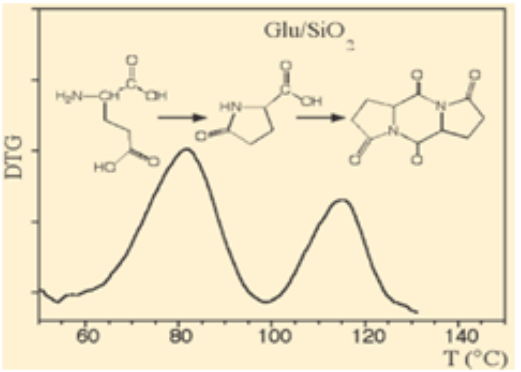

Figure 2 : Réactivité thermique de l'acide Glutamique, Profil DTG [2]

[Références] Références
[1] M. Bouchoucha, M. Jaber, L. Delmotte, C. Methivier and J.-F. Lambert, *J. Phys. Chem. C,* 2011, 115, 19216 – 19225.
[2] M. Bouchoucha, M. Jaber, T. Onfroy, B. Xue and J.-F. Lambert, *J. Phys. Chem. C,* 2011, 115, 21813 – 21825.

Séparateur de cellules diélectrophorétique fabriqué par écriture directe 3D

N. Guérin, H. Dalir, D. Therriault, M. Lévesque

Laboratoire de mécanique multi-échelles, École Polytechnique de Montréal, 2900, boul. Édouard-Montpetit, Campus de l'Université de Montréal, 2500, chemin de Polytechnique, Montréal (Québec) H3T 1J4

Mots clés : diélectrophorèse, micro-coextrusion, écriture directe, microfluidique

La séparation et la concentration des cellules sont deux étapes importantes lors de la préparation d'échantillons pour des tests médicaux. Aujourd'hui, elles nécessitent des appareils encombrants et coûteux. La diélectrophorèse (DEP) offre beaucoup d'opportunités afin de réduire la taille et le coût des appareils médicaux. La DEP est un phénomène par lequel des particules suspendues dans un médium ayant des propriétés différentes et soumises à un courant électrique peuvent être poussées vers des zones de haut ou de bas gradient de champ électrique. En utilisant l'écriture directe, notre équipe de recherche a mis au point un dispositif constitué de spirales de polymère photosensible plaquées d'or permettant la séparation par DEP de billes de polystyrène de tailles différentes (fig. 1). Ce dispositif 3D représente une amélioration par rapport aux dispositifs 2D, car le nombre de particules qui peut être séparé est significativement plus grand en raison de la surface totale des spirales par rapport à celle d'électrodes planes.
Malgré son potentiel, ce dispositif peut être amélioré par l'utilisation de microcanaux en forme de spirale 3D fabriqués par micro-coextrusion (fig. 2). Cette technique permet de fabriquer des filaments de polymère contenant une encre fugitive pouvant être retirée pour créer des canaux creux. L'utilisation de spirales 2D a déjà démontré son efficacité pour la séparation continue de particules. Les spirales 3D permettront une plus grande longueur tout en occupant une faible surface. Zhu, J. and X. Xuan, Curvature-induced dielectrophoresis for continuous separation of particles by charge in spiral microchannels. Biomicrofluidics, 2011. 5(2): p. 024111-13.

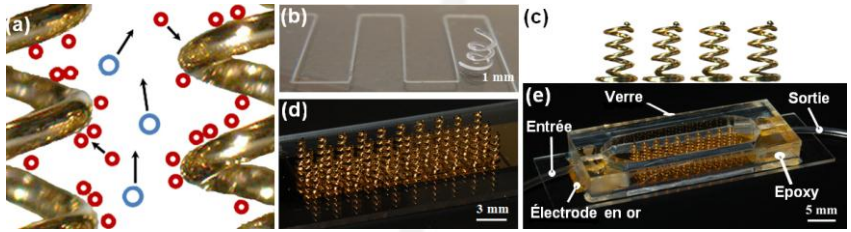

Figure 1 - Dispositif actuel de séparation par DEP. a, Représentation schématique de la séparation de particules de tailles différentes. b, Dispositif en cours de fabrication avec une spirale complétée. c, Vue de côté des spirales plaquées d'or. d, Vue d'ensemble des spirales de polyuréthane plaquées d'or. e, Dispositif complété montré avec les connexions fluidiques.

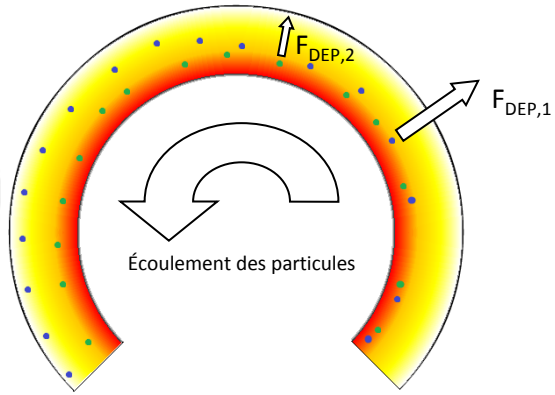

Figure 2 - Dispositif futur de séparation par DEP**.** Le canal en spirale est soumis à un champ électrique non uniforme découlant de l'application d'une tension entre les extrémités du canal. Deux types de particules différents (représentées par les points bleus et verts) sont soumis à des forces différentes ($F_{DEP,1}$ et $F_{DEP,2}$). Ces forces poussent les particules vers l'extérieur de la spirale. La différence d'intensité de ces forces permet une séparation physique entre les types de particules permettant de les récupérer dans des réservoirs séparés à l'aide d'une division dans le canal.

Références

Zhu, J. and X. Xuan, Curvature-induced dielectrophoresis for continuous separation of particles by charge in spiral microchannels. Biomicrofluidics, 2011. 5(2): p. 024111-13.

Combining Microflow Cytometry to Whispering Gallery Modes in Microspheres to Achieve Efficient and Accurate Biosensing

R. Lessard[1], L. S. Verret[1], A. Paquet[1], M. Charlebois[1], Ch. Rivière[2], P. Deladurantaye[2], O. Mermuth[2], C. Nì. Allen[1]

[1]Centre d'optique, photonique et laser (COPL), 2375 rue de la Terrasse, Québec, Canada, G1V 0A6
[2]Institut National d'Optique (INO), 2740 rue Einstein, Québec, Canada, G1P 4S4

Keywords : whispering gallery modes, microspheres, biosensors, refractometry, microflow cytometry

Whispering gallery mode (WGM) biosensing techniques show sensitivities exceeding that of the extensively documented plasmon surface resonance technology [1]. We report an innovative label-free biosensor based on statistical analysis of WGM spectral shifts in polystyrene and melamine fluorescent microspheres using a custom microflow cytometer. Along with extremely precise refractometry, WGM analysis enables detection of nanometer-sized analytes demonstrating promising possibilities for virus, bacteria and molecular detection [2]. To achieve this, the carefully chosen fluorophore-doped microspheres are mixed with *Bacilus globigii* spores in aqueous solution [3]. Then, the syringe pump pushes the solution through the fiber optic flow cell where a laser beam illuminates the region of interest in the microflow cytometer. This device provides a low-cost and user friendly solution to enhance spectrum acquisition rates due to the considerable amount of microspheres flowing through the excitation area per unit time [4]. Finally, the WGM spectra are statistically investigated using an algorithm to determine a reliable value for the refractive index since the exact radius of the microsphere scanned is unknown [5]. This refractive index becomes an effective value for the local perturbation caused by *B. globigii* on the microsphere surface and hence, determines whether or not bacteria are adsorbed by comparing to a control sample. We achieve a limit of detection of 1.9E9 spores/mL corresponding to 5 to 10 bacteria adsorbed on the microsphere surface.

References

[1] F. Vollmer, S. Arnold, Nat. Meth. **5**, 591, 2008.
[2] M. Noto et al., Appl. Phys. Lett. **87**, 2005.
[3] X. Fan et al., Anal. Chim. Acta. **620**, 8, 2008.
[4] P. J. Crosland-Taylor. Nat. **171**, 37, 1953.
[5] M. Charlebois et al., Nanoscale Res. Lett. **5**, 524, 2010.

Les microcavités optiques : biosenseurs pour la détection de bactéries

H. Ghali[1], P. Bianucci[1], Y.-A. Peter[1]

[1]École Polytechnique de Montréal, Département de génie physique, 2500 chemin de Polytechnique, Montréal, Québec, Canada, H3T 1J4

Mots clés : microcavités, fonctionnalisation, couplage, biosenseur, détection

Les microcavités optiques sont des structures capables de confiner la lumière à des échelles micrométriques. Ce confinement est basé sur la réflexion totale interne de la lumière à l'interface entre la cavité et le milieu externe. Les dispositifs se servant de ces cavités connaissent une large gamme d'applications, allant des microlasers aux dispositifs optiques quantiques. Dans ce projet, nous étudions les applications biomédicales des microcavités en silice, telles que la biodétection sans marquage de bactéries. Afin que le biosenseur soit spécifique à un type particulier de bactéries, une série d'étapes de fonctionnalisation est effectuée. La surface de la cavité est tout d'abord couverte d'une couche de poly (éthylène glycol)-silane (PEG-Silane). Les protéines dérivées des phages spécifiques aux bactéries voulant être détectées sont alors introduites. Le lien entre les bactéries et les phages créent une perturbation du champ de la cavité, entrainant ainsi un déplacement du pic de résonance. Cette variation dans le spectre de transmission est causée par un effet réactif. Les spectres sont obtenus par le couplage d'une lumière laser rouge (635 nm) à l'intérieur de la cavité à travers une fibre effilée (figure 1).

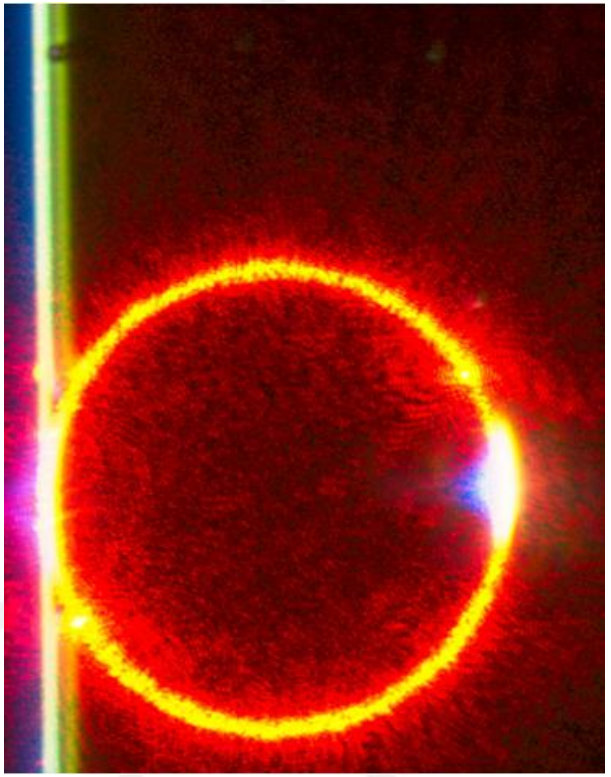

Figure 1 – Image obtenue avec une caméra dans le visible du laser rouge (635 nm) couplé à l'intérieur d'une microcavité à travers une fibre effilée.

Nanopore and Nanochannel Device: a New Approach for Single-Molecule DNA Analysis and Manipulation

Yuning Zhang, Jean-Luc Rukundo, Philip Novosad, Walter Reisner

McGill University, Physics Department, 3600 rue University, Montréal, Canada, H3A 2T8

Mots clés : nanotechnology, nanopore, nanochannel, DNA

Nanopore and nanochannel based devices are robust methods for biomolecular sensing and single DNA manipulation. Nanopore-based DNA sensing has attractive features that make it a leading candidate as a single-molecule DNA sequencing technology. With a special fluidic cell, DNA Molecules can be electrophoretically threaded through artificial SiNx nanopores (2nm to 20 nm). We are trying to prove translocation time of partially denatured ds-DNA is highly sequence depended. Nanochannel based extension of DNA, combined with enzymatic or denaturation-based barcoding schemes, is already a powerful approach for genome analysis. We believe that there is revolutionary potential in devices that combine nanochannels with nanpore detectors. In particular, due to the fast translocation of a DNA molecule through a standard nanopore configuration, there is an unfavorable trade-off between signal and sequence resolution. With a combined nanochannel-nanopore device, based on embedding a nanopore inside a nanochannel, we can in principle gain independent control over both DNA translocation speed and sensing signal, solving the key draw-back of the standard nanopore configuration. We will show our recent progress on device fabrication and characterization. In particular, we demonstrate that we can detect - using fluorescent microscopy - successful translocation of DNA from the nanochannel out through the nanopore, a possible method to 'select' a given barcode for further analysis. In particular, we show that in equilibrium DNA will not escape through an embedded sub-persistence length nanopore, suggesting that the embedded pore could be used as a nanoscale window through which to interrogate a nanochannel extended DNA molecule.

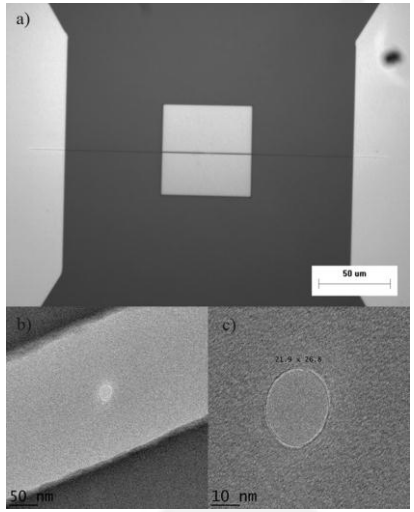

Figure 1: a) microscope image of 120 nm deep nanochannel across 200 nm thick SiNx window; b) TEM image of a nanopore embedded in a nanochannel; c) TEM image of a focus electron beam fabricated SiNx nanopore (~23 nm, zoomed in view of picture b).

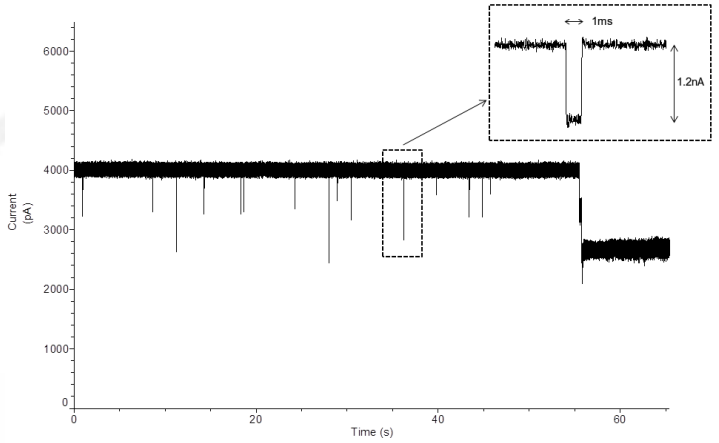

Figure 2: current trace of lambda DNA translocate through a sub 10 nm pore, showing series of current blockages.

De nouvelles membranes lipidiques sur surface nanostructurée pour étudier la diffusion de médicaments Présentation de NanoQuébec

S. Nirasay[1], J.P. Claverie[1], I. Marcotte[1], Y. Mouget[2], A. Badia[3], G. Leclair.*[4]

[1]Nanoqam, Département de chimie, UQAM, Case postale 8888, Succ. Centre-ville, Montréal, Canada, H3C 3P8
[2]Corealis Pharma, 200 boulevard Armand Frappier, Laval, Canada, H7V 4A6
[3]UdeM, Département de chimie, C.P. 6128, succursale Centre-ville, Montréal, Canada, H3C 3J7
[4]UdeM, Faculté de pharmacie, C.P. 6128, succursale Centre-ville, Montréal, Canada, H3C 3J7

Mots clés : PAMPA, perméation membranaire, bicouche phospholipidique, polydopamine

Le Parallel Artificial Membrane Permeability Assay (PAMPA) est employé dans l'industrie pharmaceutique pour étudier les médicaments administrés oralement. Il évalue la diffusion des molécules actives à travers une membrane artificielle mimant la paroi intestinale. Un filtre poreux imprégné de lipides dissous dans du n-décane compose cette membrane. Toutefois ce modèle comporte des faiblesses. Les phospholipides déposés directement sur le filtre peuvent former des couches multilamellaires et obstruer les pores de celui-ci. La perméation peut alors s'avérer anormalement lente et non représentative de la perméation réelle des molécules testées. Aussi, des interactions entre lipides et filtre induisent une perte de mobilité des lipides, allant à l'encontre de la nature fluide d'une membrane biologique.L'objectif est de concevoir de nouvelles membranes qui ressemblent davantage à la structure lipidique des parois de l'intestin, et les adapter sur des cellules de Franz ou des plaques multi-puits pour un criblage haut débit. Plus spécifiquement, ce nouveau modèle sera formé d'un film polymère sur filtre nanoporeux, qui supportera une bicouche de phospholipides. Le polymère limitera les effets de friction entre lipides et filtre et conservera la fluidité d'une biomembrane. Les premiers travaux avec la polydopamine comme biopolymère candidat sont prometteurs et des premiers tests de perméation ont été réalisés sur deux médicaments : la famotidine et l'acétaminophène.En améliorant la technologie PAMPA, nous espérons diminuer le nombre de molécules thérapeutiques potentielles écartées trop tôt dans le processus de découverte de nouveaux médicaments. Nous déterminerons également de façon plus efficace leurs propriétés d'absorption.

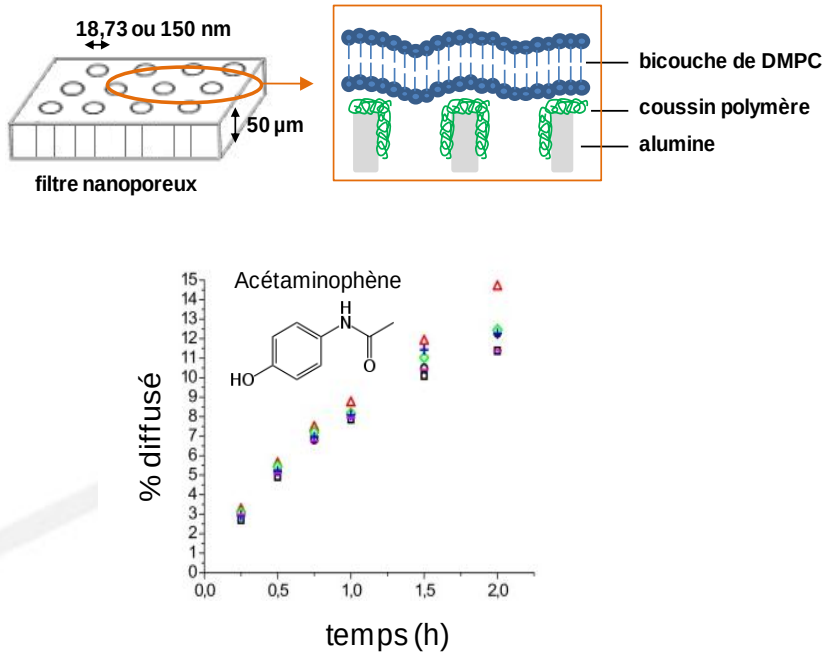

Figure 1 – Résumé graphique du projet

[Références] Références
[1] Nirasay, S., Mouget, Y., Marcotte, I., Claverie, J.P., Supported Bilayer on a Nanopatterned Membrane as Model PAMPA Membranes, *International Journal of Pharmaceutics* (2010).

Conductivity and fluid admittance profiles in a charged nanopore

G. Virdi[1], M.I. Glavinovic[2]

Departments of [1]Mechanical Engineering and [2]Physiology, McGill University, 3655 Sir William Osler Promenade, Montreal, QC, H3G-1Y6, Canada

Keywords : Poisson-Nernst-Planck, Navier-Stokes, nanofluidic pore

The charged particles and water transport through nanofluidic pores is governed by the concentration, pressure and potential gradients. Understanding their interplay is critical for reliable delivery of drugs, and for understanding of the mechanism of exocytosis. During exocytosis the hormones, transmitters or peptides are extruded through the fusion pores, whose conductance can change rapidly, but it is less clear how much this is owing to the change of pore radius, or of the conductivity of the nanopore. The physics of the problem was simulated using a coupled set of Poisson–Nernst–Planck and Navier–Stokes equations [1] in a computational domain consisting of a charged cylindrical pore flanked by two compartments and in the presence of the concentration, potential and pressure gradients between two compartments (Fig. 1). The potential and the pressure were additionally perturbed to estimate the electrical conductivity and fluid admittance. The current mainly flows near the pore wall, where the electrical conductivity is the highest owing to the presence of fixed charges. The fluid specific admittance declines gradually becoming zero at the wall (no-slip). Approximately in the middle between the pore center and the pore wall the fluid admittance and the water flow peak.

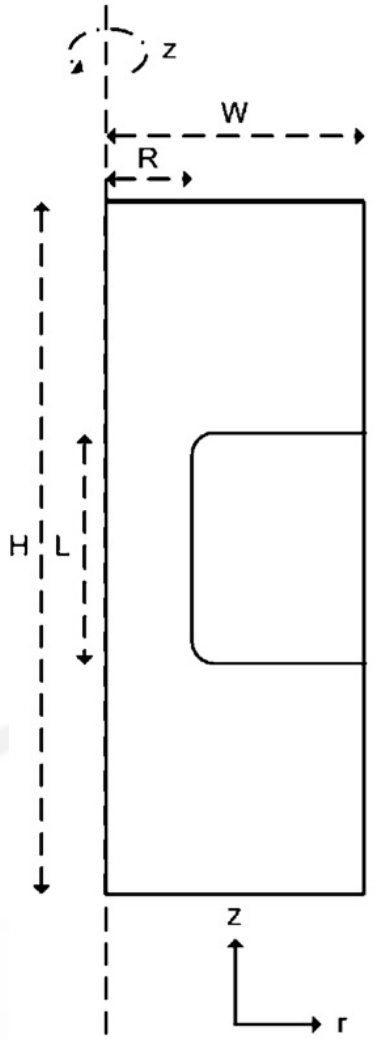

Figure 1. Semi-schematic of the hemi-section of the computational domain consisting of the cylindrical nanopore and two compartments—an upper (vesicular) and a lower (extra-cellular) compartment. Three-dimensional model is generated by the rotation of the hemi-section about the central axis by 180°. Fusion pore radius R is 3nm, whilst the pore length L is 10nm. The radius W the compartments representing the vesicular and extracellular spaces is 11nm. The total length of the computational domain including the fusion pore and two compartments is 30.0nm.

References
[1] G. De Luca, M.I. Glavinovic (2007) Biochimica et Biophysica Acta 1768, 264-279.

Towards a Nano-Plasmonic Polymerase Chain Reaction and other applications of highly localised nanoscale heating

P.J.R. Roche[*1], L.Beitel[2], R.Khan[2], M.Cheung[3] J.Thiemann[4], M. Trifiro[2], V. Chodavarapu[2], A.G. Kirk[1]*

[1]The Photonic Systems Group, McGill University, 3480 University St. room 753, Montreal, Quebec, Canada H3A-2A7
[2]Lady Davis Institute for Medical Research at the Jewish General Hospital, 3755 Côte Ste-Catherine Road, Montreal, Quebec, H3T 1E2
[3]McGill University, Department of Electrical and Computer Engineering, Room 642, 3480 University Street, Montreal, Quebec, Canada H3A 2A7
[4]Telecommunication & Signal Processing Lab, Multimedia Signal Processing, Dept. of Electrical and Computer Engineering, McGill University, Montreal, Quebec

Mots clés : nanotechnologies, expertise, leadership

The polymerase chain reaction (PCR) is one of the fundamental pillars of molecular biological investigations. It requires thermocycling between denaturing, annealing and elongation temperatures to allow the enabling thermophilic polymerase to function. Commercial instrumentation usually applies infra red radiation or solid state heaters to achieve this. Recent work has demonstrate the ever increasing miniturisation of the reaction to picoliter volumes [1], but to truely miniaturise and control the method of heating must function on a nanoscale. In this work we present a demonstration of thermocycling using nano plasmonic elements and explore the potential for rapid and conventional thermocycling required for conducting PCR and theoretically discuss how the reaction maybe reduced to a single particle. In addition we will demonstrate current biological challenges that must be overcome to realise the system. Discussion will be provided on to the further applications of nanoscale plasmonic heating and its potential applications.

References :

[1] Megapixel digital PCR, Kevin A Heyries, Carolina Tropini, Michael VanInsberghe, Callum Doolin, Oleh I Petriv, Anupam Singhal, Kaston Leung, Curtis B Hughesman, Carl L Hansen, *Nature Methods,* 8, 649–651 (2011)

Fabrication and Modeling of Polydimethylsiloxane Replicates of Shallow Etched Porous Silicon to create a Randomized Nanocomb Structure for Tune-able DNA Separation

P.J.R. Roche[*1], M.Cheung[2] Daisy Daivasagaya2, M. Trifiro[3], V. Chodavarapu[2], A.G. Kirk[1]*

[1]The Photonic Systems Group, McGill University, 3480 University St. room 753, Montreal, Quebec, Canada H3A-2A7
[2]McGill University, Department of Electrical and Computer Engineering, Room 642, 3480 University Street, Montreal, Quebec, Canada H3A 2A7
[3]Lady Davis Institute for Medical Research at the Jewish General Hospital, 3755 Côte Ste-Catherine Road, Montreal, Quebec, H3T 1E2

Mots clés : nanotechnologies, expertise, leadership, modelling, DNA

Soft lithography replicates of porous silicon have been produced for the eventual application to DNA separation analysis. The porous silicon templates create a complex range of structures in relief in PDMS. COMSOL modeling has been applied to describe the characteristics of fluidic flow, electrical field distribution and the effect of deformation upon the internal dimensions of the complex separation matrix. The randomized nature of structure prevents DNA strains taking the line of least resistance through as would occur with a geometric micropillar array. Collapse and fracturing observed in high aspect micro-pillar is reduced and an increase in the repatriation of strands is seen within the matrix that could improve separation of a complex DNA mixture upon the basis of size.

Quantum semiconductor photonic biosensor for rapid detection of bacteria in water

W.M. Hassen[1], E. Frost[2], J.J.Dubowski[1],

[1]*Laboratory for Quantum Semiconductors and Photon-Based BioNanotechnology, Department of Electrical and Computer Engineering, Université de Sherbrooke, Sherbrooke, Québec J1K 2R1, Canada*
[2]*Department of Microbiology and Infectiology, Faculty of Medicine and Health Sciences, Université de Sherbrooke, Sherbrooke, Québec J1H 5N4, Canada*
http://www.dubowski.ca

Keywords : Quantum semiconductors, Photoluminescence, Biosensors, Photonic Biosensing, Bacteria detection

In the quest for development of alternative methods of rapid detection of human/animal pathogens, we have been investigating photonic response of quantum semiconductor microstructures to the presence of viruses and bacteria specifically immobilized on semiconductor surfaces. The modification of semiconductor band bending near the surface and reduction of the hole/electron ratio of surface carrier capture cross-section by an electric charge of biomolecules is the main mechanisms contributing to the detection. Most viruses and bacteria carry a net negative electric charge, for which an increase of the PL signal is expected upon immobilization of such particles on the surface of undoped, or lightly n-doped III-V semiconductor. We have addressed detection of *E. coli* using PL emission from GaAs/$Al_{0.33}Ga_{0.67}As$ microstructures capped with a 5-nm thick GaAs layer [1]. The functionalization of the samples was achieved by using either alkanethiol SAMs, or glutaraldehyde based aldehydization of the surface of a thin Si_3N_4 film deposited atop the GaAs surface. The negative electric charge of the bacteria immobilized on the surface of antibody-functionalized microstructures contributed to the increased PL emission from GaAs. The samples exposed to different concentrations of bacteria allowed monitoring the dynamics of the bacteria immobilization observed over a period of several hours. The results indicate that the investigated method allows detection of *E. coli* at 10^4 CFU/ml within less than 120 min. The antibody-based architecture of the method makes it possible to address detection of numerous biomolecules, including pathogenic strains of bacteria.

References

[1] Duplan, V., E. Frost, and J.J. Dubowski, *A photoluminescence-based quantum semiconductor biosensor for rapid in situ detection of Escherichia coli.* Sensors and Actuators B: Chemical, 2011. **160**(1): p. 46-51.

Effect of Superparamagnetic Iron Oxide Nanoparticles on the Physiochemical Properties of Amyloid-β Protein Fibrillation

S. Sheibani[1,2], M. Mahmoudi[3], H. Vali,[1,2]

[1]Facility for Electron Microscopy Research, McGill University, Montréal, QC
[2]Department of Anatomy and Cell Biology, McGill University, Montréal, QC H3A 2B2
[3]Institute for Nanoscience and Nanotechnology, Tehran, Iran

Key word: Superparamagnetic iron oxide nanoparticles, amyloid fibrillation, transmission electron microscopy

Surface coated superparamagnetic iron oxide nanoparticles (SPIONs) are recognized as promising materials for nanodiagnostics owing to their biocompatibility, unique magnetic properties and capacity for as use as multi-modal contrast agents. Diagnosis and treatment of various brain diseases (e.g., multiple sclerosis) are among the proposed uses of SPIONs. Therefore, a complete understanding of their interactions with amyloid-β protein (Aβ) and other amyloidogenic proteins is essential. Here we present a study of the effects of SPION surface coating charge and thickness on the fibrillation kinetics of Aβ under different solution conditions. Observation in transmission electron microscopy showed that a surface area dependent “dual” effect was observed with lower concentrations of SPIONs inhibiting fibrillation, while higher concentrations enhanced the rate of Aβ fibrillation, as had been observed previously in charged polystyrene nanoparticles . Coating charge influenced the concentration at which the acceleratory effects were observed. The positively charged SPIONs promote fibrillation at significantly lower particle concentrations compared to either negatively charged or essentially uncharged SPIONs. This suggests that in addition to the presence of particles effecting the concentration of monomeric proteins in solution (and thereby the nucleation time), the influence of binding on protein conformation also needs to be considered.

Reference
S. Linse et al., (2007) Nucleation of protein fibrillation by nanoparticles. Proc. Natl. Acad. Sci. USA 104: 8691-8696.

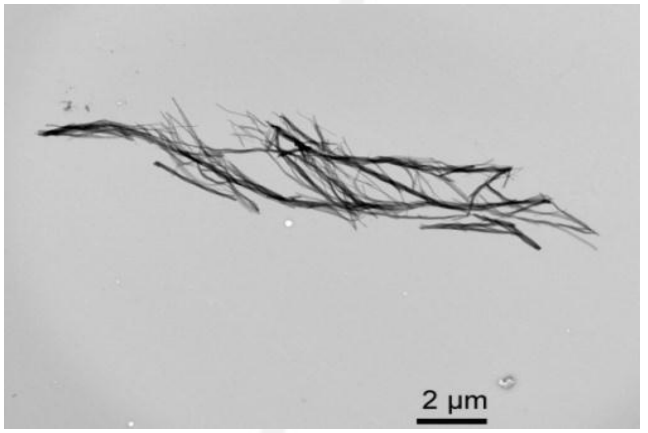

TEM image of Aβ fibrils after incubation for 2400 min in the absence of SPIONs. Protein concetration is 0.5 µM.

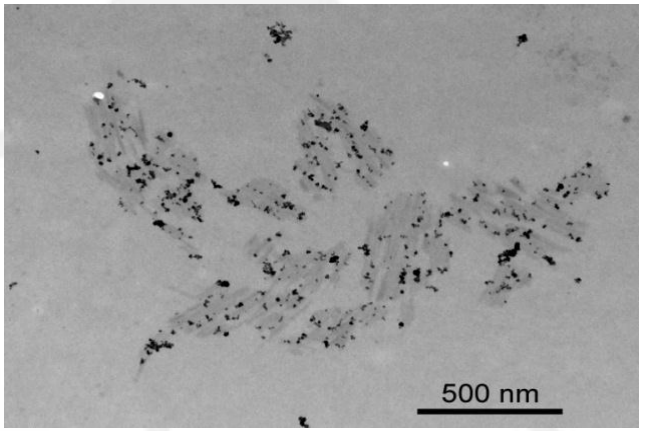

TEM image of Aβ fibrils after 2400 min incubation of Aβ monomers (0.5 µM) with double layer plain dextran-coated SPIONs (100 µg/ml).

Application of phase shift ring down measurement approach to microcavities for biosensing

*M. Imran Cheema[1], Simin Mehrabani[2], Ahmad A. Hayat[3], Yves-Alain Peter[3], Andrea M. Armani[2], and Andrew Kirk[*1]*

[1] ECE Dept. McGill University, Montreal, Canada
[2]Department of Chemical Engineering and Materials Science, University of Southern California, Los Angeles, California, USA
[3] Engineering Physics Dept. Ecole Polytechnique, Montreal, Canada

Key words: Cavity ring down spectroscopy, microcavity, biosensing

Optical resonant microcavities with ultra high quality factors (Q~10^8-10^9) have a great potential for ultra sensitive biosensing as a single photon will interact with a biological sample many times. Until now, most work on microcavity biosensors has been based on measurement of the resonant wavelength shift ($\lambda_{resonant}$) induced by binding event on surface of the microcavity. The binding event also influences the quality factor (Q) of the microcavity, however tracking of the quality factor, as a function of the binding event, has always been ignored by researchers. Moreover, measurement of the wavelength shift is not immune to intensity fluctuations of the laser source and thus overall performance of the biosensor is degraded. One of the promising methods to overcome these issues is to use phase shift cavity ring down spectroscopy, a well established technique for sensing absorption of gases with free space optical cavities. Here, we show simultaneous measurement of the quality factor and the wavelength shift by using phase shift cavity ring down spectroscopy in a biosensor by tracking changes in $\lambda_{resonant}$ and Q for disassociation phase of biotin-streptavidin system in a liquid flow cell containing a bioconjugated toroidal microcavity. We found that the disassociation curves are in good agreement with the previously published results.

PATCH detection: nano-machine functioning as a Probe for Amplification, Target Competition for Hybridization.

K. Boissinot[1], R. Peytavi, M. Boissinot[1], M.G. Bergeron[1]*

[1]. Centre de recherche en infectiologie de l'Université Laval, Centre de recherche du CHUQ, Québec City (Qc), Canada.

Mots clés : DNA amplification, microarray, multiplexing, integration.

Integration of biochemical reactions in microfluidic lab-on-chip devices is desirable for numerous applications. Such methods allow for automation of complex processes that would otherwise require trained personnel. When several techniques are combined on the same chip, such as sample preparation, enzymatic amplification and microarray hybridization, the complexity of the chip design augments rapidly. We need to develop methods that combine one or more of these steps so that they can be performed simultaneously and/or in the same physical space to ease integration. We have devised a nano-machine capable of combining PCR amplification and microarray hybridization in the same reaction chamber, operating in a single buffer. This nano-machine is a labeled oligonucleotide designed with different target sequences and secondary structures. First, it is used as a probe during amplification, which triggers its irreversible structural modification. Specific recognition of the unlabeled target is critical for this function. Second, modified nano-machines hybridize to microarray capture probes while non-modified nano-machines hybridize weakly or not at all. Multiplex detection is possible through the use of multiple nano-machines and spatial localization of different capture probes on microarray. We have demonstrated that both amplification and hybridization can be performed in PCR buffer. Modification happens only when the amplification target is present. Hybridization of the modified form of the nano-machine to a specific capture probe showed a signal-to-noise ratio of 2.5-10 as compared to the non-modified form. Optimisation and integration of the PATCH detection nano-machine into a lab-on-chip system that can perform thermal cycling and microarray fluorescence readings is ongoing.

Portable platform for rapid real-time hybridization and detection of nucleic acids.

K. Boissinot[1], M. Boissinot[1], S. Chapdelaine[1,3], M. Geissler[2], D. Béliveau-Viel[3], J.-F. Gravel[3], T. Veres[2], D. Boudreau[3], M.G. Bergeron[1]*

[1]. Centre de recherche en infectiologie de l'Université Laval, Centre de recherche du CHUQ, Québec City (Qc), Canada.
[2]. Conseil national de recherches Canada, Institut des matériaux industriels (IMI), Boucherville (QC), Canada.
[3]. Department of Chemistry and Centre d'optique, photonique et laser (COPL), Laval University, Quebec City (QC), Canada.

Mots clés : real-time, portable, microfluidics

Rapid diagnostic of infectious diseases is now possible using amplification and detection techniques such as PCR, based on interactions between biomolecules. A majority of these methods are based on specific recognition of DNA by a second DNA strand, a process called hybridization. These detection methods can typically reach an analytical sensitivity of 83 aM (10 copies/test). Furthermore, when detection of multiple analytes (targets) is necessary, spatial and/or optical localization can be used for multiplexing. We have developed a microfluidic device in which probe-grafted particles are captured as single layers in separate micro-channels. This device can then be inserted on a portable real-time hybridization and detection instrument that can analyze up to 8 different DNA targets. Nucleic acids 5.78 nm in length (capture probes) were immobilized on such particles for specific hybridization and detection of complementary targets. Amplification of 1000 copies of nucleic acids from Group B streptococci (GBS) or from vaginal-anal clinical samples (containing or not GBS) were performed to label and increase the number of targets. Afterwards, the hybridization, detection and washing steps were completed in less than 15 minutes, whereas an answer could be provided within 5 min by real-time fluorescence analysis. Using this portable platform we demonstrated real-time hybridization, detection and identification of unknown clinical samples and single nucleotide polymorphisms (SNPs). Our procedure is faster than microarray-based technologies and does not require an expensive confocal slide scanner. Such a system, by also integrating nucleic acid amplification in the microfluidic device, could provide completely automated on-chip detection of viral and bacterial pathogens.

Nanostructures plasmoniques pour la biodétection

M. Maisonneuve, A-P. Blanchard-Dionne, V. Latendresse, S. Patskovsky, M. Meunier

Laboratoire Plasmonique et Procédés Laser, École Polytechnique de Montréal, 2500 chemin de Polytechnique, Montréal (Québec) H3T 1J4

Mots clés : nanostructures, biocapteurs, résonance plasmonique

Les biocapteurs à résonance plasmonique de surface offre un cadre unique pour effectuer des tests de biodétection à très haute résolution. En effet ce type de capteur permet de mesurer des changements d'indice de l'ordre de $1x10^{-7}$ RIU (unité d'indice de réfraction), ce qui correspond typiquement à mesurer une concentration de quelques picogrammes par millilitre d'une unité biologique. Plusieurs applications sont dédiées à l'analyse de composé biochimiques et d'autres à la détection de pathogènes et maladies. Notre recherche est axée sur le second point, principalement basée sur l'élaboration de différentes plateformes plasmoniques pour la détection de la leucémie. Un nouveau type de capteur plasmonique basé sur des nanostructures périodiques creusées dans de minces films d'or offre un nouveau cadre pour exploiter ce type de capteur. De par la miniaturisation du montage nécessaire et la simplification de celui-ci, ce type de structure permet de réaliser plusieurs détections simultanées de différents analytes biologiques. Il sera aussi présenté l'analyse des différentes réponses optiques, telle que la polarisation [1] et la phase [2] émanent de ces structures ; paramètres permettant d'affiner les résolutions des dispositifs présentés. L'utilisation de telles structures dans l'imagerie sera aussi démontrée, permettant leur usage pour la détection de gros objets biologiques (bactérie, cellule). Enfin, l'intégration de ces structures sur un substrat de silicium sera présentée permettant de réaliser une seule puce exposant le senseur biologique et la détection optique [3].

Références

[1] A-P. Blanchard-Dionne, L. Guyot, S. Patskovsky, R. Gordon, and M. Meunier, "Intensity based surface plasmon resonance sensor using a nanohole rectangular array," Opt. Express **19**, 15041-15046 (2011).
[2] M. Maisonneuve, O. d'Allivy Kelly, A-P. Blanchard-Dionne, S. Patskovsky, and M. Meunier, "Phase sensitive sensor on plasmonic nanograting structures.," Opt. Express **19**, 26318-26324 (2011).
[3] L. Guyot, A-P Blanchard-Dionne, S. Patskovsky, and M. Meunier, "Integrated silicon-based nanoplasmonic sensor," Opt. Express **19**, 9962-9967 (2011).

Electrochemically Controlled Microcantilever Biosensor

Y. Nagai[1], M. H. Izadi[3], J. Dulanto-Carbajal[3], R. Sladek[1, 2, 5, 6], R. B. Lennox[4], P. Grutter[3]

[1]Research Institute of the McGill University Medical Centre, [2]McGill Universtiy and Genome Quebec Innovation Centre, Department of [3]Physics, [4]Chemistry, [5]Medicine and [6]Human Genetics, McGill Universtiy

Mots clés : Biosensor, Micromechanical cantilever, Electrochemistry, DNA hybridization

The use of micromechanical cantilevers (microcantilevers) as biological sensors is a new and rapidly developing technique. One of the applications of microcantilevers involves the detection of molecules such as DNA, in both single strand and double strand states [1,2]. Changes in the surface stress of a microcantilever can be indicative of interactions between its chemically functionalized surface and biomolecules. This change in the surface stress induces a measurable deflection of the microcantilever. We report the development of an oligonucleotide-based electrochemical cantilever biosensor that can transduce specific biomolecular interactions into cyclic stress patterns in response to an externally applied periodic potential (Figure in black). Distinct stress patterns were observed for a bare gold cantilever (Figure in blue), for a cantilever functionalized with single stranded DNA oligonucleotides (Figure in red) and for a cantilever with double stranded hybridized oligonucleotides tethered to its surface (Figure in green). The changes in the stress patterns are caused by the competitive adsorption of ions in the hybridization buffer and mechanical changes in the tethered oligonucleotide [2]. A similar cyclic change in cantilever stress results from the interaction between a DNA aptamer and its cognate ligand, demonstrating the broad applicability of this technology to other biosensors.

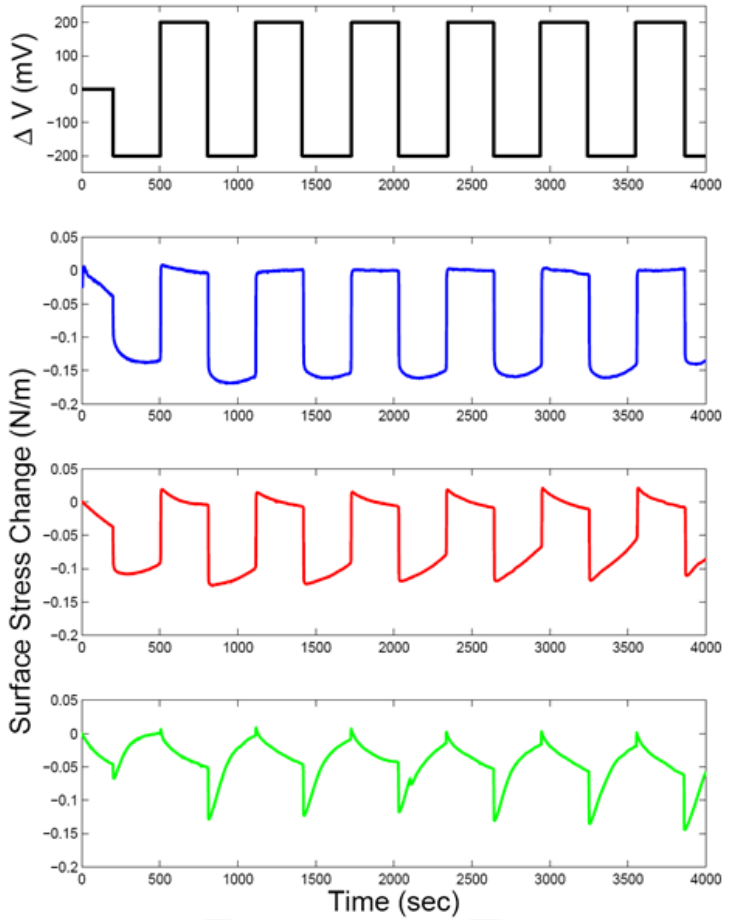

Figure shows periodic square wave of +/-0.2 V (black) and stress changes from the bare gold cantilevers (blue), 25mer probe DNA on gold cantilevers (red), double strand DNA probe on the gold surface (green).

References
[1] McKendry et al., PNAS 99, 9783 (2002)
[2] Fritz et al. Science 288, 316 (2000)
[3] Lipkowski et al., Electrochimica Acta, 43, 19 (1998)

Genomic and Epigenetic Mapping in Nanofluidic Devices

Robert L. Welch, Yi Cao, Ilja Czolkos, W. Reisner

McGill University, Department of Physics, 3600 rue University, Montreal, H3A 2T8, Canada

Keywords: nanofluidics, DNA mapping, yeast, *Staphylococcus aureus*, epigenetics

In the recent years, the capability to fabricate nanometre-sized structures less than 100 nm in feature size has led to the application of such structures in nanofluidic devices for the purpose of the mapping of DNA – the molecule which encodes any organism's genome. The technique for DNA mapping introduced by Reisner *et al.* allows for the mapping of single DNA molecules to identify structures within a genome by using a sequence-sensitive dye (Fig. 1). [1] Single DNA molecule-mapping overcomes the problem of ensemble averaging over the genomes of several cells, which is a limitation of high-throughput sequencing. We present our recent advances in mapping the genomes of baker's yeast (*Saccharomyces cerevisiae*) which is a model organism for human cells. Furthermore, we are mapping strains of *Staphylococcus aureus*, which is a problematic pathogenic germ due to its widespread acquired resistance to common broad-spectrum antibiotics. Genetic screening is a useful technique to identify resistances which are encoded in the bacteria's genome. Furthermore, it is a suggested measure in pushing back resistances. [2] Additionally, we present our progress on site-specific labelling of DNA to probe for hypermethylated areas. These areas are of importance for the identification of abnormal methylation patterns which are implicated in a number of diseases, including cancer. [3] Here, the use of nanofluidics is of great benefit since it allows for the mapping of DNA molecules of single cells.

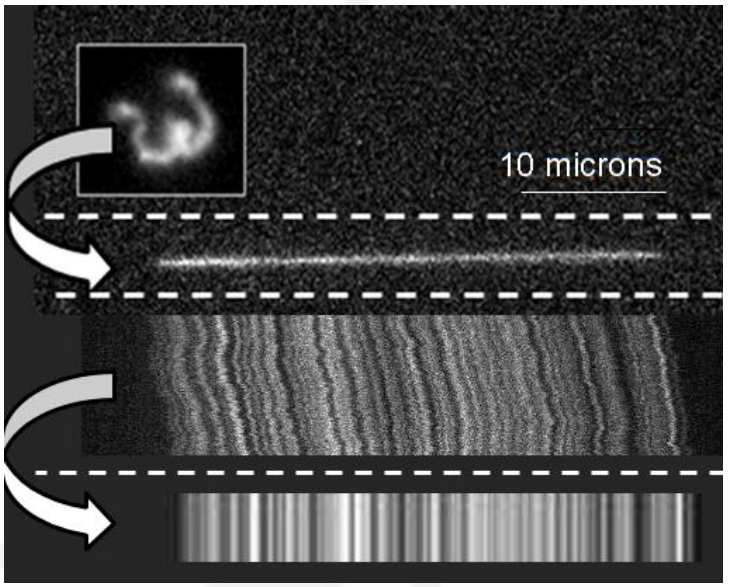

Figure 1: Principle of DNA mapping. A fluorescently stained, coiled DNA molecule (top panel) is forced into a nanochannel of approximately 100 nm in height and width, which entails that the DNA is stretched out. Partial melting of the DNA leads to varying brightness of the dye, depending on the DNA's sequence (lower panel). After image processing, the DNA molecule appears as a barcode that contains sequence or structural information (last image).

References

[1] W. Reisner, N. B. Larsen, A. Silahtaroğlu, A. Kristensen, N. Tommerup, J. O. Tegenfeldt, and H. Flyvbjerg (2010) *Proc. Natl. Acad. Sci. U. S. A.* **107**, 13294–13299.
[2] M. F. Q. Kluytmans-VandenBergh and J. A. J. W. Kluytmans (2006) *Clin. Microbiol. Infect.* **12 (Suppl. 1)**, 9–15.
[3] M. Esteller (2007) *Nat. Rev. Genet.* **8**, 286–298.

Chitosan buffering capacity: implications for gene delivery

I. Richard[1], *M. Thibault*[1], *M. Lavertu*[1], *G. De Crescenzo*[1], *M. Buschmann*[1]

[1]École Polytechnique de Montréal, CP 6079, Succ. Centre-Ville, Montréal, Qc, H3C 3A7

Keywords: gene delivery, chitosan, buffering capacity, proton sponge effect.

In non-viral gene delivery, a cationic polymer having a high buffering capacity in the endosomal pH range, ~4.5 to ~7, can mediate escape from the endosome by the proton sponge effect [1]. In this proposed escape mechanism, the acidification of the endosome or lysosome by the additional pumping of protons into the endosome, along with the concurrent influx of chloride ions causes an increase in osmotic pressure which can lead to vesicle rupture [2]. According to previous studies, polyethylenimine (PEI) has a higher buffering capacity (i.e. potentially better candidate for proton sponge effect) than chitosan [3]. However, in these studies the polymers were compared on a weight concentration basis. Since chitosan possesses a higher monomer molecular weight than PEI, its concentration of protonable amino groups is lower than for PEI for the same weight concentration. In this study, the polymers buffering capacities were therefore compared at equal amino group concentrations. Titration experiments were performed to quantify the buffering capacity of chitosan and PEI. Chitosan and PEI acid-base behaviour were analysed with a Poisson-Boltzmann mean-field theory and an Ising model, respectively. Acid-base behaviour of all polymers is well described by their respective model. This study shows that at equal amino group concentration, chitosan has a better buffering capacity than PEI in the pH range relevant to endocytic pathways. The apparent weak buffering capacity of chitosan reported in the literature is the result of an artefact in the methodology used. The proton sponge effect must be considered as a possible endosomal escape mechanism for chitosan.

References

[1] Boussif, Behr et al., Proc. Natl. Acad. Sci. USA, 92 (1995): 7297-7301.
[2] Putnam et al., PNAS, 98; 3 (2001): 1200-1205.
[3] Mao, Leond et al., Journal of Controlled Release, 70 (2001): 399-421.

Développement d'un biomatériau possédant un contraste brillant en imagerie par résonance magnétique à l'aide des technologies plasmas

M. Létourneau[1,2],G. Laroche[1,2], M.-A. Fortin[1,2]*

[1]Axe métabolisme, santé vasculaire et rénale, Centre de recherche du Centre hospitalier universitaire de Québec (AMSVR-CRCHUQ), Groupe de recherche en imagerie moléculaire (GRIM) and Centre de recherche sur les matériaux avancés (CERMA), 10 rue de l'Espinay, Québec, QC G1L 3L5, Canada
[2]Département de génie de mines, de la métallurgie et des matériaux, Université Laval, Québec, QC G1V 0A6, Canada

Mots clés : nanoparticules magnétiques, agent de contraste, imagerie par résonance magnétique, relaxométrie

Au cours des dernières années, les interventions en médecine ont subi un progrès fulgurant, devenant de moins en moins invasives tout en permettant leur suivi par imagerie médicale.[1] Traditionnellement, les interventions endovasculaires sont imagées par fluoroscopie de rayons X (FRX). Un inconvénient majeur de cette technique est l'utilisation de rayonnement ionisant. L'imagerie par résonnance magnétique interventionnelle (IRMi) est une nouvelle technique qui pallie à l'inconvénient principal de la FRX. C'est ainsi que de nouveaux matériaux biocompatibles et visibles en IRM doivent être développés.[2] L'approche ici est de fabriquer un tel matériau à base de polymère sur lequel on greffe des nanoparticules paramagnétiques ultra-petites. Le projet est divisé en trois grandes séquences : 1) la synthèse de nanoparticules à partir de sel de manganèse, qui constituent un agent de contraste (AC) positif en IRM (fig.1); 2) l'activation de groupements amines sur du téflon à l'aide d'un plasma d'azote et d'hydrogène à pression atmosphérique; 3) le greffage de l'AC sur le polymère activé (fig.2) . Les nanoparticules ont été caractérisées par DLS (taille hydrodynamique), MET (taille du cœur), ATR-FTIR (propriétés chimiques) et TD-NMR (propriétés relaxométriques). L'utilisation conjointe de XPS et de dérivation chimique permet de déterminer la densité d'amines en surface du polymère suite à l'activation. Après le greffage des particules sur le polymère, celui-ci est visualisé en IRM (1T). Cette étude démontre la faisabilité d'utiliser un matériau polymère apparaissant brillant en IRM clinique.

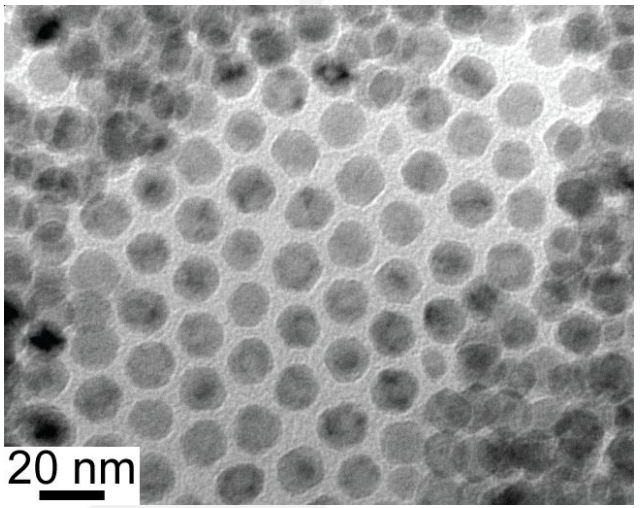

Figure 1 – Nanoparticules observées par TEM (taille moyenne = 12.7 ± 1.0 nm).

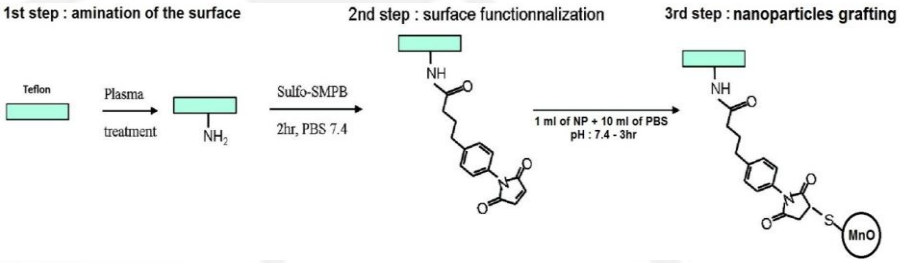

Figure 2 – Stratégie de greffage des nanoparticules sur une surface de téflon.

Références
[1] Kos, S.; Huegli, R.; Bongartz, G. M.; Jacob, A. L.; Bilecen, D. Eur Radiol 2008, 18, (4), 645-57
[2] Unal, O.; Li, J.; Cheng, W.; Yu, H.; Strother, C. M. J Magn Reson Imaging 2006, 23, (5), 763-9

Rapid redox-responsive degradation and facile bioconjugation of polyester-based block copolymer micelles as controlled drug delivery nanocarriers

Samuel Aleksanian, John Oh

Concordia University, 7141 rue Sherbrooke Ouest, Montreal, Canada, H4B 1R6

Keywords: Block copolymer, ATRP, degradation, disulfide

Well-defined amphiphilic block copolymer micelles are promising platforms as effective drug delivery carriers for cancer research. These micelles consist of hydrophobic cores, enabling the encapsulation of anticancer therapeutics, surrounded with hydrophilic coronas, ensuring colloidal stability and biocompatibility. More desirable is the degradation in response to external stimuli in cellular components, which enable the controlled release of encapsulated drugs in targeted disease cells, particularly cancer cells through bioconjugation. Recently, we have developed a new method employing a combined polycondensation and atom transfer radical polymerization to synthesize well-controlled thiol-responsive block copolymers. These copolymers consist of a hydrophilic polymethacrylate block and hydrophobic polyester blocks having disulfides positioned repeatedly on the hydrophobic backbone, thus exhibiting fast degradation in response to redox reactions. Aqueous self-assembly formed colloidally stable micellar aggregates with monomodal distributions, which were analyzed using tensiometry for critical micellar concentration, as well as dynamic light scattering, transmission electron microscopy, and atomic force microscopy for size and morphologies. Furthermore, the new method enabled facile bioconjugation of ssABP micelles with biotin (Vitamine H) demonstrating the applicability of our system towards active targeting. These important results suggest that new polyester-based block copolymer micelles hold a promise as tumor-targeting controlled delivery vehicles.

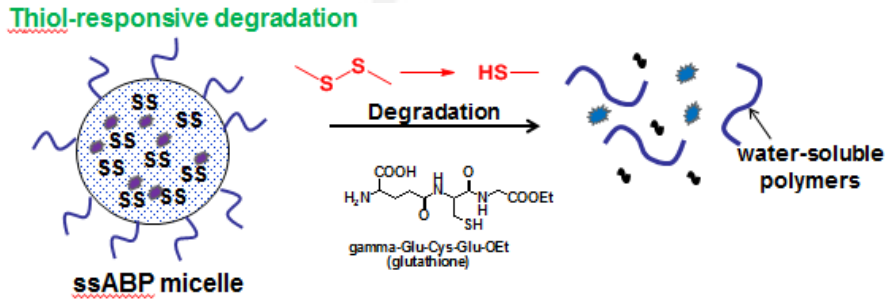

Figure 1 – Thiol responsive degradation of amphiphilic block copolymers

References

[1] W. Reisner, N. B. Larsen, A. Silahtaroğlu, A. Kristensen, N. Tommerup, J. O. Tegenfeldt, and H. Flyvbjerg (2010) *Proc. Natl. Acad. Sci. U. S. A.* **107**, 13294–13299.

[2] M. F. Q. Kluytmans-VandenBergh and J. A. J. W. Kluytmans (2006) *Clin. Microbiol. Infect.* **12 (Suppl. 1)**, 9–15.

[3] M. Esteller (2007) *Nat. Rev. Genet.* **8**, 286–298.

Highly Ordered Nanostructured Templates for Glucose Biosensors

C. A. Horwood[*1], H. A. El Sayed[1], V. I. Birss[1]*

[1]Department of Chemistry, University of Calgary, 2500 University Drive NW, Calgary, AB, Canada, T2N 1N4

Key Words: Biosensors, Glucose Oxidase (GOx), Tantalum nanotubes, Amperometric detection

Diabetes is a lifelong metabolic disorder that affects over 170 million people worldwide, with an incidence rate of approximately 2.5% (1). Other complications, such as blindness, cardiovascular and kidney disease, can be minimized by frequent measurements of blood glucose and administration of insulin (2). Currently, the primary method used for determining blood glucose involves pricking the finger and using a portable meter to measure the glucose concentration. A continuous and convenient way of monitoring blood glucose is not only crucial for ease of use, but also for the reduction of associated complications. We have developed a highly sensitive and biocompatible glucose biosensor by embedding an enzyme (glucose oxidase (GOx)) into a porous conducting matrix of iridium (Ir) nanoparticles (3). Ir-based electrodes are conductive, stable to dissolution, biocompatible, function in aerated or deaerated conditions, and have a linear electrochemical response up to 70 mM of glucose (3). However, the microstructure of these sensing layers, and thus their glucose response, are not always reproducible. Thus, a more ordered and reproducible sensor structure is sought.As a means of producing electrodes with more ordered structures and enhanced sensor reproducibility, a one-step method of preparing stable, well aligned tantalum oxide (Ta_2O_5) nanotubes of varying diameter and length has been developed (Figure 1). Various approaches of depositing Ir nanoparticles and GOx into the nanotubes are being examined, including sputter deposition followed by thermal dewetting, as depicted in Figure 2. The impact of this method on the location and distribution of Ir and GOx, as well as on the glucose response, will be discussed.

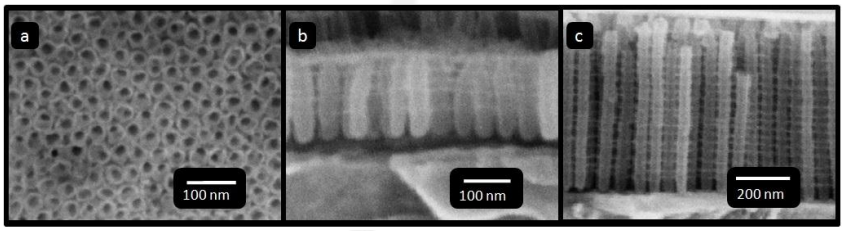

Figure 1 – FE-SEM images of Ta_2O_5 nanotubes formed by anodizing Ta in an HF/H_2SO_4 solution; (a) plan view, (b,c) cross-sectional images.

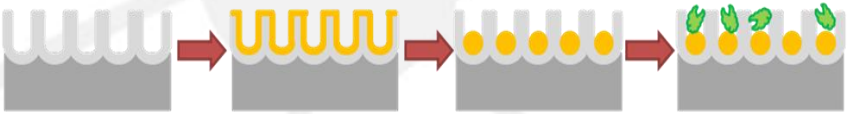

Figure 2 – Schematic showing planned formation of Ta2O5 nanotubes, sputter deposition of Ir, followed by thermal dewetting and deposition of GOx.

References
[1] King, H.; Sicree, R.; Wild; Roglic, G.; Green, A. *Diabetes Care* **2004,** *27* (5), 1047-1053.
[2] The Diabetes Control and Complication Trial Research Group. *New England Journal of Medicine* **1993,** *329,* 997-1036.
[3] Irhayem, E. A.; Elzanowska, H.; Jhas, A. S.; Skrzynecka, B.; Birss, V. I. *J. Electroanalytical Chemistry* **2002,** *153,* 538-539.

Low Molecular Weight Chitosan Nanoparticulate System at Low N:P Ratio for Nontoxic Polynucleotide Delivery

M. Alameh, D. De Jesus, M. Jean, R.M Derbali, M. Benhammadi, C.Y. Chang, V. Darras, M. Thibault, M. Lavertu, M.D Buschmann, A. Merzouki

[1]Institute of Biomedical Engineering, Department of Chemical Engineering, Ecole Polytechnique de Montréal, Montréal, Canada

Keywords: Chitosan, siRNA, Non viral delivery systems, qPCR, Transfection efficiency

Chitosan, a natural polymer, is a promising system for the therapeutic delivery of both plasmid DNA and siRNA. Reports attempting to identify its optimal parameters for siRNA delivery were inconclusive with high molecular weight chitosan at high amine-to-phosphate ratio (N:P ratios) apparently required for efficient transfection. Here we show, for the first time, that low molecular weight chitosan (LMW-C) formulations at low N:P ratios are suitable for the *in vitro* delivery of siRNA. LMW-C nanoparticles at low N:P ratios were positively charged (ζ-potential ~ 20mV) with an average size below 100 nm as demonstrated by Dynamic Light Scattering and Environmental Scanning Electron Microscopy respectively. Nanoparticles were spherical, a shape promoting decreased cytotoxicity and enhanced cellular uptake. Nanoparticle stability was effective for at least 20h at N:P ratios above 2 in slightly acidic pH 6.5. At higher basic pH of 8 these nanoparticles were unravelled due to chitosan neutralisation, exposing their polynucleotide cargo. Cellular uptake ranged from 50% to 95% in three different cell lines as measured by cytometry. Increasing chitosan MW improved nanoparticle stability as well as their ability to protect the oligonucleotide cargo from nucleases at supraphysiological concentrations. The highest knockdown efficiency was obtained with the specific formulation 92-10-5 that combines sufficient nuclease protection with effective intracellular release. This system attained mRNA knockdown > 70%, similar to commercially available lipoplexes, without apparent cytotoxicity. Contrary to previous reports, our data demonstrates that LMW-C at low N:P ratios are efficient and non toxic polynucleotide delivery systems capable of transfecting a plethora of cell lines.

In vitro evaluation and physico-chemical characterization of low molecular weight chitosan-siRNA nanoparticles targeting the ApolipoproteinB: a feasibility study.

R.M Derbali, M. Alameh, M. Jean, C.Y Chang, M. Thibault, M. Lavertu, V. Lascau, M. Nelea, M.D. Buschmann, A. Merzouki.

[1]Institute of Biomedical Engineering, Department of Chemical Engineering, Ecole Polytechnique de Montréal, Montréal, Canada

Keywords: Atherosclerosis, Apolipoprotein B, Chitosan, siRNA, HepG2 cell line

Apolipoprotein B (ApoB) is mainly found in low density lipoproteins (LDL) and is an essential structural component of this biochemical assembly. LDLs are able to move high quantities of cholesterol to peripheral tissues. LDLs play key role in the initiation and preservation of atherogenic inflammation, since they accumulate in the arterial intimae activating the innate immunity and fueling the adaptive immunity. Therefore controlling ApoB gene expression is an interesting approach for the prevention of atherosclerosis. Chitosan, a natural cationic family of polymers of β-1,4 N-acetyl glucosamine and glucosamine, has already been successfully used for gene delivery[1-4]. Chitosan-siRNA-ApoB nanoparticle size and ζ-potential varied from 90 to 128 nm and 23 to 38 mV respectively depending on chitosan parameters. Chitosan-siRNA-ApoB nanoparticles were stable for at least 20 hours at pH 6.5 for N:P ratio above 2. At higher pH of 8, nanoparticles were unravelled at low N:P demonstrating the necessity of higher N:P ratios for increased stability. These nanoparticles were able to protect the nucleic acid cargo when challenged with extra-physiological concentration of nucleases with a clear indication of molecular weight dependence. *In vitro* evaluation of uptake efficiency was performed in three different cell lines using cytometry. Uptake efficiency ranged from 50-90% depending on the cell line. Gene knockdown efficiency was evaluated in the HepG2 using real time PCR (qPCR) and reached a twofold decrease in gene expression. These preliminary data indicate that siRNA delivery using chitosan is a promising approach for the potential treatment of atherosclerosis *in vivo*

References

1. Lavertu M, Methot S, Tran-Khanh N, *et al.* High efficiency gene transfer using chitosan/DNA nanoparticles with specific combinations of molecular weight and degree of deacetylation. Biomaterials 2006; **27**: 4815-4824.
2. Howard KA, Rahbek UL, Liu X, *et al.* RNA interference in vitro and in vivo using a novel chitosan/siRNA nanoparticle system. Mol Ther 2006; **14**: 476-484.
3. Liu X, Howard KA, Dong M, *et al.* The influence of polymeric properties on chitosan/siRNA nanoparticle formulation and gene silencing. Biomaterials 2007; **28**: 1280-1288.
4. Katas H, Alpar HO Development and characterisation of chitosan nanoparticles for siRNA delivery. J Control Release 2006; **115**: 216-225.

Chitosan-based nanoparticles for GLP-1 gene delivery and DPP-IV gene silencing of *in vitro* cell lines relevant to type 2 diabetes.

Jean M. , Alameh M., Chang C.Y., Thibault M., Lavertu M., Darras V., Nelea M., Lascau V., Buschmann M.D., Merzouki A.

Institute of Biomedical Engineering, Department of Chemical Engineering, École Polytechnique, P.O. Box 6079, Station Centre-ville, Montréal, Québec, Canada H3C 3A7

Keywords : Gene delivery system, siRNA, Chitosan, GLP-1, Dipeptidyl peptidase-4 (DPP-IV).

Glucagon like peptide 1 (GLP-1), an incretin hormone that regulates blood glucose level post-prandially, is used for the treatment of type 2 diabetes mellitus. However, native GLP-1 pharmacokinetics reveals low bioavailability due to degradation by the ubiquitous dipeptidyl peptidase IV (DPP-IV) endoprotease. In this study, the glucosamine-based polymer chitosan was used as a cationic polymer-based *in vitro* delivery system for GLP-1, DPP-IV resistant GLP-1 analogues and siRNA targeting DPP-IV mRNA. We found chitosans to form spherical nanocomplexes with these nucleic acids, generating two distinct non-overlapping size ranges of 141–283 nm and 68–129 nm for plasmid and siRNA, respectively. The low molecular weight high DDA chitosan 92-10-5 (degree of deacetylation, molecular weight and N:P ratio (DDA–Mn–N:P)) showed the highest plasmid DNA transfection efficiency in HepG2 and Caco-2 cell lines when compared to 80–10–10 and 80–80–5 chitosans. Recombinant native GLP-1 protein levels in media of transfected cells reached 23 ng/L while our DPP-IV resistant analogues resulted in a fivefold increase of GLP-1 protein levels (115 ng/L) relative to native GLP-1, and equivalent to the Lipofectamine positive control. We also found that all chitosan–DPP-IV siRNA nanocomplexes were capable of DPP-IV silencing, with 92–10–5 being significantly more effective in abrogating enzymatic activity of DPP-IV in media of silenced cells, and with no apparent cytotoxicity. The versatility of these specific formulations to deliver plasmid DNA and siRNA render their use promising as a combined in vivo therapy for the control of type 2 diabetes.

Novel, rapid and label-free assay format for proteases detection and drugs screening using various transducers.

Chiheb Esseghaier[1], Andy Ng[1], M. Zourob[1]*

[1]Institut national de la recherche scientifique, Centre – Energie Matériaux Télécommunication, 1650, Boul. Lionel Boulet, Varennes (Québec) J3X 1S2, Canada

Mots clés : HIV protease, label-free, detection

Proteases constitute one of the main classes of biomolecules which play a critical role in multitude of physiological processes and cellular metabolisms. Protease activity could be used as a biomarker and as a potential target for therapeutic intervention [1]. In this work, we designed a very simple, highly-stable and inexpensive assay format for proteases and drugs screening suitable for various transducers. Furthermore, the assay is label-free, highly-sensitive and does not need any washing steps/ liquids or surface blockage. We demonstrated the assay for HIV-1 protease detection and drugs screening. The developed assay was tested with impedance, surface plasmon resonance, localized surface plasmon resonance (LSPR) and lateral flow-assays.

The assay relied on anchoring a HIV-1 protease substrate peptide linked with magnetic bead to the N-terminal and immobilized to gold surface via the sulfhydryl side chain of cysteine at the C-terminal. We placed a permanent magnet at the edge of the sensing area to collect rapidly the cleaved magnetic beads. We recorded a significant shift in signal (SPR, LSPR, impedance) due to the release of the magnetic bead as a result of the cleavage of the immobilized peptides by the HIV-1 protease. The developed assay was able quantify HIV-1 protease inhibition activity of two commercial AIDS drugs candidates (Nelfinavir mesylate hydrate and Saquinavir mesylate) with acceptable accuracy. The developed sensing layer has the potential to perform analysis with real samples.

Different conditions were optimized such as bead size and material, incubation time, and peptide spacer linkers between the magnetic beads and gold surface immobilization site for various transducers. The detection limit was as low as 10 pg/ml of HIV protease with analysis time of a few minutes. We will also present various signal amplification mechanisms.

References

[1] López-Otín C, Matrisian LM.Emerging roles of proteases in tumour suppression. (2007) Nat. Rev. Cancer. 7(10) 800-808

A label-free Multiplexed impedance-based immunosensor for brain tumor biomarkers

R. Elshafey[1], A. Ng[1], C. Tlili[1], A. Abulrob[2], A. Tavares[1] *and M. Zourob[1]**

[1]*INRS Énergie, Matériaux et Télécommunications, Varennes, Quebec, Canada*
[2] NRC Institute for Biological Sciences, Ottawa, ON, Canada

Keywords: MDM2, EGFR, impedance, multiplexing, brain biomarkers

The presence of multiple biomarkers is very important in early detection and in the diagnosis of complex diseases such as cancer [1] for which the detection of a single maker is found to be inadequate. Screening can be improved by providing the information necessary for robust diagnosis at different disease stages. In particular, it allows reliable early stage detection and routine follow-up on the effectiveness of treatment. Glimoas are the most common primary human brain tumor; they represent about 1% of all cancers and 2.5% of all cancer deaths. There is increasing evidence that the different stages of brain tumor are developed through different pathways. Primary glioblastoma multiformae(GBMs) overexpress epidermal growth factor receptor (EGFR) and murine double minute2 (MDM2). Secondary GBMs exhibit platelet-derived growth factor receptors-α (PDGFR-α) overexpression. Therefore, the screenings of these biomarkers can provide simple tool for the the brain tumor classification into grades, and facilitates the diagnosis and prognoses. Herein we focus on the developing of an array of disposable gold electrodes for multiplexed detection of these biomarkers in brain tissue, by functionalizing gold surface with antibodies specific for these biomarkers. Our detection platform, a label-free impedimetric immunosensor, is highly sensitive and selective. The detection limit of the MDM2 and EGFR is as low as 1 pg/ml as shown in Figure (1, 2). We believe this multiplexed detection platform will provide a cost-effective, highly sensitive, easy and simple method of diagnosis and delivers prognostic information for brain tumor monitoring. Furthermore, this label-free electrochemical biosensor array has high potential for low-volume multi-analyte sensing capabilities along with high sensitivity for the instant diagnostic and personalized care.

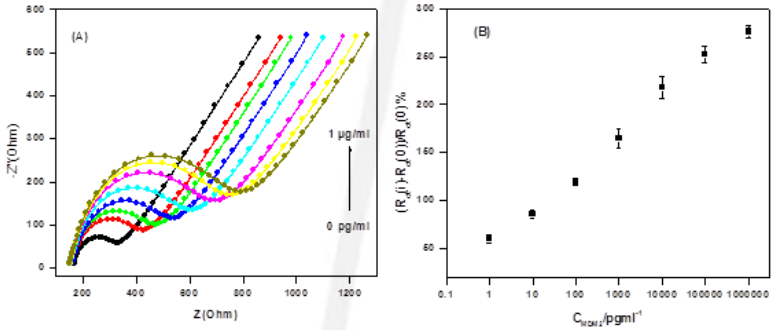

Figure 1 (A) Impedance response of the EA/Ab/Cys/Au modified electrode upon adding different concentrations of MDM2 protein from 0pg/ml-1µg/ml in 10mM $[Fe(CN)_6]^{4-/3-}$ at pH 7.4, (B) calibration plot corresponding to the increase of relative electron-transfer resistance ($\Delta R_{et}/R_{et}$ (0) % of the immunosensor with concentration of MDM2. Error bars show the standard deviation of three repetitive measurements.

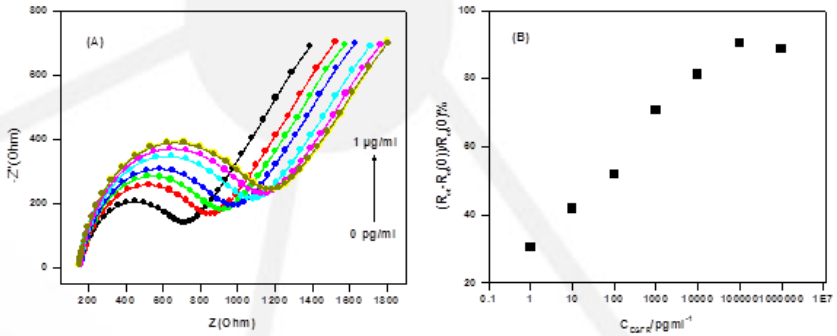

Figure 2 (A) Impedance response of the EA/Ab/Cys/Au modified electrode upon adding different concentrations of EGFR protein from 0pg/ml-1µg/ml in 10mM $[Fe(CN)_6]^{4-/3-}$ at pH 7.4, (B) calibration plot corresponding to the increase of relative electron-transfer resistance ($\Delta R_{et}/R_{et}$ (0) % of the immunosensor with concentration of EGFR.

References

[1] J.D. Wulfkuhle, L.A. Liotta, E.F. Petricoin, Proteomic applications for the early detection of cancer. Nat. Rev. Cancer 3, 267–275, 2003.

Characterization by continuous flow magnetophoresis of therapeutic microcarriers relying on embedded nanoparticles to allow navigation in the vascular network

G. Vidal[1], S. Martel[1]

[1] Department of Computer and Software Engineering, NanoRobotics Laboratory, Ecole Polytechnique de Montreal (EPM), P.O. Box 6079, Station Centre-ville Montreal, Canada, H3C 3A7

Keywords: magnetic nanopartciles, magnetophoresis, targeted drug delivery

Magnetic Resonance Navigation (MRN) is an approach in which magnetic untethered entities are navigated through the vascular network by inducing a propelling force on nanoparticles embedded in microcarriers using an upgraded Magnetic Resonance Imaging (MRI) scanner in order to reach specific regions through the vascular network. The magnetic movement of such particles under the influence of a magnetic gradient is called magnetophoresis and is usually used as a technique for separation of microparticles, because magnetophoretic velocity depends on the size and the corresponding magnetic susceptibility; then particles with different magnetic characteristics will show different deflection patterns when subject to a given magnetic gradient and a given fluid flow. For proper MRN operations, it is fundamental to have reliable data on magnetophoretic velocity (i.e. deflection pattern) for a given diagnostic or therapeutic entity. Furthermore, magnetic aggregation during MRN is unavoidable and will most likely result in different magnetophoretic velocities. This work presents a preliminary design to perform magnetophoretic velocity measurements in the bore of a clinical MRI scanner. A suspension of microcarriers of 40 µm in diameter is pumped into a microfluidic chamber. Video analysis is performed to evaluate the effect of the flow rate on the deflection of magnetic particles and magnetic aggregations.

References

[1] N. Pamme, A. Manz. On-Chip Free-Flow Magnetophoresis: Continuous Flow Separation of Magnetic Particles and Agglomerates, Analytical Chemistry, Vol. 76, No. 24, 2004.
[2] J.B. Mathieu, S. Martel. Aggregation of magnetic microparticles in the context of targeted therapies actuated by a magnetic resonance imaging system, Journal of Applied Physics, Vol. 106, Issue. 4, 2009.
[3] S. Martel, M. Vonthron. Interactive System for Medical Interventions Based on Magnetic Resonance Targeting, The Fourth International Conference on Advances in Computer-Human Interactions, ACHI 2011.

Logiciel de navigation de cathéter magnétoguidé

B.Conan, S.Martel

Laboratoire de Nanorobotique, Ecole Polytechnique de Montréal, Département de Génie Informatique, Pavillon Lassonde, local M-4505 2500, Chemin de Polytechnique Montréal, Qc, Canada, H3T 1J4

Mots clés : nanorobotique, biomédical logiciel, navigation

L'un des grands défis de la médecine moderne, est le traitement du cancer. Le laboratoire de Nanorobotique de l'école Polytechnique travaille au développement d'une nouvelle méthode permettant de cibler les tumeurs afin d'y délivrer directement les substances thérapeutiques, permettant de ce fait d'utiliser des concentrations plus élevées de médicament tout en limitant leur toxicité secondaire. Cette technique repose sur la navigation de particules ferromagnétiques encapsulant le médicament, dans un IRM. Afin d'acheminer les particules le plus près possible des tumeurs, elles passent dans un cathéter, lui-même doté d'un embout spécialement conçu[1] pour être guidé magnétiquement à l'intérieur des vaisseaux sanguins à l'aide de la même plateforme. Afin de pouvoir effectivement déplacer le cathéter dans les bifurcations souhaitées lors d'une opération, il est nécessaire de mettre en place une architecture logicielle[2] adaptée aux contraintes d'une application clinique, permettant de contrôler la navigation du dispositif. Cela passe d'abord par la mise en place d'une cartographie en 3D des vaisseaux sanguins, à partir d'une angiographie IRM, permettant d'extraire les données géométriques qui nous intéressent, puis par le développement d'une interface de guidage ergonomique, destinée au personnel soignant. Nous traiterons dans cette affiche de la construction du protocole d'imagerie et de l'interface logicielle intégrée à cette plateforme innovatrice.

Références

[1]Lalande V., Gosselin F.P. and Martel S., "Catheter Steering Using a Magnetic Resonance Imaging System", 32nd Annual International Conference of the IEEE Engineering in Medicine and Biology Society, August31 - september4, Buenos Airos, Argentina, EMBC 2010.

[2] Chanu A., Felfoul O., Beaudoin G., and Martel S. "Adapting the software platform of MRI for the real-time navigation of endovascular untethered ferromagnetic devices," Magnetic Resonance in Medicine, vol. 59, no. 6, June 2008, p 1287-97

3-D reconstruction of microvasculature using magnetic resonance images of superparamagnetic nanoparticles

N. Olamaei, F.Cheriet and S.Martel

Ecole Polytechnique Montreal

Key words: MRI contrast agents, superparamagnetic nanoparticles, susceptibility artifact

In MRI, supeparamagnetic nanoparticles induce a perturbation in the local magnetic field homogeneity in a much larger scale than their real size. If the degree of the distortion reaches the size of a typical clinical MRI pixel, the particle becomes visible in an MR image in the form of a signal loss. While the ability to visualize microvasculature using clinical imaging modalities remains to be improved, this concept initiates an approach for micro-vasculature visualization using biodegradable microparticles encapsulating magnetic nanoparticles [1] .In a previous study, we showed that a single 15 μm diameter microsphere with high susceptibility can be shown in MR images of a clinical scanner [2]. In the current study, a numerical simulation is used to simulate the 3D reconstruction of microvasculature using magnetic nanoparticles. The field induced by sphere magnetic particles can be approximated by that of a dipole:

$$\vec{B}(\vec{r}) = B_0\hat{z} + \frac{\mu_0}{4\pi}\left(3\frac{(\vec{m}.\vec{r})\hat{r}}{r^5} - \frac{\vec{m}}{r^3}\right)$$

Magnetic microparticles were released in an unknown simulated microvasculature network (Figure 1). The microparticles were scanned in different slices and at time intervals equal to the temporal resolution of the system. The slice with the highest signal loss represented the position of a particle on the Z-axis (Figure 2). By recording the X, Y, and Z coordinates of the particles, points were generated to reconstruct their travel trajectory through different bifurcations. The trajectories were assembled to build up a 3D distribution of the local microvasculature network. The final image was registered with the reference scan. The average error was found to be 0.6 *mm*.

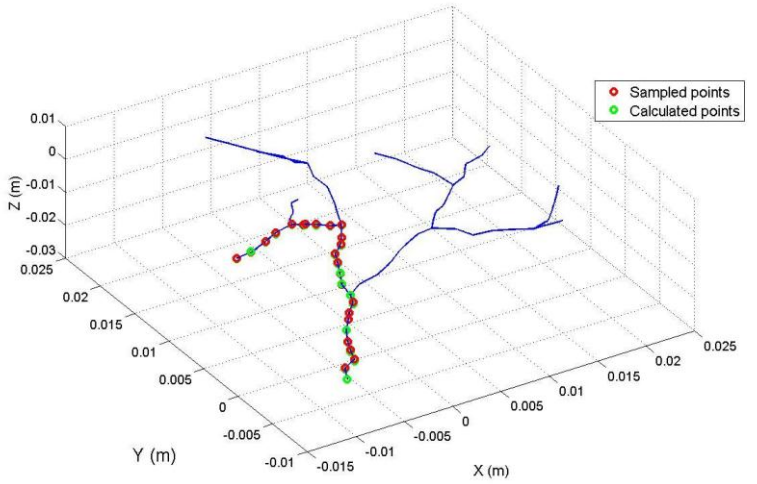

Figure 1 – Calculated points are superimposed on real points on 3D simulated vascular network

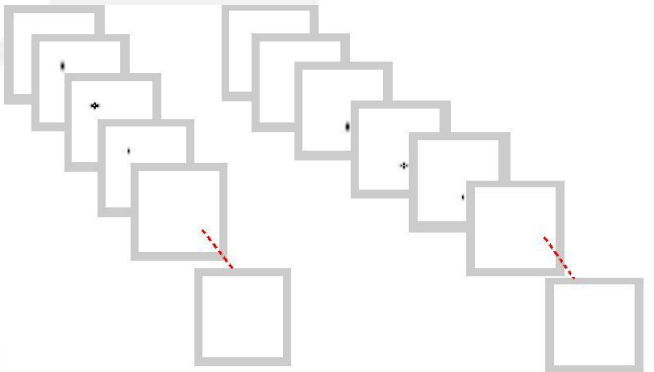

Figure 2 – Coronal image slides at two different acquisitions.

References

[1] P. Pouponneau*, et al.*, *Biomaterials,* vol. 30, pp. 6327-6332, Nov 2009.

[2] N. Olamaei*, et al.*, *Conf Proc IEEE Eng Med Biol Soc,* vol. 2010, pp. 4355-8, 2010.

Navigation d'un embout de fil-guide magnétique par une plateforme IRM modifiée

M. Vonthron[1], V. Lalande[1], B. Conan[1], C. Tremblay[1], S. Martel[1]*

[1]Laboratoire de Nanorobotique, École Polytechnique de Montréal, Montréal, QC, Canada

Mots clés : navigation magnétique, thérapie ciblée, imagerie interventionnelle, microrobotique médicale

Nous guidons un fil-guide muni d'un embout ferromagnétique de 0.9mm de diamètre afin de permettre une cathéterisation améliorée en Imagerie par résonance magnétique (IRM), sans recourir à des techniques d'imagerie ionisantes. La navigation du fil-guide est assurée par une plateforme de guidage logicielle et matérielle ajoutée à un IRM clinique qui permet au praticien de voir la position de son fil-guide et de le guider à l'aide d'une force magnétique. Cette force de guidage magnétique est produite par des bobines de gradients additionnelles portant l'amplitude de gradients magnétique atteignables à 400mT/m au lieu de 40mT/m sans affecter les autres composantes de l'IRM.
À ce système est adjoint un algorithme de positionnement en IRM par sélection hors résonance du dispositif avec une précision de 0.6mm. La position du dispositif est superposée avec une reconstruction 3D du modèle vasculaire afin de suivre le déplacement du fil-guide sur une carte vasculaire. Quatre lapins sont utilisés pour montrer l'efficacité de l'ensemble de la plateforme. Le fil-guide est guidé magnétiquement avec succès dans les artères rénales droite et gauche ainsi que dans l'artère mésentérique supérieure. La localisation de l'embout est fiable et est confirmée par une méthode d'imagerie classique. Cette plateforme à l'amplitude magnétique hors du commun ouvre la voie à une navigation de dispositifs thérapeutiques aussi petits que 50µm, permettant une libération de médicaments au plus près des zones ciblées.

Enchantement of Surface Plasmon Resonance Biosensors using Gold Nanocubes

A. Abumazwed[*1], *A. Kirk*[1]

Department of Electrical and Computer Engineering, McGill University, McConell, 606, 3480 University Street, Montreal, Quebec, H3A2A7

Key words: Gold nanorods, Surface Plasmon Resoance, Aspect ratio

We present a study of gold nanocubes and their optical properties. These nanocubes are compared to nanorods in terms of plasmonic properties. Both the nanocubes and the nanorods should have the same volume and the same aspect ratio for the sake of comparison. The Finite Difference Time Domain (FDTD) method is used for the study of optical properties using OptiFDTD package.
The gold nanocubes have an enhanced local electric field at the corners and the extinction is also increased if compared to two nanorods with the same spacing. This can be useful in many applications such as biosensors. Both the nanorod and the nanocubes have the same volume and aspect ratio (AR=1.5). As can be shown in Figure (1), the Longitudinal Surface Plasmon Resoance (SPR) is increased whereas for the nanocylinders is not affected.This enhancement is more pronounced in the case of transverse SPR as shown in Figure 2 where the incident E field is horizontally polarized. The effect of spacing between the two nanocubes is also shown in Figure 2. The optimum spacing is 10 nm for the two nanocubes as it corresponds to the highest resoance obtained. For nanorods with the same spacing, it can be noticed that they have less resonance than that of gold nanocubes.

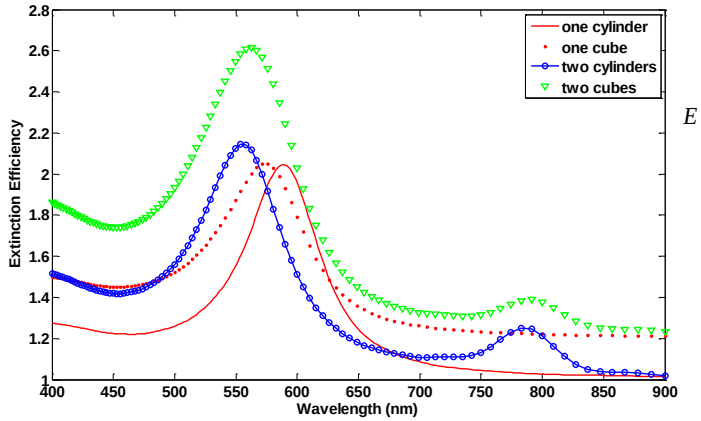

Figure 1 – Improved LSPR, Longitudinal Mode

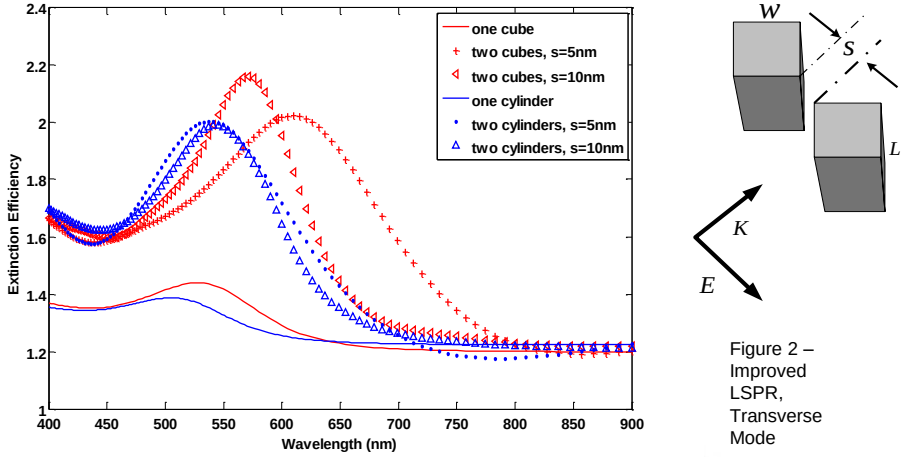

Figure 2 – Improved LSPR, Transverse Mode

In Situ Health Monitoring of Adhesively Bonded Joints during Fatigue Using Carbon Nanotube Network

Roham Mactabi[*1], Iosif D. Rosca[1], and Suong V. Hoa[1]*

Concordia University, Department of Mechanical and Industrial Engineering

Keywords : nanotube, fatigue, adhesive joint

Adhesive joints have widespread applications in aerospace and automotive industries, but predicting catastrophic failures during dynamic loads is very difficult due to the inaccessibility of the bonded interface. We have developed a new technique based on carbon nanotube (CNT) sensors that can monitor the bond integrity and is capable to predict failure well in advance. The conductive network inside the adhesive is very sensitive to crack initiation, propagation and delamination, therefore in-situ measurement of the bond resistance is capable of recording events that lead to failure. In 90% of the samples the change in bond resistance remains below 10% of the initial value up to approximately 80% of the fatigue life, and then the resistance increases rapidly due to crack propagation and interfacial delamination. As the increase in resistance typically occurs over a few hundreds to thousand cycles it is possible to define a resistance that corresponds to a safety limit before catastrophic failure. Moreover, the addition of 1 wt% MWCNTs inside the adhesive increased the joints shear strength and fatigue life by 10% and 20% respectively. The decrease in electrical resistance due to addition of only 0.5 wt% was more than 7 orders of magnitude.

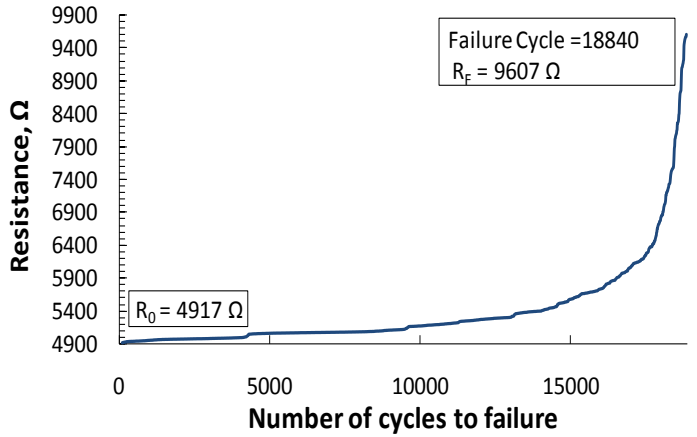

Figure 1 – Electrical resistane signature for single lap joint with 0.5wt% MWCNTs

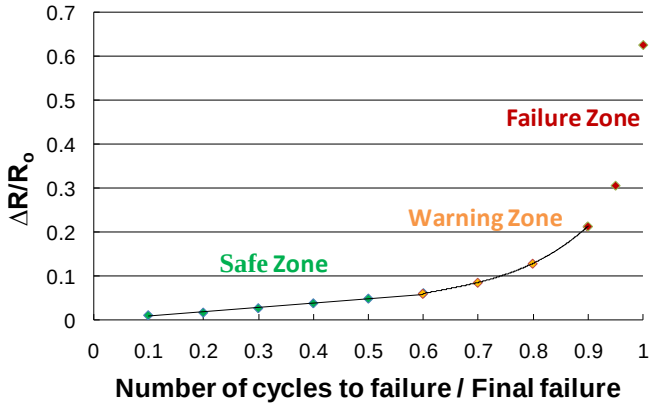

Figure 2 – Average electrical resistance signature for single lap joints with 0.5 wt% MWCNTs

Références

[1] S.G. Prolongo, M. Gude, J. Sanches, A. Urena. 2009. “Nano Reinforced Epoxy Adhesives for Aerospace Industry,” The Journal of Adhesion, 85(4-5):180-199.

[2] Yi-Ming Jen, Chih-Wei Ko. 2010. “Evaluation of Fatigue Life of Adhesively Bonded Aluminum Single-Lap Joints using Interfacial Parameters,” International Journal of Fatigue, 43(1-2):330-340.

[3] Erik T. Thostenson, Tsu-Wei Chou. Carbon Nanotube Networks: Sensing of Distributed Strain and Damage for Life Prediction and Self Healing. Adv. Mater., 2006, Vol. 18, p. 2837:2841.

Nanosondes SERS basées sur des nanoparticules d'alliage or-argent produites par laser femtoseconde

D. Rioux[*1], *S. Osseiran*[1], *S. Besner*[1], *N. Tam*[2], *I. Auberach-Ziogas*[2], *A. Albanese*[2], *A. Lee*[2], *G. Zheng*[2], *E. Kumacheva*[2], *W. Chan*[2], *M. Meunier*[1]

[1]École Polytechnique de Montréal, 2500 chemin de Polytechnique, Montréal, Québec, Canada, H3T 1J4
[2]University of Toronto, 27 King's College Circle, Toronto, Ontario, Canada, M5S 1A1

Mots clés : nanoparticules, SERS, alliage, champ sombre, biocompatibilité

Les nanosondes Raman basées sur les nanoparticules (NPs) plasmoniques constituent un nanomatériau très prometteur pour la détection du cancer. Les NPs sont marquées à l'aide d'un colorant Raman et ensuite fonctionnalisées pour s'attacher à des récepteurs spécifiques de cellules cancéreuses. La majorité des travaux de recherche utilisent des NPs d'or en raison de son excellente biocompatibilité. Toutefois, il est bien connu que l'argent possède de meilleures propriétés plasmoniques que l'or. Son utilisation pour des applications biomédicales est cependant incertaine en raison de sa toxicité potentielle. Nous proposons d'utiliser des NPs d'alliage or/argent produites par ablation laser femtoseconde. Cette approche devrait permettre le meilleur des deux mondes avec des NPs ayant un meilleur signal Raman que l'or et une meilleure biocompatibilité que l'argent. Ces nanoparticules ouvrent également la voie à l'imagerie multiplexée par la microscopie en champ sombre. Nous fabriquons les NPs d'alliage par ablation laser femtoseconde en milieu liquide. La taille des nanoparticules (10 à 40 nm) dépend des paramètres laser, de la concentration des NPs ainsi que de l'usage d'agents stabilisants. La composition des alliages est contrôlée par la quantité d'or et d'argent utilisée lors du processus d'alliage. L'amplification du signal Raman pour divers colorants (Crystal Violet, Malachite Green, Rhodamine 6G) adsorbés à la surface des NPs est mesurée et comparée à une modélisation théorique. Dans les deux cas, on observe que le signal SERS des NPs d'alliage peut être jusqu'à 10 fois plus élevé que celui de l'or pur, selon la longueur d'onde d'excitation. Nous avons également effectué des mesures de cytotoxicité *in vitro* afin d'évaluer la biocompatibilité des NPs d'alliages.

Molybdophosphate d'ammonium immobilisé sur silice mésoporeuse pour l'adsorption sélective du radiocésium en milieu aqueux

Solange Schneider, Adriana Caldas Garcez, Mélodie Tremblay, Freddy Kleitz, Dominic Larivière**

Département de Chimie, Université Laval, Québec, G1V0A6, QC, Canada
*E-mail: freddy.kleitz@chm.ulaval; Dominic.Lariviere@chm.ulaval.ca

Mots clés : silice mésoporeuse, radiocésium, hétéropolyacide

Les sources de radiocésium (135,137Cs) sont utilisées commercialement dans les domaines médicaux et industriels. Il existe plusieurs méthodes, telle la spectroscopie-γ, permettant de détecter de faibles concentrations de Cs-137. Cependant, l'analyse du ratio 135Cs/137Cs, qui permet de caractériser la source, ne peut être obtenue que par spectrométrie de masse[1], et seulement si l'élément a été préalablement séparé chimiquement. Cette étude porte sur la séparation du Cs+ par l'utilisation d'adsorbants à base d'ammonium molybdophosphate (AMP), sel connu pour être sélectif au Cs+, supportés sur silice mésoporeuse. Les silices mésoporeuses permettent d'augmenter la surface de contact avec l'échantillon et de stabiliser l'échangeur de cations pour des perspectives de régénération. La technique se révèle efficace et permet d'isoler sélectivement le Cs+ dans une matrice aqueuse. L'analyse du Cs+ est effectuée par ICP-MS. Synthèse et caractérisation des adsorbants et résultats d'adsorption de Cs+ seront présentés.

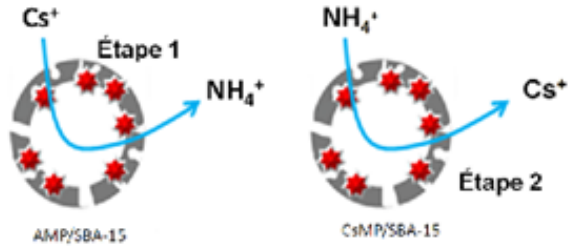

Figure 1: Procédé d'échange Cs^+-NH_4^+

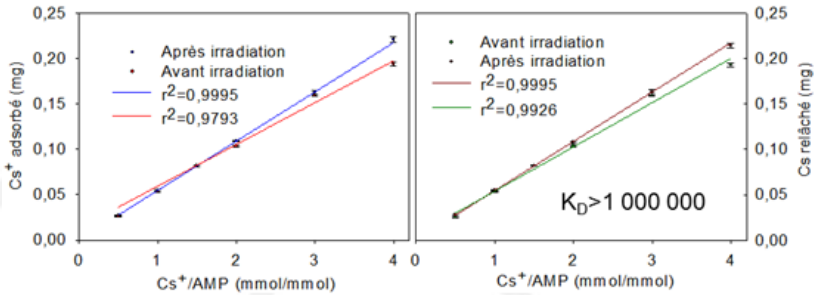

Figure 2: Adsorption et élution du césium en fonction du ratio Cs/AMP avant et après irradiation-γ

Références
[1] a) V.F. Taylor, V.F.; Evans, R.D.; Cornett, R.J., J. Env. Radioact. 2008, 99, 109. b) Caruso, S.; Gunther-Leopold, I.; Murphy, M.F.; Jatuff, F.; Chawla, R., Nucl. Instr. Meth. Phys. Res. A 2008, 589, 425.
[2] Gaur, S., J. Chrom.-A 1996, 733, 57.
[3] Epov, V.N., Larivière D., Reiber K.M., Evans R.D., Cornett R.J., J. Anal. At. Spectrom. 2004, 19, 1225.

Atomic Force Microscopy tools for Biology

Monserratt Ayon[1,2], Stella Xing[1,2], Matthew Rigby[1], MegumiMori[3], Sarah Perez[1,2], Margaret Magdesian[4,5], Svetlana Komarova[2], David Colman[4,5] and Peter Grütter[2,3]

[1]Department of Physics, McGill University, Montreal, Quebec H3A 2T8, Canada.
[2] Dentistry Department, McGill University, Montreal, Quebec H3A 0C7, Canada.
[3]Program in NeuroScience, McGill University, Montreal, Quebec H3A 2B4, Canada.
[4]Program in NeuroEngineering, McGill University, Montreal, Quebec H3A 2B4, Canada.
[5]Montreal Neurological Institute and Hospital, McGill University, Montreal, Quebec H3A 2B4, Canada.

Key words: AFM, mechanotransduction, cell-injury, microfluidics, SNOM

In the Bio AFM group we combine AFM with various modalities of optical microscopy technique to study and manipulate live cells under physiological conditions. Micro-damage of bone tissue is known to regulate bone turnover. Single cells were mechanically stimulated by AFM indentation leading to membrane deformation, or micro-injury. We found qualitative differences in calcium responses as a function of loading forces. This suggests that cell micro-injury can play an important role in linking bone tissue micro-damage and stimulation of bone remodeling. Extracellular ATP is a known signaling mediator among bone cells. We assumed that ATP is released from the stimulated cell in an amount proportional to the extent of the injury to mathematically model the signaling cascade, thus providing new insights into cell-cell communication. Different types of insults can trigger axonal degeneration in the central and peripheral nervous system. Using AFM nano-compression techniques and microfluidics we evaluated the mechanical response of individual neuronal axons, the reversibility of the damage and the three dimensional aspects of neurons undergoing compression. Elucidating the specific mechanisms that initiate axonal degeneration open up new avenues to improve safety equipment design, injury diagnosis and to identify ways to protect and regenerate axons. Scanning Near Field Optical Microscopy (SNOM), used in combination with AFM provides a powerful method to examine the dynamics of proteins in a cell We have developed a combined AFM/SNOM system for operation in liquids without compromising sensitivity due to increased damping. We demonstrate this by observing the layering of water above a surface.

CONFÉRENCE NANOQUÉBEC 2012

Micro-nano systèmes

HYATT REGENCY, MONTRÉAL

www.nanoquébec.ca

Effects of Grain Size and Frequency on Internal Friction in Nanocrystalline Thin Films and Nanowires of Aluminum

K. Das[1], D. Almecija[1], G. Sosale[1], S. Vengallatore[1]*

[1]Department of Mechanical Engineering, McGill University, Montréal, Canada

Mots clés : microelectro-mechanical systems (MEMS), performance, nanomaterials, internal friction

Measuring internal friction in ultrathin films and nanowires can provide useful insight into the effects of scale on their mechanical behavior and guide the design of high-Q micro/nanomechanical resonators. Using a single-crystal silicon microcantilever platform [1] that calibrates dissipation against the fundamental limits of thermoelastic damping, we have measured the effects of grain size and frequency on internal friction at room temperature in sputtered thin films of aluminum with thickness of 60 nm and 120 nm. Internal friction in 100 nm thick films reduced by a factor of 2.5 when the average grain size increased from 90 nm to 390 nm, suggesting that grain-boundary sliding contributes significantly to dissipation in these films. For constant film thickness and grain size, internal friction reduced monotonically by a factor of two as the frequency increased from 50 Hz to 50 kHz. Using the same platform, we also measured internal friction in nanowires of aluminum that were patterned at the root of the microcantilevers using electron-beam lithography. The thickness of these polycrystalline nanowires ranged from 50 nm to 100 nm, and their width from 118 nm to 396 nm. These nanowires were patterned in arrays with center-to-center spacing of 1 micrometer. Internal friction in the nanowires was essentially the same as in the thin films for frequencies ranging from 6.5 kHz to 24.5 kHz, suggesting that lateral confinement does not significantly affect dissipation in aluminum. The details of these measurements, and their implications for the mechanisms of internal friction in nanomaterials, will be presented.

Références

[1] G. Sosale, S. Prabhakar, L. Frechette and S. Vengallatore, J. Microelectromechanical Systems, vol. 20, pp. 764-773 (2011).

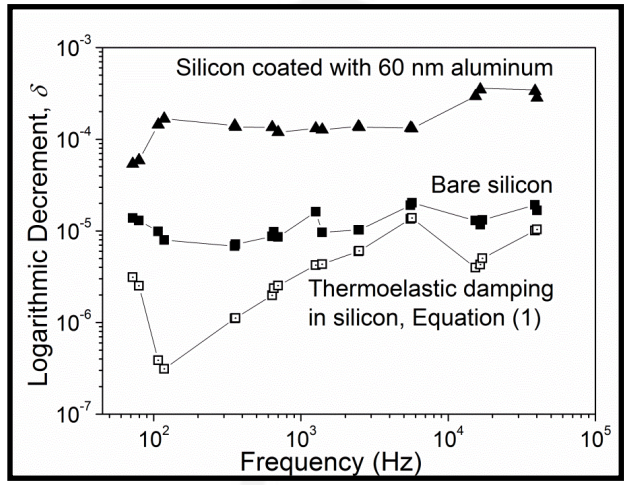

Figure 1 – Frequency dependence of damping at room temperature in bare silicon microcantilevers and in silicon microcantilevers coated with 60 nm thick films of aluminum.

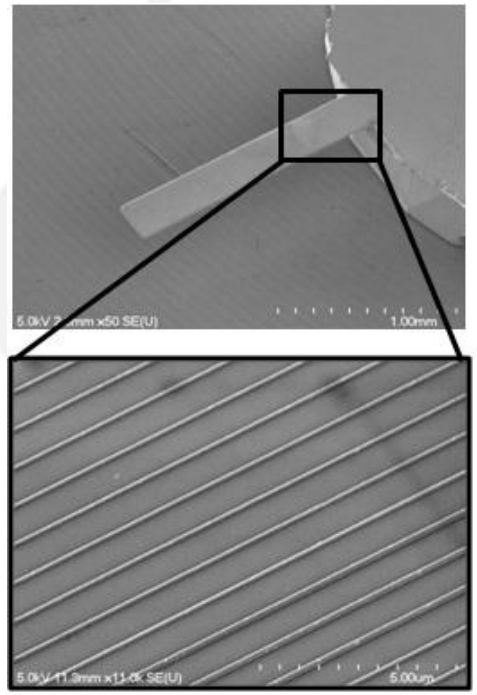

Figure 2 – A silicon microcantilever with an array of aluminum nanowires patterned at the root of the microcantilever.

Non-volatile single electron memory using a floating nanogate approach

M. Guilmain[*1], W. Xuan[2], J.-F. Morissette[1], S. Ecoffey[1], A. Beaumont[2], D. Drouin[1]*

[1]Centre de Recherche en Nanofabrication et Nanocaractérisation, Université de Sherbrooke, Canada, J1K 2R1.
[2]Institut des Nanotechnologies de Lyon, INSA de Lyon, F-69621Villeurbanne cedex France.

Key words: single electron memory simulation, retention time, write/erasing time

Metallic Single Electron Transistors (SETs) are devices that exhibit a high potential for future electronic circuits because of their power efficiency and their stacking capability which enables their integration in 3D high density circuits. A SET consists of an island separated from two electrodes (source and drain) by tunnel junctions. A voltage applied on a third electrode (gate) can inhibit the Coulomb Blockade Effect (CBE) and modulate the drain current.

The approach to fabricate a single electron memory (SEM) is to add a floating gate between the island and the gate of a SET. Charging the floating gate is done from the island (or from the gate) through a Fowler-Nordheim (FN) process. The gate voltage will control the number of charge in the memory point. Figure 1 presents a SEM electrical schematic.

Figure 2 shows that the presence of an electron on the floating gate changes the threshold voltage of the SET by shifting the ID-VG characteristics. This simulation was performed with MARSSEA [1] at 300 K. The source and drain junctions are 8 nm-thick TiO2 giving a capacity of 0.06 aF, FN junction is 5.5 nm-thick HfSiO4 giving a capacity of 0.35 aF and CG = 2 aF. The change of the threshold current can be used to develop a memory architecture based on this device.

The capacity control of the FN junction and the choice of dielectrics for SEM fabrication is a big challenge. Simulations show that the speed and the retention time of such SEMs make them potential competitors for both DRAM and hard drives.

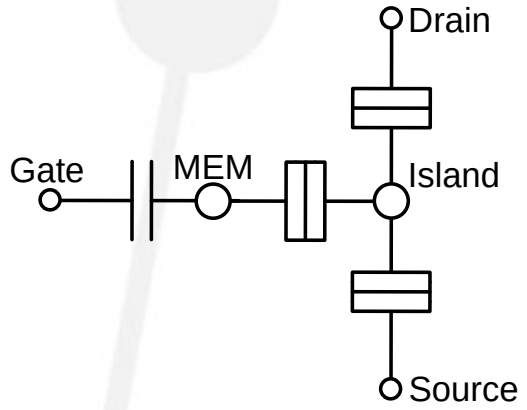

Figure 1 – SEM electrical schematic

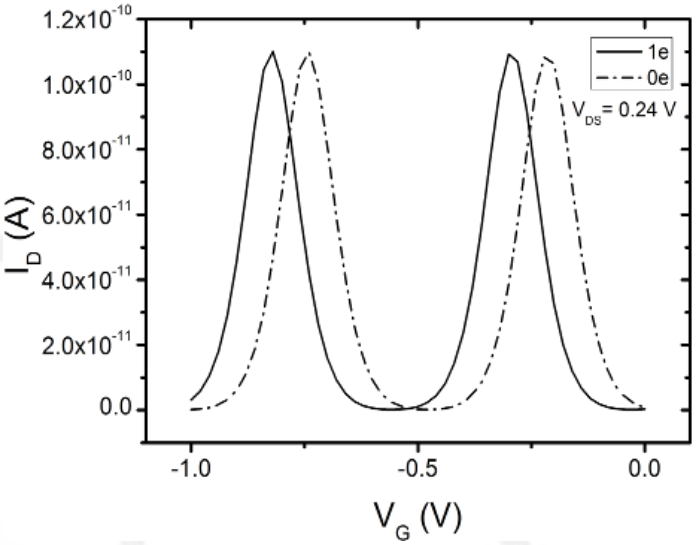

Figure 2 – MARSSEA simulation of SEM ID-VG curves with and without an electron on the floating gate.

References
[1] A. Beaumont, PhD thesis, INSA-Lyon (2005).
[2] C. Dubuc et al., Solid-State Electronics, vol. 53, (2009), page 478.

Nanoscale Characterization of Silicon-based Negatives Electrodes for Lithium-ion Batteries by Electron Energy Loss Spectroscopy and Transmission Electron Microscopy

M. Gauthier [1,2], P. Moreau[2], D. Mazouzi[2], B. Lestriez[2], L. Roué[1] and D. Guyomard[2]*

[1]INRS-Énergie, Matériaux et Télécommunications, 1650 boulevard Lionel Boulet, Varennes, Québec, Canada, J3X 1S2
[2]Institut des Matériaux Jean Rouxel, UMR 6502 CNRS – Université de Nantes, 2 rue de la Houssinière, BP 32229, 44322 Nantes Cedex 03, France

Keywords: Li-ion batteries, Si-based negative electrode, TEM, EELS

The development of both hybrid electric vehicles (HEV) and all-electric vehicles (EV) requires batteries with higher energy and power densities to compete with heat engines. One way of improvement of battery performance is through the development of new electrode materials. In the case of Li-ion batteries, silicon is a promising alternative to graphite anode, as its theoretical specific capacity is about ten times higher than that of graphite. Nevertheless, the use of Si is compromised by a ~280% volume expansion which generates a large capacity fade during cycling [1]. In order to better understand the failure mechanisms taking place in these electrodes, advanced characterization tools must be developed. For this purpose, Transmission Electron Microscopy (TEM) and Electron Energy Loss Spectroscopy (EELS) are promising techniques in the characterization of lithium batteries materials at the nanometric scale [2]. In this work, we studied by TEM/EELS composite electrodes containing nano-sized Si, carbon and a binder (carboxymethylcellulose), prepared in a buffer solution at pH 3 and at pH 7 [3]. The aim of this study is to have a better understanding of the interaction between the different electrode components and to highlight the key role of the pH in this interaction. The TEM-EELS technique offers precise information on the morphology and on the nanoscale composition of the composite electrode, as illustrated in Figure 1.

References
[1] J.-S. Bridel, T. Azais, M. Morcrette, J.-M. Tarascon and D. Larcher, *Chem. Mater*., **22**, 1229 (2010).
[2] J. Danet, T. Brousse, K. Rasim, D. Guyomard and P. Moreau, *Phys. Chem. Chem. Phys*., **12**, 220 (2010).
[3] D. Mazouzi, B. Lestriez, L. Roué and D. Guyomard, *Electrochem. Solid-State Lett*., **12**, A215 (2009).

a)

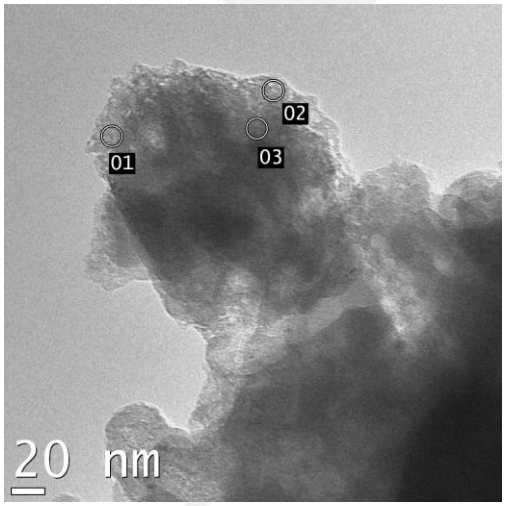

b)

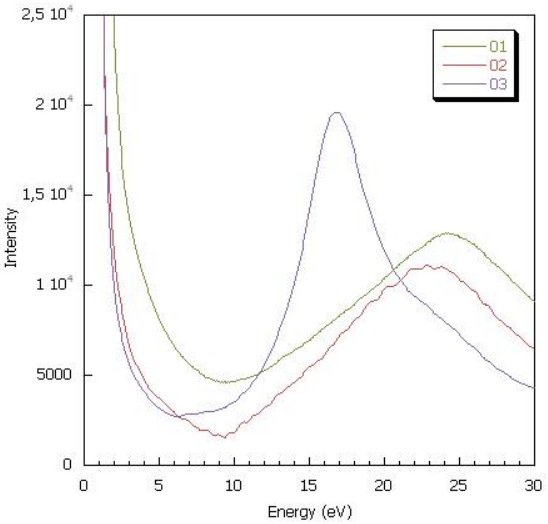

Figure 1 – (a) Post-mortem TEM image of a Si-C-CMC electrode prepared in buffered solution at pH 3. (b) Low-energy loss spectra obtained on the areas labeled 1, 2 and 3.

Design, synthesis and characterization of C_{60} derivative as *n* type materials

*Antoine Lafleur Lambert, Simon Rondeau-Gagné, Jean-François Morin**

University Laval 1045, avenue de la Médecine, Pavillon Alexandre-Vachon, Québec (Québec) G1V 0A6, Canada.

Mots clés : Energy, Fullerene (C_{60}), Photovoltaics

To achieve long term development and preservation of the environment, considering a renewable energy source such as solar energy is particularly interesting. Organic plastics and small molecules photovoltaïcs devices are at the center of interest of many research groups seeking to improve and complete the energetic contribution offered by inorganic solar cells. Such devices are made from an electron giving (*p* type) conjugated polymer and an electron accepting (*n* type) compound, usually a fullerene C_{60} derivative. These two mixed together form the active layer of the bulk-heterojunction solar cells as bicontinuous phases wherein charges are generated at the phases interfaces. The *p* type hereafter transports electron holes and the *n* type transports electrons throughout the device.PCBM[1] (phenyl-c61-butyric methyl ester) a soluble and commercially available compound is considered the standard[2] accepting moiety. However, PCBM is not necessarily the optimal acceptor for every kind of p-active polymer. Therefore, research is underway at the Fonctionals Organics Materials Laboratory, directed by Prof. Jean-François Morin, to design and synthesize better electron accepting compounds. A first series was synthesized to modulate the electronic properties of the fullerene. Through this modulation we aimed to increase the electronic level of the LUMO therefore enhancing the open-circuit current (V_{oc}). The V_{oc} is one of the parameters responsible for the efficiencie of photovoltaïcs devices[3]. This series consist of fullerene derivatives bearing a phenylalkoxy group atttached through an alkynyl bond. Subsequently, a secondary group is attached to the fullerene, this group brings further modulation.A second type of derivative was synthesized using a monosubstituted and unsymmetrical diketopyrrolopyrrole (DPP) moiety. This compound should allow photogeneration of electrons by the electron acceptor in the device, thus enhancing the general efficiency of the device by creating more charges.

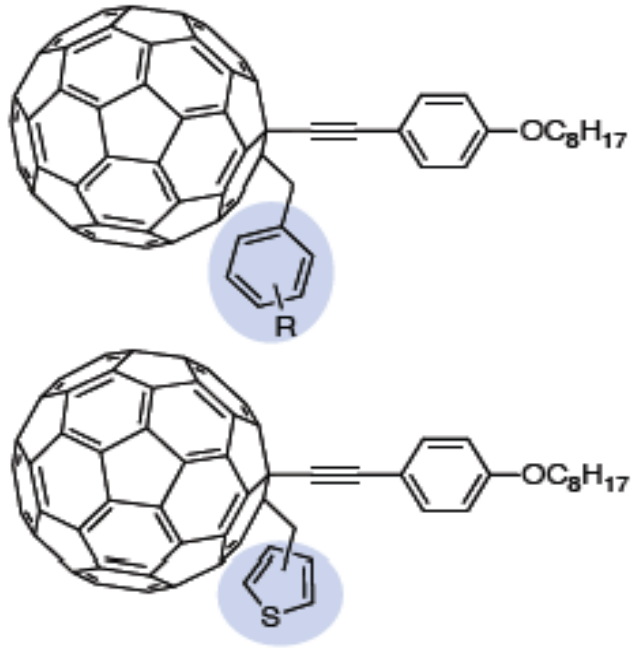

Figure 1: C_{60} derivatives with different LUMO energy level.

Références
1.Jan C. Hummelen, Brian W. Knight, F. LePeq, Fred Wudl, Jie Yao, Charles L. Wilkins J. Org. Chem., **1995**, 60 (3), pp 532–538]
2.L. Zheng, Q. Zhou, X. Deng, M. Yuan, G. Yu, Y. Cao, *J. Phys. Chem. B.* **2004**, *108*, 11921-11926
3.B. C. Thompson, J. M. J. Fréchet, *Angew. Chem. Int. Ed.* **2008**, *47*, 58-77.

Single Electron CMOS-Like One Bit Full Adder

D. Griveau[1], S. Ecoffey[1], R. M. Parekh[1], M. A. Bounouar[1,2], F. Calmon[2], J. Beauvais[1], D. Drouin[1]

[1]3IT, Université de Sherbrooke, Sherbrooke, QC, Canada; [2]Lyon Institute of Nanotechnology, University of Lyon, INSA-Lyon, F-69621 Villeurbanne Cedex, France.

Mots clés : Energy efficiency, full adder, single-electron transistor, hysteresis.

Since two decades, single electron transistors (SETs) have been seen as very good candidates for the future of low power electronics [1]. While SET logics have been theoretically demonstrated [2] and proved their fundamental capabilities for computation, SET building blocks, like one-bit full adder (FA) cell could be integrated with CMOS logic. Hybrid SET-CMOS FAs and SET-FAs [3] simulation studies were already made in order to evaluate and compare their performance and energy efficiency with low power CMOS. In this paper, the SET-FA is implemented in a logic called static CMOS-like SET logic. Existing CMOS transistor-based designs can easily be ported to this technology. In most of systems the adder is part of the critical path that determines their overall performance. This is why enhancing the performance of the 1-bit full-adder cell is a significant goal. To increase the energy efficiency, a hysteresis (H) operating mode [4] is implemented in our SET-FA. Moreover, serial and parallel SET designs are introduced to improve our SET-FA characteristics. The serial design of SET inverter consumes less than 90.4 pW while it dissipates 4.21 nW in CMOS technology. This paper presents a comparative study of a one-bit-full-adder cell based on metallic single-electron transistors with its 22 nm CMOS counterpart. A gain of 70% of the total average power consumption of the CMOS-FA is realized with the SET-FA cells.

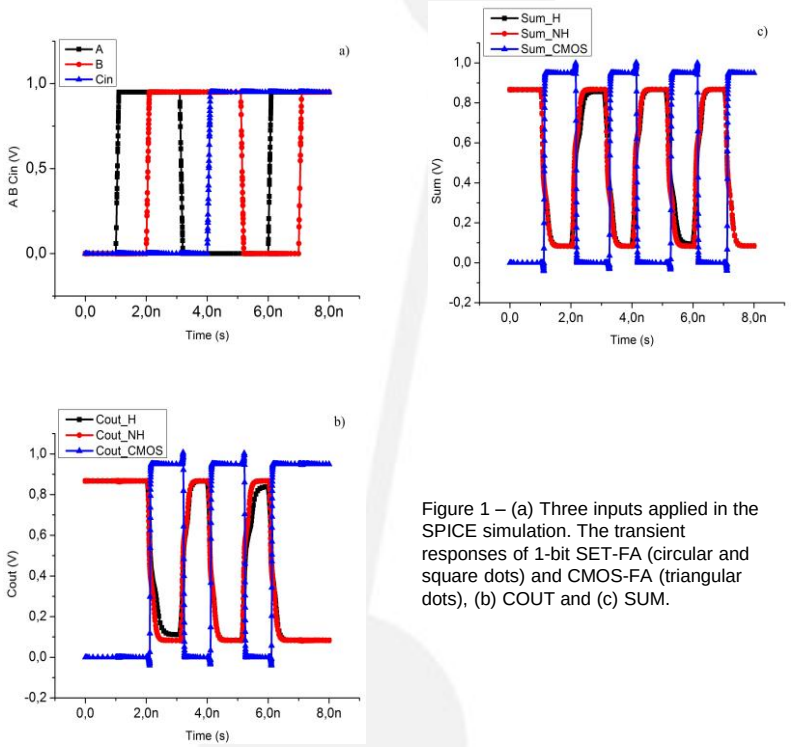

Figure 1 – (a) Three inputs applied in the SPICE simulation. The transient responses of 1-bit SET-FA (circular and square dots) and CMOS-FA (triangular dots), (b) COUT and (c) SUM.

Implementation (V_{DD} = 0.95 V)	Delay (ps)		Power consumption (nW) at 200 MHz	Power-delay product (ns x nW)	
	COUT	SUM		COUT	SUM
SET-H-FA	177	220	67.6	11.9	14.9
SET-NH-FA	162	203	71.2	11.5	14.4
CMOS-FA	85	125	234.9	19.9	29.4

Tableau 1 - Performance comparison of the SET Full Adders and CMOS Full Adder

Références
[1] ITRS, *ERD*, 2011.
[2] J. R. Tucker, *J. Appl. Phys.*, vol. 72, no. 9, pp. 4399–4413, Nov. 1992.
[3] J. Lee, J. H. Lee, I.-Y. Chung, C.-J. Kim, B.-G. Park, D. M. Kim and D. H. Kim, *IEEE Transactions on Nanotechnology*, vol. 10, no. 5, pp. 1180-1190, Sept. 2011.
[4] M.-Y. Jeong, B.-H. Lee and Y.-H. Jeong, *J. Appl. Phys.*, vol. 40, pp. 2054–2057, Mar. 2001.

Solvation structures of ionic liquids at a gold electrode

A. Labuda, P. Grütter

Department of Physics, McGill University, Montréal, Québec.

Mots clés : ionic liquid, atomic force microscope, cyclic voltammetry, solvation.

The prospect of building electrochemical supercapacitors based on ionic liquids requires a thorough understanding of the dynamics occurring at the electrode interface. These interfacial properties are often probed by various electrochemical and optical methods. However, conflicting data hinder advancements in our understanding of this solid-liquid interface. Atomic force microscopy (AFM) provides complementary information about the solvation structures with nanometer resolution in three dimensions, which can be compared with molecular dynamics to verify predictions and fine-tune modeling parameters. In this study, the oscillatory solvation structure of the BMIM][PF6] and gold interface is probed by AFM and correlated to electrochemical signatures observed by cyclic voltammetry.

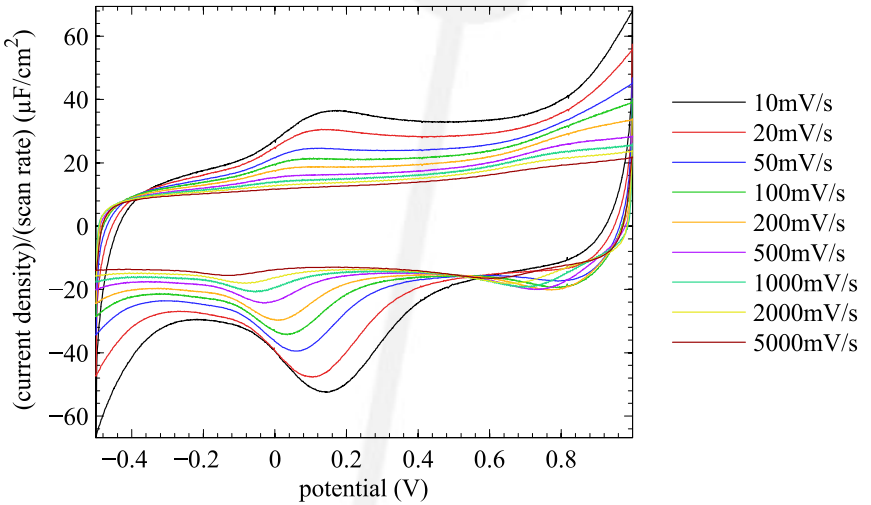

Figure 1 – Cyclic voltammetry of the Au(111) surface in [BMIM][PF_6] displaying the scan rate dependence of the current density.

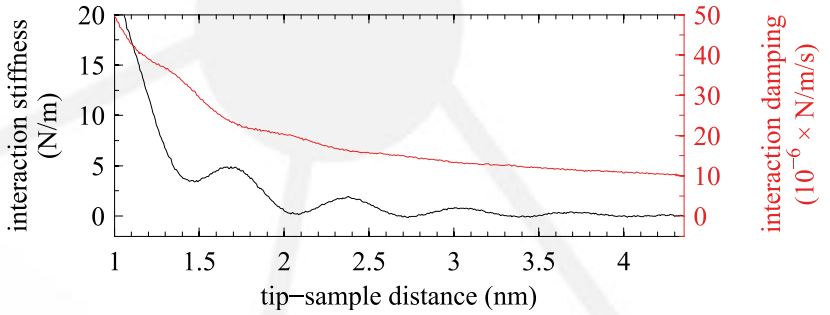

Figure 2 – Approach curve towards the Au(111) electrode in [BMIM][PF_6]. An oscillatory stiffness profile is observed, and a monotonically increasing damping profile.

Références

[1] W. Reisner et al. Directed self-organization of single DNA molecules in a nanoslit via embedded nanopit arraysPNAS 2009 106 (1) 79-84

High-performance nanocrystalline multilayered heterostructures for low-cost optoelectronic devices and architectures

X. Ma[1], F. Xu[1], J. Benavides[1], S. G. Cloutier[*1,2]*

[1]Department of Electrical and Computer Engineering, University of Delaware, 140 Evans Hall, Newark, Delaware, U.S.A., 19711.
[2]Département de Génie Électrique, École de Technologie Supérieure, 1100 rue Notre-Dame Ouest, Montréal, Canada, H3C 1K3.

Mots clés : nanocrystals, self-assembly, light-emitting diodes, solar cells

In recent years, self-assembled nanocrystalline films such as shown in Figure 1(a) have offered a unique material platform for a new generation of ultra low-cost optoelectronic devices with promising performances including FETs, photodetectors and solar cells. More recently, these structures have also been explored as a way of producing new low-cost light-emitting diode architectures. Currently, polymer-based light-emitting diodes offer good performances for the visible, but not the near-infrared. As an example of added functionality, we demonstrate how lead-chalcogenide nanocrystalline film structures can be used to form hybrid polymer-nanocrystal heterostructures with superior properties [1]. It is also known that self-assembled nanocrystalline films can be used to form very decent low-cost photovoltaic devices. However, we also show in Figure 1(f) that the overall performances of such structures can be significantly improved by forming a hybrid heterojunction between nanocrystalline films and an interconnected metal-oxide nanowire-based collector. As such, this presentation will focus especially on hybrid multilayered optoelectronic structures developed in our lab and how they were used to form: (1) polymer-nanocrystal heterostructures for high-performance near-infrared light-emitting diodes and (2) hybrid multilayered nanocrystalline structures for low-cost depleted-heterojunction solar cells. Based on these promising results, we believe these low-cost and high-performance nanocomposites will create new paradigms for several key applications such as lighting & displays, biomedical devices, lab-on-a-chip, flexible optoelectronics, night-vision and photovoltaics.

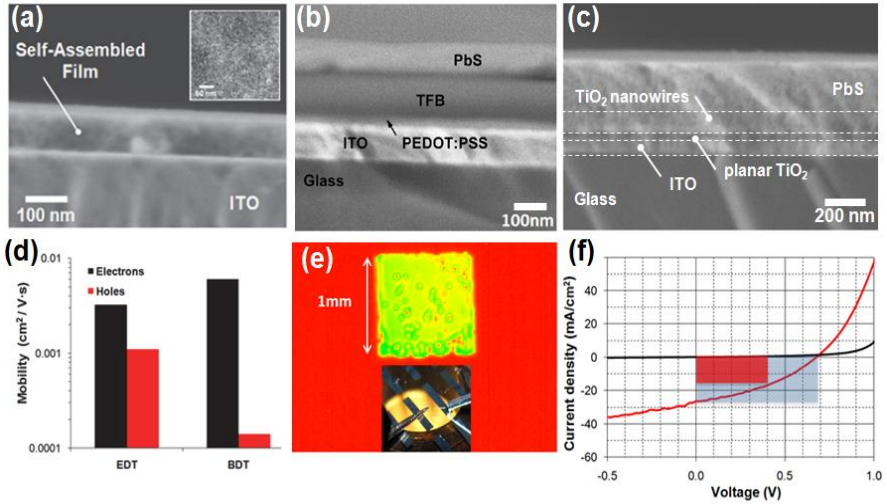

Figure 1 – High-performance nanocrystalline multilayered heterostructures for low-cost optoelectronic devices and architectures. (a) Self-assembled PbS film structure obtained by directed nanocrystal self-assembly using dithiol ligand-exchange treatment. **(b)** Hybrid multilayered polymer-nanocrystal heterostructure. **(c)** Hybrid multilayered nanocrystal-nanowire heterostructure. **(d)** Comparison of the electron and hole mobilities for nanocrystalline film structures cross-linked using ethanedithiol (EDT) and benzenedithiol (BDT) ligand-exchange treatment. **(e)** Emission of a low-cost hybrid near-infrared LED produced using the multilayered structure shown in (b). **(f)** Typical current-voltage characteristics for a nanocrystalline solar cell produced using the multilayered structure shown in (c).

Références

[1] X. Ma, F. Xu, J. Benavides and S. G. Cloutier, *Organic Electronics* **13**, 525-531 (2012).

Conductivity through an atomically-defined gold-tungsten interface

D. J. Oliver,[1] J. Maassen,[1] M. El Ouali,[1] W. Paul,[1] T. Hagedorn,[1] Y. Miyahara,[1] Y. Qi,[2] H. Guo,[1] and P. H. Grütter[1]

[1]Department of Physics, McGill University, Montreal, QC H3A2T8, Canada
[2]General Motors R&D Center, 30500 Mound Road, Warren, MI 48090-9055

Key words : nanoelectronics, SPM, nanoindentation, contact mechanics

Through atomically-characterized nanoindentation experiments and first-principles quantum transport calculations, we examine a mechanically-formed electrical nanocontact between gold and tungsten. We show, theoretically and experimentally, that the conduction across the metal-metal interface is drastically reduced due to the fundamental mismatch between s-wave and d-wave modes of electron conduction. Defects and disorder are a further major source of conduction losses. The technique and these findings are relevant to a diverse range of fields: molecular electronics, nanoscale contact mechanics, scanning tunneling microscopy, and semiconductor device design.A key challenge in all nanoscale electrical measurements, including transport measurements on molecules[1] and nanomaterials[2] and quantum break-junction experiments, is to accurately determine the area over which contact is made, especially as size is scaled down. This uncertainty prohibits quantitative testing and refinement of theoretical models against experimental data.[2] Junction area may be inferred from conductance, but this approach prevents any conclusions to be made about the relationship between conductance and area.To achieve an accurate knowledge of contact geometry, we have employed field ion microscopy (FIM), for direct atomic imaging of the probe tip. This capacity is incorporated into a scanning probe arrangement operating in ultra-high vacuum (UHV), capable of simultaneous current and force measurement.

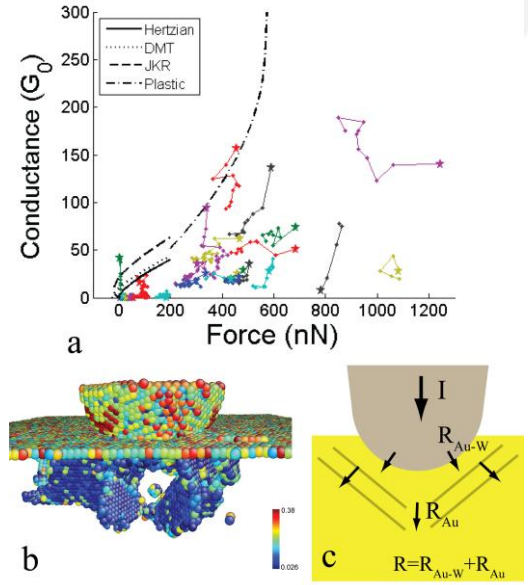

Figure 1 – a. Conductance values vs. applied force for series of indents of a 4.1 nm-radius W tip into Au. b. Molecular dynamics simulations of indentation of the same W tip into Au, showing plastic defects. c. Schematized conduction pathway through the W-Au junction.

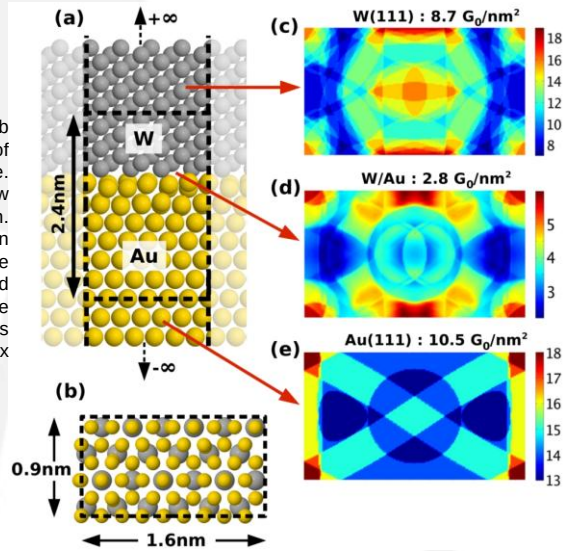

Figure 2 – Results from ab initio transport calculations of an W(111)-Au(111) interface. a. Side-view and b. plan-view of the simulated configuration. c-e. Plots of the transmission in reciprocal space for pure W, the W-Au interface, and Au, respectively. The interface reduces conductance nearly ~4x relative to either pure metal.

Références
1 K. Moth-Poulsen and T. Bjornholm, Nat. Nano. 4, 551 (2009).
2 F. Leonard and A. A. Talin, Nat. Nano. 6, 773 (2011).

Ultrathin Titanium Passive Devices Fabrication

S. Ecoffey, J.-F. Morissette, M. Guilmain, C. Nauenheim, D. Drouin

Centre de recherche en nanofabrication et nanocaractérisation CRN², Université de Sherbrooke, 2500 bld. de l'université, Sherbrooke QC, J1K 2R1.

Keywords: CMP, e-beam lithograhy, titanium, nanowire, MIM capacitor.

Chemical mechanical planarization has first been used in the back-end-of-line for multilevel metallization in the early 1990s [1]. It has then been introduced in the front-end-of-line through the shallow trench isolation technology in 1995. After incremental developments, it has been integrated in the 45 nm technology node as a solution for high-k metal gate structures and it shows nowadays a great potential for 32 nm and future applications such as FINFET, phase change memory, or 3D integration [1]. This paper presents physical and electrical characterizations of fabricated ultrathin titanium passive devices embedded in silicon dioxide. The nanowires and Ti/TiO2/Ti metal-insulator-metal capacitors are fabricated with a flexible process based on a nanodamascene technology. Successive chemical mechanical planarizations allow the fabrication of devices with titanium thicknesses down to few nanometers. A model of the titanium resistivity versus thickness based on Fuchs-Sondheimer and Mayadas-Shatzkes theory [2] is proposed. This model considers the electron scattering at line edge interfaces and grain boundaries for ultrathin metal films combined with devices electrical resistance measurements during the process (see Figure 1). This allows the evaluation of the remaining metal thickness and thus the realization of ultrathin titanium passive devices. The proposed methodology can be used with any kind of metal or dielectric that can be evaporated or deposited by atomic layer. The device geometries are not limited, and with this technology we have fabricated 20 nm wide and few nanometer thick titanium nanowires and capacitors (see Figure 1 and Figure 2) [3-4].

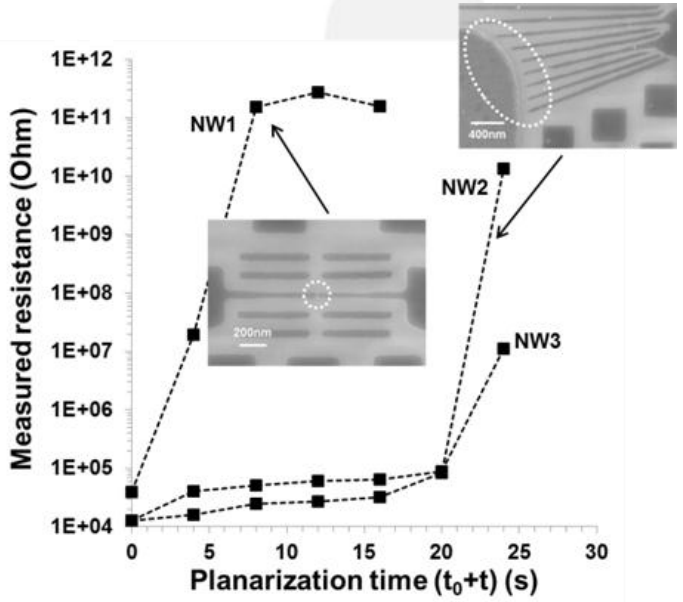

Figure 1 – Titanium nanowires measured resistances as a function of successive CMP steps. The SEM micrographs represent an interrupted nanowire line (NW1) and an interrupted contact electrode (NW2) [3].

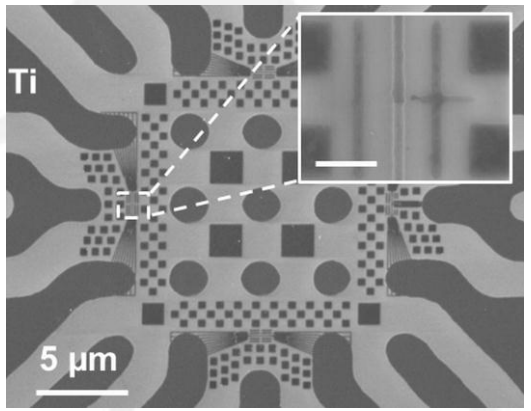

Figure 2 – SEM images of fabricated CMP titanium micro/nanostructures embedded in silicon oxide. The inset is a zoom on a Ti/TiO2/Ti capacitor (the scale-bar represents 200 nm) [4].

References
[1] J. M. Steigerwald, IEDM Technical Digest, December 2008.
[2] J.-W. Lim *et al*., Applied Surface Science, vol. 217, no. 1-4, 2003.
[3] S. Ecoffey *et al.*, 11th International Conference on Nanotechnology, Portland, August 15-19, 2011.
[4] S. Ecoffey *et al.*, JVST B, Volume 29, Issue 6, 2011.

Nanocomposite materials for three-dimensional microsensors

R. D. Farahani[1], M. A. El Khakani[2], M. Lévesque[1], D. Therriault[1]*

[1]Center for Applied Research on Polymers and Composites (CREPEC), Mechanical Engineering Department, École Polytechnique de Montréal, C.P. 6079, Succ. Centre-Ville, Montreal (QC), Canada H3C 3A7
[2]Institut National de la Recherche Scientifique, INRS-Énergie, Matériaux et Télécommunications, 1650 Blvd. Lionel-Boulet, Varennes (QC), Canada J3X 1S2

Keywords: carbon nanotubes, nanocomposites, microsensors, UV-assisted direct-write fabrication, photopolymers

Until now, most of the researches undertaken on using nanotubes in microelectronics like microsensors have been limited to the use of an individual nanotube, bulk nanotubes or polymer nanocomposite films [1-3]. Due to the size order of an individual nanotube or their bulk physical state (i.e., powder of entangled structures), manufacturing and manipulation of these materials is quite challenging [4, 5]. For nanocomposite-based sensors, two-dimensional (2D) and three-dimensional (3D) shape optimization have not reached their full potential, partly because of the lack of suitable and cost-effective manufacturing techniques. Here, we present the design and microfabrication of geometry-controlled microsensors made of carbon nanotube-based nanocomposites with the ultraviolet-assisted direct-write (UV-DW) technique. The technique consists of a computer-controlled robot that moves an extrusion apparatus along *x*, *y* and *z* axes. The UV-curable nanocomposite materials are extruded through a capillary nozzle by an applied pressure and are simultaneously photopolymerized under UV light. The flexibility of this fabrication method enabled to cost-effectively fabricate 2D and 3D patterned freestanding microsensors. The manufactured sensors geometries matched the programmed robot paths, which show the high capability of the technique. The electromechanical performance of the strain sensors was assessed under tension or compression in a dynamic mechanical analyzer. Electromechanical measurements revealed that the sensors are highly sensitive to small mechanical disturbances, especially for lower nanotube loadings when compared to traditional metallic or nanocomposite films. The present manufacturing method offers a new perspective for manufacturing highly sensitive 3D freestanding microstructured strain- and easily-manipulated biosensors.

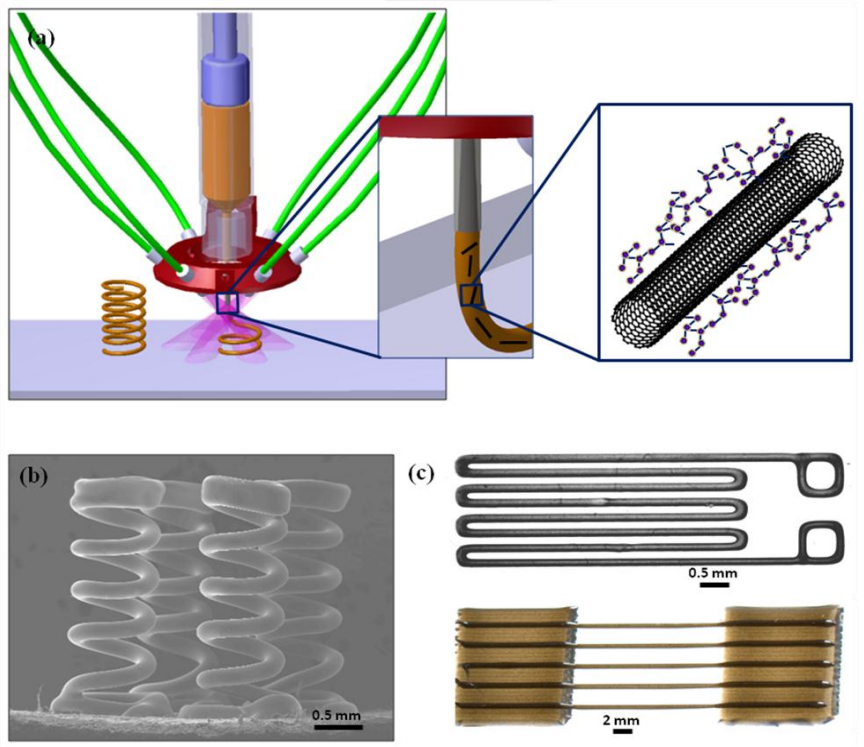

Figure 1 – (a) Schematic representation of the UV-assisted direct-writing of microstructures using single-walled carbon nanotubes/epoxy nanocomposites, (b) SEM image of a three-dimensional freestanding nanocomposite microsensor consisting of four identical microsprings, and (c) optical images of two two-dimensional microsensors similar to traditional strain gauges. To fabricate these microstructures using the UV-DW technique, the nanocomposite is extruded through a capillary micronozzle by an applied pressure and is partially cured shortly after extrusion under UV illumination.

References
[1] Hu N, Yin G, Karube Y, Liu YL, Li Y, Fukunaga H. A carbon nanotube/polymer strain sensor with linear and anti-symmetric piezoresistivity. Journal of Composite Materials. 2011;45(12):1315-1323.
[2] Ji TS, Jung SY, Xie JN, Varadan VK. Flexible Strain Sensors Based On Pentacene-Carbon Nanotube Composite Thin Films. 7th IEEE Conference on Nanotechnology, 2007;1-3, 375-378.
[3] Liu Y, Chakrabartty S, Gkinosatis DS, Mohanty AK, Lajnef N. Multi-walled carbon nanotubes/poly(L-lactide) nanocomposite strain sensor for biomechanical implants. 2007 Ieee Biomedical Circuits and Systems Conference. 2007:119-122.
[4] Atashbar MZ, Bejcek B, Singamaneni S, Santucci S. Carbon nanotube based biosensors. Proceedings of the IEEE Sensors 2004; 1-3:1048-1051.
[5] Kong J, Franklin NR, Zhou CW, Chapline MG, Peng S, Cho KJ, et al. Nanotube molecular wires as chemical sensors. Science. 2000;287(5453):622-625.

Metallic SET based Logic Cells: Evaluation & Comparison of Power Concumption with their CMOS Couterparts

M. A. Bounouar[1, 2], A. Beaumont[2], F. Calmon[2], D. Drouin[1]

[1]3IT-CRN2, Dept. of Electrical and Computer Engineering, Universite de Sherbrooke, Sherbrooke, QC, Canada
[2]Lyon Institute of Nanotechnology, University of Lyon, INSA-Lyon, F-69621 Villeurbanne Cedex, France

Keywords: Metallic Single Electron Transistor (SET), Low power consumption, Room Temperature Operation, Nanoelectronic logic gates

Single Electron Transistors have the potential to be a very promising candidate for future computing architectures due to their low voltage operation and low power consumption. In this paper, logic cells based on metallic SET operating at room temperature and up to 125 °C were designed. An evaluation of the energy consumption and a comparison with their equivalents in CMOS technology has been made. By using accurate SET model which closely matches experimental SET characteristics (Fig.1) [1, 2], SET-based logic cells provide a significant consumption reduction as compared with their CMOS counterparts (Table I). SETs based circuits rely on tunnel junctions through which electrons can flow in a controlled manner. By applying an appropriate gate voltage, we can control charge transfer through the SET and then switch it from OFF state (Coulomb Blockade) to ON state (current conduction). By using the second gate capacitance, the Coulomb Oscillations can be shifted and we obtain SETs transistors with *P*-type and *N*-type behavior. Therefore, it is possible to build Boolean logic with both pull-up and pull-down devices. The main advantage to use SETs that way is to reuse existing knowledge and design tools at very little cost and effort while overcoming fundamental physical restriction of CMOS technology. Indeed, SETs can be used to realize logic functions using the same CMOS architectures. Architectures based on SETs may offer a new computational paradigm with low power consumption and low voltage operation. This may be a real alternative to decrease power consumption significantly in future circuits.

Références
[1] M. A. Bounouar et al., "Single Electron Transistor Analytical Model for Hybrid Circuit Design," proc. of IEEE – NEWCAS conference, pp. 506- 509, 2011.
[2] C. Dubuc, et al., "Current conduction models in high temperature single electron transistor," Solid State Electronics 53, pp. 478-482, 2009.

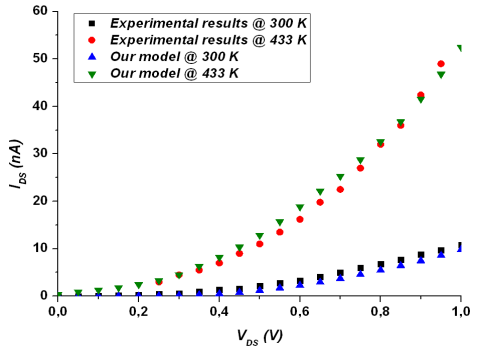

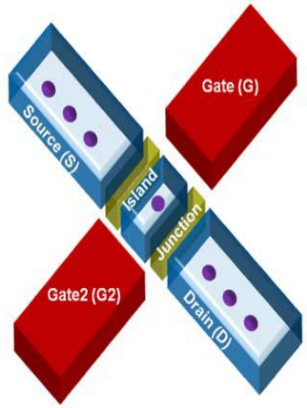

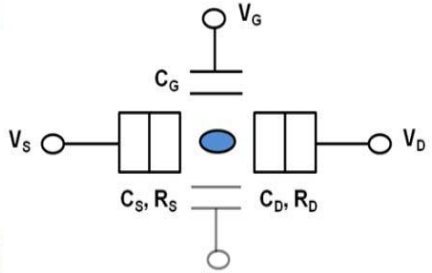

Figure 1 – Structure of a SET and equivalent electrical model. I_{DS}-V_{DS} characteristics for V_{GS} = 0 V calculated at different temperatures according our model [1] and experimental results [2] at *300K* and *433K*

	CMOS 65 nm		CMOS 28 nm		SET	
	25 °C	125 °C	25 °C	125 °C	25 °C	125 °C
INVERTER	70 nW	105 nW	25 nW	55 nW	650 pW	1.75 nW
NAND 2	160 nW	210 nW	55 nW	85 nW	400 pW	1 nW
NOR 2	160 nW	210 nW	45 nW	80 nW	950 pW	2.5 nW
1-Bit SRAM	2 µW	2.5 µW	620 nW	820 nW	4 nW	10 nW

Table I – Logic gates Average power consumption in CMOS 65nm, 28nm & SET for 25 and 125 °C

Raman Spectroscopy hyperspectral imager based on Bragg Tunable Filters

S. Marcet[1], M. Verhaegen[1], S. Blais-Ouellette[1], and R. Martel[2]

[1]Photon etc., 5795 Avenue de Gaspé, Montréal, Québec H2S 2X3, Canada
[2] Département de chimie, Regroupement Québécois sur les Matériaux de Pointe (RQMP), Université de Montréal, Montréal, Québec H3C 3J7, Canada

Keywords: Imaging, Bragg tunable filter, hyperspectral

A new type of Raman spectroscopy hyperspectral imager based on Bragg tunable filter has been developed by University of Montreal and Photon etc. Because the signal from Raman diffusion is much weaker than other optical characterization techniques, maximum efficiency is required from the imager. The standard methods, point-to-point measurements or imagers using liquid crystal tunable filters, increase substantially the acquisition time because of the downtime of mechanical displacements of the sample or the low filter transmission and polarization sensitivity. The decision to use spectral rather than spatial scanning allows for saving in acquisition time while keeping high spatial and spectral resolutions. The technology of Bragg tunable filter has an efficiency of 90%, allowing for non-destructive molecular analysis with high sensitivity. The transmission is continuously tunable over 400 nm with a spectral resolution of 0.2 nm (down to 2 cm^{-1}). A single wavelength of the entire image is filtered through a Bragg tunable filter where a single wavelength is diffracted and transmitted; other wavelengths are refracted and split from the optical path. The beam is then focalized on a CCD camera where a monochromatic image is formed. Wavelengths are scanned by changing the angle of incidence of the beam on the Bragg tunable filter. We present hyperspectral Raman images of Si/Ti structured wafer taken with a spectral resolution of 0.2 nm on the whole field of view of the microscope.

Design and microfabrication of through substrate vias integrable with thin films Piezoelectric structures

G. Mirshekari, M. Brouillette and L. G. Fréchette

Department of Mechanical Engineering, Université de Sherbrooke, Sherbrooke, Canada, J1K 2R1

Keywords: Through Substrate Via, Piezoelectric Transducers, Packaging

The poster demonstrates the design and microfabrication procedure of a novel Through Substrate Vias (TSV) that allows backside connection to the SOI device layer and is high temperature compatible for less restricted subsequent processing. Various existing approaches [2], [1] either induce a topology on the wafer surface, include metals that cannot sustain high temperature or do not use high quality insulators. In the present microfabrication, it is desired to use the vias to connect sol-gel derived piezoelectric structures from the backside. This imposes a number of specifications for the TSV process such as surface topology, thermal resistance, diffusion of contaminations and residual stresses. Thus, a microfabrication procedure has been introduced that uses SOI wafer. The first step is deep wet etching of cavities in the handle layer using a PECVD oxide mask on both sides. The next step is the deep etching of very narrow circular trenches in the device layer to create an electrically isolated island in the device layer. These trenches are then covered and sealed by deposition and patterning of a PECVD oxide layer. The substrate is then thermally oxidized and the buried oxide at the bottom of the via etched from the backside using a spray coated photoresist. Both sides of the substrate then metalized using lift-off photolithography as shown in Fig. 1. The microfabricated vias show the expected properties including small resistance between the front and backside metal pads as well as excellent isolation from the ground and the small capacitance between vias and the ground.

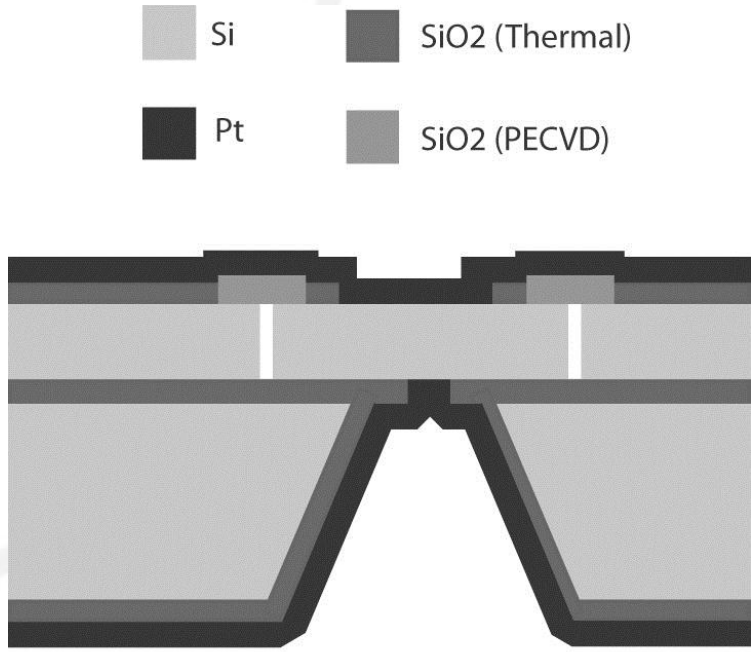

Figure 1 – The structural details of microfabricated vias

Références
[1] T. Bauer, “High Density Through Wafer Via Technology”, NSTI-Nanotech 2007, Santa Clara, USA, May 20-24, 1997, pp.116-119.
[2] J. H. Wu, J. A. del Alamo, “Fabrication and Characterization of Through-Substrate Interconnects”, IEEE Transaction on Electron Devices, Vol. 57, No. 6, pp. 1261-1268, 2010

Towards Synthesis of High-quality Water-soluble Near-infrared Emitting Core/shell PbS/CdS Quantum Dots

H. Zhao, M. Chaker, D. Ma

Institut National de la Recherche Scientifique, 1650 Boulevard Lionel-Boulet Varennes, Québec J3X 1S2, Canada

Keywords: Near infrared, Quantum dot, core/shell, PbS

A two-step approach (formation of a PbS/CdS core/shell structure followed by water transfer via amphiphilic polymers) was developed for the first time to synthesize high-quality water-soluble NIR-emitting PbS-based quantum dots (QDs) [1]. The CdS shell efficiently increases the structural stability of PbS QDs during water transfer and leads to a significantly enhanced quantum yield (QY) as high as 30% in phosphate buffered saline buffer. To the best of our knowledge, this is the highest value obtained so far for water-soluble near-infrared emitting PbS-based QDs. In addition, the PbS/CdS core/shell QDs in buffer show a good photostability under continuous illumination, comparable to that of PbS QDs dispersed in an organic phase. Further improvement of QY and photostability was made by optimizing core/shell structures [2,3]. By carefully varying the initial size of PbS QDs and finely tuning cation exchange experimental conditions, we are able to synthesize PbS/CdS core/shell QDs with a similar PbS core size of 4.4 ~ 4.5 nm yet different CdS shell thickness (0.2 to 2.3 nm). We study the effect of the shell thickness on the optical properties of these QDs after water transfer via polymer. It was found that the QY reaches the maximum of 33% when the shell thickness is ~ 0.7 nm. Further investigation on a series of core/shell samples with different core size and different shell thickness confirms that ~ 0.7 nm is an optimal shell thickness for the various core sizes investigated herein, consistently yielding the maximum QY and reasonably good photostability.

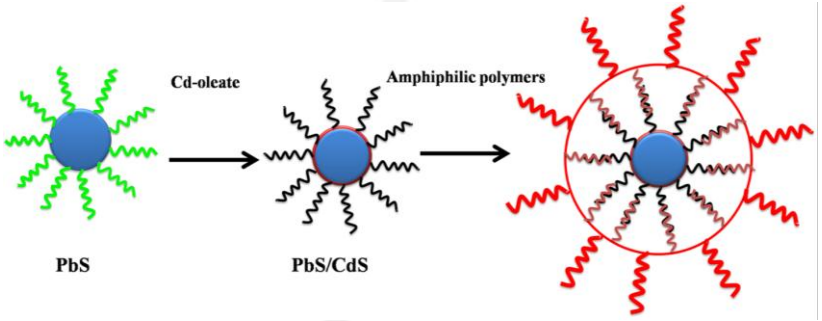

Figure 1 The two-step approach for synthesizing water-soluble PbS/CdS QDs.

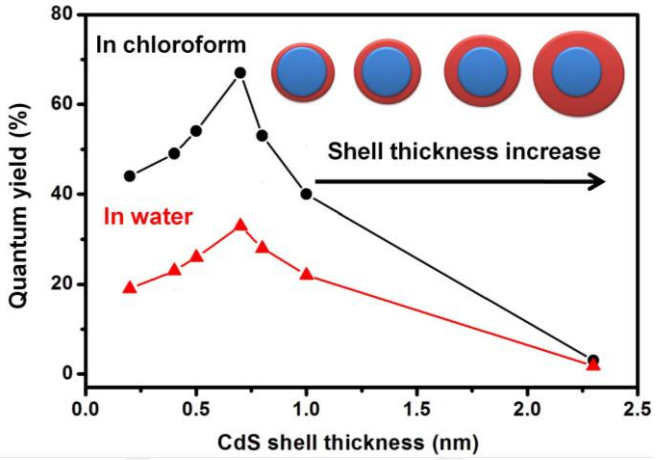

Figure 2 The QY of PbS/CdS QDs before and after water transfer as a function of CdS shell thickness. The solid lines are guides to the eye. Inset: PbS/CdS QDs with varying core size and constant CdS shell thickness of 0.7 nm.

Reference
[1] H. Zhao, D. Wang, T. Zhang, M. Chaker and D. Ma, Chem. Commun., 2010, 46, 5301–5303.
[2] H. Zhao, M. Chaker and D. Ma, J. Mater. Chem., J. Mater. Chem., 2011, 21, 8898-8904. (Highlighted by RSC publishing)
[3] H. Zhao, M. Chaker and D. Ma, J. Mater. Chem., 2011, 21, 17483–17491.

Conception and fabrication of Quantum Cellular Automata based on a single electron transistor process

G. Droulers[*1], S. Ecoffey[1], M. Pioro-Ladrière[2], D. Drouin[1]*

[1]*Nanofabrication and Nanocharacterization Research Center, Université de Sherbrooke, Sherbrooke, Quebec J1K 2R1, Canada*
[2]*Physics Department, Université de Sherbrooke, Sherbrooke, Quebec, J1K 2R1, Canada*

Mots clés : Quantum Cellular Automata, nanodamascene, single electron transistor, Coulomb blockade.

As the MOSFET is further scaled down, the increase in undesirable quantum effects and the need for better energy efficiency is driving the development of new technologies and computational methods. The quantum cellular automata (QCA) paradigm, where two excess electrons are confined in two of four quantum dots placed at the corners of a square, was introduced in 1993 [1]. Since then, many theoretical and experimental demonstrations have been made. However, room temperature operation is still a challenge especially to integrate QCA to usable, everyday life technologies. Here, we propose a QCA platform that has the potential to work at room temperature. Our platform is based on the nanodamascene process [2], used for the fabrication of room temperature single electron transistor (SET). The project consists of two parts, the first being simulation of a QCA half-cell based on the current technology process and the second, the fabrication and characterization of prototypes. I will present the basic operation scheme of QCA as well as the model used to predict electrical characteristics of these cells. The design and current state of the fabrication will also be shown. This new paradigm of computing with the position of a few electrons instead of the flow of many should provide a great reduction in the power consumption of future electronic circuits. The proposed process being compatible with standard CMOS processes also provides an advantage by facilitating the transition to new technologies including hybrid circuits as the MOSFET is ultimately scaled down.

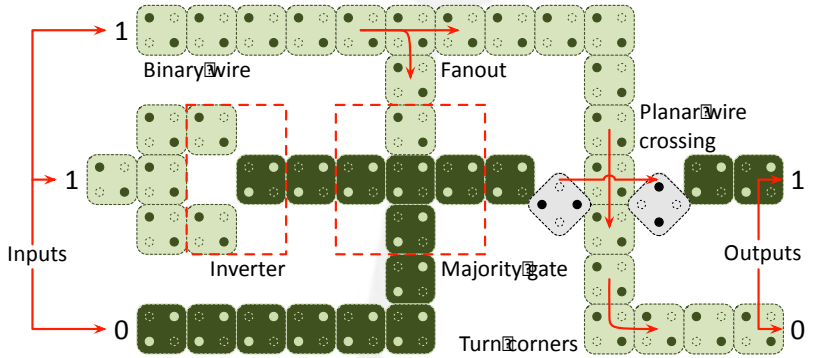

Figure 1 – Fictional circuit showing the different cell functional arrangements: binary wire, corners, fan-out, planar wire crossing, inverter and majority gate.

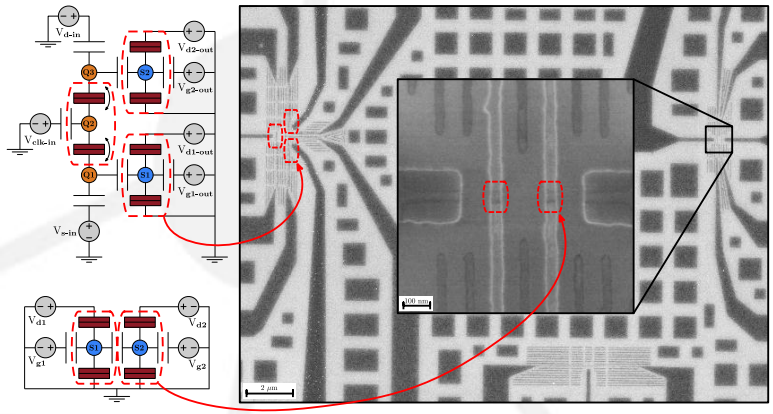

Figure 2 – Comparison between electrical circuit and fabricated devices (QCA half-cell with SET electrometers for readout). QCA circuit contains a third central dot to implement a clocking scheme by providing a “null” state.

Références
[1] C. S. Lent *et al*., NANOTECHNOLOGY (1993), 49.
[2] A. Beaumont *et al.,* IEEE Electron Device Letters (2009), 766.

Nano-mixing: A technique to overcome intrinsic liquid phase self diffusion barrier via spinning magnetic nanoparticles.

P. Hajiani[*1], *F. Larachi*[1]

Chemical Engineering Department, Laval University, Québec, Canada, G1V 0A6

Keywords : Nanomixing, magnetic nanoparticle, rotating magnetic field, liquid self diffusion coefficient, process intensification

Magnetic nanoparticles (MNPs) constituted of a magnetic core, like magnetite (Fe_3O_4) particle coated with surfactant layer, have attracted significant interest in diverse areas of engineering and research. Small particle size and magnetic properties of suspended MNPs in a liquid matrix allows manipulation at a distance by an appropriate external magnetic field while anchored to metal catalysts, enzymes or therapeutic drug agents. Owing to this feature, MNPs have been involved in many applications where mixing in micro-scale is also a critical issue, like catalytic reaction[1, 2], separation[3] and drug delivery[4, 5]. We explore here MNPs as easily separable nano-scale mixing devices. We present a mixing technique which uses magnetite nanoparticles as nano-stirrers subjected to a rotating magnetic field (RMF) generating small vortices in liquid phase. Using this technique, we intensified self diffusion coefficient of motionless water in a static diffusion cell. We also promoted significantly lateral mixing along the channel in a Taylor dispersion capillary tube relative to that in absence of MNPs or magnetic field. Moreover, we speculated hydrodynamic effect of such lateral mixing on laminar velocity profile as the result of an approach to a plug flow-like flat profile.

References

[1] L. Z. Gao, J. Zhuang, L. Nie, J. B. Zhang, Y. Zhang, N. Gu, T. H. Wang, J. Feng, D. L. Yang, S. Perrett and X. Yan, *Nat. Nanotechnol.*, 2007, 2, 577-583.
[2] V. Polshettiwar, R. Luque, A. Fihri, H. Zhu, M. Bouhrara and J.-M. Bassett, *Chem. Rev.*, 2011, 111, 3036-3075.
[3] H. H. Yang, S. Q. Zhang, X. L. Chen, Z. X. Zhuang, J. G. Xu and X. R. Wang, *Analytical Chemistry*, 2004, 76, 1316-1321.
[4] A. Ito, M. Shinkai, H. Honda and T. Kobayashi, *J. Biosci. Bioeng.*, 2005, 100, 1-11.
[5] I. Giouroudi and J. Kosel, *Recent Pat. Nanotechnol.*, 2010, 4, 111-118.

Tip enhanced Raman spectroscopy for chemical characterization of nano-structures

Mischa Nicklaus[1], Andreas Ruediger[1]

[1]INRS-EMT, Université du Québec, 1650, Boul. Lionel-Boulet, Varennes J3X 1S2

Keywords : Near field microscopy, Raman spectroscopy, scanning probe microscopy, ferroelectrics

Nano-electronics and biotechnology call for analytical methods with nanometer precision. Common techniques that provide such high resolutions are electron microscopy (SEM) and scanning probe microscopy (e.g. STM and AFM). Although some of these techniques can probe the topography of the sample with atomic resolution, the chemical and structural information remains unknown. Chemically-sensitive methods like Raman or IR-spectroscopy are physically limited by the diffraction limit of light and thus do not provide access to the nano-scale. With the goal of making chemical characterization available at nanometer resolution, we are working on tip enhanced Raman spectroscopy (TERS). This aperture-less near-field scanning microscopy is based on an atomic force microscope that uses localized surface plasmons at the apex of the microscopy tip (Figure 1) to generate an optical near-field of a few nanometers in diameter. While scanning the surface of the sample, the plasmons at the tip act as light source for the Raman spectroscopy (Figure 2) and the chemical structure of the sample can be mapped with molecular sensitivity. Our system is specifically designed to allow the characterization of insulating and opaque samples. We are therefore using a tuning fork AFM operated in shear force mode with electro-chemically etched gold tips. The optical access for the confocal Raman measurement is established from the side. We are presenting scans of carbon nanotubes with 15 nm optical resolution and first TERS spectra of $PbTiO_3$ nano structures.

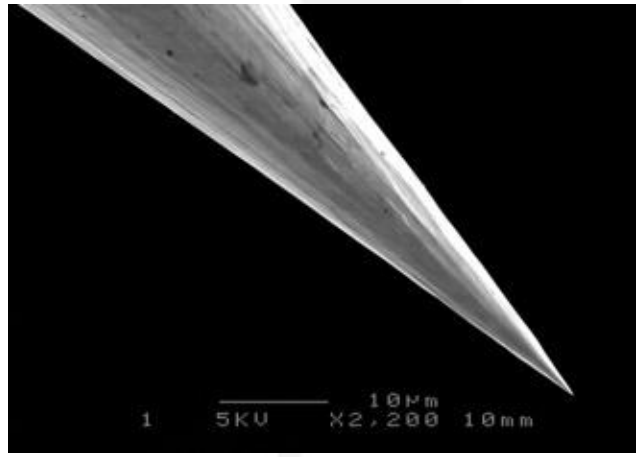

Figure 1 – SEM image of an electro-chemically etched gold tip for tip enhanced Raman spectroscopy.

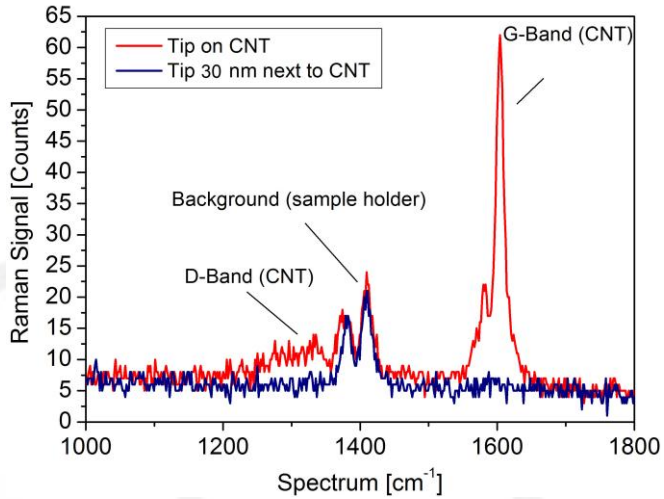

Figure 2 – Tip enhanced Raman spectrum of a carbon nanotube (red). The blue curve shows the loss of the G-band when the carbon nanotube is positioned 30 nm away from the tip. This demonstrates the position dependence and thus the high lateral resolution of TERS.

Synthesis of Gold Nanoparticles in a Microreactor Environment

H. SadAbadi[1], S. Badilescu[1], M. Packirisamy[1], R. Wuthrich[1]*

[1] Optical Bio-Micro Systems Lab, Department of Mechanical Engineering, Concordia University, 1455 de Maisonneuve Blvd. West, Montreal (Quebec), Canada H3G 1M8

Mots clés: Gold Nanoparticles, Synthesis, Microreactor, Microfluidic system

Metal nanoparticles have attracted much attention due to their unique properties associated with their dimensions. In particular, the optical and electronic properties of gold nanoparticles have been extensively studied, and various applications were reported such as biotechnology and medicine, bio-imaging, bio-sensing, and gene and drug delivery. In this work a polydimethylsiloxane (PDMS) microreactor is designed and fabricated by using the SU8 technology (Figure 1). The chloroauric acid (HAuCl4.3H2O) is used as the gold precursor and a sodium citrate solution is used as a reducing agent and stabilizer. Preliminary results showed that, upon introduction of the two solutions into the microreactor chamber, the reduction process starts immediately. The UV/Vis spectra of the output solution show the appearance and gradual increase of Au plasmon band with time which is shown in Figure 2. Scanning electron microscopy (SEM) is used for measuring the size distribution of the synthesized gold nanoparticles. The output of the reactor is collected from the chamber at different times and is dropped on a silicon wafer for SEM imaging. Experiments performed at the macro-size show that, the reduction process is endothermic. However, our results showed that in a microfluidic environment, the process can be performed even at room temperature. Miniaturized heating pads (Polyimide Heaters from Watlow®) were used in conjunction with the microreactor. The heating elements are integrated in the reaction micro chamber and the effect of temperature is studied. In order to improve the mixing of the reactants, a mixing element should be integrated with the microreactor.

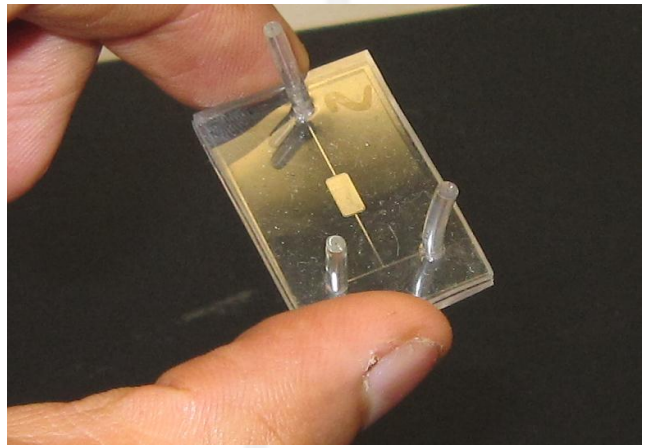

Figure 1 – Fabricated PDMS microreactor, the channel widths are 150 µm and the size of microreactor chamber is 2×4mm.

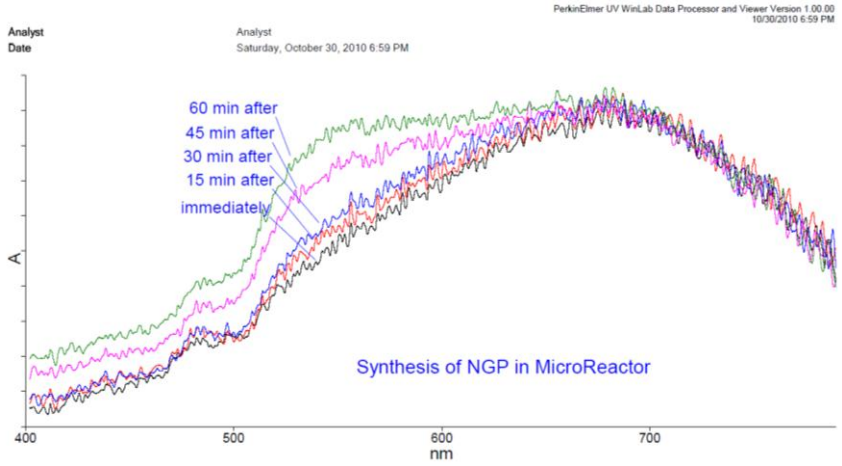

Figure 2 – The spectra of the solution inside the microreactor during the first hour of the reaction.

Nanostencil mask lithography problems and solutions

Jeffrey R Bates[1], Shawn Fostner*[2], Yoichi Miyahara[1], Peter Grutter[1]

[1] McGill University, Department of Physics, Montréal, Canada, H3A 2T8
[2] University of Canterbury, Department of Physics and Astronomy, Christchurch, New Zealand

Keywords : nanostencil lithography, focused ion beam milling, gallium implantation, stencil deformation

The standard techniques used for fabrication of sub-micron device features include electron beam lithography, interference lithography, extreme UV and x-ray lithography. An alternative to these fabrication techniques is nanostencil lithography. Nanostencil lithography avoids possible contamination sources such as resist coatings, solvents and etching and also has the possibility of fabrication and measurement being performed while maintaining ultra high vacuum (UHV) conditions. Despite these benefits, there are many obstacles to nanostencil lithography. We will show some issues when using nanostencil lithography then propose solutions to these issues. A commonly used fabrication technique, focused ion beam (FIB) milling, can implant gallium ions that can influence the growth of material deposited though the nanostencil as shown in figure 1. This problem may be mitigated by thinning the nanostencil using a reactive ion etch which may remove the gallium ions. Another obstacle can occur when stencils made using FIB are baked in air, significant deformation can occur to the stencil, which is possibly caused by gallium catalyzed oxidation. By baking the stencil in UHV oxidation induced deformation can be avoided [1]. Stencil deformation that occurs when stressed metal is deposited onto the nanostencil can also be detrimental to pattern replication as shown in figure 2. By adding stencil stiffening structures into the membrane it provides a sufficiently large bending moment that stencil deformation can be made negligible [1].

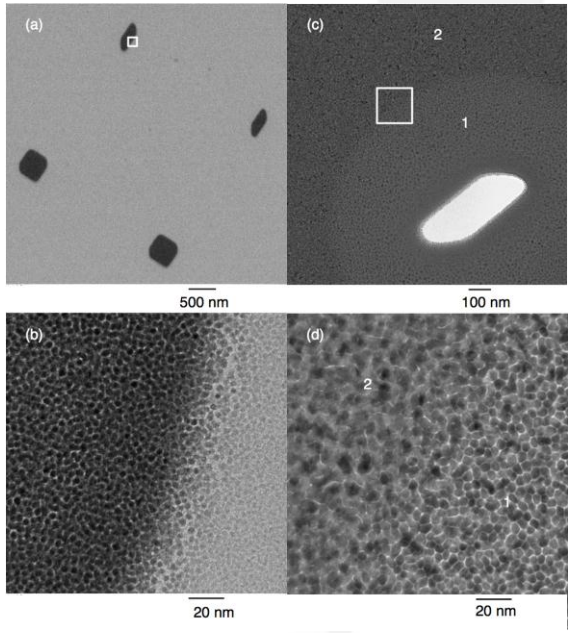

Figure 1 – Bright field TEM images of: (a) Permalloy nanostructures fabricated using FIB nanostencil. (b) Zoom in on nanostructure in (a). (c) FIB-milled nanostencil used to make (a) after permalloy deposition, with permalloy film visible featuring two morphology zones surrounding milled hole (d) Zoom in on area in (c). Note that morphology in (b) is the same as region 1, the FIB damaged region, in (d).

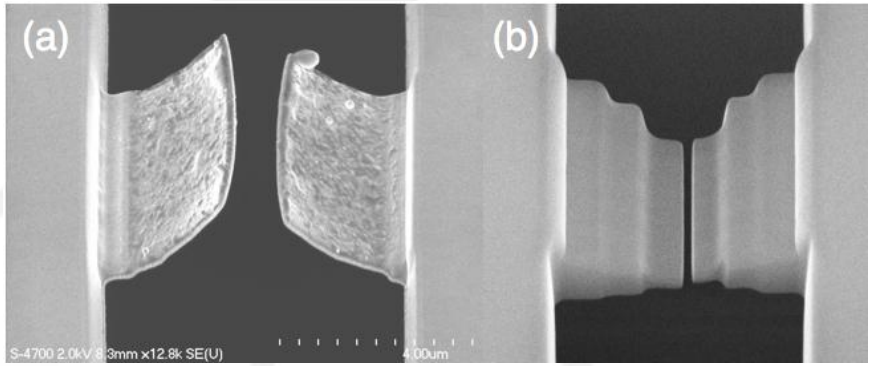

Figure 2 –A comparison of the stencil deformation of normal and stiffened membrane structures with Ta films deposited on the backside. (a) Uncompensated structure with 45 nm of Ta and significant deformation. (b) Reinforced structure with 27 nm Ta and no visible deformation

Références
[1] S. Fostner, S. A. Burke, J. Topple, J. M. Mativetsky, J. Beerens, and P. Grutter, Microelectronic Engineering 87, 652 (2010).

Enhanced optical properties of gold nanorod polyvinyl alcohol nanocomposite film

Stefan Stoenescu*[a], Simona Badilescu[a], Muthukumaran Packirisamy[a], Vo-Van Truong[b]

[a]Dept. of Mechanical Engineering, Concordia Univ., EV 4.219, 1515 St.Catherine West, Montreal, QC, Canada H3G 2W1 [b]Dept. of Physics, Concordia Univ., Loyola Science Complex, 7141 Sherbrooke West, Montreal, QC, Canada H4B 1R6

Keywords : anisotropic, gold nanorods, nanocomposite film, dichroic ratio

The strong optical absorption, scattering and local electric field enhancement associated with the longitudinal Surface Plasmon Resonance (SPR) of gold nanorods (AuNRs) have important applications in imaging, sensing, nonlinear optics, thermal therapy and data encoding. However, in normally cast polymer based nanorod composite films, the NRs orientation is random and only those more or less aligned with the electric field of the linearly polarized incident light have the most favorable orientation for the excitation of the longitudinal SPR mode. Thus, only a fraction of the embedded NRs is useful for the intended applications. Therefore, producing composite films of fully aligned NRs would greatly enhance the device efficiency. In this work, we have developed polyvinyl alcohol composite films containing well aligned AuNRs by uniaxial drawing using a specially designed mechanical device. The chemical composition of the polymer was optimized to allow for high drawing ratios. The macroscopic properties of the nanocomposite film were characterized by SEM and UV-Visible spectroscopy using linearly polarized light. The average orientation angle of the AuNRs was calculated based on a statistically significant number of NRs and its standard deviation was found to be close to zero. The linear dichroic ratio of the stretched nanocomposite film was calculated based on the ratio of the peak absorbance of the incident light parallelly polarized, to that of the light polarized perpendicularly to the NRs axes.

References

[1] J. Perez-Juste, B. Rodrigues-Gonzales, P. Mulvaney, M. Liz-Marzan, Optical Control and Patterning of Gold-Nanorod-Poly(vinyl alcohol) Nanocomposite Films, Adv. Funct. Mater. 2005, 15, 1065-1071

[2] C. J. Murphy, C. J. Orendorff, Alignment of gold nanorods in polymer composites and on polymer surfaces, Adv. Mater. 2005, 17, 2173-2177

[3] J. Li, S. Liu, Y. Liu, F. Zhou, Z-Y Li, Anisotropic and enhanced absorptive nonlinearities in a macroscopic film induced by aligned gold nanorods, Applied Physics Letters 96, 2010

Solvent-cast Direct-write Assembly of 3D Thermoplastic Nanocomposites Microstructures

*Shuangzhuang Guo, Daniel Therriault**

Center for Applied Research on Polymers and Composites (CREPEC), Mechanical Engineering Department, École Polytechnique de Montréal, C.P. 6079, Succ. Centre-Ville, Montréal (QC), Canada H3C 3A7

Keywords : Microfabrication, Nanocomposites, Direct-write, Scaffolds, Biomaterial.

Poly(lactic acid) (PLA) is a biodegradable and biocompatible thermoplastic derived from renewable plant sources. The direct-write assembly offers the ability to rapidly and precisely fabricate functional materials in various complex 3D structures from a broad array of materials. In this work, we developed a PLA nanocomposite solution used as an ink to fabricate 3D periodic micro scaffolds by direct-write assembly. In this process, the polymer PLA and the nanofillers (i.e., nanoclay) were well distributed in a volatile solvent to form a viscous solution. This polymer solution was then loaded into a syringe and extruded through a micro nozzle during the robotic deposition. Due to the rapid solvent evaporation, the filament behavior changed from fluid-like to solid-like right after its extrusion out of nozzle to facilitate the shape retention of the deposited features. The PLA nanocomposite solutions were used to build 2D planar filaments on a substrate, and 3D scaffolds for various filament diameters (40 ~ 250 μm). The fabrication parameters for the ink micro-extrusion process such as the applied pressure, the nozzle and filament diameter, the robot velocity and the ink apparent viscosity were investigated by capillary flow analysis. The morphology of extruded filaments was characterized by SEM. Dynamic mechanical analysis (DMA) using a film tension clamp was performed for the nanocomposite filaments featuring different nanoclay contents, and nozzle diameters. This novel direct-write approach using thermoplastic nanocomposite solutions can be readily extended to other polymers and enables a broad array of applications including tissue engineering scaffolds, stimuli-responsive materials and microelectronic devices.

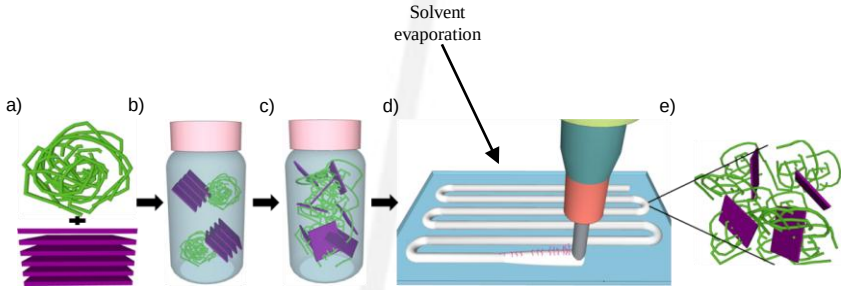

Figure 2 Microscopy images of six layers 3D scaffold fabricated with 25% (PLA-nanoclay) composite solution under pressure 1120 kPa and robot velocity 1mm/s with 100 μm nozzle: (a) Top view, (b) Slight inclined top view, (c) Side view. Scale bar: (a, b) 1 mm, (c) 250 μm.

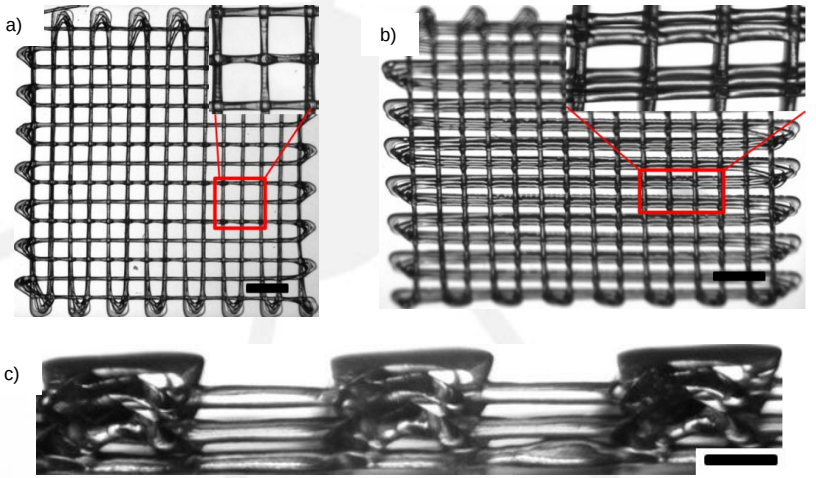

Figure 1 Schematic of solvent-cast direct-write process with thermoplastic-based nanocomposite solution: (a) PLA and nanoclay, (b) adding PLA and nanoclay into solvent, (c) Stirring and ultrasonication, (d) Direct-write process with nanocomposite solution, (e) nanocomposite.

References

[1] J. Perez-Juste, B. Rodrigues-Gonzales, P. Mulvaney, M. Liz-Marzan, Optical Control and Patterning of Gold-Nanorod-Poly(vinyl alcohol) Nanocomposite Films, Adv. Funct. Mater. 2005, 15, 1065-1071

[2] C. J. Murphy, C. J. Orendorff, Alignment of gold nanorods in polymer composites and on polymer surfaces, Adv. Mater. 2005, 17, 2173-2177

[3] J. Li, S. Liu, Y. Liu, F. Zhou, Z-Y Li, Anisotropic and enhanced absorptive nonlinearities in a macroscopic film induced by aligned gold nanorods, Applied Physics Letters 96, 2010

Croissance et caractérisation des boîtes quantiques d'InAs/GaAs pour des applications solaires

J. Zribi[*1], *D. Morris*[1], *R. Arès*[2]

[1]Département de physique et [2]Département de génie mécanique, Université de Sherbrooke, Sherbrooke, Québec J1K 2R1, Canada.

Mots clés: cellules solaires, boîtes quantiques, épitaxie par jets chimiques

Les cellules solaires à boîtes quantiques ont attiré l'attention dernièrement dans le domaine du photovoltaïque [1-4]. Les boîtes quantiques (BQs) sont insérées dans la cellule centrale d'une structure multi-jonction InGaP/InGaAs/Ge afin d'augmenter l'absorption optique dans la gamme 900-1200 nm et ainsi améliorer l'efficacité de conversion lumière-électricité. Dans ce travail, nous étudions, pour la première fois, la croissance et la caractérisation de BQs d'InAs/GaAs crues par épitaxie par jets chimiques. Cette technique d'intérêt pour le photovoltaïque permet de croître de grandes cellules avec une bonne qualité cristalline et à ce à coût réduit. Les propriétés des BQs ont été caractérisées par microscopie à force atomique et par spectroscopie de photoluminescence. Les objectifs du travail visent la croissance de telles cellules solaires, l'optimisation de leurs caractéristiques à travers un meilleur contrôle des conditions de croissance ainsi qu'une compréhension des mécanismes physiques affectant la dynamique des photoporteurs. Pour cette étude, les BQs ont été crues à 465°C pour différentes quantités d'InAs déposées (Fig. 1). Pour un dépôt de 0.95 monocouche (ML) d'InAs, le mode de croissance est bidimensionnel. À partir de 1.58 ML d'InAs des îlots 3D commencent à se former. À 2.07 ML, la densité de BQs atteint 4.45 × 10^{10} cm^{-2}. Ces BQs émettent à 1.2 eV (Fig. 2). Des travaux liés à l'intégration des BQs dans une jonction p-i-n de GaAs pour l'étude de leurs propriétés optoélectroniques et pour la caractérisation de leur efficacité de conversion sont en cours.

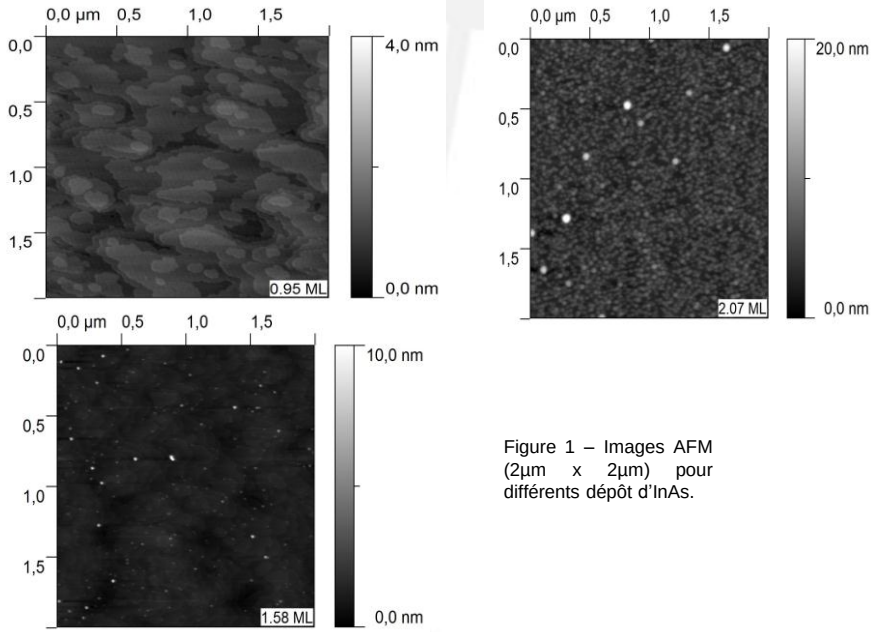

Figure 1 – Images AFM (2µm x 2µm) pour différents dépôt d'InAs.

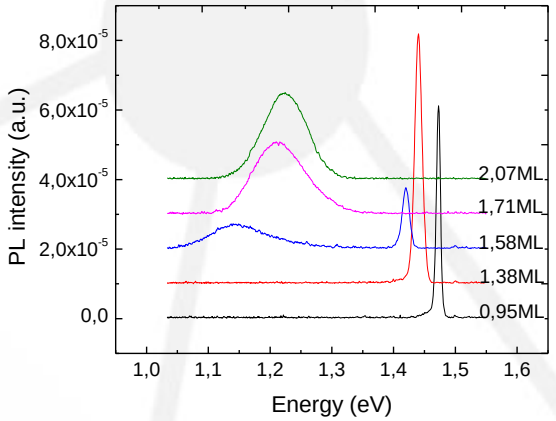

Figure 2 – Spectres de photoluminescence d'une série d'échantillons avec différentes quantités d'InAs déposées.

Références

[1] S. Suraprapapich, S. Thainoi, S. Kanjanachuchai, S. Panyakeow, Quantum dot integration in heterostructure solar cells, Solar Energy Materials & Solar Cells, **Vol. 90**, pp. 2968–2974, 2006.

[2] V. Aroutiounian, S. Petrosyan, A. Khachatryan, Quantum dot solar cells, **Vol. 89**, Journal Of Applied Physics, pp. 2268-2271, 2001.

[3] A.J. Nozik, Quantum dot solar cells, Physica E, pp. 115-120, 2002.

[4] A. Marti, N. Lopez, E. Antolin, E. Canovas, C. Stanley, C. Farmer, L. Cuadra, A. Luque, *Novel* semiconductor solar cell structures: The quantum dot intermediate band solar cell, Thin Solid Films, pp. 638 – 644, 2006.

Modélisation du transport percolatif dans les réseaux de nanotubes de carbone de dispersion et de structure variables.

L.-P. Simoneau[*1], A. Rochefort*[1]

[1]Polytechnique de Montréal, Département de génie physique et Regroupement québécois sur les matériaux de pointe (RQMP), Montreal, Canada

Mots clés : nanotechnologies, nanotubes de carbone, réseaux percolatifs

Le fonctionnement des dispositifs d'affichage et des cellules photovoltaïques repose typiquement sur l'emploi d'électrodes transparentes et celles-ci sont majoritairement rigides, cassantes et coûteuses. Une solution de remplacement ne possédant pas ces défauts est donc hautement désirable et pourrait être trouvée dans les réseaux percolatifs de nanotubes de carbone (CNTs) ou de nanorubans de graphène (GNRs). L'étude computationnelle de ces réseaux de nanostructures permet l'exploration des processus physiques sous-jacents ainsi que l'optimisation des caractéristiques fonctionnelles. Toutefois, la plupart des études allant dans ce sens limitent la description des jonctions CNT-CNT à un seul paramètre constant [1], alors qu'il s'agit en fait du facteur limitant dans la propagation des porteurs de charge [2]. Nous avons développé des algorithmes Monte-Carlo permettant d'étudier le transport de charges dans des réseaux de CNTs et de GNRs bi- et tridimensionnels incorporant des distributions réalistes de résistance de contact. Nos algorithmes génèrent des réseaux aléatoires à l'aide de nombreux paramètres qui peuvent être ajustés pour représenter des réseaux expérimentaux de CNTs, de GNRs ou des hybrides de différentes nanostructures. Nous évaluons alors la conductance totale des réseaux générés en se basant sur les conductances de contact individuelles, qui sont quant à elles déduites des propriétés locales du réseau. En faisant varier les distributions stochastiques de ces conductances de contact, nous reproduisons des résultats expérimentaux pour des réseaux de CNTs [3].

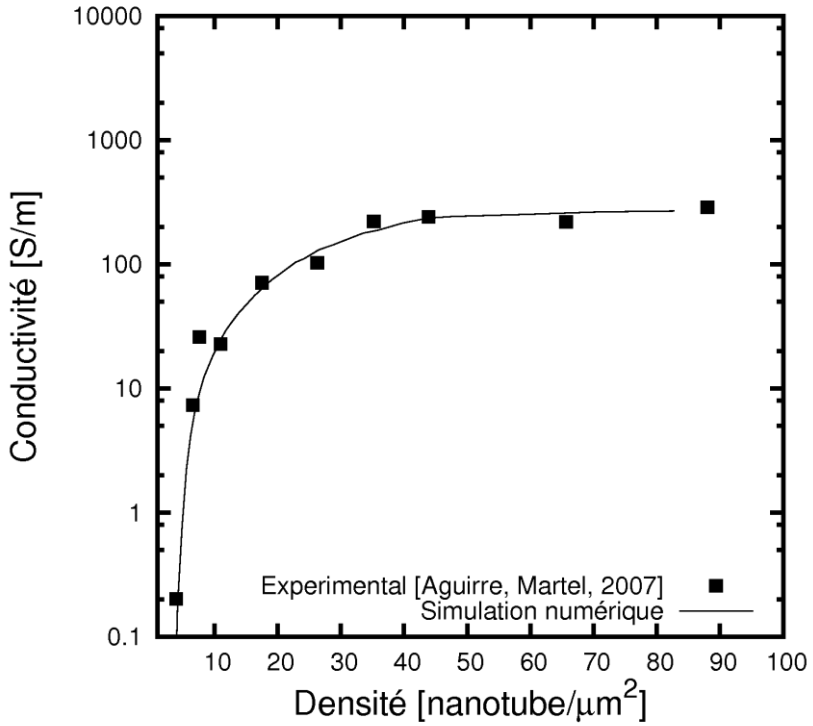

Figure 1 – Évolution de la conductivité en fonction de la densité de recouvrement du substrat par les nanotubes. Résultats numériques pour un réseau de 23X23 µm comparés à des résultats expérimentaux obtenus avec un réseau de 50X100 µm [3]. Les nanotubes simulés ont les mêmes distributions de longueur, de diamètre et d'orientation que celles rapportées par les expérimentateurs. Les distributions de conductance de contact sont MM: Lorentz(8E-8,16E-9) SS: Normal(8E-9,4E-9) MS: Normal(8E-11,8E-12) (les unités sont en siemens).

Références

[1] Hicks J, Behnam A, Ural A. Resistivity in percolation networks of one-dimensional elements with a length distribution. Physical Review E. 2009; (April 2008):1-4.
[2] Nirmalraj PN, Lyons PE, De S, Coleman JN, Boland JJ. Electrical connectivity in single-walled carbon nanotube networks. Nano letters. 2009; 9 (11):3890-5
[3] Aguirre CM. Carbon Nanotube Networks for Thin Film Electronic Applications, Ph.D. Thesis. 2007

.

Scanning probe investigation of resistive switching in TiO_2 thin films

M. Moretti[*1], M. Nicklaus[1], C. Nauenheim[1], A. Ruediger[1]*

[1]INRS-EMT, 1650 Boulevard Lionel-Boulet, Varennes J3X 1S2, Québec

Keywords : non-volatile memories, resistive switching, conductive AFM

The concept of resistive switching paves the way to non-volatile data storage with non-destructive read-out and promising scaling behavior ($4F^2$) due to a two-terminal structure that can be realized in crossbar arrays. Such structures have been realized by electron beam lithography and showed reproducible resistance changes down to 100 nm linewidth with excellent R_{on}/R_{off} ratios after electroforming. Their integration e.g. in CMOS-backend circuits critically depends on further downscaling. A downscaling ability investigation has been conducted by scanning probe microscopy with a conductive Pt-Ir coated tip of a beam-deflection cantilever on a 30 nm TiO_2 thin film deposited by reactive sputtering on a Pt bottom electrode. Our conductive AFM scans displaying an estimated lateral resolution of 3 nm in current indicate a globally homogeneous conductivity that locally reflects the granularity of the structure (columnar growth) with a reduced conduction along the grain boundaries. Attempts to electroform the thin film failed and resulted in an irreversible modification of the surface morphology (hillocks of 20 nm height). However, even without electroforming, we achieved On-Off ratios of 4 which is in agreement with literature[1]. In a subsequent series of experiments we investigated the effect of mechanical compression by tapping mode microscopy on the properties of resistive switching. After tapping, we achieved a noticeable compression of 3% and a decreased conductivity by a factor of 130. However, the On-Off ratio remains unchanged, we observe the same ratio for the compressed even for two different SET voltages.

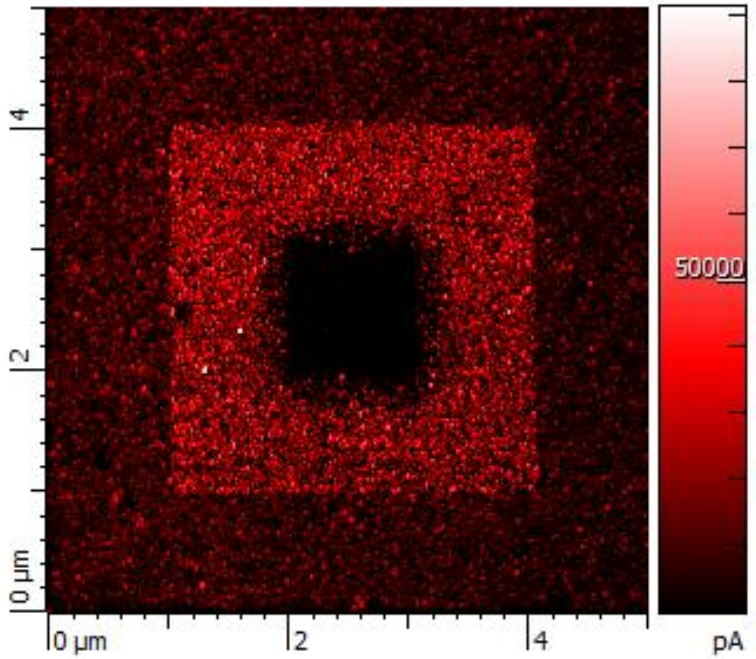

Figure 1 – Current map (5 by 5 micron^2) with the pristine sample (outside) and the sample exposed to a negative bias (center) and positive bias (in between) of 7V. The read voltage was 1V.

Références

[1] L. Yang, C. Kuegeler, K. Szot, A. Ruediger, R. Waser, "The influence of copper electrode on the resistive switching effect in TiO2 thin films studied by conductive force microscopy", Applied Physics Letters, 95 (2009) 013109..

Disassembling glancing angle deposited films for high-throughput nano-column characterization

J.M.A. Siewert[1], J.M. LaForge[1], M.T. Taschuk[1], M.J. Brett[1,2]

[1]Department of ECE, University of Alberta, Edmonton, Alberta, T6V 2V4, Canada
[2]NRC National Institute for Nanotechnology, Edmonton, Alberta T6G 2M9, Canada

Keywords : nanocolumns, GLAD, characterization, thin-films, broadening

Glancing angle deposition (GLAD) uses physical vapour deposition with substrate rotation to grow forests of highly customizable nanocolumns. Providing precise control over column shape in metals, oxides, and organics, GLAD films facilitate applications in the realms of chromatography, optical filtering, and organic photovoltaics.[1] With growing application of GLAD films, however, comes an increasing need to understand and engineer their growth mechanics – especially for the common "vertical post" nanocolumn morphology. Vertical post shape is typically described by $d = \omega_0 h^p$, where d is column diameter, h is height, and ω_0 and p are material dependent constants describing diameter and broadening.[2] Based on theoretical growth models, p is predicted to lie between 5/16 and 1/2. While many GLAD materials have been characterized for p, no reliable trends have yet been obtained.[3–5] Groups generally measure p from cross-sectional SEM images, recording diameters of clearly distinct posts at various film heights. This is labour-intensive and produces data with large scatter. Alternatively, focused ion-beam cross sections of GLAD films[5] can produce precise measurements, but are impractical for characterizing films' ensemble properties. In both cases, limited numbers of measurements restrict what can be learned. To overcome these limitations, we have developed an automated characterization method for GLAD nanocoloumns. Using this technique, we have measured p and ω_0 as a function of pitch for TiO_2 vertical post films, testing the theoretical limits on p and quantifying an important dependence on substrate rotation that may ultimately enhance our control of nanocolumn morphology and device performance.

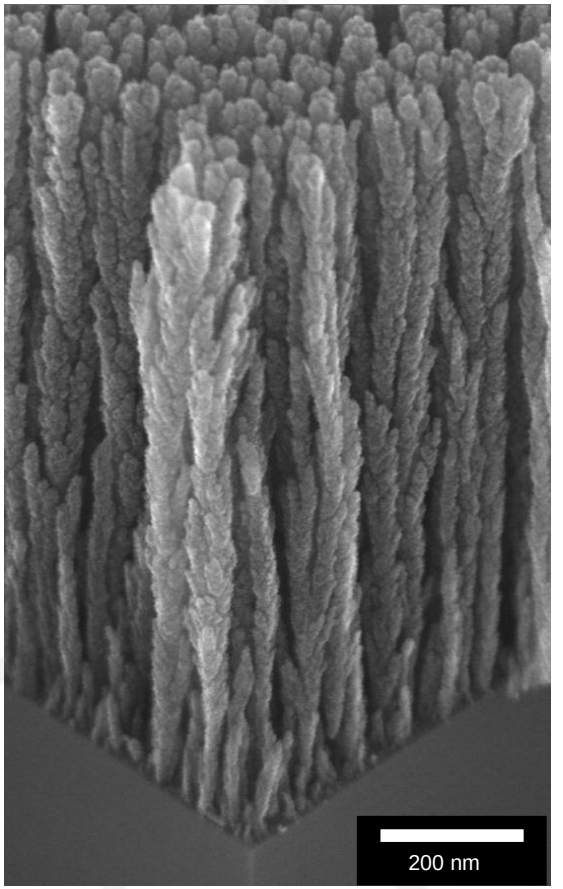

Figure 1 – Sample of a TiO_2 glancing angle deposited (GLAD) film used in this study, demonstrating one of the simplest nanocolumn morphologies available to the GLAD technique. Individual columns exhibit both branching and broadening effects which both have important ramifications for GLAD applications.

Références
[1]M. T. Taschuk et al. in "Handbook of Deposition Technologies for Films and Coatings," 3rd ed., (Ed: Peter Martin), Elsevier, Oxford:2010.
[2] T. Karabacak, et al. *Phys Rev B* 68:12, 2003.
[3] C. M. Zhou & D. Gall *JAP* 103:1, 2008.
[4]C. Buzea et al. *Nanotechnology* 16:10, 2005.
[5] K. M. Krause, et al. *Langmuir* 26:22, 2010.

Développements Récents de l'Intégration 3D de SET Métalliques sur CMOS pour une Application Mémoire

N. Jouvet[1,2], M.A. Bounouar[1,2], B. Lee-Sang[2], A. Lecestre[2], S. Ecoffey[2], C. Nauenheim[2], A. Beaumont[1], S. Monfray[3], A. Ruediger[4], F. Calmon[1], A. Souifi[1], D. Drouin[2]

[1]Institut des nanotechnologies de Lyon, INSA, UMR CNRS 5270, 7 Avenue Jean Capelle, 69621 Villeurbanne Cedex, France
[2]3IT-Université de Sherbrooke, 2500 Boulevard Université, J1K 2R1 Sherbrooke, Canada
[3]ST Microelectronics, 850 Rue Jean Monnet, 38920 Crolles, France
[4]INRS-Energie, Matériaux et Télécommunications, 1650 Boulevard Lionel-Boulet, J3X 1S2 Varennes, Canada

Mots clés : Transistor Mono-électronique, Hybridation SET-CMOS, Nanodamascène, SRAM, Architecture 3D

A cause de limitations physiques liées à une constante miniaturisation, l'industrie des semi-conducteurs explore le développement de nouvelles technologies pour complémenter les fonctions CMOS [1]. Parmi celles-ci, le transistor mono-électronique (SET) est prometteur à cause de son ultra basse consommation et de sa nature unique qui permet la réalisation de fonctions logiques complexes à l'aide d'un nombre réduit de dispositifs [2]. Ce travail présente le procédé nanodamascène de fabrication de SETs métalliques dans le *back end of line* de transistors CMOS, et l'utilisation d'outils de simulation pour le développement d'une cellule mémoire constituée de SETs. Des observations SEM et AFM, combinées avec des caractérisations électriques à température ambiante ont été réalisées sur des SETs aux dimensions relâchées fabriqués sur des CMOS. Elles tendent à montrer la viabilité du processus de fabrication nanodamascène. On a aussi exploré le potentiel de circuit nanoélectroniques constitués de SETs grâce aux simulations d'une cellule mémoire SRAM. En utilisant les caractéristiques physiques théoriquement atteignable par déposition de couche atomique (ALD), on démontrera que la cellule peut fonctionner jusqu'à une température de 398K, et que la puissance consommée est inférieure à celle d'un circuit équivalent formé de CMOS 65nm. Afin de prendre avantage, à la fois de la faible puissance consommée des transistors mono-électroniques, et des forts courants émis par les CMOS, un circuit hybride 3D SET CMOS est proposé.

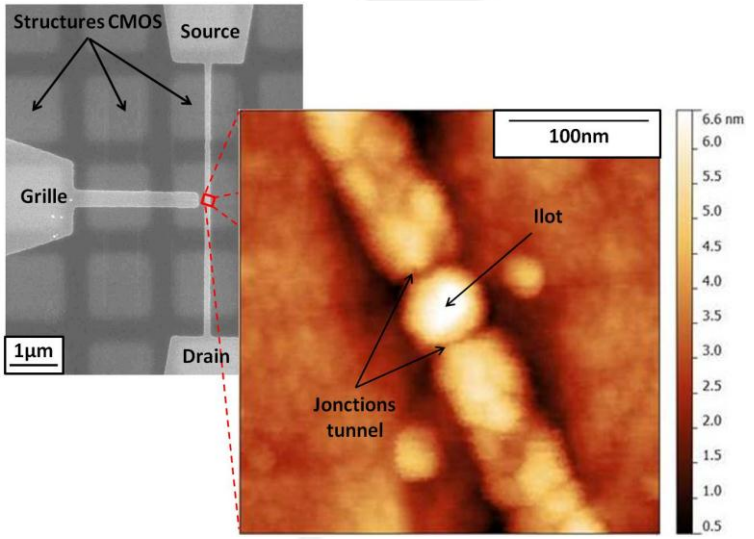

Figure 1 – Image SEM d'un transistor mono-électronique au dessus de structures de la couche CMOS après CMP (figure de gauche). La source et le drain sont liés par le canal. Un ilot a été déposé. L'image AFM montre clairement l'îlot et les jonctions tunnel du transistor mono-électronique.

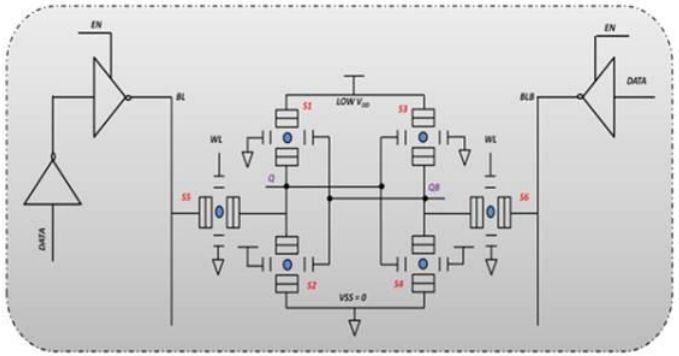

Figure 2 – Schéma d'une cellule mémoire SRAM 1-Bit composée uniquement de transistor mono-électroniques.

Références

[1] G. Bourianoff; M. Brillouet; R.K. Cavin; T. Hiramoto; J.A. Hutchby; A.M. Ionescu; K. Uchida. Nanoelectronics Research for Beyond CMOS Information Processing, Proceedings of the IEEE, 2010

[2] Y. Ono, A. Fujiwara, K. Nishiguchi, H. Inokawa, Y. Takahashi. Manipulation and Detection of Single Electrons for Future Information Processing, JAP, 2005

Impact of Sidewall Roughness on Integrated Bragg Gratings

A. D. Simard[*1], N. Ayotte[1], Y. Painchaud[2], S. LaRochelle[1]*

[1]Centre d'optique, photonique et laser, Université Laval, Québec, Canada, G1V 0A6
[2]TeraXion, 2716 Einstein St., Québec, Qc, Canada, GP 4S8

Keywords : Bragg gratings, integrated optics devices, optical filter, silicon photonics.

There are currently major research efforts worldwide to develop photonic integrated circuits for telecommunication applications using Silicon-on-insulator (SOI). The goal is to provide a low-cost small-footprint platform to integrate several functions on the same photonic chip. One type of components typically required for WDM systems are optical filters with flexible and precise spectral responses. Integrated Bragg grating (IBG) structures in SOI could provide greater tuning properties, compared to fiber Bragg gratings, through the plasma dispersion or the thermo-optic effects. However, to achieve elaborate spectral responses, long structures must be obtained. Very recently, curved photonic wires were proposed to minimize device footprint [1, 2]. This structure, in a spiral shape, could allow large scale integration without having a significant impact on the grating spectral response [1]. However, since waveguide width fluctuations have a large impact on the mode effective index in waveguides with high index contrast, such as photonic wire in SOI, sidewall roughness severely degrade the grating spectrum [3] (Figure 1). In this paper, we address this issue by showing that only low spatial frequency components of the noise are relevant to the calculation of the IBG spectral response (Figure 2). Furthermore, we present an IBG emulator that allows estimation of expected fabrication yield of specific gratings given that the fabrication process is well characterized. Finally, the analysis of apodized gratings is used as an example to illustrate how this modeling can help to reduce development cost by first studying robustness of IBG designs to fabrication limitations.

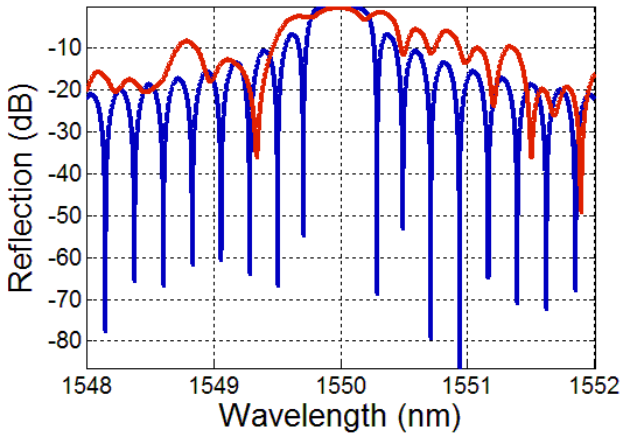

Figure 1 – Comparison of a typical ideal Bragg grating reflection spectrum (in blue) with one affected by sidewall roughness (in red).

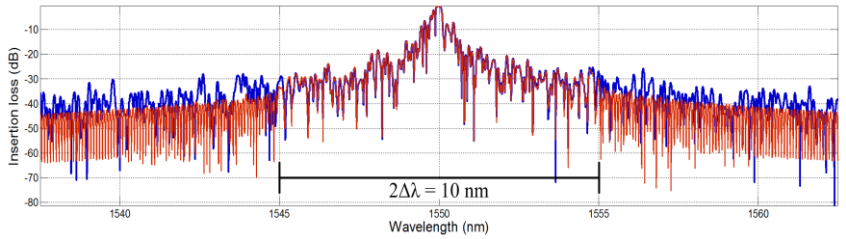

Figure 2 – Comparison of an IBG simulated without the low-pass filtering approach (in blue) with one using an ideal low-pass filter with a threshold frequency associated with ± 10 nm bandwidths.

Références
[1] A. D. Simard, Y. Painchaud, and S. LaRochelle, "Integrated Bragg Gratings in Curved Waveguides," in *the 23rd Annual Meeting of the Photonics Society*, Denver, USA, 2010, ThU3.
[2] S. Zamek, D. T. Tan, M. Khajavikhan, M. Ayache, M. P. Nezhad, and Y. Fainman, "Compact chip-scale filter based on curved waveguide Bragg gratings," *Opt. Lett.*, vol. 35, nº. 20, pp. 3477–3479, Oct. 2010.
[3] A. D. Simard, N. Ayotte, Y. Painchaud, S. Bedard, and S. LaRochelle, "Impact of Sidewall Roughness on Integrated Bragg Gratings," *J. Lightwave Technol.*, vol. 29, no. 24, pp. 3693-3704, Dec. 2011.

Nanopatterning and Nanocomposites In Microfluidic Microbial Fuel Cells

B. Nearingburg[1], A. L. Elias[1]

[1]Department of Chemical and Materials Engineering, University of Alberta, 7'th Floor ECERF, 9107-116 St, Edmonton, Alberta, Canada, T6G 2V4

Keywords : nanopatterning, nanocomposites, microfluidics, fuel cells

In a global environment dominated by concerns for clean and renewable sources of energy methods to maximize energy production and energy losses are keenly sought. Our proposed method works towards addressing these concerns by bringing together the promising fields of nanofabrication and biotechnology to create bioelectrical energy generation systems in the form of microfluidic microbial fuel cells (µMFCs). Such devices apply techniques found in micro and nanofluidic processing with the natural metabolic processes of microorganisms such as algae and cyanobacteria to produce chemical gradients capable of generating electrical current [1, 2]. As the interactions between microbes and external environments occur on a micro and nano-scale, both the chemical and physical nature of surfaces within the µMFC devices must be carefully engineered and characterized on the nanometer scale. Our work involves engineering of advanced materials to optimize favourable interactions of microbes with both electrode and non-electrode surfaces within the µMFC device with the goal of optimizing efficiency of energy production. Techniques such as nanoscale lithography are used to alter the structure of thin film electrodes to increase electroactive surface area and microbial adhesion. Other methods such as incorporating nanoparticle containing photopolymerizable polymer composites are used to enhance the functionality of proton exchange membranes while altering the effects of bio-fouling.

References

[1] Logan, B. E. et al, “Microbial Fuel Cells: Methedology and Technology”, Environmental Science and Technology, 40 (17) 2006, 5181-5192.
[2] Wang, H. Y. et al, “Micro-sized microbial fuel cell: A mini-review”, Bioresource Technology, 102 (1) 2011, 235-243.

Conception of a lab-on-a-chip for fluorescence detection applications using quad junction photodetector and hybrid optical filter

Thierry Courcier[†‡], Charles Richard[‡], Stéphane Martel[ᶠ], Luc Ouellet[ᶠ], Patrick Pittet[†], Guo-Neng Lu[†], Paul Charette[‡], Vincent Aimez[‡]

[†]Equipe conception INL, UMR 5270 CNRS-UCBL, Villeurbanne, France
[‡]Laboratoire de Biophotonique et d'Optoélectronique, CRN², Sherbrooke, Canada
[ᶠ]Teledyne DALSA, 18 boul. de l'Aéroport, Bromont, Québec, J2L1S7, Canada

Mots clés : lab-on-a-chip, photodetector, Buried-Quad-Junction, fluorescence, optical filter

For the implementation of fluorescence detection within lab-on-a-chip, weak signal detection is a key issue resulting from short optical paths. Special attention should also be paid for the design of an efficient on chip optical filtering associated to a sensitive CMOS photodetector [1]. We report multi-wavelength detection performances of a Buried-Quad-Junction pn-photodetector and the ongoing work on a hybrid optical filter.The proposed BQJ photodetector structure [2] has been designed in a CMOS 0.8 µm High Voltage Teledyne DALSA process. It consists of four stacked buried pn-junctions reverse biased which operate in photoconductive mode. Each junction has a specific spectral response (fig 1) which allows quantification up to four contributions. More advanced signal processing such as synchronous detection and dedicated preamplification is being implemented to determine fluorescence contributions from quantum dots and organic dyes. A new interference filter has been designed based on the CRN² deposition process allowing a high refraction coefficient for nitride thin-films (n above 2.5 @ 532nm) while keeping an absorption coefficient k under $10^{-3}cm^{-1}$. This 1.13µm thick Si_3N_4/SiO_2 (5/4) interferential filter allows an attenuation of -21.8dB at 532nm and only -0.65dB at 650nm (fig 2). Combined with an absorbing filter of around 1µm thick, we obtain a quasi-uniform attenuation over -43dB over a wide angular dispersion [0°- 60°].Next milestones cover integration of the interference filter on the BQJ and characterization of optimized electronics. Fluorescence measurements with up to four dyes will be performed to show the multi-labeling capability of the proposed BQJ structure with associated signal processing.

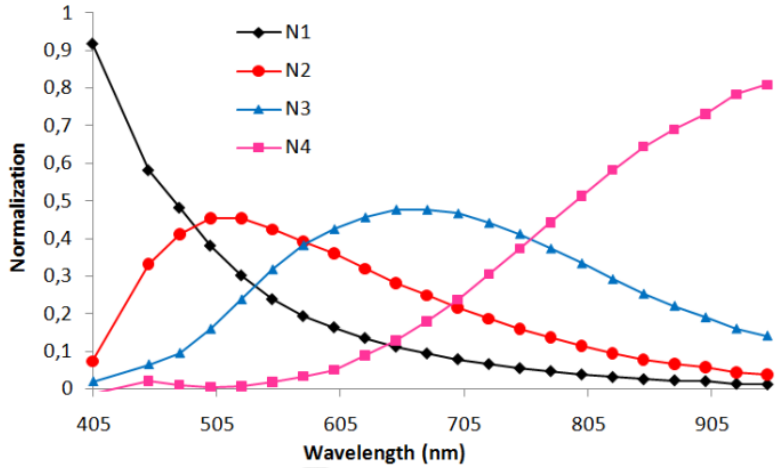

Figure 1: Normalization of BQJ outputs (Reverse bias: 1.5V for each junction)

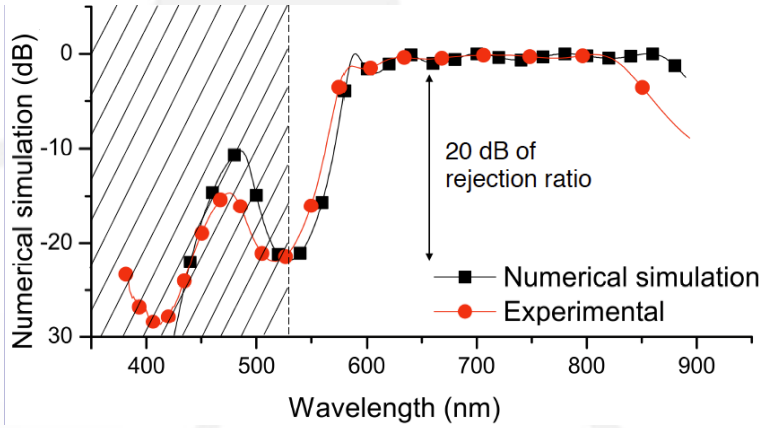

Figure 2 : Transmission (dB) of 9 layers filter deposited by PECVD. ~1.1µm thick

[Références]
[1] Richard, C.; Pittet, P.; Martel, S.; Ouellet, L.; Lu, G.N.; Aimez, V.; Charette, P.G.. *Integration of hybrid optical filter with buried quad pn-junction photodetector for multi-labeling fluorescence detection applications*. In proceedings of IEEE Design, Test, Integration & Packaging of MEMS/MOEMS symposium 2011.
[2] Richard, C.; Courcier, T.; Pittet, P. ;Martel, S.; Ouellet, L.; Lu,G. N. ; Aimez,V. and Charette, P. G., *CMOS buried Quad p-n junction photodetector for multi-wavelength analysis.* Optics Express Vol. 20, Iss. 3, pp. 2053–2061 (2012)

Spontaneously Self-assembled Nano-hillocks

Soroush Nazarpour[*,1], Mohamed Chaker*[1]

[1]INRS énergie, matériaux et telecommunications, 1650, boulevard Lionel Boulet, Varennes, QC, Canada J3X 1S2

Keywords: Nano-hillocks, AFM image processing, Fractal analysis, Coble creep, Stress

In contrast to artificially ordered schemes, such as those currently used in integrated circuits, “self-assembled” processes may enable the creation of complex device architectures that rely on the intrinsic ability of the system to organize itself into ordered patterns. Development of such processes requires extensive studies revealing the dominant parameters governing the ordering process. For instance, arrays of regularly ordered nano-islands on the surface are of great interest of technologies such as field emitters for vacuum microelectronic devices. Indeed, nano-hillocks are nanometric islands that heterogeneously appear on the surface of metallic films. To understand the controlling mechanism of hillock formation, this study combines the experimental efforts in growth of nano-hillocks of Pd with mathematical analysis of their AFM topographic images. Pd thin films in different thickness were deposited at 300°C onto $SrTiO_3$ single crystalline perovskite substrate. Structural and mechanical analyses were performed resulting into measurement of accumulated residual stress in thin films. Next, hillocks were identified through topographic images of the surface and data were fed into image processing WS×M software. Flooding process and fractal analysis assisted into removal of background noise (surface roughness) resulting into detection of well-separated nano-hillocks (Fig 1). This enables to calculate the geometrical parameters of nanohillocks. As a result, strong correlation has been found between the total hillock surface area and residual stress generated in the films (Fig 2). Application of this knowledge on thin films of columnar grain led to formation of the arrays of hillocks, well distributed over the pocket grain boundaries.

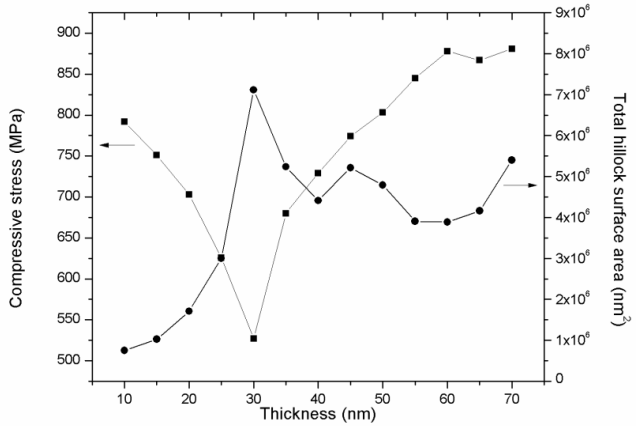

Figure 1 – Variation of compressive stress and total hillock surface area versus thickness of Pd films.

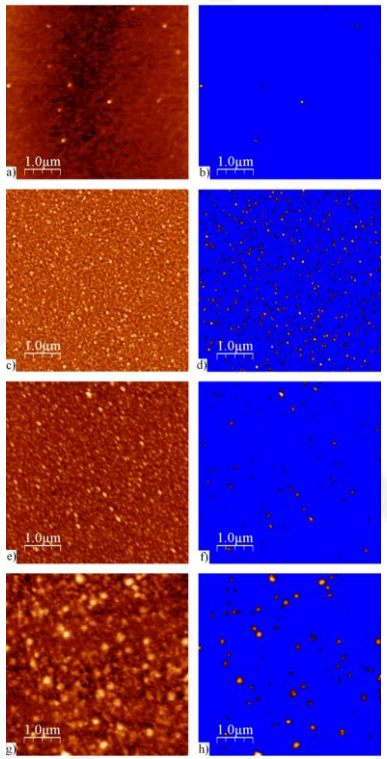

Figure 2 – AFM topographic images of 15nm (a), 30nm (c), 45nm (e), and 60nm (g), and noise removed images of 15nm (b), 30nm (d), 45nm (f), and 60nm (h) thickness of Pd film.

Références

[1] Faucher, L. et al. Ultra-small PEGylated Gd2O3 nanoparticles (submitted Feb 2012).

[2] Guillet-Nicolas R, Bridot JL, Seo Y, Fortin MA, Kleitz F (2011) Enhanced relaxometric properties of MRI “positive” contrast agents confined in three-dimensional cubic mesoporous silica nanoparticles. *Advanced Functional Materials* (Wiley) (accepted)

Fabrication de bobines planaires comme remplacement à des bobines solénoïdales dans un miroir déformable ferrofluidique

G. Gingras[1], D. Brousseau[2], S. A. Charlebois[1]

[1]Université de Sherbrooke, 2500, boul. de l'université, Sherbrooke, Canada, J1N 2R1
[2]Université Laval, 2325, rue de l'Université, Québec, Canada, G1V 0A6

Mots clés : Bobine planaire, microfabrication, électrodéposition, ferrofluide, miroir liquide

L'optique adaptative permet de compenser les fluctuations du milieu dans lequel se propage la lumière (air, eau, tissus vivants) afin d'améliorer la qualité d'une image. Cette technique utilise des miroirs déformables dont certains sont réalisés à l'aide de liquides magnétiques (ferrofluides) déformés par le champ magnétique produit par plusieurs bobines (actionneur). Lors d'une conférence de NanoQuébec en 2008, une équipe s'est formée alliant l'expertise de production des nanoparticules composant le ferrofluide, de conception de systèmes d'optique adaptative [1] et de microfabrication dans le but de pousser la miniaturisation des actuateurs, d'en augmenter l'efficacité et de proposer une approche manufacturable à coût raisonnable. Le projet a permis de réaliser des réseaux de bobines planaires de plusieurs dimensions afin de remplacer les bobines solénoïdales assemblées à la main dans les prototypes antérieurs et dont le diamètre ne pouvait que difficilement être réduit en dessous d'un millimètre. Le diamètre des bobines planaires fabriquées actuellement varie entre 400µm et 4.8mm (Figure 1). Des simulations ont été réalisées sur la structure des bobines et l'épaisseur du ferrofluide pour comprendre le profil et l'amplitude des déformations. Une bobine planaire permet de créer une déformation plus de 5 fois plus intense qu'une bobine solénoïdale en plus d'être plus étroite (pour un même rayon, densité de conducteur, courant et épaisseur de ferrofluide.) Cette plus grande efficacité permet de diminuer la taille de la bobine et donc d'augmenter le nombre de pixels par mm². Les mesures et tests effectués sur ces deux types de bobine ont validé les résultats des simulations (Figure 2).

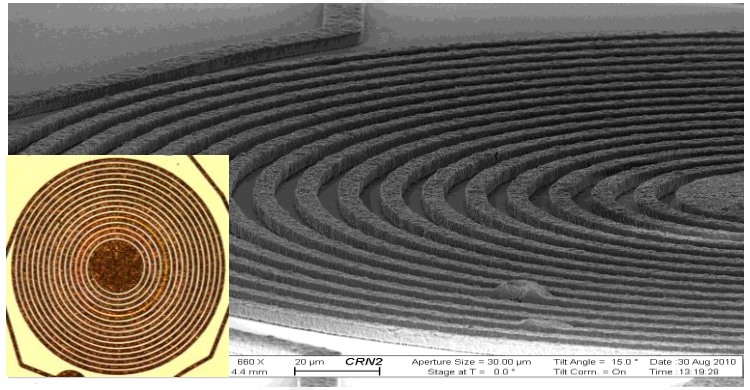

Figure 1 – Image SEM et optique d'une bobine de 400µm de diamètre

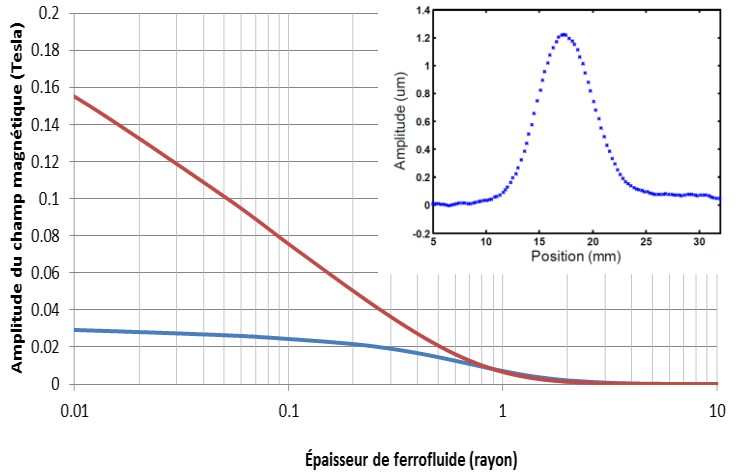

Figure 2 –Amplitude du champ magnétique selon l'épaisseur de ferrofluide pour une bobine planaire.Mesure d'une déformation créée par une bobine planaire de 4.8mm de diamètre (droite)

[Références] Références
[1] Brousseau, D. (2008). Comportement spatial de miroirs déformables à base de liquide magnétique. Doctorat en physique, Faculté des études supérieures de l'Université Laval, Québec

Carbon nanotube-based solar collectors for solar-thermal and photovoltaic applications

Nathan Hordy[*1], Larissa Jorge [1], Sylvain Coulombe[1], Jean-Luc Meunier[1]*

[1]*Plasma Processing Laboratory - PPL, Department of Chemical Engineering, McGill University, Montreal, QC, Canada*

Keywords: Carbon nanotubes, solar thermal, photovoltaics, quantum dots

With consumer demand expected to double in the next 40 years, there is no doubt that energy will be one of the most important issues of the 21st century. However, as concerns for global warming continue to grow, traditional energy supplies, such as fossil fuels, will need to be replaced by clean and renewable alternatives. Solar energy, given its abundance and global availability, is a natural choice to help meet the demands of our energy-hungry world. The Sun's radiation can be converted into two useful forms of energy: heat and electricity. Solar thermal collectors, which generate heat, and photovoltaics (PV) that generate electricity, are currently used world-wide in applications ranging from hot water heating to large scale electricity production. Both of these methods of energy production are considered promising, but currently are hampered by high costs and low conversion efficiencies. In this work we propose the use of CNT nanofluids as direct solar thermal collectors and decorated CNT arrays for enhanced PV applications. The large surface area and unique properties of CNTs lead to an improvement in collection efficiency and reduction in material costs. In solar thermal processes, a nanofluid can act as both a volumetric solar collector and the heat transfer fluid. For PV, a 3-D CNT array offers a large surface area for deposition of semiconductor quantum dots and a highly conductive material for efficient electron transport. Different decorating methods are being explored, such as laser ablation and chemical vapor deposition, to reduce the use of toxic chemicals and the number of processing steps. In this poster, we present an overview of the Plasma Processing Laboratory synthesis capabilities for functionalized CNTs, stable CNT nanofluids, and CNT-based heteronanostructures (e.g. CdSe quantum dots decorated CNTs) for solar applications.

Fast Non-Volatile Memristive Memory on CMOS

C. Nauenheim[1,2], M. Moretti-Poisson[1], S. Ecoffey[2], A. Lecestre[2], A. Ruediger[1], D. Drouin[2]

[1]INRS-EMT, 1650 bld. Lionel Boulet, Varennes, Canada, J3X 1S2
[2]3IT, Université de Sherbrooke, 2500 bld. de l'Université, Sherbrooke, J1K 2R1

Keywords : nanofabrication, resistance switching, resistance random access memory, 1R1T architecture

Resistance switching thin films provide the basis for a memory system that offers a high storage density due to a small foot print of 4 F^2 (minimum feature size) and a low energy consumption mutually dependent by its non-volatility. TiO_2 is a commonly accepted prototype material for the application in future Resistance Random Access Memories and is generally recognized as 'memristor' [1, 2]. It is compatible to existing Si technology, offers small fabrication costs and has no environmental impact. Notably, it features write times that are essentially smaller than those of modern FLASH memories in combination with multiple memory levels per storage cell, as shown in Fig.1. The SEM picture in Fig.2 images a device that is defined by a junction of two 100 nm wide Pt, respectively Ti metal lines sandwiching a 30 nm thick TiO_2 layer. Physically and technically, this concept allows a downsizing to several ten nanometers. However, the fabricated cells show a reliable and reproducible resistance state change as a response to 10 ns pulses with a total resistance ration of 2-3 orders of magnitude (Fig.1) [3]. As this layer stack is not depending on epitaxial growth or a high temperature margin, it is our intention to attach these memory cells directly on a CMOS system, which provides direct addressing and information read-out. This solution presents a short and mid-term solution for non-volatile solid state memory, especially for low power mobile applications, and circumvents the need of a complex operation layer for passive memory crossbar arrays.

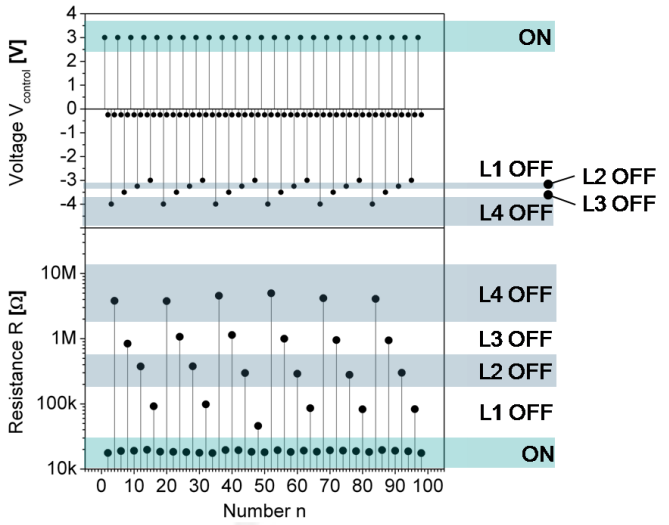

Figure 1 – Multilevel resistance switching caused by 10 ns pulses. The upper graph presents the operation voltages and the lower graph the resistance levels indicating the stored information [3].

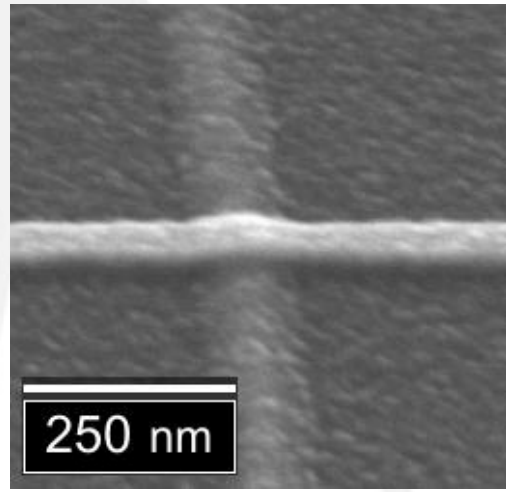

Figure 2 – SEM image of a single resistively switching junction creating a 0.01 µm² large memory cell.

References
[1] L. Chua, Appl. Phys. A 102, 765 (2011).
[2] J.J. Yang, et al., Nature Nanotechnol. 3, 429 (2008).
[3] C. Nauenheim, et al., ULIS 2009, 135 (2009).

Structuration de couches minces de $Ca_xBa_{1-x}Nb_2O_6$ par gravure plasma.

S. Vigne[1], J. Munoz[2], S. Delprat[1], J. Margot[2], M. Chaker[1]*

[1] Laboratoire de Micro et Nanofabrication, INRS-EMT, Varennes, Canada, J3X1S2
[2]Département de Physique, Université de Montréal, Montréal, Canada, H3C 3J7

Mots clés : Gravure plasma ICP, électro-optique, CBN

Le $Ca_xBa_{1-x}Nb_2O_6$ (CBN-x), est un matériau électro-optique comparable au $LiNbO_3$ mais avec des propriétés électro-optiques supérieures (1). La structuration des couches minces de ce matériau est un défi important pour réaliser des composants optiques. En ce sens, une étude systématique de la gravure du CBN par plasma a été réalisée. La gravure du CBN a été étudiée suivant différents paramètres : la nature du mélange de gaz, la température ainsi que l'énergie des ions dans le plasma. Il est montré que ce matériau est très inerte à la chimie du plasma (chloré ou fluoré), quelque soit la température (Figure 1) et l'énergie des ions. En comparant les expériences réalisées avec des modèles théoriques de gravure (2), il est prouvé que la gravure du CBN par plasma est principalement physique dans tous les cas. La verticalité des parois est critique pour des applications optiques. Son évolution en fonction de la température et du mélange de gaz a donc été observée. Le masque de gravure a été réalisé en nickel, matériau très résistant. À température ambiante, les angles des parois du CBN sont proches des valeurs habituelles de gravure physique tandis qu'à plus haute température, une réaction chimique renforce le masque de nickel. Ceci redresse les parois jusqu'à près de 80° pour les conditions optimales (Figure 2). Si elle est étendue à la gravure d'autres matériaux inertes et/ou difficiles à graver, les profils de gravure pourraient être améliorés.

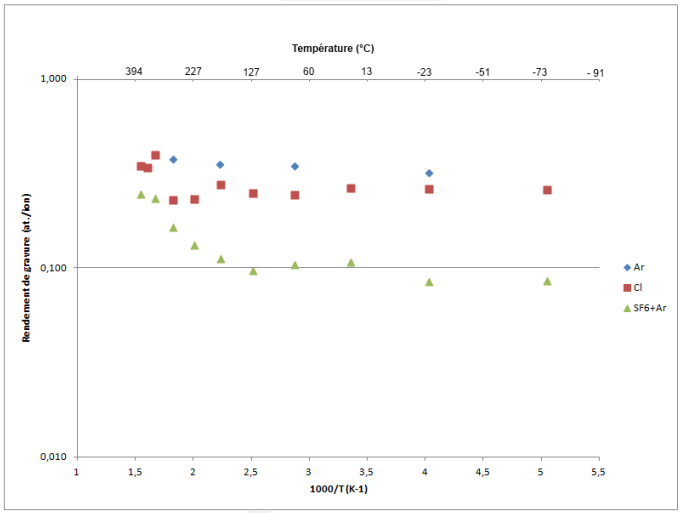

Figure 1 – Rendement de gravure du CBN en fonction de la température pour différents plasmas

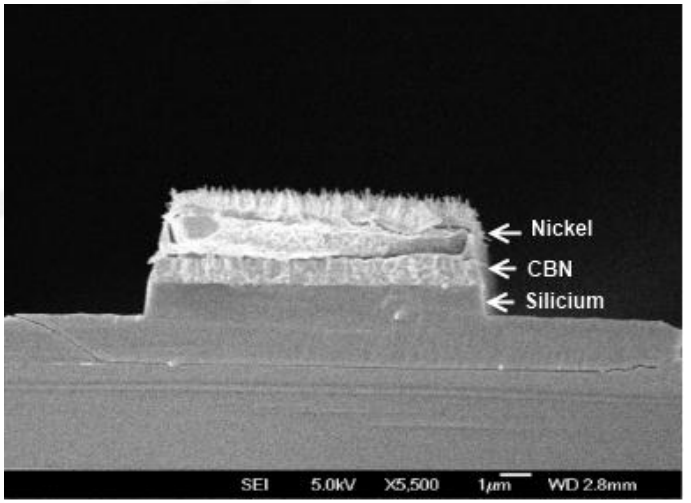

Figure 2 – Parois de gravure à haute température

Références
1[] *Pockels response in Calcium barium niobate thin films.* R. Helsten, L. Razzari, M. Ferrera, P.F. Ndione, M.Gaidi, C. Durand, M. Chaker, R. Morandotti. 2007, Applied Physics Letters, Vol. 91, p. 261101.
[2] Y. Yamamura, Y. Itikawa, N. Itoh. *Angular Dependance of sputtering Yields of monoatomic solids.* Nagoya, Japan : s.n., 1983. IPPJ-AMReport.

Self-Assembly of Polymer Nanowires for Efficient Plastic Solar Cells

B.J. Worfolk[1,2], W. Li[1,2], K.D. Harris[2], J.M. Buriak[1,2]*

[1]Department of Chemistry, University of Alberta, Edmonton, Alberta, Canada, T6G 2G2
[2]National Institute for Nanotechnology, Edmonton, Alberta, Canada, T6G 2M9

Keywords: nanotechnology, plastic solar cells, hole transport layer, carboxylated polythiophenes, concentration gradients

The global energy demand is rapidly increasing, as a result of growing population and economic wealth. It is projected that by the year 2050, the earth's energy demand will double, straining global energy availability.[1] It is critical that both inexpensive and carbon-neutral energy sources are investigated to complement traditional energy sources. Plastic solar cells (PSCs) have the potential to provide inexpensive and reliable power with significantly reduced manufacturing and installation costs.[2] Typically, PSCs consists of two electrodes: a transparent anode for the collection of holes and a reflective cathode for electron extraction. A bulk heterojunction photoactive layer is used for photon absorption and charge generation, while interfacial layers between the electrodes and photoactive layer allow efficient extraction of charges. The hole transport layer (HTL) is commonly applied to transparent indium tin oxide (ITO) anodes (Figure 1a), and this layer reduces the energetic hole extraction barrier, blocks electrons and improves interfacial roughness. A conjugated regioregular carboxylated polythiophene (P3CPenT), is introduced as an HTL for PSCs.[3,4] P3CPenT rapidly self-assembles into nanowires in solution (Figure 1b). These NWs can be cast as a film on ITO, reducing concentration gradients of the subsequent photoactive layer (Figure 1c). PSCs incorporating P3CPenT NWs as the HTL have a higher fill factor (FF, 0.67) and power conversion efficiency (PCE, 3.7%) compared to devices with conventional PEDOT:PSS. We propose that using a carboxylated derivative of the conjugated donor material as an HTL is a general strategy for energetic matching and improved morphology in plastic solar cells.

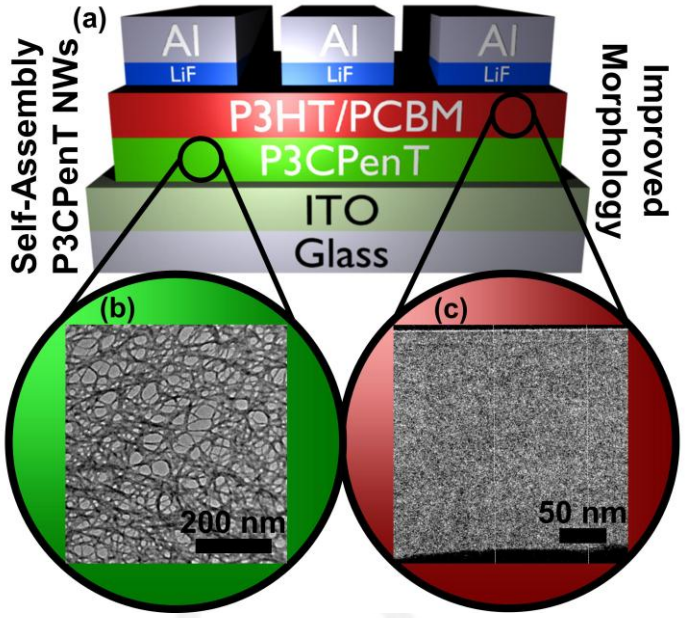

Figure 1 – (a) The PSC device architecture, (b) a transmission electron microscope (TEM) image of self-assembled polymeric nanowires, and (c) cross-sectional TEM analysis of the P3HT/PCBM photoactive layer morphology.

References
[1] N.S. Lewis and D.G. Nocera. *Proc. Nat. Acad. Sci. U.S.A.*, 103, 15729, **2006.**
[2] T.D. Nielsen, C. Cruickshank, S. Foged, J. Thorsen and F.C. Krebs. *Sol. Energy Mater. Sol. Cells, 94,* 1553*,* **2010**.
[3] B.J. Worfolk, D.A. Rider, A.L. Elias, M. Thomas, K.D. Harris and J.M. Buriak. *Adv. Funct. Mater.*, 21, 1816, **2011**.
[4] B.J. Worfolk, W. Li, P. Li, T.C. Hauger, K.D. Harris and J.M. Buriak. *Submitted to J. Mater. Chem.*, Manuscript #JM-ART-01-2012-030576 , **2012.**

Air-Stable and Efficient Inverted Low Bandgap Plastic Solar Cells

B.J. Worfolk[1,2], T.C. Hauger[1,2], K.D. Harris[2], M. Leclerc[3], J.M. Buriak[1,2]*

[1]Department of Chemistry, University of Alberta, Edmonton, Alberta, Canada, T6G 2G2
[2]National Institute for Nanotechnology, Edmonton, Alberta, Canada, T6G 2M9
[3]Département de Chimie, Université Laval, Quebec City, Quebec, Canada, G1V 0A6

Keywords: nanotechnology, plastic solar cells, air stable, low bandgap polymers, air stable

Solar energy is a widely abundant resource. In fact, there is sufficient sunlight hitting the earth in 1 hour to power the entire planet for an entire year.[1] Alberta and western Canada have greater photovoltaic (PV) potential than many PV leading countries such as Germany and Japan. In order to fully utilize this abundant resource, solar panel material and installation costs must be significantly reduced to reach grid parity, making PVs a cost competitive energy source to consumers. Plastic solar cells (PSCs) have the potential to generate low-cost renewable energy as a result of solution processing and scalable manufacturing using roll-to-roll printing.[2] A major challenge for the commercialization and widespread adoption of PSCs is short lifetimes with many degradation pathways. One major contributor to the degradation of PSCs is poly(3,4-ethylenedioxythiophene):poly(*p*-styrenesulfonate) (PEDOT:PSS), a common anodic buffer layer, which can etch electrodes and migrate throughout devices. Electrostatic layer-by-layer (eLbL) nanoscale assembly of anionic PEDOT:PSS and cationic polythiophenes (Figure 1a) can stabilize PEDOT:PSS components, leading to longer PSCs lifetimes. These films serve as polymeric cathodic buffer layers for inverted-mode PSCs (Figure 1b).[3,4] We demonstrate long-term stability of poly[(3-hexylthiophene)-2,5-diyl] (P3HT):6,6-phenyl-C_{61}-butyric acid methyl ester ($PC_{61}BM$) PSCs under encapsulation for 10,000 h and air stable low bandgap polymer:$PC_{71}BM$ devices for over 1500 h. PV devices with the latter architecture achieved power conversion efficiencies of over 5.6% and present a bright future for both efficient and stable plastic solar cells.

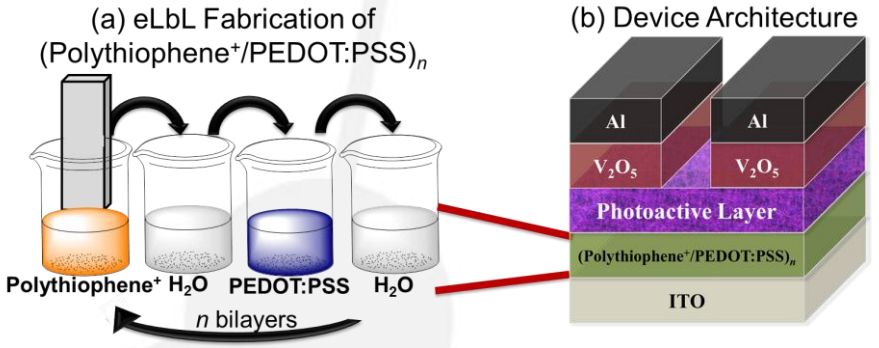

Figure 1 – (a) The eLbL fabrication process of polymeric thin films, and (b) the PSC inverted device architecture.

References
[1] N.S. Lewis and D.G. Nocera. *Proc. Nat. Acad. Sci. U.S.A.*, 103, 15729, **2006.**
[2] T.D. Nielsen, C. Cruickshank, S. Foged, J. Thorsen and F.C. Krebs. *Sol. Energy Mater. Sol. Cells, 94,* 1553*,* **2010**.
[3] D.A. Rider, B.J. Worfolk, K.D. Harris, A. Lalany, K. Shahbazi, M.D. Fleischauer, M.J. Brett and J.M. Buriak. *Adv. Funct. Mater.*, 20, 2404, **2010**.
[4] B.J. Worfolk, T.C. Hauger, K.D. Harris, D.A. Rider, J.A.M. Fordyce, S. Beaupré, M. Leclerc and J.M. Buriak. *Adv. Energy. Mater.*, In Press, DOI: 10.1002/aenm.201100714, **2012**.

Nanoplasmonics from Marine Diatoms

A.R Hajiaboli[1], J. Hiltz[1], G. Singh[1], T. Gonzalez[1], E.lowe-Dacarie[2], G. fussmann[2], R.B. Lennox[1], M. P. Andrews[1]

[1] Chemistry Department, McGill University, Montreal, Canada
[2] Biology Department, McGill University, Montreal, Canada

Keywords: Nanophotonics, Diatoms, Nitzschia Palea, FDTD, Biotemplate

Marine diatoms are single cell phytoplankton that are responsible for a significant percent of the global oxygen supply. They are striking for their magnificent hierarchies of periodic patterns of pores that are structured over nanometer to micrometer length scales in the biogenic silica comprising the exoskeleton shell (frustule) of the organism. Species dependent patterns generated by the more than 200 000 kinds of diatoms have attracted the interest of nano- and materials scientists. The frustule offers a renewable, biotemplate for developing nanostructured materials. Among the diatoms, *Nitzschia palea* exhibits a complex frustule topography that resembles the warp and weft pattern of woven glass. In this work, we present techniques to make nanoplasmonic structures by solid-state dewetting of thin films of gold on *Nitzschia* frustules. The spatial distribution and morphologies of the resulting plasmonic features are strongly determined by frustule topography. The latter is the source of curvature instabilities for dewetting, while the pores and valleys provide periodic trapping sites for nanoparticles. The outcome of dewetting events is revealed through combinations of SEM and AFM and numerical calculation. With full wave 3D-FDTD calculations, we analyze optical properties and waveguiding characteristics of the woven frustules. Our calculations reveal that the frustule may function as a defusing medium for guiding and propagating light. We conjecture a possible evolutionary role for the patterned silica frustule in photosynthesis.

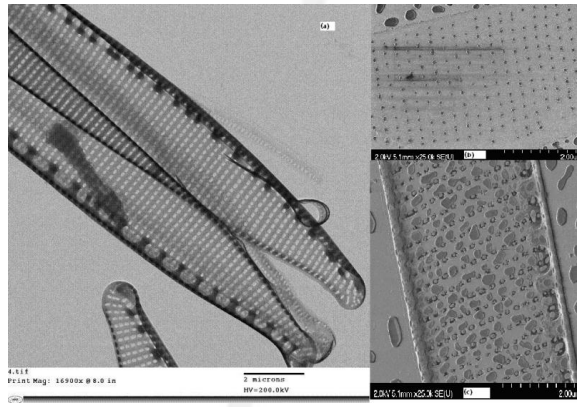

Figure 1 – (a) TEM image of Nitzschia Palea, (b) and (c) are SEM images of structure after dewetting of 10 nm gold films in 550° C for 60 minutes and in 600° C for 120 minutes respectively.

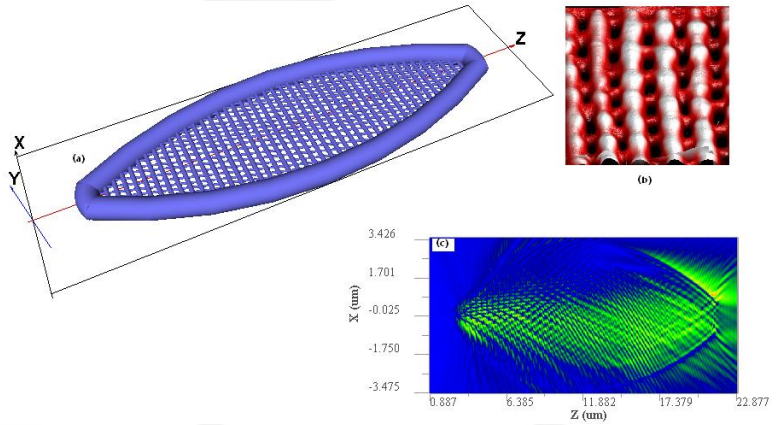

Figure 2 – (a) 3D schematic of the frustule that exhibits the rhombic lattice of Weft and warp strips, (b) AFM image of Frustule of Nitzschia Palea , (c) Electromagnetic field distribution due to excitation of small aperture UV-NIR broadband source from left to right direction. The schematic shows intensity of the H_y field from top view.

Références
[1] Ostiguy, C. et al. (2009). “A good practice guide for safe work with nanoparticles: the Quebec approach.” J. Phys. Conf. Ser. **151**.
[2] Déclaration universelle sur la bioéthique et les droits de l’homme, http://portal.unesco.org/fr/ev.php-URL_ID=31058&URL_DO=DO_TOPIC&URL_SECTION=201.html
[3] Rapport de la Commission Européenne en vue d’une définition des nanomatériaux, http://eur-lex.europa.eu/LexUriServ/LexUriServ.do?uri=OJ:L:2011:275:0038:0040:EN:PDF,

Transfert de charge induit dans des nanorubans de graphène par une modification de l'environnement

C. Archambault[*1], *A. Rochefort*[1]

[1]Département de génie physique, École Polytechnique de Montréal, C.P. 6079, Succursale Centre-ville, Montréal, Québec, H3C 3A7

Mots clés : graphène, nanorubans, transfert de charge

Le graphène est un matériau très prometteur en électronique à cause de sa très grande mobilité électronique. La conception de dispositifs requiert par contre un matériau semiconducteur plutôt qu'un semi-métal comme le graphène. Heureusement, il devient semiconducteur lorsqu'il est sous forme de nanorubans [1, 2]. Ainsi, des transistors constitués de tels rubans entre deux électrodes métalliques ont déjà vu le jour [3, 4]. Les interactions électroniques entre un ruban et des contacts métalliques, qui peuvent s'avérer critiques à une aussi petite échelle de grandeur, demeurent toutefois méconnues.Dans cette optique, nous présentons les résultats de calculs de structure électronique, basés sur la théorie de la fonctionnelle de la densité (DFT), de nanorubans finis en contact avec des électrodes d'or. Il a été possible de mettre en évidence l'hybridation des orbitales frontières du graphène avec les états métalliques. De plus, on observe un transfert de charge du graphène vers le métal qui s'étend au-delà de la région située immédiatement sous les contacts. Dans le cas des rubans à bordures zigzag, le transfert de charge s'effectue principalement via les états de bord des nanorubans. Dans un autre ordre d'idées, on peut aussi envisager de tirer profit de la présence d'une couche moléculaire auto-assemblée sur le graphène pour doper le nanoruban, mais aussi pour former un canal de conduction additionnel. Nos premiers calculs montrent que la nature chimique de la couche semble plus importante que la structure du nanoruban de graphène sur l'ordre de grandeur du dopage.

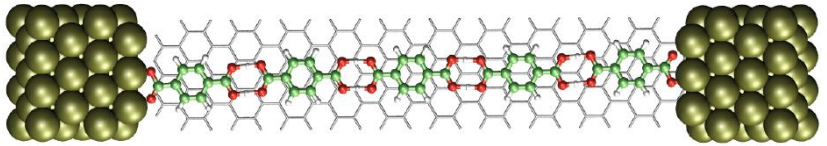

Figure 1 – Pentamère d'acide téréphtalique adsorbé sur un ruban de graphène entre deux contacts métalliques.

Références
[1] K. Nakada, M. Fujita, G. Dresselhaus et M. Dresselhaus, Phys. Rev. B **54**, 17954 (1996).
[2] M. Han, B. Özyilmaz, Y. Zhang et P. Kim, Phys. Rev. Lett. **98**, 206805 (2007).
[3] X. Wang, Y. Ouyang, X. Li, H. Wang, J. Guo et H. Dai, Phys. Rev. Lett. **100**, 206803 (2008).
[4] Z. Chen, Y.-M. Lin, M. J. Rooks, P. Avouris, Physica E **40**, 228 (2007).

Étude de la mécanique des fluides classique et quantique à l'échelle du nanomètre

G. Dauphinais[1], M. Savard[1], S. Neale[1], et G.Gervais[1]

[1]Département de physique de l'Université McGill, Ernest Rutherford building, Université McGill, 3600 rue University, Montréal, Canada, H3A 2T8

Mots clés : Nanofluidique quantique, Nanofabrication, Microscopie électronique en transmission (MET)

À l'échelle nanométrique, on peut se demander si les lois régissant la dynamique des fluides sont les mêmes que pour l'écoulement des fluides à notre échelle. De fait, nous avons des raisons de penser que dans le cas d'un fluide classique, l'écoulement à travers une structure nanométrique peut différer de celle à plus haute échelle (par exemple, l'absence notoire de turbulence à petite échelle). Dans le cas quantique, il est prédit que l'hélium liquide devienne un "un liquide de Luttinger" dans des structures de 2nm de diamètre [1]. Cet état liquide, prédit depuis les années 50, correspond à l'état fondamental d'un fluide quantique en une dimension. Afin d'étudier ces questions, des nano-pores ont été fabriqués dans de minces couches suspendues de nitrure de silicium amorphe. En utilisant un faisceau d'électrons focalisés par microscopie électronique en transmission (MET), des diamètres entre 0.7 nm et 100 nm ont été atteints. La relaxation structurelle de nano-pores fabriqués par faisceau focalisé d'électrons a été observée. Dépendamment du diamètre initial du nano-pore et de sa longueur, deux phases distinctes ont été identifiées. Un montage expérimental permettant la mesure de l'écoulement de masse d'hélium causé par l'application d'une différence de pression a été réalisé. La mesure de conductance de nano-pores ayant un diamètre compris entre 25 nm et 315 nm a été effectuée [2]. Nous avons également mesuré l'écoulement de l'hélium superfluide à travers une nanostructure de 40 nm de diamètre et nous en avons extrait les vitesses d'écoulement critiques [3], une étape intermédiaire nécessaire avant d'entreprendre l'étude de nanostructures avec des diamètres de l'ordre du nanomètre. Finalement, les prochaines avenues de recherche ouvertes par ces travaux, ainsi que la nano-fabrication utilisant un MET seront discutées.

Références

[1] Helium-4 Luttinger Liquids in Nanopores, Adrian Del Maestro, Massimo Boninsegni, and Ian Affleck, Phys. Rev. Lett. 106, 105303 (2011).

[2] Flow Conductance of a Single Nanohole, M. Savard, C. Tremblay-Darveau and G. Gervais, Phys. Rev. Lett. 103 , 104502 (2009).

[3] Hydrodynamics of Superfluid Helium in a Single Nanohole, M. Savard, G. Dauphinais and G. Gervais, Phys. Rev. Lett. 107, 254501 (2011). Selectionné en tant qu' "Editor's suggestion".

Transfert biomimétique : de la luciole vers la diode électroluminescente

N. André[1], L. A. Francis[1,3], A. Giguère[1], A. Bay[2], J.-P. Vigneron[2], V. Aimez[1]

[1]CRN², Université de Sherbrooke, Sherbrooke (Canada)
[2]Groupe de Photonique du Vivant, FUNDP, Namur (Belgique)
[3]ICTEAM, UCL, Louvain-la-Neuve (Belgique)

Mots clés : DEL, biomimétisme, extraction de lumière, lithographie par écriture directe

Autrefois reléguées à des marchés ciblés et de faible volume, les diodes électroluminescentes (DELs) révolutionnent toutefois déjà le monde de l'éclairage grâce à la spectaculaire croissance de leur efficacité énergétique et leur durée de vie record. Les projections annoncent des avancées technologues majeures concernant les DELs d'ici à 2025 [1]. Cependant, plusieurs problèmes technologiques limitent l'efficacité d'extraction de photons des DELs en raison de l'emplacement de la zone radiative : se trouvant à l'intérieur du semiconducteur, une majorité de photons restent piégés au sein de la diode [2]-[3]. Dans ce travail, nous visons à augmenter l'extraction des photons dans les DELs à base de nitrure de gallium (GaN) au départ d'une photonique bio-inspirée. Comme modèle, la structure des écailles de la paroi de l'abdomen des lucioles a été identifiée par simulation comme étant à l'origine d'une amélioration de 75% de l'extraction lumineuse de l'insecte [4]. Ces écailles forment des prismes juxtaposés de dimensions micrométriques présentant une géométrie en « toits d'usine » (Fig. 1). Cette géométrie naturelle est ensuite adaptée pour correspondre à la différence de longueur d'onde d'émission et d'indice de réfraction rencontrée dans les diodes GaN. En ce sens, nous avons reproduit la géométrie spécifique de l'abdomen des lucioles par lithographie en 3 dimensions à partir d'une écriture laser directe dans la photorésine (Fig. 2). L'impact de la structuration de surface est ensuite évalué par une étude macroscopique moyenne fournissant la dépendance entre la puissance électrique et l'émission optique.

Fig. 1 : Structuration de la surface de l'abdomen d'une luciole, avec coupe transversale de la paroi.

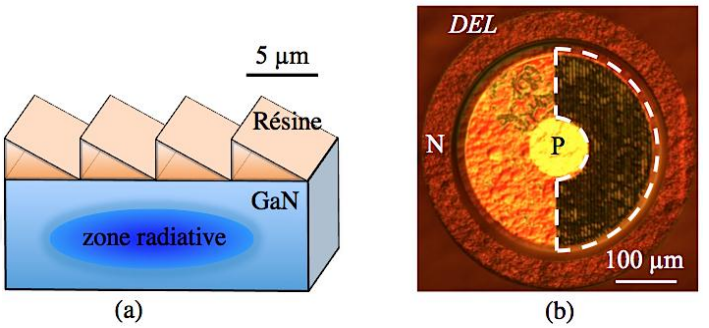

Fig. 2 : Structuration de la surface d'une DEL à base de nitrure de gallium (GaN) par écriture directe dans la photorésine : (a) schéma et (b) réalisation de principe.

Références
[1] U.S. Department of Energy, Technology Roadmap, 2010.
[2] S. Pimputkar *et al.,* Nature Photonics, **3,** 180-182, 2009.
[3] A. I. Zhmakin, Physics Reports, **498**, 189–241, 2011.
[4] A. Bay *et al.*, Proceedings of SPIE, **7401**, 740108-740119, 2009.

Building foundations for nanoelectronics: growth of ultra-thin insulating films on iron surfaces

Antoni Tekiel, Jessica Topple, Peter Grütter*

Department of Physics, McGill University, Montreal, H3A 2T8, Canada

Keywords : Ultra-thin insulatin films, nanoelectroni devices, atomic force microscopy

Thin insulating films of metal oxides and alkali halides grown on a variety of metal substrates, such as Ag(001), Mo(001) and Fe(001), attract considerable attention due to applications in heterogeneous catalysis and magnetoelectronic devices. Insulator-on-metal systems are also ideal model systems for nanoelectronic applications where a molecular device located on the surface can be controlled by electric field induced by the back electrode. However, well-defined and fully crystalline MgO thin layers are difficult to fabricate and are usually oxygen deficient. Currently there is no system described where the film could be grown with small number of defects in a layer-by-layer mode allowing for full control of thickness and uniformity.In this work we use ultra-high vacuum noncontact atomic force microscopy (NC-AFM), Kelvin probe force microscopy (KPFM) and low energy electron diffraction (LEED) to investigate the morphology of MgO films (prepared by reactive deposition method) and NaCl films grown on Fe(001) surfaces. We demonstrate that NaCl can be grown in a layer-by-layer mode providing atomically flat films with much less defects than the MgO films, and thus is a very promising material for developing crystalline insulating ultra-thin films. We present results of 0.75-10 ML thick films grown under various conditions and discuss their possible applications in nanoelectronic devices.

One-step Passivation of Silicon Nanocrystals in a Silica Matrix by Pulsed Laser Deposition

D. Soubane [1], R. Nechache [1,3], A. Dadvand [2] and F. Rosei [1]

[1]Institut National de la Recherche Scientifique, Centre Energie, Matériaux et Télécommunications Varennes Québec J3X 1S2 (Canada)
[2]Department of Chemistry McGill University Montreal, Québec, H3A 2K6 (Canada)
[3] NAST Center & Department of Chemical Science and Technology, University of Rome Tor Vergata, Via della Ricerca Sceintifica 1, 00133 Rome (Italy)

Keywords: Novel approach, Anneal-free process, Photo-luminescent Si-ncs, passivation, optical gain

Many years after the fabrication of the first transistor, bulk silicon crystal still monopolizes microelectronic, photovoltaic and MEMS technologies. So far, due to its indirect band gap, photonic industry is restricted to direct-band gap III-V materials. Fortunately, at nanoscale silicon shows amazing features [1-3]. Hence, a sparking hope has risen to keep evolution of Moore and beyond-Moore law. The advantage of silicon based photonics is its ability to adapt elegantly to complementary metal-oxide-semiconductor technology except it suffers from problems such as high temperature silicon nanocrystals (Si-ncs/SiO_2) processing which involves further constraints to the integration of Si-ncs in photonics devices. For this reason, special effort has been devoted to find out a way to form Si-ncs/SiO_2 at lower temperature and subsequently simplify the integration of Si-ncs in waveguide and light generation applications [4]. The current work is an ideal response to such a technological issue. In effect, with our novel approach we have shown that it is possible to crystallize Si-ncs in a silica matrix at lower temperatures (cf figure 1). This finding will help opening a pathway to all-in Si-photonic and telecommunication technology. Using laser pulsing technique, we succeeded, to confine and rapidly passivate Si-ncs within silica. X-ray diffraction and Raman spectroscopy measurements reveal the formation of silicon nanocrystals and silica. Moreover, via optical process modeling, we have shown ~470 and 970 meV upper-shift from Si-bulk band gap, highlighting then the quantum confinement effect for the freshly grown and annealed Si-ncs/SiO_2, respectively. Importantly cool Si-ncs show a potential for optical gain in the near infra-red (NIR) region (cf Fig. 2).

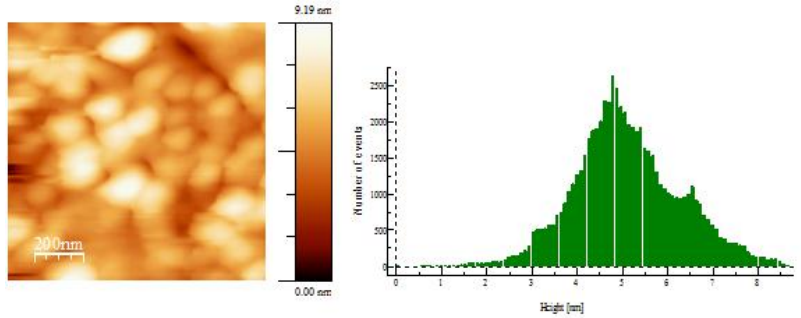

Figure 1: right: AFM surface morphology of heat treated sample ((3.10^{-5} Torr) left: size distribution of Si-annealed ncs/SiO_2

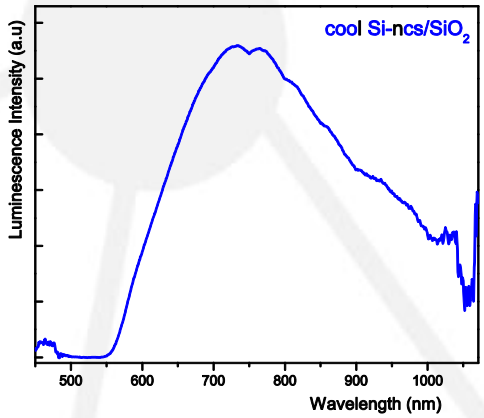

Figure 2: Room temperature photoluminescence spectrum of anneal-free Si-ncs/SiO_2 grown by pulsed laser deposition at oxygen partial pressure 7.3.10^{-4} torr.

References
[1] L. T. Canham, Appl. Phys. Lett. 57, 1046
[2] N. Daldosso and L. Pavesi Chap.1 Silicon photonics Edit. L. Khriatchev World Scientific Publishing Co. Pte. Ltd. 2009
[3] L. Pavesi, L. Dal Negro, C. Mazzoleni, G. Franzo, F. Priolo, Nature 408, 23, 2000
[4] J. Wang, X. F. Wang, Q. Li, A. Hryciw, A. Meldrum, Phil. Magazine, 87:1, 11-27, 2007

Simulateur rapide « particle-in-cell » de procédés de nano fabrication.

M. Laberge[*1], J. Margot[1], M. Chaker[2]*

[1]Département de physique, Université de Montréal, Montréal (Québec), Canada
[2]INRS-Énergie, matériaux et Télécommunications, Varennes (Québec), Canada

Mots clés : plasma, gravure, dépôt, particle-in-cell, couche mince

La géométrie finale des couches minces après gravure ou dépôt est fortement influencée par la formation de nanostructures tout au long du procédé. En lien avec l'avancée rapide de la réduction de la taille des composantes, des processus physiques négligeables à plus grande échelle deviennent dominants lorsque la taille des profils s'approche de l'échelle nanométrique. L'identification et la meilleure compréhension de ces différents processus sont essentielles pour améliorer le contrôle des procédés et poursuivre la « nanométrisation » des composants des dispositifs électroniques. Un simulateur de type particle-in-cell (PIC) en deux dimensions, s'appuyant sur les méthodes Monte-Carlo (MC), a été développé pour étudier l'évolution initiale du profil lors de procédés de nano fabrication. Le domaine de gravure est discrétisé en cellules carrées représentant la géométrie initiale du masque et du système. L'injection de particules se fait à l'aide de l'intégration par méthode (MC) des différentes distributions en énergie, en angle et en flux des espèces considérées pour les procédés simulés. La modélisation (MC) de l'interaction des différentes espèces avec la surface permet de simuler les divers mécanismes de gravures sèches tels que la pulvérisation, la gravure chimique réactive et la gravure réactive ionique. Le modèle permet également la simulation de systèmes de dépôt de couche mince, comme le dépôt en phase vapeur et le dépôt par faisceau d'ions. Des comparaisons entre les simulations de pulvérisation du Pt par un plasma d'Ar, ainsi que la gravure réactive de Si par Cl_2 seront présentées. Finalement, les effets du bombardement ionique de faible énergie lors du dépôt en phase vapeur pour le remplissage de tranchées nanométriques sera abordé.

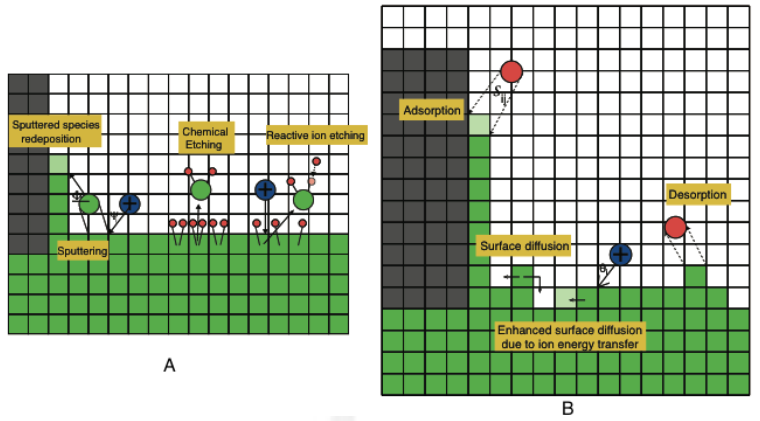

Figure 1 – Schématisation des trois mécanismes principaux de gravure simulée (A) et des différents processus de surface pris en compte par le simulateur (B)

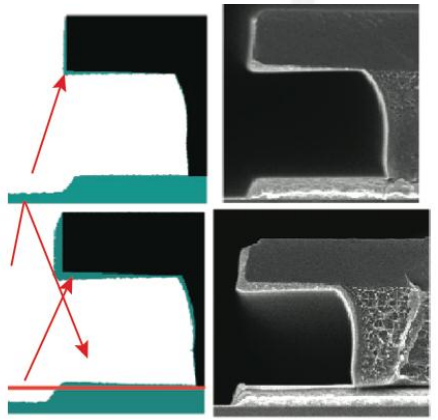

Figure 2 –La simulation d'un profil de gravure de platine par un plasma d'argon de haute densité reproduit bien à la fois la tranchée gravée et le redépôt des espèces pulvérisées.

References
[1] N. Mizutani and T. Hayashi, Journal of Vacuum Science & Technology A: Vacuum, Surfaces, and Films 19, 1298 (2001)
[2] T.P. Schulze, Efficient Kinetic Monte Carlo Simulation, October (2007)
[3] L. Zhang and Z. Zhang, Radiation Effects and Defects in Solids 160, 337-347 (2005)
[4] Z. L. Zhang and L. Zhang, Radiation Effects and Defects in Solids 159, 301-307 (2004)
[5] J. Saussac, Ph.D. dissertation, Université de Montréal (2009)
[6] S. Delprat, M.C. Haker, and J .Margot, Japanese Journal of Applied Physics 38, 4488-4491 (1999)
[7] S. Delprat, M. Chaker, and J. Margot, J. Appl. Phys. 89, 29 (2001)
[8] S. L. Lai, D. Johnson, and R. Westerman, J. of Vacuum Science & Technology A: Vacuum, Surfaces, and Films 24, 1283 (2006)

Floating concentration gradients in a microfluidic quadrupole

Mohammad A. Qasaimeh[1], Thomas Gervais[2], and David Juncker[1]

[1]Biomedical Engineering Département and Génome Québec Innovation Centre, McGill Université, Montréal, Québec, H3A 1A4 Canada.
[2]Département of Engineering Physics, École Polytechnique de Montréal, Montréal, Québec, H3C 3A7 Canada.

Mots clés : microfluidics, concentration gradients, quadrupoles

We introduce two new concepts in the field of microfluidics; the microfluidic quadrupole (MQ) and the floating concentration gradients. Also, we developed theoretical framework that describe our experimental observations of these concepts. The MQ is analogous to the two-dimensional electrostatic quadrupole, however, solutes can be added to the MQ giving rise to convection-diffusion phenomena. The MQ was created by simultaneously injecting and aspirating fluids from two pairs of opposing apertures in a narrow gap formed between a microfluidic probe (MFP) [1] and a substrate, Figure 1. A stagnation point (SP) was formed at the center of the quadrupole where the two streams meet head-on. Following the injection of a solute through one of the fluidic poles, a stationary, "floating" concentration gradient formed across the SP and the interface between the two streams, Figure 2. The generated gradients could be used for cell chemotaxis studies and overcome the problem of culturing cells inside microchannels, thereby allowing controlable and predictable chemotaixs studies to be performed within the well-established culture protocols. Furthermore, there is virtually no fluid flow coincident with the SP, thus permitting the study of cell responses caused by the pure concentration gradients. The generated gradients can be rapidly tuned and moved, therefore allowing the study of several cells under various conditions during the same experiment, which increase the throughput. Our results lay the foundation for future theoretical analysis of fluidic multipoles in combination with convective-diffusive mass transport, as well as for the experimental application of MQs and floating gradients [2].

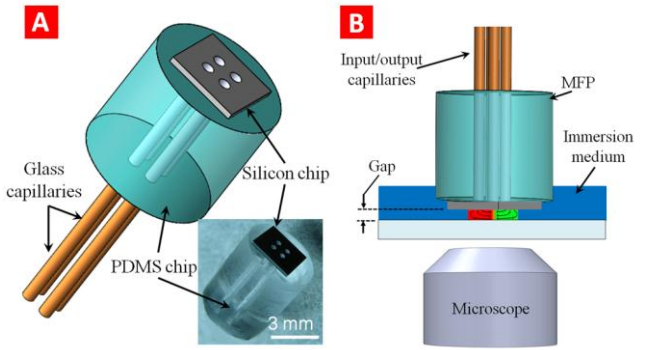

Figure 1 – The developed microfluidic probe (MFP) for generating microfluidic quadrupole and floating concentration gradients. (a) 3D representation of the MFP; it has four apertures that are arranged at the corners of a virtual square. It is fabricated out of a Si chip and a PDMS adaptor. The PDMS adaptor is used to connect each aperture to an independent syringe pump via a glass capillary. A micrograph of the MFP is shown in the inset. (b) The MFP is placed in parallel to the bottom substrate (i.e. cell culture) for forming a narrow gap, while being immersed in the surrounding medium (i.e. cell medium).

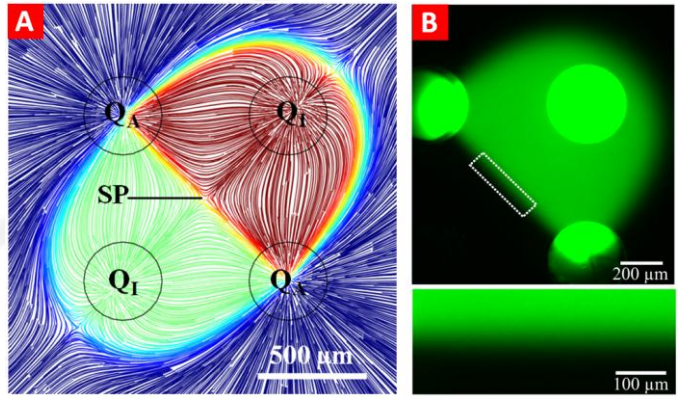

Figure 2 – A microfluidic quadrupole (MQ) and floating concentration gradients. Two opposite apertures of the MFP were used for injections (Q_I = 10 nl/s), and the other two for aspirations (Q_A = 20 nl/s). (A) 3D simulations revealing the quadrupolar flow field, the generated stagnation point (SP), the injected chemicals confinements, and the floating concentration gradients across the SP and all along the interface of the two injected solutions. (B) A micrograph obtained using an inverted microscope showing the generated gradient of fluorescein. Solutions of fluorescein and water alone were injected through the top right and bottom left apertures, respectively, and aspirated back in through the other two apertures. A close up view of the concentration gradient corresponding to the white rectangle is shown in the inset.

Références

[1] D. Juncker, H. Schmid, E. Delamarche. Multipurpose microfluidic probe. *Nat Mater* 4(8):622-628, 2005.
[2] M.A. Qasaimeh, T. Gervais, D. Juncker. Microfluidic quadrupole and floating concentration gradient. *Nat Commun* 2:464, 2011.

Réalisation de structures MOS sur GaN par dépôt PECVD d'oxyde de silicium

A. Chakroun[1], A. Jaouad[1], V. Aimez[1] et R. Arès[1]*

[1]CRN2 : Centre de Recherche en Nanofabrication et Nanocaractérisation, 2500 boulevard de l'université, Sherbrooke, Québec, Canada, J1K 2R1

Mots clés : Nitrure de gallium (GaN), passivation, états de surface, PECVD, MOS

Le nitrure de gallium (GaN) est un matériau semiconducteur à large bande interdite directe qui suscite un intérêt croissant du fait de ses propriétés électriques, thermiques et mécaniques particulièrement attractives. Pour pouvoir profiter pleinement des avantages de ce matériau plusieurs verrous technologiques doivent être surmontés. La réalisation d'une bonne interface isolant/GaN est indispensable pour développer une technologie MOS fiable sur ce matériau. La passivation de la surface du GaN, en vue de réduire la densité des états d'interface et de lever l'ancrage ('pinning') du niveau de Fermi, est une étape majeure pour améliorer les performances et la fiabilité des dispositifs électroniques et optoélectroniques sur GaN. Nous rapportons des résultats expérimentaux sur la passivation de la surface du GaN par dépôt PECVD d'oxyde de silicium (SiO_x). Des capacités métal-oxyde-semiconducteur (MOS) ont été fabriquées sur une couche de n-GaN non intentionnellement dopée (Fig. 1). Les mesures *C-V* montrent une bonne modulation du potentiel de surface, avec un très faible décalage de la tension de bande plate, une faible hystérésis et aucune dispersion notable en fréquence (Fig. 2). En appliquant la méthode de Terman, une faible densité d'états de surface (D_{it}) de l'ordre de 10^{10} $eV^{-1}.cm^{-2}$ est extraite à partir des courbes *C-V* à 1 MHz. Les mesures *I-V* montrent un faible courant de fuite et un champ électrique de claquage supérieur à 5 $MV.cm^{-1}$ [1]. Le procédé de passivation de la surface du GaN par dépôt PECVD d'oxyde de silicium présente un potentiel prometteur pour la réalisation de transistors MOSFETs sur GaN.

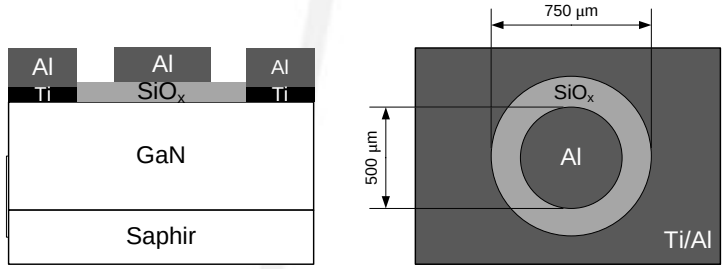

(a) Vue de coupe (b) Vue de dessus

Figure 1 – (a) vue de coupe et (b) vue de dessus des capacités MOS fabriquées.

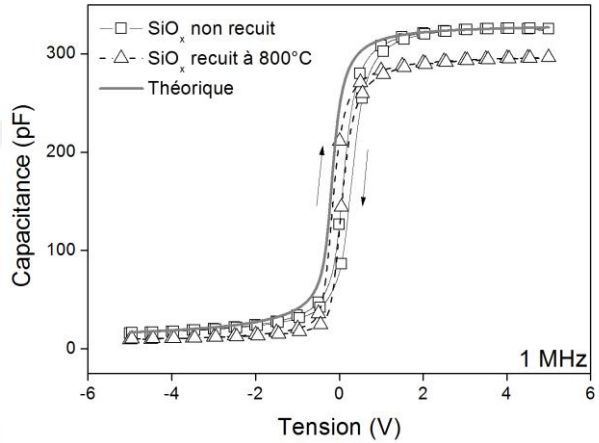

Figure 2 – Caractéristiques *C-V* à 1MHz des capacités MOS fabriquées avec une couche de SiO_x déposée par PECVD.

Références

[1] A. Chakroun, A. Jaouad, A. Giguère, V. Aimez et R. Arès, *IEEE Transactions on Electron Devices, 2012 (soumis)*

Nanofabrication de cages à photon en silicium par un procédé descendant (*top-down*)

G. Beaudin[*1], C. Sieutat[2], P. Rojo Romeo[2], J.-L. Leclercq[2], V. Aimez[1]*

[1]Centre de recherche en nanofabrication et nanocaractérisation (CRN²), Université de Sherbrooke, Sherbrooke, Canada, J1K 2R1
[2]Institut des nanotechnologies de Lyon (INL), Lyon, France

Mots clés : nanosctructure, photonique, procédé Bosch, gravure par plasma à couplage inductif (*ICP*), électrolithographie

Un des buts de la photonique est d'arriver à confiner de la lumière dans le plus petit espace possible aussi longtemps que possible. Ceci est accompli par des dispositifs appelés microcavités. Récemment, un nouveau dispositif a été imaginé pour confiner les photons dans toutes les directions (3D) : la cage à photon [1].
Ce dispositif est un ensemble circulaire de piliers ayant un fort contraste d'indice avec le milieu et dont la hauteur atteint 10 µm pour un diamètre submicronique (voir Figure 1). Bien qu'une méthode ascendante (*bottom-up*), c'est-à-dire de faire croître des piliers, soit envisageable pour fabriquer ces dispositifs, les défis associés sont importants notamment en ce qui concerne la directionalité des piliers. Grâce aux techniques avancées de nanolithographie et de gravure profonde sur silicium, nous avons pu réaliser les structures géométriques requises par la méthode descendante (*top-down*), c'est-à-dire la gravure de piliers.
Étant donné que le silicium possède un indice de réfraction élevé (autour de 3,5), cela permet de réaliser des structures ayant l'effet de confinement optique désiré. Un procédé de triple gravure par plasma à couplage inductif (*ICP*) a été développé pour transférer des motifs nanométriques, écrits par électrolithographie, dans la couche supérieure d'un substrat de silicium-sur-isolant (*SOI*). Cette technique a une grande flexibilité ce qui permet non seulement de fabriquer des cages ayant des piliers circulaires (voir Figure 2), mais également des piliers rectangulaires. De plus, avec cette technique, il est aussi possible d'ajouter d'autres dispositifs photoniques tels que des jonctions « Y ».

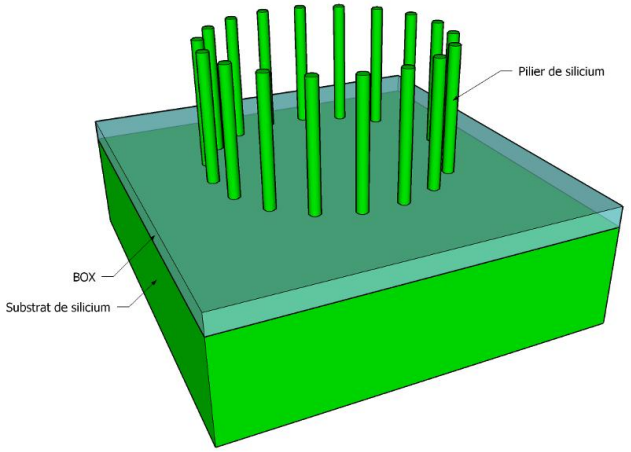

Figure 1 – Schéma 3D d'une cage à photon

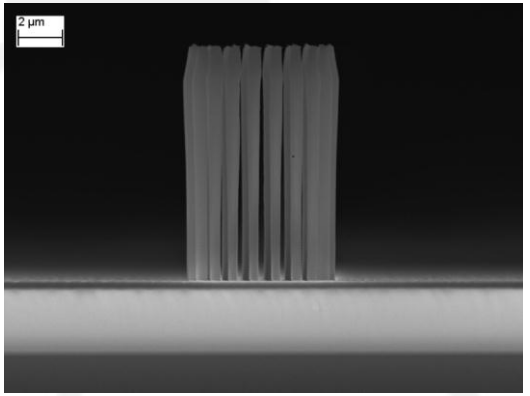

Figure 2 – Photo d'une cage à photon ayant des piliers circulaires fabriquée par un procédé descendant

Références
[1] C. Sieutat, *et al.* (2010) 3D harnessing of light with photon cage, *Proceedings of the SPIE - The International Society for Optical Engineering*, vol. 7712, no. 16, p. 77120E.

Étude de couches minces de Carbone Amorphe Fluoré pour le développement de moules pour la nano-impression

M. Bossard[*1,2], *B. Le Drogoff*[1], *M. Zelsmann*[2], *S. Delprat*[1], *J. Boussey*[2], *M. Chaker*[1]

[1]Laboratoire de Micro et Nano-fabrication – INRS/Centre Énergie, Matériaux et Télécommunications, 1650 Boulevard Lionel Boulet, J3X 1S2 Varennes, Canada
[2]Laboratoire des Technologies de la Microélectronique – CNRS/UJF – Grenoble 1/CEA-LTM, 17 avenue des Martyrs, 38054 Grenoble cedex 9, France

Mots clés : Nano-impression, Lithographie, Matériaux antiadhésifs

La nano-impression assistée par ultraviolets est une technique de lithographie impliquant le contact sous pression d'un moule sur un photopolymère. Les moules sont habituellement faits en silicium ou en silice fondue pour bénéficier des procédés de micro-fabrication issus de la micro-électronique. Néanmoins, l'énergie de surface élevée de ces matériaux limite leur utilisation car les résines utilisées en nano-impression ont tendance à coller aux moules. Des mono-couches fluorées auto-assemblées ont donc été mises au point pour réduire l'énergie de surface des moules et faciliter le démoulage. Toutefois, il a été démontré que ces couches perdent leur efficacité après quelques impressions à cause d'une dégradation par des radicaux libres photo-induits [1].

Le carbone amorphe ou *Diamond-Like Carbon* (DLC) fait partie des matériaux pressentis pour des applications en nano-impression assistée par ultraviolets de par ses propriétés mécaniques, sa transparence aux ultraviolets et son inertie chimique. L'ajout de fluor dans les films permettrait d'exalter les propriétés de surface recherchées pour faciliter le démoulage [2,3].

Nous avons optimisé des couches minces de DLC déposé par rf-PECVD et avons modifié les paramètres de dépôt pour incorporer du fluor. Notre étude montre que les films contenant 20% de fluor ($F_{[20\%]}$-DLC) sont un bon compromis pour la nano-impression. Des moules réalisés par lithographie électronique à partir de $F_{[20\%]}$-DLC et de DLC non fluoré ont été soumis à des impressions successives (Figure 1) qui ont montré que les propriétés de réplication du $F_{[20\%]}$-DLC ont une durée de vie au moins douze fois supérieure à celle du DLC non fluoré.

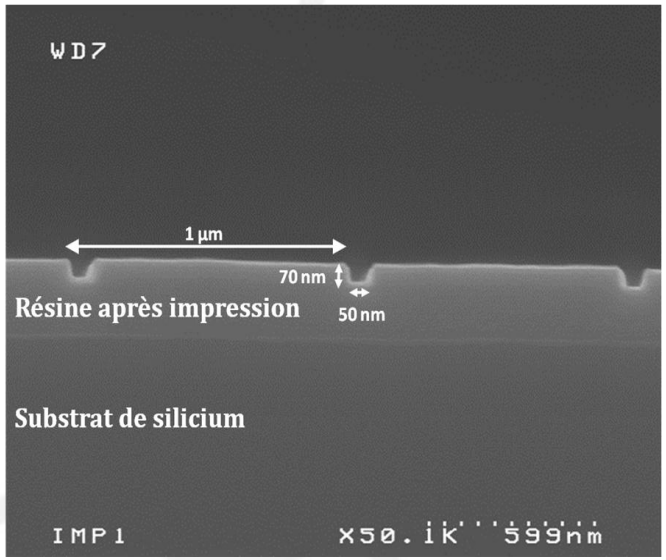

Figure 1 – Résultat d'impression de lignes de 50 nm issues d'un moule en $F_{[20\%]}$-DLC dans une résine photosensible. (Notez que l'épaisseur résiduelle n'a pas été optimisée.)

Références
[1] D. Truffier-Boutry, A. Beaurain, R. Galand, B. Pelissier, J. Boussey, M. Zelsmann, *Microelec. Eng. 87* (2010) 122-124.
[2] A. O. Altun, J. H. Jeong, J. J. Rha, D. G. Choi, K. D. Kim, E. S. Lee, *Nanotechnology 17* (2006) 4659-4663.
[3] M. Schvartzman, S. J. Wind, *Nanotechnology 20* (2009) 145306.

Nanofabrication de boîtes quantiques pour la manipulation ultra-rapide du spin d'un électron.

J. Camirand Lemyre[*1], C. Bureau-Oxton[1], S. Rochette[1], M. Pioro-Ladrière[1]*

[1]Université de Sherbrooke, 2500 Boulvard de l'Université, Sherbrooke, Québec, J1K 2R1.

Mots clés : nanotechnologies, nanoélectronique, spintronique, traitement de l'information

Notre habileté à traiter l'information a entraîné la société actuelle dans une révolution technologique inégalée, dans laquelle l'informatique joue un rôle central. Or, les méthodes actuelles pour traiter l'information n'utilisent pas directement les propriétés quantiques de la matière qui régissent notre univers. En tirant parti de ces propriétés, il est possible de créer un nouveau processeur d'information quantique dont les performances surpasseraient celles de l'informatique actuelle. Pour qu'un tel processeur puisse voir le jour, il faut parvenir à contrôler l'unité fondamentale de l'informatique quantique, le bit quantique (qubit). Étant soumis à la même mécanique que les atomes, à savoir la mécanique quantique, l'électron peut être utilisé comme qubit [1,2]. Grâce aux avancées dans le domaine des nanotechnologies, la manipulation de la charge électrique est devenue si précise qu'il est désormais possible de piéger des électrons individuels à l'aide de dispositifs nommés boîtes quantiques. Ceci ouvre la porte à la manipulation d'un élément intrinsèque à l'électron, le spin. L'opération la plus élémentaire pour contrôler le spin électronique est la rotation du spin. Or, les méthodes de rotation actuelles sont trop lentes et l'information quantique est perdue avant la fin d'une seule opération. Pour contrer ce problème majeur, de forts gradients de champ magnétiques peuvent être utilisés pour les rotations [3]. Dans notre approche, ces gradients seront produits par des micro-aimants placés sur des boîtes quantiques. Aussi, l'utilisation de doubles boîtes quantiques en aluminium oxydé[4] (voir figure 1) nous permettra de maximiser ces gradients et d'accroître la vitesse de rotation du spin.

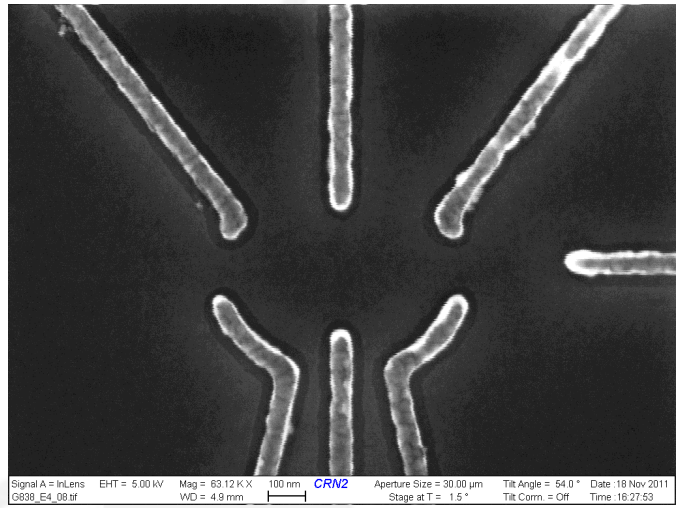

Figure 1 – Image prise au microscope électronique montrant une double boîte quantique formée par des grilles d'aluminium d'une largeur de 60nm. Les dispositifs sont fabriqués en utilisant l'IMC matériaux et dispositifs quantiques et l'IMC micro et nanofabrication de l'Université de Sherbrooke.

Références

[1] D. Loss and D. P. DiVincenzo. (1998) Physical Review A, Vol.57, p.120–126.
[2]. R. Brunner, Y.-S. Shin, T. Obata, M. Pioro-Ladrière, *et al*. (2011) Physical Review Letter, Vol.107, No.146801.
[3] W. Coish and D. Loss. (2007) Physical Review B, Vol.75, No.161302.
[4] W. H. Lim et al. (2009) Physics Letters, Vol. 94, No.173502.

A carbon nanotube-based sensor for measuring compressive stress on a flexible surface.

J. Genest[1], K. S. Kim[2], P. Boissy[3], G. Soucy[2], J. Beauvais[1]

[1]Department of electrical and computer engineering, Université de Sherbrooke, Canada
[2]Department of chemical engineering, Université de Sherbrooke, Canada
[3]Department of surgery, Université de Sherbrooke, Canada

Keywords : Carbon nanotubes, Strain sensing, Piezoresistivity

Since their discovery, numerous applications based on single-walled carbon nanotubes (SWCNTs) have been proposed in various fields. The extensive interest for SWCNTs is mainly attributed to their superlative properties, which offer outstanding opportunities for developing novel multifunctional devices. In particular, the combination of good electrical conductivity and mechanical strength of SWCNTs has opened-up new possibilities for design and fabrication of next-generation transducers, which can be embedded into many intelligent materials or structures. Here, we report the fabrication of simple compressive stress sensors based on the high piezoresitivity of SWCNTs.

Directly grown SWCNT films and purified films were fabricated for this study [1] and connected to electrodes. The mechanical properties of both types of films were measured by nano-indentation and compressive strain probing. The piezoresistive behavior of the two types of film was analyzed (figure 1) and a model based on tunneling conduction between nanotubes can be used to describe it. Under strain, the tunneling distance is expected to change, causing an alteration in the overall resistance of the films [2].

Compressive stress sensors were fabricated. Purified SWCNT films were deposited on PCB-flex substrates and capped with a molded polydimethylsiloxane (PDMS) layer. The device mechanical response under cyclic compressive strain was characterized. Despite the capping material viscoelastic properties, the system mechanical response is reproducible over each cycle.

In summary, we report straight forward approach for the fabrication of compressive stress sensors on a flexible substrate using SWCNT films. The SWNCT sensors produced exhibit high piezoresistive sensitivity to normal pressure.

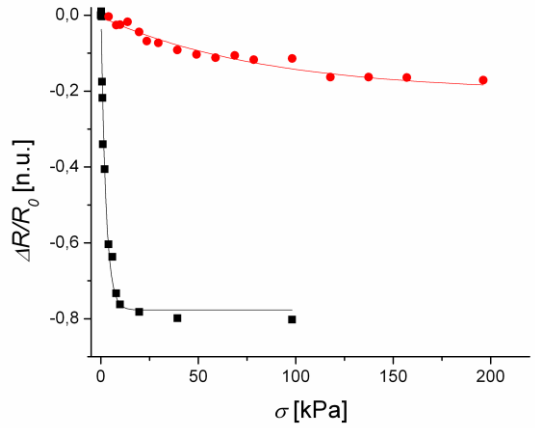

Figure 1 – Piezoresistance of the directly grown SWCNT films (square) and the purified films (circles) under corresponding stress

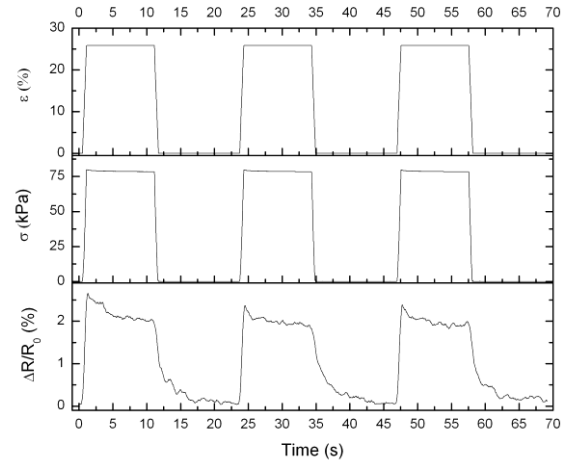

Figure 2 – Resulting mechanical stress and relative resistance variation on a SWCNT sensor.

References
[1] Kim, K. S., et al., J. Phys. Chem. C (2009) 4340.
[2] Genest, J. G., et al. J. Appl. Phys. (2012) 023502.

Excimer laser processing of III-V quantum semiconductor surfaces for selected area bandgap engineering

R. Beal, N. Liu, Kh. Moumanis, V. Aimez, J.J. Dubowski

Institut Interdisciplinaire d'Innovation Technologique (3IT), Département de Génie Électrique et Informatique, Université de Sherbrooke, Sherbrooke, QC

Mots clés : Quantum Well Intermixing, Excimer Laser, Laser-surface interaction, Photonic Integration

The development of III/V photonic integration requires multi bandgap wafers in order to concentrate on a same chip waveguiding, light emission, phase tuning or amplification functions. To obtain such structures, we have employed UV Laser Induced Quantum Well Intermixing (UV-QWI) The UV-QWI technique is a post-growth bandgap tuning process, with the potential to deliver cost-effectively some complex multi-wavelength wafers. The process was applied to InP/InGaAs/InGaAsP quantum well (QW) structures, using ArF (l=193 nm) and KrF (l=248 nm) excimer laser irradiations in different environments. A subsequent rapid thermal annealing induces diffusion of the laser created surface point defects into the semiconductor structure. These diffusion blur the QW profile due to an enhanced intermixing of the barrier and well species. Thus, the selective area bandgap variation can be controlled by adjusting laser irradiation dose (fluence and number of pulses) and annealing parameters. In order to optimize the bandgap tuning process, we have investigated dependence of the sample surface morphology on the laser irradiation dose and irradiation environments, such as air [1], water vapour, vacuum and SiO_2 [2][3]. A combination of characterization techniques based on atomic force microscopy (AFM), x-ray photoelectron spectroscopy (XPS), ellipsometry and photoluminescence (PL) enabled us to demonstrate that the UV-QWI process has the ability to deliver multi wavelength patterns, with a high spatial selectivity, 100 nm of PL peak wavelength variation over 10 µm distance, and large blue shift (over 130 nm), without major variation of the PL intensity. The results suggest that the UV-QWI process has the potential to deliver the QWI material without its quality being significantly compromised. The UV-QWI approach is currently tested for the fabrication of a multi-bandgap multi-section superluminescent diode [4], a device that should allow versatility in the output spectral shape and power..

Références

[1] Genest, J.; Beal, R.; Aimez, V.; Dubowski, J.J.; ArF laser-based quantum well intermixing in InGaAs/InGaAsP heterostructures; Applied Physics Letters, v 93, n 7, p 071106-1-3, (2008)

[2] Liu, N.; Moumanis, K.; Dubowski, J.J.; ArF excimer laser-induced quantum well intermixing in dielectric layer coated InGaAs/InGaAsP microstructures; 4th Pacific International Conference on Applications of Lasers and Optics, PICALO (2010)

[3] Liu, N.; Moumanis, K.; Dubowski, J.J.; Surface morphology of SiO2 coated InP/InGaAs/InGaAsP microstructures following the irradiation with ArF and KrF excimer lasers; Proceedings of SPIE - The International Society for Optical Engineering, v 7920, Laser Applications in Microelectronic and Optoelectronic Manufacturing (LAMOM) XVI (2011)

[4] Beal, R.; Liu, N.; Moumanis, K.; Aimez, V.; Dubowski, J.J.; Multi section bandgap tuned superluminescent diodes fabricated by UV laser induced quantum well intermixing, 2011 ICO International Conference on Information Photonics (IP), p 2 pp., (2011)

Harvesting lost photons using NIR Up-Converting CdSe/NaYF4:Yb,Er Nano-Heterostructures

Afshin Dadvand[a,b], Chenglin Yan[a,b], Dmitrii F. Perepichka[b], and Federico Rosei[a]

[a]*INRS–EMT, Université du Quebec 1650 Boul. Lionel Boulet, J3X 1S2 Varennes (QC) Canada,* [b]*Department of Chemistry and Center for Self-Assembled Chemical Structures, McGill University, 801 Sherbrooke Street West, Montréal, Quebec, Canada H3A 2K6*

Keywords: Nano-particles, N95, Penetration, Cyclic flow, MPPS.

Multi-component hetero-nanostructures containing two or more nanosized components arranged in a controlled manner are of fundamental and practical significance for many rapidly developing fields.[1] An interaction between the components of such systems may significantly improve the application performance and even induce new chemical [2] and electronic properties.[3] In this research work, we are interested in exploring energy transfer from lanthanide materials to CdSe because of its semiconducting properties.[4] If sub-band-gap energy photons could efficiently be up-converted and used to create hole-electron pairs in a semiconductor, such system would allow to break a fundamental limitation of single junction photovoltaic devices. We note that energy transfer from $NaYF_4$:Yb,Er into CdSe has been recently shown for a core-shell structure.[5] However, using silica shell to attach CdSe to the lanthanide nanocrystals precludes electronic interaction between the CdSe and renders its semiconducting properties irrelevant. Therefore, the aim of this research is to develop a simple method for the synthesis of nanoheterostructures consisting of lanthanide-doped $NaYF_4$ nanocrystals dendritically decorated with CdSe quantum dots (QDs). The investigation of photoconductivity of the device based on CdSe/NaYF4:Yb,Er nano-heterostructures is thoroughly carried out. For the synthesis of nano-heterostructures, a seeded growth method is used to synthesize heterostructures consisting of CdSe to a core of $NaYF_4$:Yb,Er nanocrystals. The two-contact devices are prepared by spin-coating of solution of studied nanoparticles in toluene on Si/SiO_2 substrates pre-patterned with Au electrodes, which is aimed to study its photoconductivity.

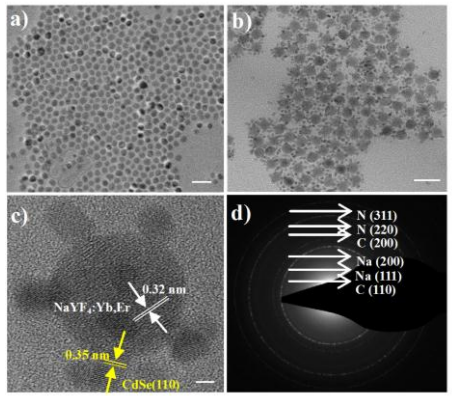

TEM images of original NaYF4:Yb,Er nanocrystals (a) and CSNY hetero-nanostructures (b and c). SAED pattern of a CSNY hetero-nanostructure (d). Scale bar is: 50 nm (a, b) and 3 nm (c). N represents NaYF4:Yb,Er; C represents CdSe.

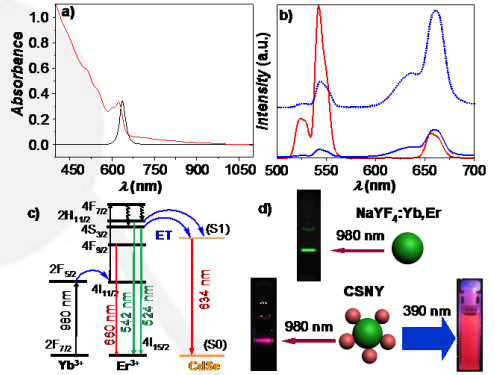

(a) Absorption and emission spectra of CSNY excited at 390 nm; (b) emission spectra of the seed NaYF4:Yb,Er nanocrystals (red) and of resulting CSNY (blue; dotted line shows an expansion of the same) in toluene (~1 wt%) excited at 980 nm); (c) a simplified schematic of the excitation and ET in CSNY; (d) photographs of the emission from NaYF4:Yb,Er nanocrystals (top) and CSNY heterostructures (bottom).

References

[1] Mokari, T.; Sztrum, C.; Salant, A.; Rabani, E.; Banin, U. Nat. Mater. **4** (2005) 855; (b) Catala, L.; Brinzer, D.; Prado, Y.; Gloter, A.; Stephan, O.; Rogez, G.; Mallah, T. Angew. Chem. internat. Edit, 1 (2009) 183.
[2] Lim, B.; Jiang, M.; Camargo, P.; Cho, E. C.; Tao, J.; Lu, X.; Zhu, Y.; Xia, Y. Science, **324** (2009) 1302.
[3] Gudiksen, M. S.; Lauhon, L. J; Wang, J. F; Smith, D. C; Lieber, C. M. Nature, **415** (2002) 617.
[4] Grieve, K.; Mulvaney, P.; Grieser, F. Curr. Opin. Colloid Interface Sci. **5** (2000) 168.
[5] Li, Z. Q.; Zhang, Y.; Jiang, S. Adv. Mater. **20** (2008) 4765.

Utilisation de nanocristaux de silicium en photonique intégrée

D. Barba[1], D. Koshel[1], F. Martin[1], G.G. Ross[1]

[1] INRS-EMT, 1650 Boul. Lionel Boulet, Varennes Canada, J3X 1S2

Mots clés : cristaux photoniques, nanocristaux de silicium, gain optique, laser

L'incorporation de matériaux nanocristallins au sein de systèmes nanostructurés permet d'envisager de nouvelles applications en photonique intégrée. La réalisation de réflecteurs et de filtres de Bragg à base de nanocristaux de silicium (nc-Si) luminescents rend possible l'intégration monolithique de sources émettrices 'tout silicium', pouvant considérablement améliorer l'interconnectivité des éléments entrant dans la composition de nombreux dispositifs optoélectroniques.
Le développement de cette nouvelle classe de matériaux repose sur la conception d'architectures submicrométriques et périodiques (Figure 1), dont les propriétés optiques ont pu être modélisées avant d'être caractérisées [1]. La fabrication de cristaux photoniques à base de nc-Si comporte une succession d'étapes dérivant toutes de procédés entièrement compatibles avec la technologie SOI, tels que la réalisation de masque d'implantation ionique par lithographie de faisceau d'électrons et la synthèse de nc-Si par implantation ionique suivie de recuit. D'importantes variations de gain optique ont pu être identifiées. Celles-ci résultent d'un effet de photodéterioration de la luminescence des nc-Si [2] qu'il est possible de minimiser par un conditionnement spécifique des échantillons. De tels dispositifs intégrés pourraient servir de base au développement de nouvelles sources laser.

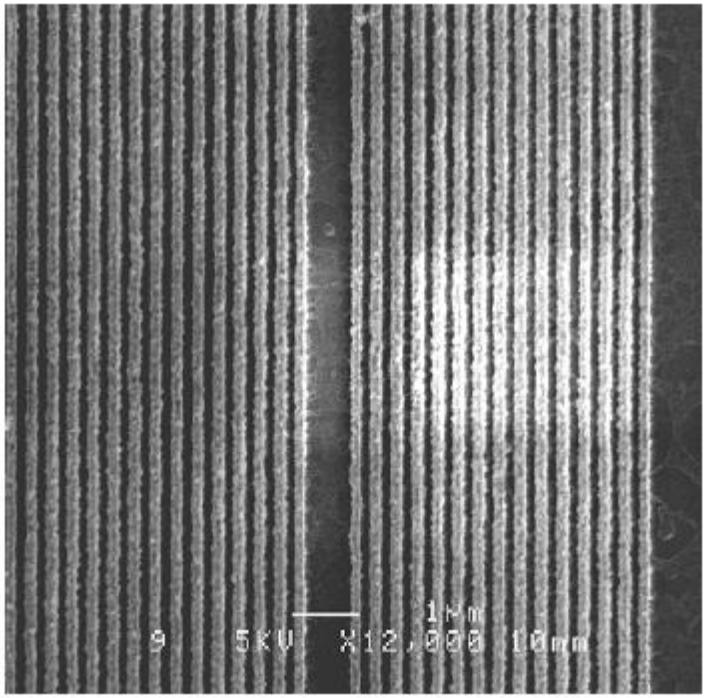

Figure 1 – Filtre optique réalisé à partir d'un réseau de Bragg contenant des nanocristaux de Si

Références
[1] D. Koshel, F. Beaudouin, D. Barba, F. Martin. G.G. Ross, J. of Lum. 131, 159 (2011).
[2] D. Koshel, D. Barba, F. Martin, G. G. Ross. J. Appl. Phys. 108, 053101 (2010).

Formation de revêtements nanométriques sur des fils utilisés dans le domaine de la microélectronique.

B. Commarieu[*1], *J. Persic*[2], *J. P. Claverie*[1]

[1]Centre de recherche, Département de Chimie, Université du Québec à Montréal, Succursale Centre-Ville, Montréal, QC, H3C 3P8, Canada
[2]Microbonds Corporate Headquarters, 151 Amber Street, Unit 12, Markham, ON, L3R 3B3, Canada

Mots clés : revêtement, nanométrique, polymère, microélectronique, microprocesseur

Ce projet en collaboration avec l'entreprise de microélectronique Microbonds a pour objectif de développer de nouveaux revêtements nanométriques sur des fils de 25µm de diamètre à base de cuivre, d'or ou encore d'argent. Ces fils conducteurs sont utilisés dans la conception des microprocesseurs pour relier les différentes puces électroniques (Figure 1). Il y a quelques années, les fils utilisés en microélectronique n'étaient pas isolés les uns des autres. Ils ne pouvaient donc pas être mis en contact ni être croisés, ce qui entrainait une importante limitation de l'ingénierie à l'intérieur des microprocesseurs. C'est pourquoi la compagnie Microbonds a développé un revêtement de polymère isolant pour ces fils permettant ainsi la mise en contact des fils entre eux sans risque de court-circuit (Figure 2). Cette innovation permet d'augmenter les rendements industriels, de diminuer les coûts de production tout en rendant possible l'obtention de microprocesseurs constitués de réseaux électriques plus denses. De nouvelles jonctions qui étaient alors jusque-là inaccessibles ont vu le jour. Il est ainsi possible de produire des microprocesseurs plus compacts présentant une consommation énergétique réduite grâce aux nouvelles jonctions améliorants les connectivités entre les puces électroniques. Notre objectif est d'améliorer le revêtement actuellement commercialisé en répondant à un cahier des charges de l'industriel très précis. Le polymère doit présenter des caractéristiques indispensables tels qu'une haute température de dégradation et de transition vitreuse, il doit adhérer fortement au cuivre, il doit être à la fois dur et cassant, etc. Le polymère doit convenir et supporter les différentes étapes de production.

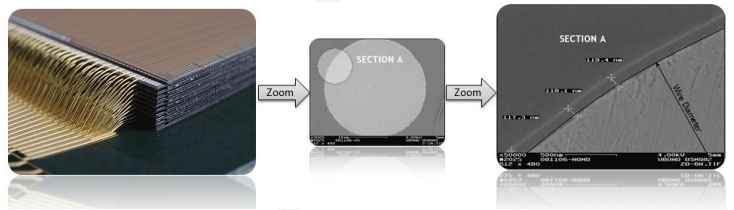

Figure 1 – Image MEB de la section d'un fil isolé par le revêtement de polymère.

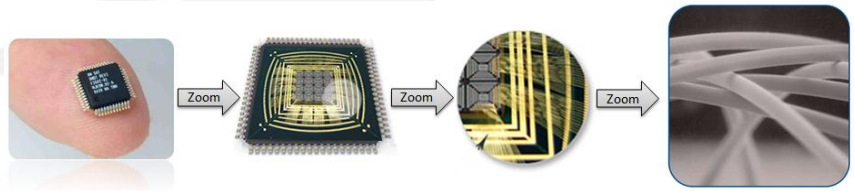

Figure 2 – Image MEB de l'architecture à l'intérieur d'un microprocesseur où il est représenté la mise en contact des fils isolés grâce au polymère (Pas de court-circuit possible).

References
[1] T. Kanit, *et al.*, "Determination of the size of the representative volume element for random composites: Statistical and numerical approach," *International Journal of Solids and Structures,* vol. 40, pp. 3647-3679, 2003

Fabrication of Silicon Quantum Dots for Quantum Information

P. Harvey-Collard[1], J.-P. Richard[2], C. Nauenheim[2,3], A. Ruediger[3], D. Drouin[2] and M. Pioro-Ladrière[1]

[1]Département de physique, Université de Sherbrooke, Sherbrooke QC J1K 2R1, Canada
[2]Département de génie électrique et génie informatique, Université de Sherbrooke, Sherbrooke QC J1K 2R1, Canada
[3]INRS-EMT, Université du Québec, 1650 bld. Lionel Boulet, Varennes QC J3X 1S2, Canada

Keywords: Quantum information, Quantum dots, Spin qubits, Nanoelectronic, Single electron transistor.

Silicon quantum dots are promising for both classical and quantum information. By using charging effects, it can be used as a single electron transistor, which is a low power logic device, a small non-volatile memory or an ultra-sensitive charge detector [1]. Moreover, by trapping single electrons and manipulating their spin degree of freedom, they can serve as qubits (quantum "transistors") [2,3]. Nevertheless, fabricating such a sensitive device is quite challenging due to its small dimensions.Here, we present a new fabrication process [4] to realize a lithographically defined silicon quantum dot (figure 1). First, a 20 nm wide and 20 nm deep trench is patterned in SiO_2 using Electron Beam Lithography (EBL) and plasma etching. The trench is then filled with amorphous silicon (a-Si) using Low Pressure Chemical Vapor Deposition. The dot is patterned using a second EBL step: a fine 20 nm resist line is aligned over the filled trench and with the gate box. The silicon is etched by a plasma to produce a standing a-Si line perpendicular to the trench. An annealing then crystallizes the a-Si and sputtered titanium fills the trench and gate box. Finally, a Chemical Mechanical Polishing (CMP) step is performed, which removes all excess material above the oxide surface, leaving only the silicon and metal inside the trench (figure 2).We will show results on the key processing steps separately, namely the plasma trench etch (line width down to 10 nm), the a-Si standing line etch (17 nm) and the CMP.

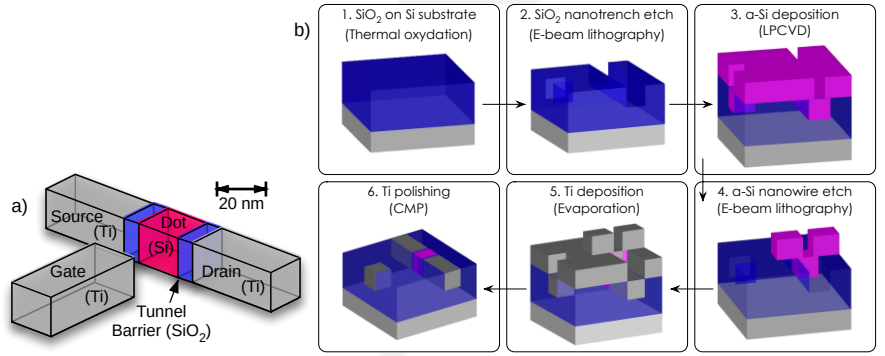

Figure 1 – a) Schematic image of the silicon quantum dot. It is connected to electrodes via SiO_2 tunnel barriers for electrical measurements and capacitively coupled to a gate electrode to control the charge state of the dot. The entire device is embedded in a silicon dioxide layer (not shown here). b) Fabrication process of the device. Material colors are the same as in a).

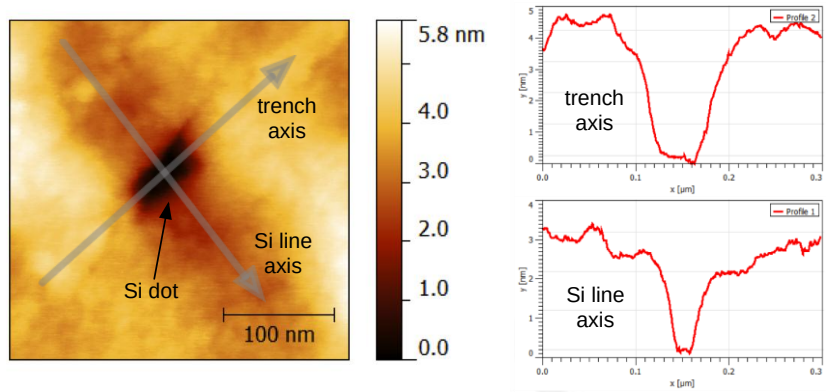

Figure 2 – Atomic Force Microscope image of a finished device. The dark region is the dot. The topography dip is due to the silicon CMP polishing rate, which is faster than the other materials. The cleanroom fabrication is realized at *IMC Micro et Nanostructures*, the cryogenic electrical characterisation is done at the *IMC Matériaux et Dispositifs Quantiques* and the Atomic Force Microscope characterization at the *IMC Laboratoire de Micro-Nanofabrication*.

References
[1] Likharev et al., Proc. IEEE **87**, 4 (1999)
[2] Ladd et al., Nature **464,** 7285 (2010)
[3] Assali et al., Phys. Rev. B **83,** 165301 (2011)
[4] Dubuc et al., IEEE Trans. Nano. **7,** 1 (2008)

Fabrication et intégration de semiconducteurs poreux pour l'isolation thermique dans les MEMS

P.J. Newby[1,2], J.-M. Bluet[2], V. Aimez[1], V. Lysenko[2], L.G. Fréchette[1]

[1]CRN2, Université de Sherbrooke, Canada
[2]Institut des Nanotechnologies de Lyon, CNRS, INSA de Lyon, Villeurbanne, France

Mots clés : silicium poreux, carbure de silicium poreux, MEMS, isolation thermique

L'isolation thermique est essentielle pour le fonctionnement de plusieurs types de micro-systèmes électro-mécaniques (MEMS). Dans les systèmes comportant des éléments chauffants, elle réduit la consommation d'énergie et l'inertie thermique. De plus, la cointégration MEMS-électronique requiert une bonne gestion thermique afin de protéger l'électronique des élévations de température. Des solutions existent mais en général elles limitent les techniques de microfabrication utilisables ou résistent mal aux hautes températures. Le silicium poreux (SiP), fabriqué par gravure électrochimique, est une alternative attrayante. La faible dimension de ses structures réduit sa conductivité thermique (CT) de 2 à 3 ordres de grandeur par rapport au Si monocristallin. De plus il est fabriqué avec des gaufres de Si cristallin, donc est compatible avec les procédés de microfabrication [1]. Au CRN2 nous avons développé un banc et les procédés de fabrication et intégration du SiP, en vue de l'utiliser comme isolant thermique dans les MEMS. Nous avons également mis au point une technique de contrôle de la CT du SiP, qui permet de la réduire davantage en l'amorphisant partiellement par implantation ionique. Ce matériau a des limites lorsqu'il est soumis à des conditions exigeantes (mécaniques, thermiques ou chimiques). Afin de pallier à cela, nous étudions actuellement un autre matériau, le SiC poreux (SiCP) [2]. Le SiC massif a des propriétés mécaniques excellentes et une très bonne inertie chimique, ce qui nous laisse supposer que le SiCP devrait être supérieur au SiP sur ces aspects. Sa CT est inconnue, mais sa nanostructure est similaire à celle du SiP, donc en le porosifiant, on devrait en principe réduire sa CT.

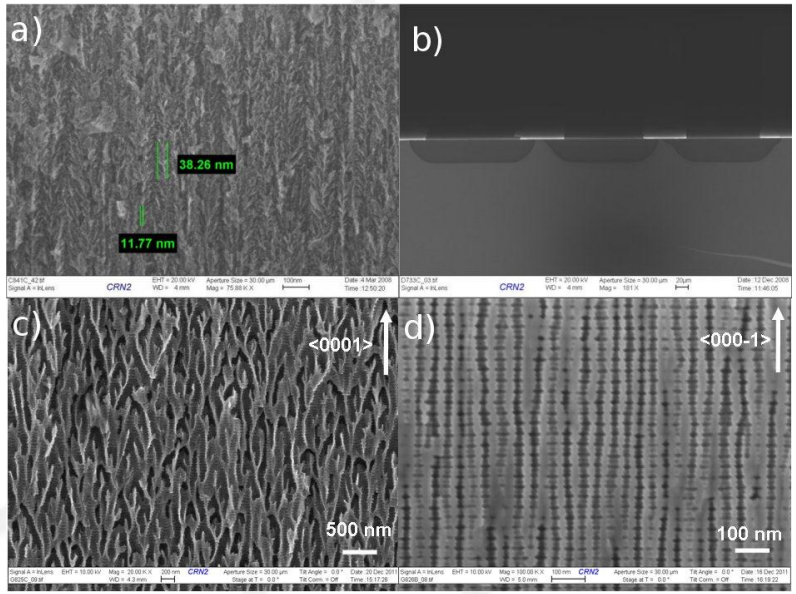

Figure 1 – Exemples de silicium et carbure de silicium poreux : a) silicium poreux, b) silicium poreux formé à l'aide d'un masque, c) carbure de silicium poreux, d) carbure de silicium poreux.

Références
[1] V. Lysenko et al. Sensors and Actuators A 99, 13, (2002).
[2] P. Newby et al. Physica Status Solidi (c) 8, 1950-1953 (2011)

Fabrication of III-V/Ge high-efficiency multijunciton solar cells

A. Turala, O. Arenas, R. Homier, G. Kolhatkar, S. Schicho, A. Jaouad, R. Arès, V. Aimez

Centre de recherches en nanofabrication et nanocaractérisation (CRN²)
Département de génie électrique et informatique, Université de Sherbrooke, 2500 boul. Université, Sherbrooke, QC, J1K 2R1, Canada

Keywords: concentrated photovoltaics, III-V multijunction solar cells, microfabrication

Multijunction solar cells (MJSC) for concentrator photovoltaic (CPV) are the most efficient photovoltaic devices, achieving 40% conversion efficiency. Further performance improvement along with reduction of manufacturing costs is necessary to make CPV systems more competitive on the solar market. In this work we propose a fabrication process of high efficiency solar cells (figure 1) for application in CPV systems with a number of modifications introduced in order to improve their performance, fully compliant to the industrial processing requirements. The solar cells were fabricated starting from triple junction III-V/Ge solar cell wafers. We have elaborated a cost-effective process of isolation of cells by wet etching through the whole epitaxial layers [1], allowing to isolate the active layers of solar cells and avoid structural damage to the cell's edges during to dicing. Isolated solar cells are then passivated on the sidewalls using PECVD-deposited silicon nitride – based antireflection and passivation coating. This film protects the cell not only from the environmental influence but also from accidental short-circuiting during die singulation and packaging step, improving manufacturing yield. The silicon nitride-based antireflective coating was optimized to minimize the reflection at wavelengths absorbed by the middle, current-limiting junction, resulting in better current matching between the top and middle junction [2]. The cells are tested for their functionality with a solar simulator at low concentration (figure 2).

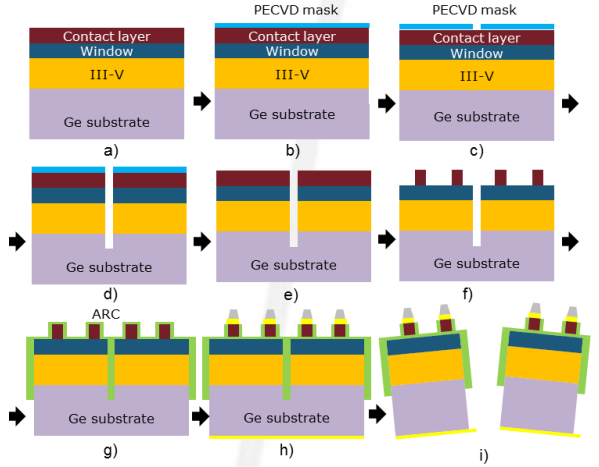

Figure 1 - Process flow of III-V/Ge solar cell fabrication with integrated isolation step: a) MJSC structure, b) stress-compensating/mask layer deposition by PECVD, c) etching of isolation trenches in PECVD mask, d) etching of isolation trenches in III-V materials and Ge, e) isolation mask removal, f) contact layer etch, g) passivation and antireflection coating deposition, h) front side and rear side electrical contacts, i) dicing.

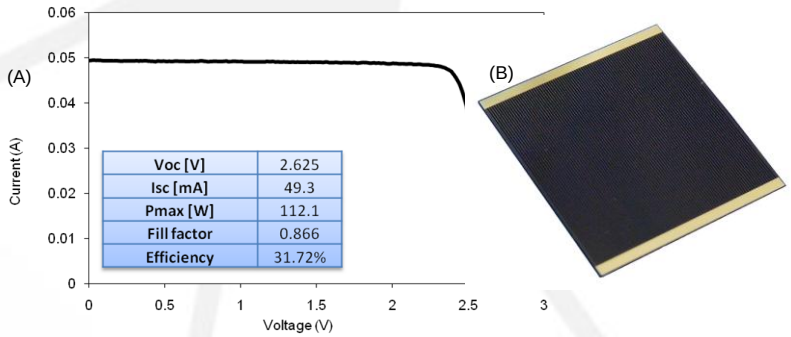

Figure 2 - (A) Illuminated I-V characteristics of a (B) solar cell (1 cm x 1 cm) at low concentration (4x) fabricated at CRN² of Université de Sherbrooke.

References

[1] A. Turala, R. Homier, A. Jaouad, R. Arès, V. Aimez, C.E. Valdivia, D. Masson, S. Fafard, S.G. Wallace, *"Yield limiting issues with etchant diffusion through a dielectric mask during non-selective wet etching of III-V materials for the isolation of multijunction solar cells"*, 7th International Conference on Concentrating Photovoltaic Systems, Las Vegas, USA, 2011

[2] R. Homier, A. Jaouad, A Turala, C.E. Valdivia, D. Masson, S.G. Wallace, S. Fafard, R. Arès, V.Aimez *"Antireflection coating design for triple-junction III-V/Ge high efficiency solar cells using low absorption PECVD silicon nitride"*, submitted to Journal of Photovoltaics, 2012

Nanomagnets for the Coherent Control of Electron Spins in Quantum Dots

C. Bureau-Oxton[*1], J. Camirand Lemyre[1], S. Rochette[1], M. Lacerte[1], M. Pioro-Ladrière[1]*

1Département de Physique, Université de Sherbrooke, 2500 boulevard de l'Université, Sherbrooke, Canada, J1K 2R1

Key Words: quantum dots, nanomagnets, nanoelectronics, spintronics, information processing

A quantum computer is a computer made from quantum bits (qubits) that takes advantage of the quantum properties of matter (intrication, superposition of states, etc.). Such a computer would allow certain calculations to be done exponentially faster than with conventional computers [1]. When an electron is confined in a quantum dot (Figure 1), its spin state can be used as a qubit. Different types of qubits can be implemented using double quantum dots. Foletti *et al.* suggested using two electrons in a double quantum dot to implement a single qubit using the singlet and T_0 triplet states as the 0 and 1 states of the quantum bit [2]. Petta *et al.* suggested a similar scheme where le singlet and T_+ triplet states are used [3]. In both schemes, a difference in the magnetic field felt by the two electrons in the quantum dot is needed, and the larger the difference in this magnetic field, the better the results. In 2008, Pioro-Ladrière *et al.* suggested adding a rectangular micromagnet to the double quantum dot, thus creating a difference in magnetic field of 13 mT between the dots [4]. We present a novel geometry of nanomagnets suggested to obtain a difference in the magnetic field of the order of 100 mT. The above-mentioned experiments will be explained in detail and it will be shown how our nanomagnets can be used in these experiments to achieve much better results (higher fidelity, better visibility and faster operation times).

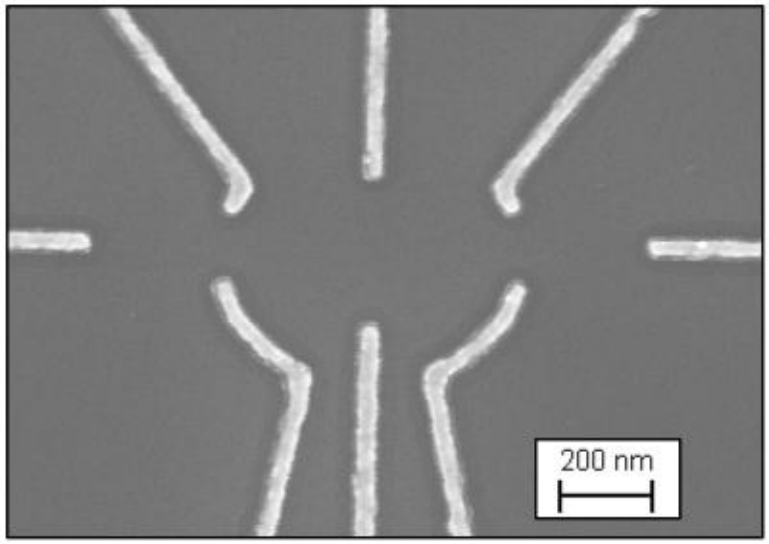

Figure 1 – Micrograph of a lateral double quantum dot taken using a Scanning Electron Microscope. The devices are fabricated using the *IMC matériaux et dispositifs quantiques* and the *IMC micro et nanofabrication* of the University of Sherbrooke

Références
[1] P. W. Shor, SIAM J. on Computing **26**, 1484 (1997).
[2] S. Foletti *et al.*, Nat Phys **5**, 903 (2009).
[3] J.R. Petta, H. Lu, A.C. Gossard, Science **327**, 669 (2010).
[4] M. Pioro-Ladrière *et al.*, Nat Phys **4**, 776 (2008).

Microbalance basée sur une cavité Fabry-Pérot asymétrique accordable

A. Poulin[*1], R. St-Gelais[1], A.-L Eichenberger[2] and Y.-A. Peter[1]*

[1]École Polytechnique de Montréal, Montréal, Canada, H3C 3A7
[2]Office fédérale de métrologie, Lindenweg 50, Wabern, Bern, Suisse, CH 3003

Mots clés : microsystème, réseaux de Bragg, Fabry-Pérot asymétrique, senseur de force

Nous présentons une microbalance optique de haute-précision pour la mesure d'échantillons macroscopiques. Les senseurs de forces sont nécessaires dans le développement de nombreux domaines de pointe allant de l'aérospatiale au biomédicale. Ils trouvent des applications tant au niveau de la recherche fondamentale qu'appliquée. Les principaux senseurs de force peuvent être classés en fonction de leur résolution et de leur charge maximale. [1] Peu de technologies permettent de mesurer avec précision des forces situées entre 1 mN et 100 mN. Pour cette gamme, seuls les dispositifs basés sur les effets piézorésistif ou piézoélectrique permettent d'atteindre de hautes performances. Néanmoins, outre la complexité et les coûts supérieurs de ce type de microsystèmes, [2] leur fonctionnement s'avère sensible au bruit électromagnétique. [3] De plus, les mesures piézoélectriques sont impossibles en mode statique. Ces technologies, contrairement aux microsystèmes optiques, sont donc mal adaptées pour des applications spatiales ou pour le développement de microbalances. Cependant, les échantillons ayant un poids situé dans cette gamme de forces sont de dimensions macroscopiques ce qui limite généralement l'utilisation des microsystèmes optiques.Le dispositif développé est présenté à la Fig. 1. Il est basé sur une cavité Fabry-Pérot asymétrique accordable composée de deux miroirs de Bragg verticaux en Silicium. L'action d'une masse sur la zone de charge engendre une déformation de la cavité et le décalage de sa réponse spectrale tel que présenté à la Fig. 2. Des échantillons pesant de 75 mg à 10 g on été pesés et des sensibilités allant jusqu'à 50 nm/mN ont été mesurées.

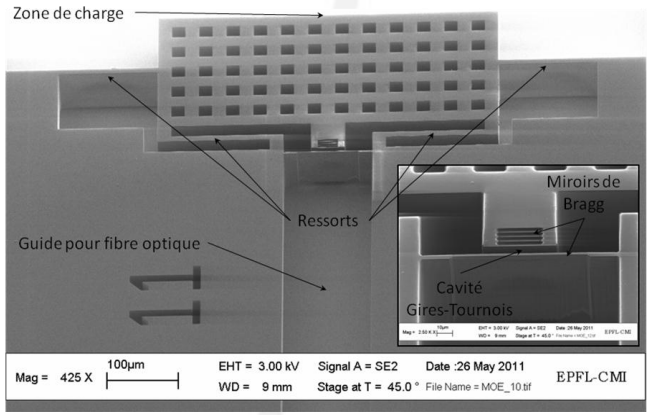

Figure 1 – Image du dispositif fabriqué prise au microscope électronique à balayage.

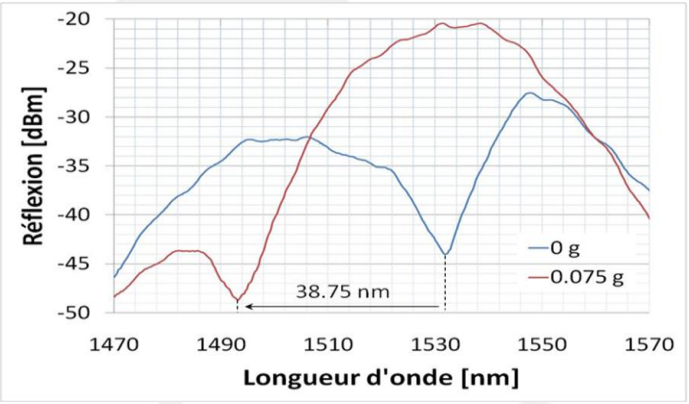

Figure 2 – Réponse spectrale de la microbalance sous l'action d'une masse de 75 mg.

Références
[1] D. Bell et al.. Journal of Micromechanics and Microengineering, Vol. 46, p. S153, 2005.
[2] D. L. Devoe. Sensors and Actuators A : Physicsl, vol. 88, p. 263-272, 2001.
[3] H. R. Shea. Poc. of SPIE, vol. 6111, 61110A, 2006.

Synthèse par ablation laser de nanoparticules de PbS et leur association avec les nanotubes de carbone pour le développement des dispositifs optoélectroniques

*I. Ka, V. Le Borgne, D. Ma, M. A. El Khakani**

Institut National de la Recherche Scientifique, INRS-Énergie, Matériaux et Télécommunications, 1650 Lionel-Boulet, Varennes, Canada, J3X 1S2

Mots clés : Nanoparticules de PbS; Nanotubes de carbone; Nanohybrids; ablation laser; Photoluminecence; Photoconduction.

La combinaison de deux ou plusieurs nanomatériaux constitue une alternative attrayante pour mieux contrôler leurs propriétés optoélectroniques. Dans ce contexte, nous avons dans un premier temps, développé un procédé de synthèse, par ablation laser, de nanoparticules de PbS permettant de contrôler leur taille moyenne de ~2 à 10 nm, et ainsi leur photoluminescence sur la plage 800-1600 nm.[1] Ensuite, nous présenterons les résultats de nos travaux sur des nouveaux matériaux nanohybrides (NHs) réalisés par ablation laser en intégrant les nanoparticules (NPs) de PbS aux réseaux de nanotubes de carbone (NTCs). Les NHs ainsi réalisés ont été caractérisés par microscopie électronique à transmission (MET), par diffraction des rayons X (XRD), par absorption UV-Vis ainsi que par spectroscopie de Photoluminescence. L'intégration de ces nanohybrides dans les dispositifs appropriés nous a permis de révéler leurs propriétés remarquables de photoconduction. En effet, l'optimisation de la quantité des NPs et de celle des NTCs, nous a permis d'augmenter la photoréponse des NHs de 30 % à plus de 1300 %. Cette performance remarquable est attribuée, non seulement, à la très haute mobilité des charges dans les NTCs, mais surtout grâce au transfert de charge ultra-efficace entre les NPs de PbS et les NTCs, que nous avons pu mettre en évidence. Ces résultats forts prometteurs font de ce genre de structures nanohybrides des candidats de choix pour les applications photovoltaïques et/ou de photodétection.

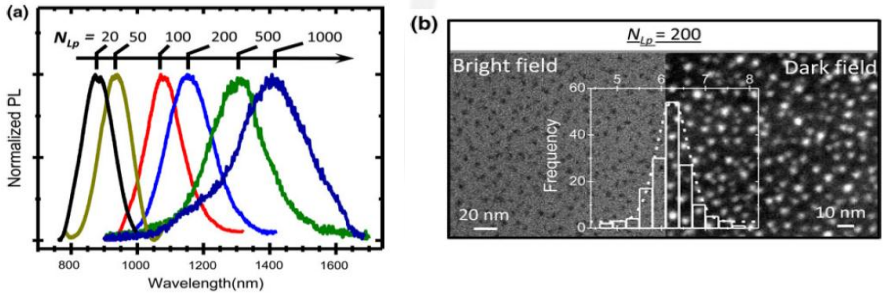

Figure 1 : (a) Spectres de photoluminescence des NPs de PbS en fonction lorsque la taille des NPs est variée de 2.5 à 8.5 nm; (b) images TEM des NPs de PbS ayant une taille moyenne de ~6 nm.

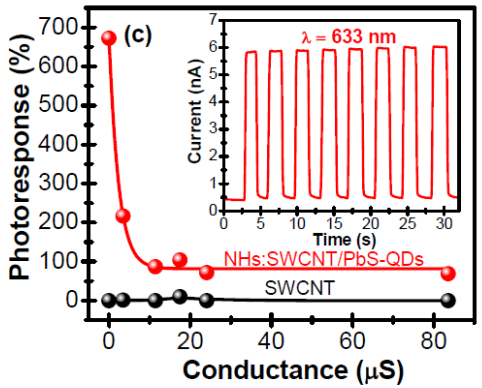

Figure 2 – Variation de la photoréponse des films de nanohybrides (NPs-PbS/SWCNTs) en fonction de l'épaisseur des films de NTCs.

References

[1] I. ka, D. Ma and M. A. El Khakani, J. Nanopart. Res., 13 (2011) 2269–2274.

Josephson Junctions and Nanobridges Fabricated with a Damascene CMP Process

A. Ramzi[*1], S. A. Charlebois[1], Philip Krant[2]*

[1]Interdisciplinary Institute for Innovations in Technology (3IT) and Department of electrical and computer engineering, Université de Sherbrooke, Quebec, Canada J1K 2R1
[2]Microtechnology and Nanoscience, Chalmers Tekniska Högskola, Gothenborg, Sweden

Keywords : Josephson junction, Nanobriges, Damascene CMP process

We report on the fabrication of Josephson junction and superconducting bridges using a damascene CMP process applied for a first time to superconductors. The demonstrated industrial reliability of damascene CMP processes on large scale semiconductor circuits is a major incentive for our research that should allow large numbers of nanometric Josephson junctions to be fabricated in both Nb and Al, the two main material employed in superconducting quantum computing (qubit) and RSFQ electronics fabrication[1, 2]. We carried out a Chemical-Mechanical Polishing (CMP) process on Nb and Al films deposited on a SiO_2 layer patterned with trenches of 100 to 300 nm of nominal depth. The process formed long bridges, 1 to 4 µm wide. The susceptibility and resistive transitions showed that CMP has no observable influence on superconductivity. We have also developed a hybrid technique that uses $Al/Al_2O_3/Al$ shadow evaporation in the trenches before the damascene CMP process (figure 1). This allows for high quality "in-situ" junction oxidation with the size reduction benefit provided by the damascene CMP process. We expect to easily reach junctions sizes below 10^3 nm^2 with capacitances in the subfemto range which are extremely difficult to fabricate by other methods. We describe these techniques and report on measurements on large bridges and junctions and on the fabrication and measurements of Al and Nb nanobridges [3].

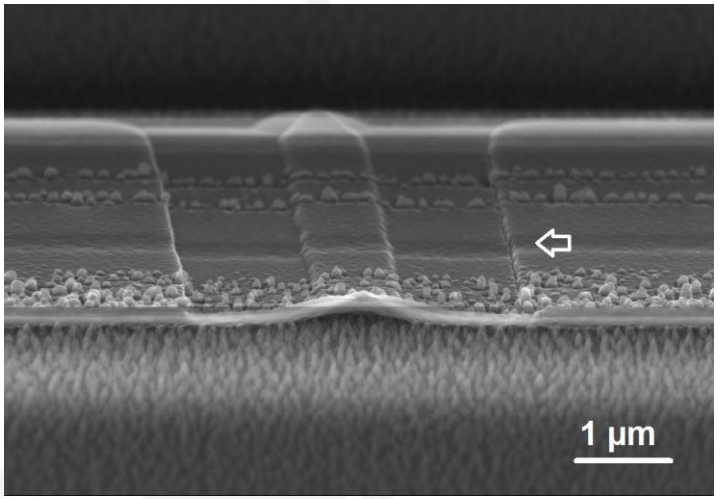

Figure 1 - Al/Al-oxide/Al Josephson junction fabricated by the hybrid process shadow evaporation/damascene. The trench are 3.5 µm wide but the shadow mask was made by photolithography (bridge 1 µm wide by 4 µm long). The arrow indicates the trench.

References
[1] Sillanpaa, M.A. Park, J.I. Simmonds, R.W., Coherent quantum state storage and transfer between two phase qubits via a resonant cavity, *Nature,* 2007, **449**, N° 7161, 438-442.
[2] Fenton J. C. Webster C. H. Warburton P. A., Materials for superconducting nanowires for quantum phase-slip devices, *Journal of Physics: Conference Series*, 2011, **286**, 012024.
[3] Vijay R. Levenson-Falk E. M. Slichter D. H. Siddiqi I., Approaching ideal weak link behavior with three dimensional aluminum nanobridges, *Appl. Phys. Let.,* 2010, **96**, 223112.
* *E-mail address : abdelaziz.ramzi@usherbrooke.ca*

Wetting robustness on hierarchically rough surfaces

A. Sarkar[1], A.M.Kietzig[1]

Department of Chemical Engineering, McGill University, 3610 University Street, Montréal, Canada, H3A 2B2

Keywords: Superhydrophobic, hierarchical roughness, penetration depth, femtosecond laser

Characterized by a near zero surface-liquid contact, superhydrophobic surfaces play a pivotal role in designing miniature scale equipments (microfluidic devices, MEMS) and self-cleaning surfaces. Superhydrophobic behavior can be provoked by introduction of a hierarchical surface roughness, i.e. co-existing features on micrometer and nanometer length scales. Superhydrophobicity can be best expressed as the resistance encountered by a water droplet in penetrating the micrometer scale roughness. Liquid penetration in the roughness valleys can be traced back to contributions from the surface topology, droplet shape and, most importantly, the velocity of a water droplet upon impact. Our work involves a two-step computational approach, which is supported by experiments. In the computational section, the penetration depth of water in roughness valleys is evaluated as a function of pressure terms corresponding to the geometry ($P_{geometry}$, for micrometer scale square pillars), the droplet shape (P_{shape}) and the velocity of impact ($P_{velocity}$). The mutually antagonistic pressures (Figure 1), namely $P_{geometry}$ and the combined effect of P_{shape} and $P_{velocity}$, determine the variation of penetration depth with the position under the droplet (Figure 2). Substitution of the penetration depth enables the analysis of wettability on a micrometer scale surface topology. The experiments involve wettability measurements on a surface ablated with femtosecond laser pulses, which can be tuned to simultaneously generate nano and micrometer scale structures. Thus, the above approach successfully incorporates a fingerprint of the droplet shape and history, and forms a prelude to designing lab on chip devices.

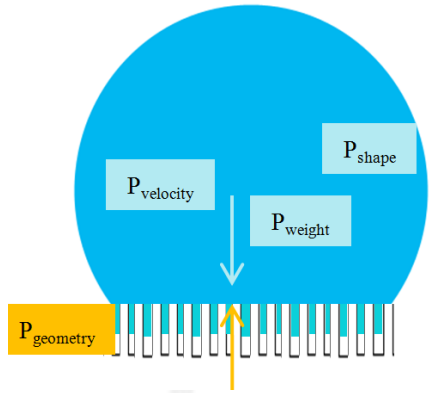

Figure 1– Pressures acting at the liquid-vapor interface within roughness valleys under the drop. The dominating pressure term determines the penetration depth.

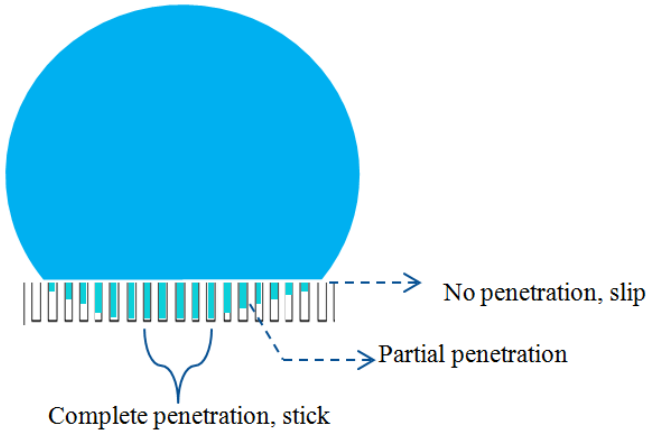

Figure 2: Above a certain threshold impact velocity, the penetration depths vary with the position under the droplet.

Fabrication et caractérisation de microcavités organiques de type *Whispering Gallery Cavities*

Tassadit Amrane[1], Francis Vanier[1], Pablo Bianucci[1], Carlos Silva[2], Richard Leonelli[2],Yves-Alain Peter[1].

[1]École Polytechnique de Montréal, 2900 Édouard-Montpetit campus de l'Université de Montréal. 2500 Chemin de polytechnique Montréal, Canada, H3T 1J4.
[2]Université de Montréal, 2900 boul. Édouard-Montpetit Montréal, Canada, H3T 1J4.

Mots clés : microcavité circulaire, modes de galeries, microfabrication, copolymère.

Les microcavités optiques à modes de galeries sont des dispositifs capables de piéger la lumière à l'échelle microscopique [1]. Elles sont utilisées pour différentes applications : milieu amplificateur, filtre spectral, dispositif pour la biodétection, etc. Pour introduire un milieu amplificateur, l'utilisation de matériaux organiques semi-conducteurs offre de nombreux avantages : ils sont faciles à structurer, peu dispendieux et disponibles pour toutes les gammes de longueur d'onde. De plus, la structure de ces microcavités assure un recouvrement optimal du matériau et du mode optique, permettant une excellente interaction entre ceux-ci. Le semi-conducteur organique utilisé est le F8BT, un copolymère photoluminescent déjà très largement étudié pour ses propriétés optiques [2].
L'application visée est la création de polaritons, particule phare de la physique fondamentale. Le polariton résulte d'un couplage fort entre un exciton et un photon. Sa création nécessite l'interaction efficace d'un matériau semi-conducteur et le mode optique d'une cavité résonnante. Un couplage fort avec l'exciton est possible si le photon est confiné suffisamment longtemps à l'intérieur de la cavité. Les matériaux organiques sont propices à la création d'excitons et les cavités obtenues ont un facteur de qualité de 10^4. La figure 1 montre une cavité de 200µm de diamètre posée sur un pied en silicium. Le disque est fabriqué à partir de trois épaisseurs. Le F8BT est pris entre une base en oxyde de silicium et une couche de parylène. Cette dernière sert de masque lors des étapes de microfabrication critiques : la photolithographie et la gravure par plasma [3].

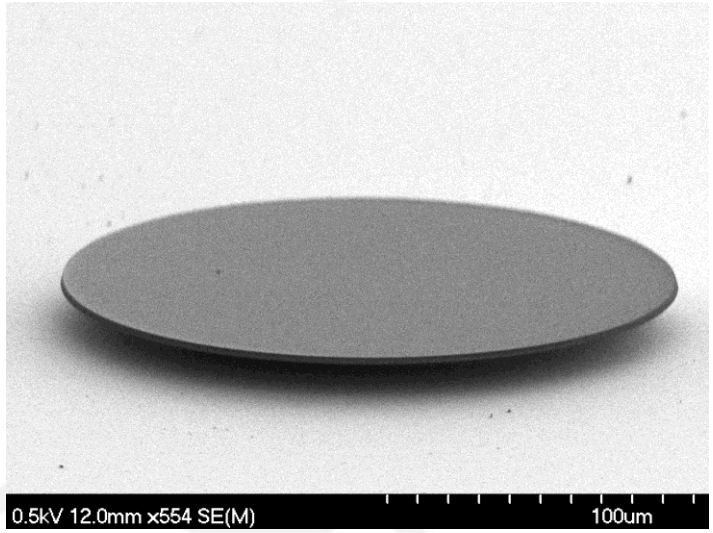

Figure 1 – Cavité organique de 200µm de diamètre suspendue sur un pied en silicium.

Références

[1] K. Vahala. Optical Microcavities, World Scientific, 2004.
[2] D. Bradley, Fluorene-based conjugated polymer optical gain media, Organic Electronics 4, 2003.
[3] H. Sirringhaus, Conjugated-Polymer-Based Lateral Heterostructures Defined by High-Resolution Photolithography, Adv. Funct. Mater, 2010.

AFM studies of triboelectricity in DLC films

C. Harnagea[*1], S. Taleb-Bendiab[1], O. Seddiki[1], F. Rosei[1]*

[1] Institut National de la Recherche Scientifique, Énergie, Matériaux et Télécommunications, Université du Québec, 1650 Boul. Lionel Boulet, Varennes, QC, J3X 1S2

Keywords: Friction, triboelectricity, scanning probe microscopy, diamond-like carbon films

Friction is a ubiquitous phenomenon represented by a force opposing the relative lateral (tangential) displacement of two bodies contacting each other. Due to its omnipresent nature, much is known from an experimental/empirical viewpoint; however, the origin of friction is still poorly understood. Macroscopic tribology is an important subfield of engineering and usually focuses on optimizing the friction coefficient and wear rate for materials of interest. To understand the origin of friction, experiments are simplified by reducing one of the surfaces in contact down to a single asperity. Such single-asperity contact measurements are performed using an atomic force microscope (AFM), which is a unique tool to detect atomic-scale forces. Triboelectricity, a phenomenon of charge separation upon rubbing certain pairs of materials, is even more complex and less understood than friction. In this study, we use an AFM to investigate the triboelectric effect. For simplification, we analyzed this effect occurring between pairs of stable, hard, and inert materials (e.g. diamond like carbon, naturally oxidized silicon). To assess the charges induced, we have analyzed the surface potential appearing at the surface of one material upon scanning in contact, repulsive mode with the AFM tip made (or coated) with another material. Being known that the environment is crucial in the process of charge separation, we performed the experiments in both ambient atmosphere and ultrahigh vacuum (UHV). In UHV, we observe a monotonic dependence of the surface potential on the previously applied normal (and thus also the friction) force (figure 1). In ambient we observe an increase of the friction coefficient of the areas previously rubbed.

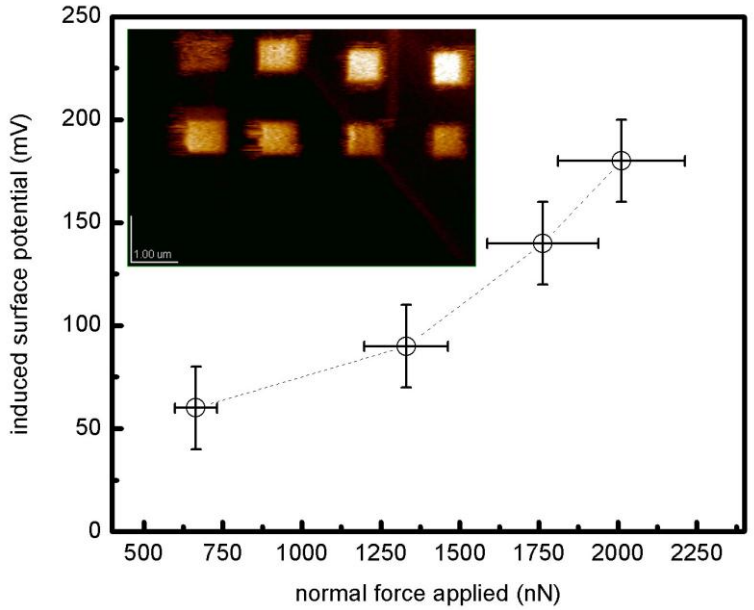

Figure 1 – Surface potential induced at the surface of a DLC film as a function of the normal force previously applied. The inset shows an example of a KPM (Kelvin Probe Microscopy) image illustrating several 1mm × 1mm regions of the surface with modified potential due to friction.

NV centers array for magnetic sensing at the nanoscale

D. Roy-Guay[*1], *A. Tallaire*[2], *D. Drouin*[3], *M. Pioro-Ladrière*[1], *D. Morris*[1]

[1]Département de physique, Université de Sherbrooke, Sherbrooke, QC, J1K 2R1, Canada, [2]LSPM, Université Paris 13, CNRS, 93430 Villetaneuse, France, [3]Département de génie électrique et génie informatique, Université de Sherbrooke

Mots clés : Nano-spintronic, Spin qubit, Quantum sensors

Nitrogen vacancy (NV) centers in diamond are nanoscale color centers preserving their qubit spin state over a very long time, a coherence time exceeding by three orders of magnitude other spin qubits [1]. Quantum bits (qubits) are two level systems that can, contrarily to classical bits, be in a superposition of states and form entangled systems. The ability of NV centers to maintain their state coherence over an extended period even at room temperature allows the creation of high spatial resolution nano-sensors, namely for biosensing [2]. Combined with the capacity to manipulate by microwave excitation and read optically their state [3], NV centers in diamond are outstanding magneto/electro meters, detecting single nuclear/electronic spins at the nanoscale (figure 1 a,b) [4,5]. We present efforts towards making an array of NV nano-detectors for magnetic field mapping (figure 1 c,d). The array (figure 2), created by localised implantation of NV centers in artificial diamond, will be mapped with a cathodoluminescence setup, composed of an electron beam to excite the color centers, while collecting the luminescence in a raster scan fashion. Developing such capability allows in-situ localization of centers and patterning of local gates for the application of high amplitude electric fields as a tuning parameter. Such tuning will enhance the magnetic field sensitivity of the NV array, resulting in a high precision magnetometer. The magnetic CCD created will be relevant to map local magnetic fields produced by micromagnets, as used in spin qubits architectures for fast qubit gates [6].

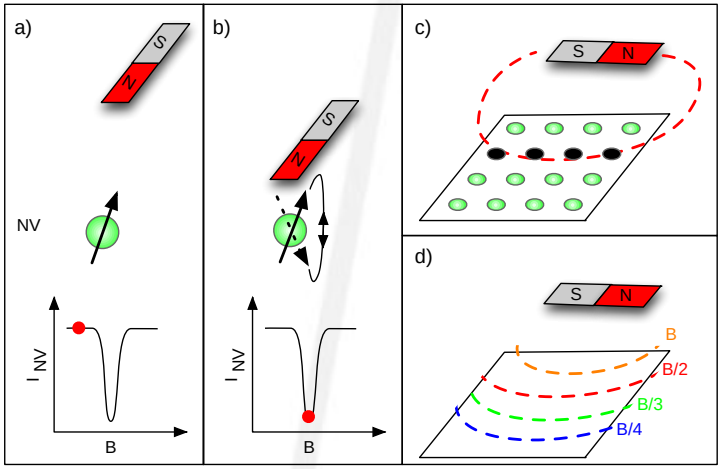

Figure 1 : a) Luminescence of the NV center under a non-resonant magnetic field. b) A resonant magnetic field applied on the NV center switches off the luminescence of the NV center. c) Mapping of a micromagnet field by an NV center array. d) Reconstructed magnetic field lines from the luminescence collected.

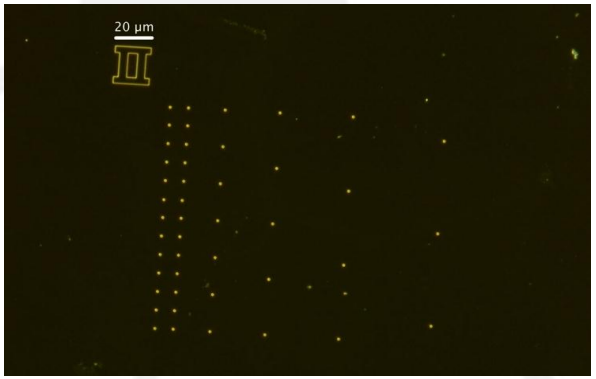

Figure 2 : Micro-implantation mask for the creation of the NV array. Measurements were made with the infrastructure of IMC Matériaux et dispositifs quantiques et IMC Micro et nanofabrication.

Références

[1] Balasubramanian, G. et al. Nature Materials **8**(5), 383–7 (2009).
[2] P., M. et al. Nature Nano 6, 358-363 (2011).
[3] Jelezko, F. et al. Physical Review Letters **92**(7), 76401 (2004).
[4] Balasubramanian, G. et al. Nature **455**, 648–651 (2008).
[5] Dolde, F. et al. Nature Physics **7**, 459-463 (2011).
[5] M. Pioro-Ladrière et al. Nature Physics **4**, 776-779 (2008).

Using GPUs to accelerate electronic transport computations

M. Harb[1], H.Guo[1]

[1]McGill University, 3600 rue Université, Montréal, Canada, H3A 2T8

Mots clés : GPU computing, Quantum Transport, tight-binding model

In the past two decades, significant progress has been achieved in the large scale fabrication of nanostructures where quantum transport properties of charge and spin are closely coupled to the discreteness of the device material. In addition to developing the appropriate theoretical formalisms and modeling tools for making quantitative and material specific predictions of device characteristics, it is important to address the computational issues that may arise.

Modern high performance computers are heterogeneous systems consisting of multi-core processors and specialized GPU. Graphics Processing Units (GPU) contain hundreds of cores, consume less power and are ideal for performing computationally intensive operations that have crippled performance in the past. We discuss our GPU implementation, the pros and cons of this kind ofapproach and present benchmarks and comparisons to several other platforms. We also present a quantum transport transport application this technique: Computing the transmission function of a ~140,000 atom Si system using four Nvida Tesla C2050 cards.

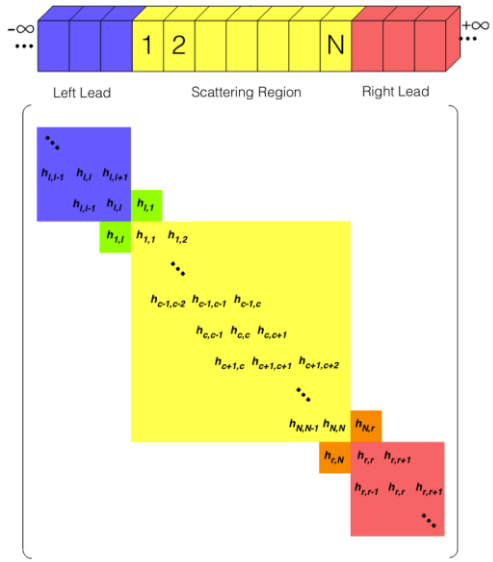

Figure 1 – A schematic of a two-probe device hamiltonian. The hamiltonian size scales linearly with the length of the scattering region and cubically with the cross-sectional area.

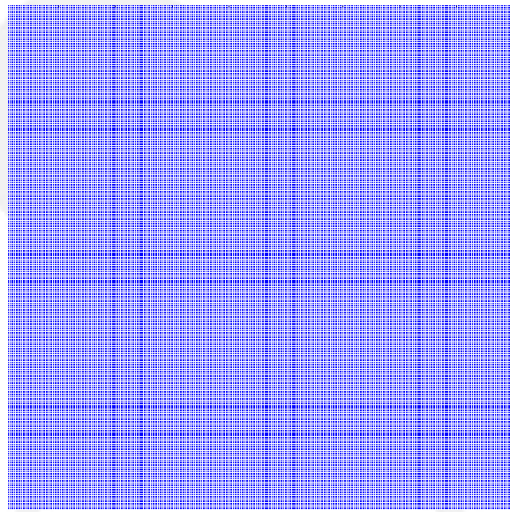

Figure 2 – Visual representation of the self-energy matrix for the electrodes of a large Si system.

Small Molecule Organic Photovoltaics at the Nanoscale

J.M. Topple, Z. Schumacher*, P. Grütter*

Department of Physics, McGill University, Montreal, QC, H3A 2T8, Canada

Mots clés : solar energy, thin films, small molecule organic photovoltaics, atomic force microscopy, nanotechnology.

Organic photovoltaics (OPVs) are a sustainable method of solar energy harvesting with dramatic fabrication advantages over more developed inorganic semiconductor solar cells. However, the power conversion efficiency of OPV devices is currently about 8.6%, compared to up to 43.5% for inorganic solar cells [1-4]. The structure of solar harvesting device active layers is crucial to performance, but little is currently known about the specific loss mechanisms responsible. We present a preliminary study of structure-function relationships in thin films of organic photovoltaic materials by simultaneous non-contact atomic force microscopy (NC-AFM) and Kelvin probe force microscopy (KPFM). Thin films of small electron donor and electron accepter molecules were thermally evaporated on KBr (001) surfaces under ultra-high vacuum. Local contact potential difference and topography were mapped with KPFM and NC-AFM to investigate corresponding optoelectronic and structural properties at the nanometre scale. Light of various wavelengths was coupled into the UHV AFM system to illuminate samples during imaging, thus allowing characterization of active OPV materials during the generation of excitons and charge carriers. Our early results demonstrate that simultaneous NC-AFM and KPFM is a powerful approach to studying fundamental physical processes in photovoltaic charge generation. Understanding structure-function relationships in OPVs will contribute to the advancement of renewable energy light harvesting devices that are clean, efficient and affordable.

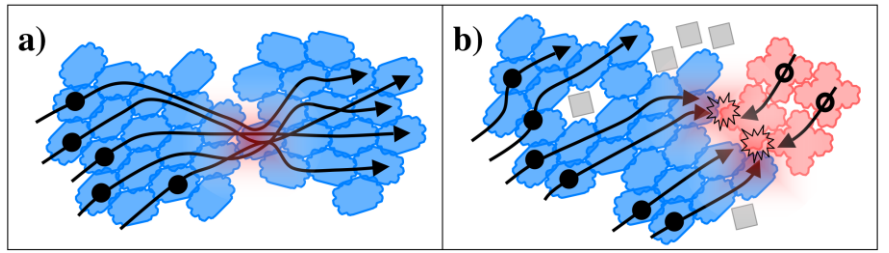

Figure 1 – Illustration depicting possible structure-dependent OPV efficiency loss mechanisms under investigation. (a) Charge flow dependent on molecular anisotropy and bottleneck structure, (b) recombination loss structure and the influence of defects

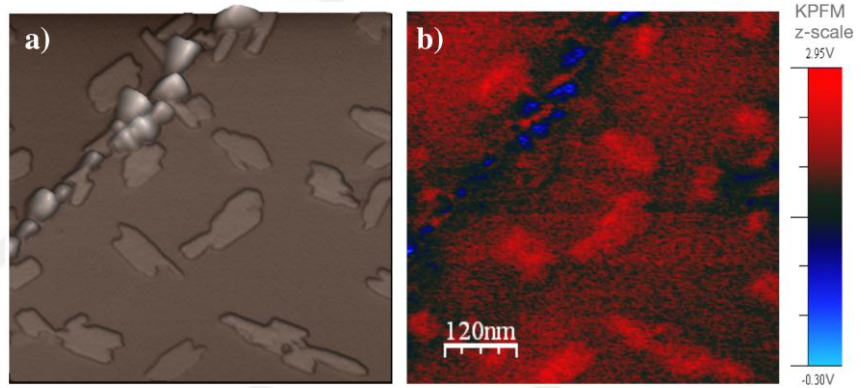

Figure 2 – Volmer-Weber growth of islands of CuPc (electron donor) and PTCDI (electron accepter) molecules on KBr (001). (a) 3D-rendered topography imaged by NC-AFM, (b) local contact potential difference imaged by KPFM

References

[1] S. H. Park, A. Roy, S. Beaupre, S. Cho, N. Coates, J.S. Moon, D. Moses, M. Leclerc, K. Lee, A.J. Heeger, Nature Photonics 3, 297 (2009).
[2] H.Y. Chen, J.H. Hou, S.Q. Zhang, Y.Y. Liang, G.W. Yang, Y. Yang, L.P. Yu, Y. Wu, G. Li, NaturePhotonics 3, 649 (2009).
[3] Y. Liang, Z. Xu, J. Xia, S.T. Tsai, Y. Wu, G. Li, C. Ray, L. Yu, Adv. Mater. 22, 1 (2010).
[4] Martin A. Green, Keith Emery, Yoshihiro Hishikawa and Wilhelm Warta, Prog. Photovolt: Res. Appl. 2010; 18:346–352

Phase Luminometric Contact CMOS Imaging and Detection of Xerogel Sensor Array

D. S. Daivasagaya, M. C. Cheung, P. J. R. Roche, V. P. Chodavarapu

Department of Electrical and Computer Engineering, McGill University, Montréal, Canada, H3A 2A7

Mots clés : CMOS optical sensors, biosensors, xerogels, sensor integration, polymer filters

We describe a compact luminescent gaseous and dissolved oxygen (O_2) and dissolved glucose sensor microsystems based on the direct integration of sensor elements with a polymeric optical filter and placed on a low power complementary metal-oxide semiconductor (CMOS) imager integrated circuit (IC). The sensor system is capable of the measurement of excited-state emission intensity and lifetimes of luminophore molecules such as tris(4,7-diphenyl-1,10-phenanthroline) ruthenium(II) ($[Ru(dpp)_3]^{2+}$) encapsulated within sol–gel derived xerogel nanoporous thin films. The polymeric optical filter is made with polydimethylsiloxane (PDMS) that is mixed with a dye (Sudan-II). The PDMS membrane surface is molded to incorporate arrays of trapezoidal microstructures that serve to focus the optical sensor signals on to the imager pixels. The molded PDMS membrane is then attached with the PDMS color filter. The xerogel sensor arrays are contact printed on top of the PDMS trapezoidal lens-like microstructures. The CMOS imager uses a 32 × 32 (1024 elements) array of active pixel sensors and each pixel includes a high-gain phototransistor to convert the detected optical signals into electrical currents. The imager can be fully integrated with a novel System-on-Chip (SoC) interface for wide-dynamic range and multi-frequency phase luminometric analysis. This new integrated sensor platform will lead to the development of robust optical sensors that incorporate (a) minimal susceptibility to excitation light source and photodetector drift, (b) insensitivity to changes in optical path, and (c) insensitivity to drift due to luminophore degradation and/or photo-bleaching.

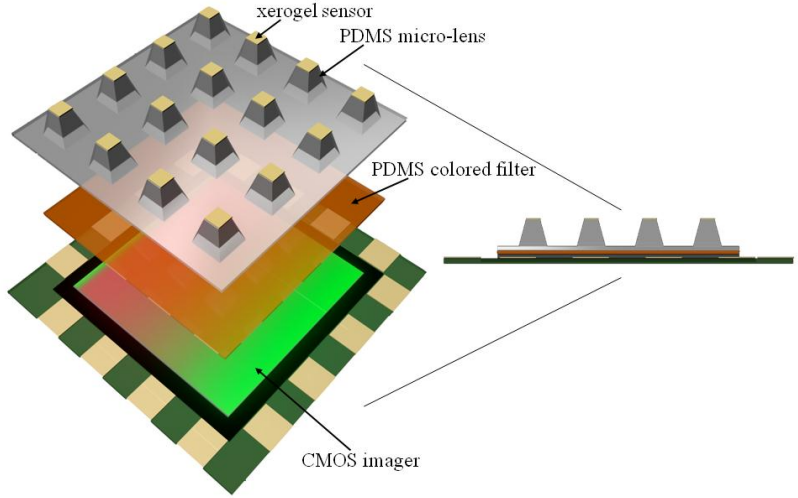

Figure 1 – Block diagram of the contact CMOS imaging sensor system

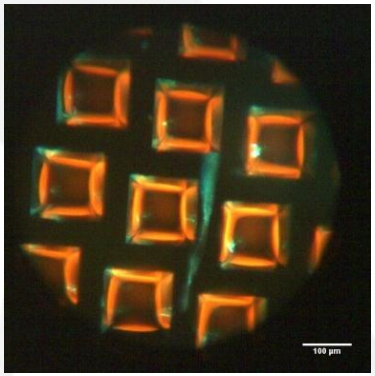

Figure 2 – Microscope view of the luminescence emission from xerogel coated lenses with excitation by a LED

Explosion de Coulomb de nano-agrégats de Carbone et Silicium

C. Chenard-Lemire[*1], L. J.Lewis[1], M. Meunier[2]*

[1]Département de Physique et RQMP, Université de Montréal, C.P. 6128, Succursale Centre-Ville, Montréal, Canada, H3C 3J7
[2]Département de Génie Physique et LP[2]L, École Polytechnique de Montréal, C.P. 6079, Succursale Centre-Ville, Montréal, Canada, H3C 3A7

Mots clés : explosion de Coulomb, ablation laser, nano-agrégat

Dans cette présentation, nous faisons l'étude de l'interaction entre des pulses laser ultra-bref de durée et de fluence variable avec des nano-agrégats de carbone et silicium. Deux mécanismes de désintégration ont été identifiés, soit l'expansion hydrodynamique et l'explosion de Coulomb [1,2,3]. L'expansion hydrodynamique est un mécanisme thermodynamique où la pression des électrons chauds pousse les ions de façon uniforme vers l'extérieur [4,5]. L'explosion de Coulomb (EC) est un processus « à froid » qui survient lorsqu'une densité de charge suffisante est accumulée à l'intérieur de l'agrégat. L'énergie de Coulomb entre les ions est relâchée sous forme d'explosion, souvent anisotropique [6,7]. Le contrôle de quel mécanisme est responsable de la désintégration est crucial pour contrôler les produits de celle-ci. Le focus de notre présentation est porté sur l'explosion de Coulomb de ces systèmes. Nous utilisons une nouvelle approche de dynamique quantique pour simuler l'interaction entre le laser et les ions et électrons du système. Nous examinons en particulier le mécanisme d'ionisation externe, où des électrons libres quittent la surface de l'agrégat, et sa relation avec l'EC. Notre analyse montre que le pic d'ionisation externe dépend fortement de la durée du pulse et que les autre paramètres tel la taille de l'agrégat et la fluence du laser affectent seulement son intensité mais non son profil. Le taux d'ionisation externe aux premiers stages de l'interaction laser-agrégat est d'importance vitale au contrôle du rôle de l'EC.

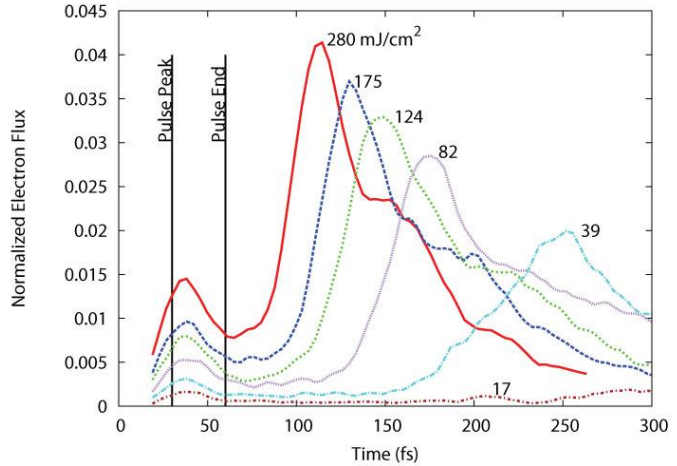

Figure 1 – Flux d'électrons sortant de la surface d'un agrégat de Si de 476 atomes à différentes fluences à durée constante de 60 fs.

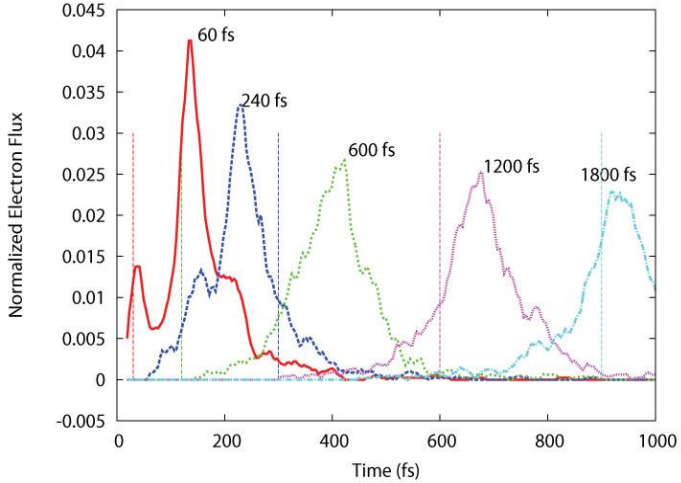

Figure 2 – Flux d'électrons sortant de la surface d'un agrégat de Si de 172 atomes à différentes durée à fluence constante de 170 mJ/cm^2.

Références
[1] Jungreuthmayer, C., Geissler, M., Zanghellini, J., and Brabec, T. (2004) Phys. Rev. Lett. 92(13), 133401.
[2] Jungreuthmayer, C., Ramunno, L., Zanghellini, J., and Brabec, T. (2005) Journal of Physics B: Atomic, Molecular and Optical Physics 38(16), 3029.
[3] Mijoule, V., Lewis, L. J., and Meunier, M. (2006) Phys. Rev. A 73(3), 033203.
[4] Ditmire, T., Donnelly, T., Rubenchik, A. M., Falcone, R. W., and Perry, M. D. (1996) Phys. Rev. A 53(5), 3379–3402.
[5] Milchberg, H. M., McNaught, S. J., and Parra, E. Oct 2001 Phys. Rev. E 64(5), 056402.
[6] Lezius, M., Dobosz, S., Normand, D., and Schmidt, M. (1998) Phys. Rev. Lett. 80(2), 261–264.
[7] Siedschlag, C. and Rost, J. M. (2002) Phys. Rev. Lett. 89(17), 173401.

Épitaxie de semiconducteurs III-V sur substrats non-standards.

*A. Boucherif, S. Tutashkonko, V. Aimez, R. Arès**

Centre de Recherche en Nanofabrication et en Nanocaractérisation (CRN2), Université de Sherbrooke, Sherbrooke, Québec, J1K 2R1, Canada

Keywords : Quantum semiconductors, Photoluminescence, Biosensors, Photonic Biosensing, Bacteria detection

Le Laboratoire d'Épitaxie Avancée (LÉA) est une infrastructure d'épitaxie des semiconducteurs III-V basée sur la technique d'épitaxie par faisceaux chimique, ou *Chemical Beam Epitaxy*. Le LÉA est intégré au Centre de Recherche en Nanofabrication et Nanocaractérisation (CRN^2) de l'Université de Sherbrooke, qui est une infrastructure majeure du réseau NanoQuébec. L'équipe de recherche du LÉA mène actuellement plusieurs travaux de recherche sur la croissance épitaxiale de couches minces sur des substrats non-standards. En effet, plusieurs des domaines technologiques les plus prometteurs nécessitant des couches minces de semiconducteurs font actuellement face à un défi majeur. La croissance épitaxiale procède normalement par le dépôt contrôlé de matériau cristallin sur la surface d'un substrat, dont la structure cristalline correspond étroitement à celle du matériau déposé. Or les nouvelles applications comme l'éclairage aux diodes électroluminescentes, les cellules solaires à haute efficacité et les dispositifs électroniques de pointe, souffrent toutes de l'absence de substrat approprié à coût viable. Il est donc impératif de développer des alternatives technologiques qui permettront de produire des couches de haute qualité sur un substrat à fort désaccord de maille. Les impacts industriels de percées dans ce domaine seront majeures. Cette affiche montre les progrès actuels au sein de l'équipe du LÉA sur la croissance de couches épitaxiales sur des substrats à fort désaccord de maille. L'approche actuelle préconisée est un procédé de porosification/recristallisation du substrat avant la croissance. Les résultats préliminaires sont prometteur pour le développement d'une alternative à faible coût aux méthodes actuellement reconnues, comme celle qu'a développé le groupe de Fitzgerald au MIT. Des résultats sur la genèse de matériau nanoporeux et la préparation du substrat sont présentées, de même que la caractérisation de couches épitaxiales sur des substrats modifiés.

Références

www.4cpv.com

Foresterie

HYATT REGENCY, MONTRÉAL

www.nanoquébec.ca

Use of Microfluidization for the Preparation of Nanocrystalline Cellulose (NCC) Reinforced Biobased Nanocomposite

Avik Khan[1], Stephane Salmieri[1], Ruhul A. khan[1], Bernard Riedl[2], Jean Bouchard[3] and Monique Lacroix[1]*

[1]Research Laboratories in Sciences Applied to Food, Canadian Irradiation Centre (CIC), INRS-Institut Armand-Frappier, University of Quebec, 531 Boulevard des Prairies, Laval, Quebec H7V 1B7, Canada.
[2]Département des sciences du bois et de la forêt, Faculté de foresterie, géographie et géomatique, Université Laval, Quebec-city, Quebec, G1V 0A6, Canada
[3]FPInnovations, 570 Boulevard St. Jean, Pointe-Claire, Quebec, H9R 3J9, Canada

Keywords: Chitosan, Nanocrystalline Cellulose, Nanocomposite films, Microfluidization, NCC Dispersion.

One of the major challenges in the area of nanocomposite is the compatibilization of the nano reinforcements with the polymer matrix to achieve acceptable dispersion of the filler within the polymeric matrix. In this study microfluidization, which is a high pressure homogenization technique, was adopted to disperse a concentrated (2% w/v) NCC suspension into chitosan matrix. Nanocomposite films prepared without microfluidization (control) exhibited no significant improvement of mechanical strength than the chitosan matrix. However, the films prepared after the microfluidization of the nanocomposite suspension (chitosan/NCC) showed significant improvement of the mechanical strength. Figure-1 represents effect of microfluidization on the chitosan/NCC suspension. Microfluidization pressure and number of cycles was optimized by measuring the mechanical strength of the nanocomposite films. A pressure of 10,000 psi and 5 cycles was found to be the optimum and the mechanical strength of the films improved by 30% than the control films (figure-2). Microfluidization was successfully applied to disperse a concentrated NCC suspension into chitosan matrix and can be considered as a suitable technique for the dispersion nano materials into polymer matrix.

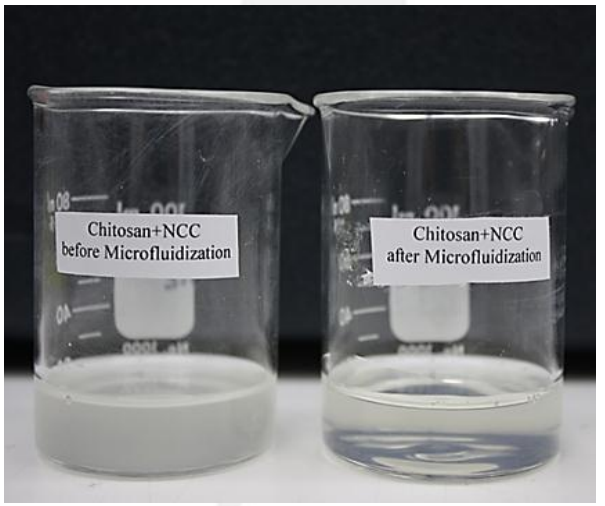

Figure 1 – Chitosan/NCC suspension before and after microfluidization (20,000 psi, 5 cycles)

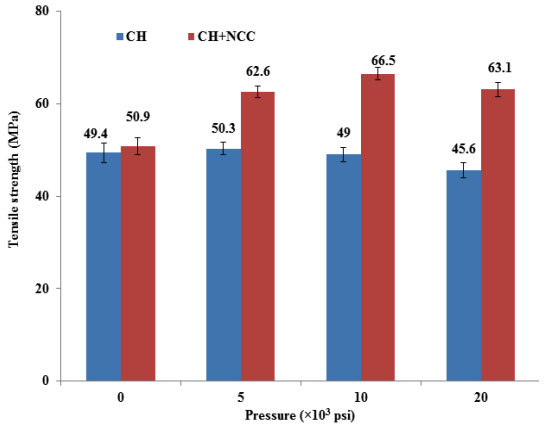

Figure 2 – Effect of microfluidization on the tensile strength of chitosan and chitosan/NCC films at different microfluidization pressures (5 cycles)

Effect of Nanocrystalline Cellulose (NCC) on the Survival of *Lactobacillus rhamnosus* ATCC 9595 in Alginate Beads During Freeze Drying and Storage

Tanzina Huq[1], Stephane Salmieri[1], Ruhul A. Khan[1], Jean Bouchard[2], Bernard Riedl[3] and Monique Lacroix[1]*

[1]Research Laboratories in Sciences Applied to Food, Canadian Irradiation Centre (CIC), INRS-Institut Armand-Frappier, University of Quebec, 531 Boulevard des Prairies, Laval, Québec, H7V 1B7, Canada
[2]FPInnovations, 570 Boulevard St. Jean, Pointe-Claire, Québec, H9R 3J9, Canada
[3]Département des sciences du bois et de la forêt, Faculté de foresterie, géographie et géomatique, Université Laval, Québec, G1V 0A6, Canada

Keywords: Alginate, Nanocrystalline Cellulose, Lactobacillus rhamnosus, Encapsulation, Freeze Drying

The main objective of this work is to observe the effect of NCC on freeze dried calcium (Ca)–alginate beads as a carrier material for the stabilization of *Lactobacillus rhamnosus* ATCC 9595. The encapsulation efficiency of the control beads was found to be 46% whereas incorporation of only 5% w/w NCC into alginate improved the encapsulation efficiency to 51%. After freeze drying, it was found that the survivability of *Lactobacillus rhamnosus* ATCC 9595 was 5.84 log CFU/mL in control bead but the survivability was 7.37 log CFU/mL when 5% w/w NCC was added to the alginate matrix (Figure-1). It was found that encapsulation with NCC enhanced the survivability of *Lactobacillus rhamnosus* ATCC 9595 during storage (4°C and 25°C at 30% RH) for up to 30 days. In conclusion, the qualities of the alginate beads were improved by incorporating NCC which acts as a reinforcing agent with the matrix had a significant influence on cell viability during freeze drying and storage.

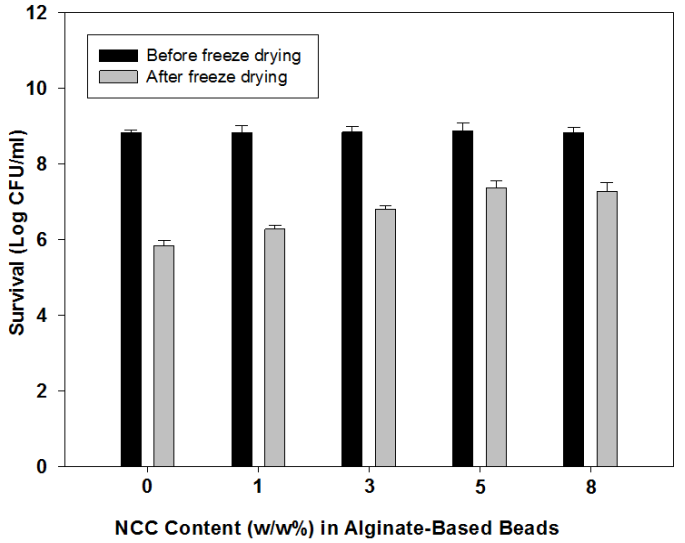

Figure-1: Effect of NCC on the survival of *L.rhamnosus* after freeze drying, as a function of NCC content in dry matrix.

Références

[1] W. Reisner et al. Directed self-organization of single DNA molecules in a nanoslit via embedded nanopit arraysPNAS 2009 106 (1) 79-84

Humidity colorimetric indicators from Self-Assembled NanoCrystalline Cellulose

Yu Ping Zhang[a], Vamsy P. Chodavarapu[a], Andrew G. Kirk[a], Mark P. Andrews*[b]

[a] Department of Electrical and Computer Engineering, McGill University, Montreal, QC, H3A2A7, Canada
[b]Department of Chemistry, McGill University, 801 Sherbrooke St West, Montreal, QC, H3A 2K6, Canada

Keywords: Humidity sensor, colorimetric, NCC, nanocrystalline cellulose, Green chemistry sensor

Safer and ecologically-friendly colorimetric indicators are key components for many applications, such as food, chemicals, biological, semiconductor and even in personal care products, such as diaper industry. NanoCrystalline Cellulose (NCC), a natural product made from wood pulp and also other biological sources, has drawn much attention recently due to its potential in this field. In this publication, we propose a humidity indicator based on an NCC film. A reversible shift in the color tint of the film (from blue to red, and back to blue) is observed upon exposure to moisture and subsequent drying. The color shift for a 10 µm thick film occurs on the timescale of few seconds. This colour change is likely caused by a variation in the chiral nematic pitch of NCC film induced by moisture. The color is a structural color originating from a combination of multilayer reflective interference and surface relief gratings. This is supported by SEM, AFM and polarized microscopy experiments. Colour changes in the diffractive spectrum were followed by spectrometry as the film reversibly transitioned from dry to wet.

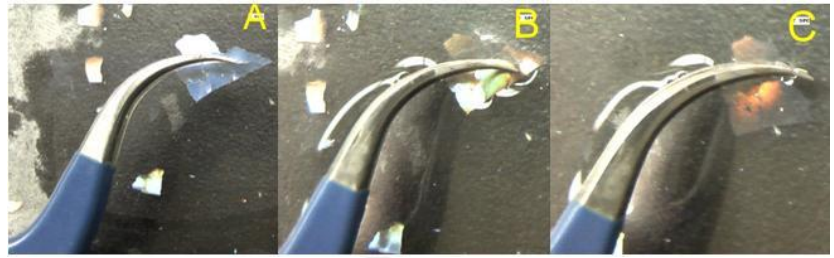

Figure 1 – color changes with time

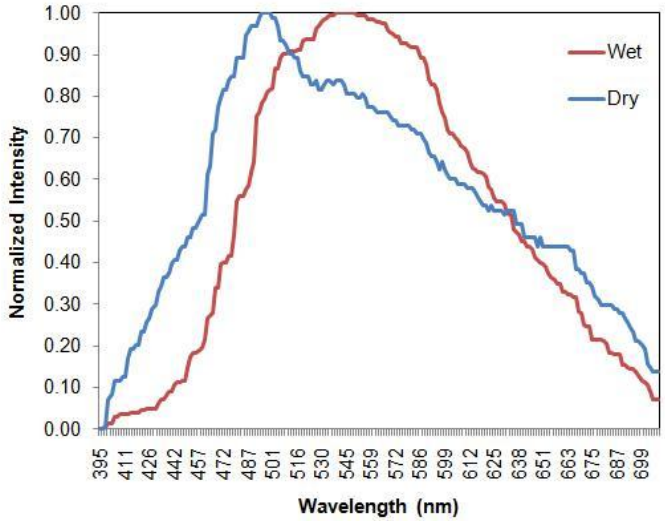

Figure 2. NCC tint color peak shift caused by moistrue

Dépôts de nano couches de ZnO par plasma sur le bois

F. Tomczak[1], B. Riedl[1]

[1]Centre de Recherche sur le Bois, Université Laval, 2425, rue de la Terrasse, Pavillon Gene-H.-Kruger, Quebec, Canada, G1V 0A6

Mots clés : Nano couches; plasma, bois, vieillissement.

L'objectif de cette étude est d'évaluer les dépôts de nano couches de ZnO par plasma sur l'érable à sucre sans et avec revêtements pour vérifier leur influences dans les propriétés superficielles du bois. Dans une première étape, les dépôts ont été réalisées sur un substrat de silice pour déterminer les effets des différents paramètres (puissance, ratio de gaz O_2 et Ar, distance et pression) sur les taux de croissance du film. Les taux de croissance varient de 0,75 à 7,5nm.min^{-1}. Dans une deuxième étape, les couches de ZnO ont été déposées sur le bois sans et avec revêtements avec différentes conditions de procédés de traitements plasma. Avec les dépôts de ZnO sur le bois sans revêtements, on observe un changement dans le comportement de la mouillabilité. Il y a un passage d'un caractère hydrophile vers hydrophobe qui se stabilise quelques jours après le traitement. Les valeurs d'angles de contacts chutent de 60 à 13°, 2 jours après le traitement et, quelques jours après, des valeurs supérieures à 100° sont trouvées. Les paramètres de couleur ont aussi été évalués, avec un changement de ΔE entre 3 à 12, dépendant de la condition du traitement. Avec la microscopie électronique de balayage, on est capable d'observer deux mécanismes différents de nucléation des nano couches et l'impact des paramètres de procédés sur la microstructure des dépôts. Comme prochaine étape, les échantillons seront soumis â des conditions contrôlées de vieillissement artificiel (radiation UV) pour évaluer l'efficacité des nano couches de ZnO sur le bois.

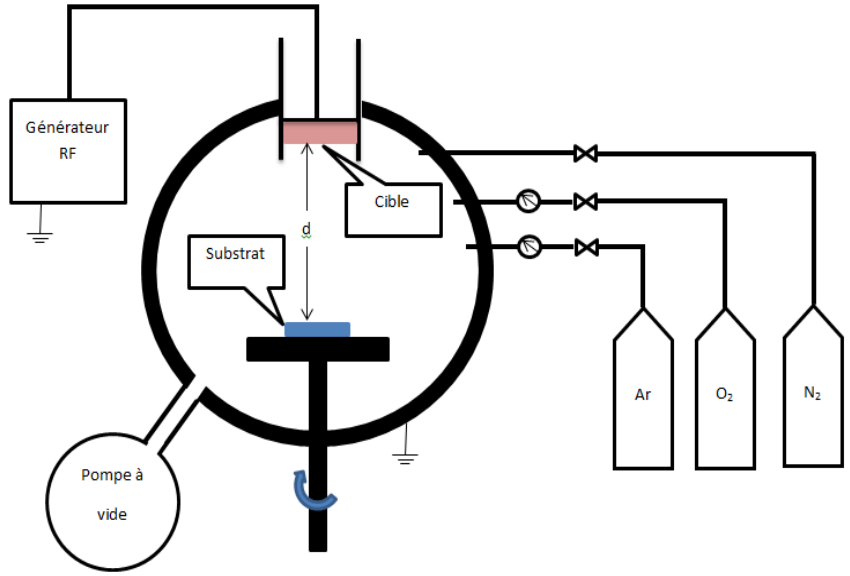

Figure 1 – Equipment pour dépôt d'oxyde de zinc par plasma

Références

[1] Aydin, Ismail; Demirk, Cenk. Activation of Spruce Wood Surfaces by Plasma Treatment After Long Terms of Natural Surface Inactivation. Plasma Chem Plasma Process, 30, pp 697-706, 2010.

[2] Podgorski, L.; Bousta, C.; Scgambourg, F.; Maguin, F. and Chevet, B. Surface Modification of Wood by Plasma Polymerisation. Pigment and Resin Technology, vol 31, Number 1, pp 33-40, 2001.

[3] Blanchard, V.; Riedl, B.; Blanchet, P. and Evans, P. Modification of Sugar Maple Board Surface by Plasma Treatment at Low Pressure. In Contact Angle, Wettability and Adhesion, Vol. 6, Koninklijke, Leiden, 2009.

Intégration de nanocelluloses dans des revêtements pour le bois

B. Poaty[1], V. Vardanyan[1], B. Riedl[1], V. Landry[2], G. Chauve[3]

[1]Centre de recherche sur le bois, Pavillon G.-H. Kruger, Université Laval, Québec (QC), Canada, G1V 0A6
[2]FPInnovations, 319 rue Franquet, Québec (QC), Canada, G1P 4R4
[3]FPInnovations, 570 boul. Saint-Jean, Pointe-Claire (QC), Canada, H9R 3J9

Mots clés : bois d'érable à sucre, vernis, peinture, cellulose nanocristalline, intégration, dispersion, renfort mécanique

La cellulose nanocristalline (NCC) a été utilisée pour améliorer les propriétés mécaniques des revêtements à base d'eau destinés aux applications sur le bois. Les films contenant la NCC ont été obtenus par dispersion de différentes concentrations de NCC dans des formulations à cuisson rapide (UV). Le bois utilisé pour tester ces formulations a été l'érable à sucre. L'influence d'un pigment, le TiO_2, a été également étudiée, pour l'obtention de formulations comme vernis ou comme peintures. Les résultats basés sur les microscopies à transmission et à force atomique ont montré que la dispersion de particules de NCC dans le film a été satisfaisante. Aucun véritable agrégat, n'a quasiment pas été observé en dessous des concentrations en NCC de 2 % w/w dans les vernis, et en dessous de 1 % dans les peintures. En dépit d'une légère diminution dans les niveaux de brillance après intégration de NCC, les valeurs restaient tout de même élevées, à savoir au minimum 76 pour les vernis et 56 pour les peintures à un angle de 60°. L'incorporation de particules de NCC dans les formulations n'a quasiment pas affectée la couleur des films de revêtement. Les tests mécaniques de résistance à l'abrasion et de résistance à l'égratignure sur les revêtements ont indiqué une amélioration de ces propriétés particulièrement pour les vernis, avec une meilleure satisfaction lorsque la dose de NCC d'ajout était de 2 %.

Préparation et imprégnation de sol-gel dans le bois

Gabrielle Boivin[1], Véronic Landry [1,2] et Pierre Blanchet [1,2]

FPInnovations, Université Laval

Mots Clés: sol-gel, bois, oxydes métalliques, vieillissement, propriétés mécaniques

Le bois est un matériau renouvelable largement utilisé pour des produits extérieurs (lambris, bardeau, etc.) et intérieurs (planchers, armoires de cuisine, meubles, etc.). Comme le bois est un matériau organique, il est sujet à la dégradation par l'oxygène, les rayons ultra-violets, l'eau et les microorganismes (Mahltig *et al*., 2008). L'amélioration des propriétés mécaniques, thermiques et chimiques du bois permettrait à l'industrie canadienne des produits du bois de rester compétitive et d'atteindre de nouveaux marchés. Le procédé sol-gel est une méthode utilisée pour synthétiser des oxydes métalliques, à partir d'une solution contenant des précurseurs métalliques, tels que des alkoxydes, pour ensuite former un gel par polymérisation inorganique. Selon le sol-gel synthétisé, différentes propriétés du bois peuvent être améliorées. Il est possible de préserver la couleur du bois, de diminuer ou de ralentir son vieillissement, d'améliorer la résistance aux moisissures et les propriétés mécaniques, etc. Dans le présent projet, des échantillons d'érable ont été imprégnés avec des sol-gels à base d'oxydes métalliques (Al_2O_3, SiO_2, ZrO_2). Les gains de masse, les profils de densité et la microscopie optique ont permis de quantifier l'efficacité de l'imprégnation dans le bois. La performance mécanique des surfaces de l'érable, un bois très dur, a été nettement améliorée par l'imprégnation de sol-gels. En effet, une amélioration notable de la résistance aux égratignures et aux impacts a été enregistrée.

Valorisation de cellulose nanocristalline comme pigment à effet dans les revêtements pour le bois

M. Vlad Cristea[*1], *V. Landry* [1, 2], *P. Blanchet* [1, 2]

[1]FPInnovations, Nanotechnologies pour les produits du bois, 319 rue Franquet, Québec, Canada, G1P 4R4
[2]Professeur associé, Université Laval, Québec, Canada, G1V 0A6

Mots clés : cellulose nanocristalline, iridescence, pigment à effet

La cellulose nanocristalline (CNC) est un nouveau matériau obtenu de l'industrie forestière québécoise qui peut grandement contribuer au développement des produits du bois à forte valeur ajoutée. Des études récentes ont relevé que la CNC tend à se comporter comme un pigment à effet. Selon la concentration de CNC dans la phase aqueuse, des structures ordonnées chirales nématiques (dits choléstériques) se forment et s'arrangent sous forme hélicoïdale. La longueur d'onde de la lumière réfléchie change avec l'angle d'observation, d'où le phénomène d'iridescence des films de CNC. Ce projet vise à développer des systèmes de finition à effet pour le bois en utilisant les propriétés iridescentes de la CNC. Différentes stratégies ont été utilisées afin d'obtenir des revêtements iridescents à partir de plusieurs types de formulations à base d'eau pour la finition du bois. Le grand défi est de contrôler le phénomène d'iridescence en préservant la structure chirale nématique de CNC dans ces systèmes de finitions. L'effet de l'ajout de différents types d'additifs organiques et inorganiques sur le phénomène d'iridescence des films avec CNC a été étudié. Les résultats montrent que la CNC est une particule à haute valeur ajoutée qui peut être utilisée avec succès dans les produits de finition pour le bois dans le but d'améliorer la compétitivité des matériaux forestiers. En même temps, ces revêtements à effet pourront également être utilisés dans les emballages intelligents, le papier électronique, les matériaux d'ingénierie avancée ainsi que les cosmétiques.

Nouveaux films de nanocellulose faits de nanocellulose cristalline stabilisée électrostériquement

Han Yang[1], Alvaro Tejado[1], Nur Alam[1], Miro Antal[1] et Theo van de Ven[1]

[1]Département de chimie, Université McGill,

Mots clés : nanocellulose, superhydrophobicité, nanofilm

Nous avons produit une nouvelle nanocellulose cristalline stabilisée électrostériquement (ENCC). Cette cellulose diffère de la nanocellulose cristalline (NCC) et des autres celluloses micro- ou nano-fibrillées.

L'ENCC peut être modifiée de diverses façons, entre autres en la réticulant. Il est possible de produire des films à partir de suspensions d'ENCC modifiée ou non.
Nous avons étudié les propriétés optiques, mécaniques et thermiques de ces films. Les films réticulés ont une meilleure résistance, une stabilité thermique améliorée et un coefficient de transmission de la vapeur d'eau réduit. Cela pourrait les rendre propres à une utilisation comme matériaux d'emballage.

Enfin, nous avons produit des films superhydrophobes en traitant les films d'ENCC au trichloromethylsilane.

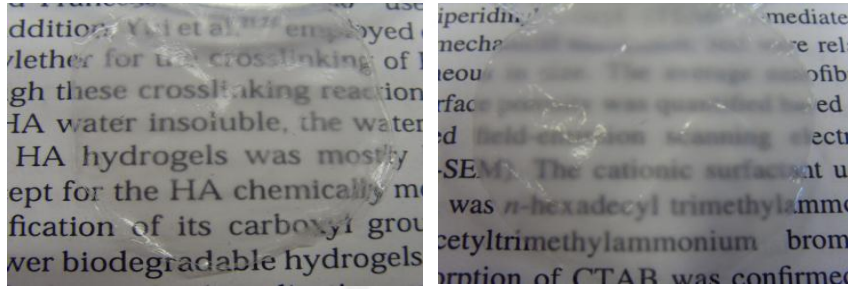

Figure 1 – Films de cellulose stabilisée électrostériquement (ENCC). À gauche le film a été réticulé après sa formation tandis qu'à droite, la suspension a été réticulée avant de former le film.

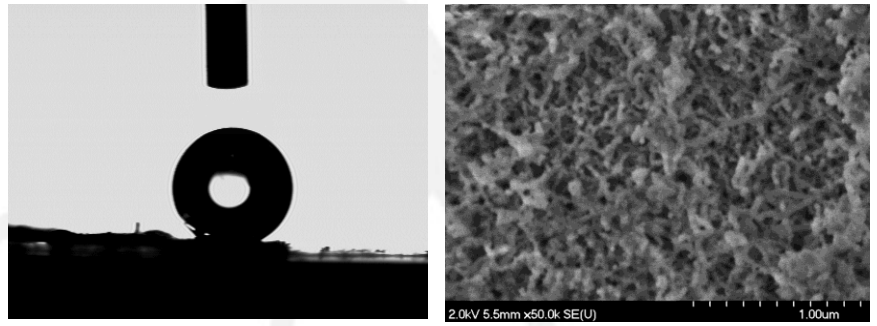

Figure 2 – Film de cellulose stabilisée électrostériquement (ENCC) devenu superhydrophobe après un traitement au trichloromethylsilane. À gauche une gouttelette d'eau perle sur la surface, à droite une image de microscopie SEM de la surface du film.

Modélisation moléculaire sur la phase cholestérique de la nanocellulose cristalline: Interactions fondamentales

P. Bourassa, S. Robert

Université du Québec à Trois-Rivières, 3351, boul des Forges, Trois-Rivières, QC, Canada, G8Z 1V3

Mots clés : nanotechnologie, nanocellulose, propriétés optiques, iridescence

La nanocellulose cristalline est un matériau naturel extrait de la fibre de bois. On l'obtient par l'hydrolyse acide de la cellulose naturelle [1]. À partir de ces cristaux, il est possible de préparer des films colorés qui montrent des propriétés iridescentes [1]. Ces propriétés optiques intéressantes sont dues à l'agencement spécifique des nanocristaux de cellulose en phase cholestérique. Pour obtenir une telle phase liquide cristalline, il faut créer une suspension aqueuse de ces nanocristaux. Pour ce faire, la surface du nanomatériau doit être modifiée afin de posséder des charges négatives. Ceci augmente la répulsion entre les particules ce qui stabilise la suspension. En évaporant l'eau, on obtient la phase cholestérique. Il est possible de modifier le pas de vis de cette phase cholestérique par l'ajout de chlorure de sodium ou autres sels dans la suspension. Ceci entraine donc un changement des propriétés optiques des films issus de ce nanomatériau : la longueur d'onde de la réflexion spéculaire diminue vers le bleu.
Pour mieux comprendre ce phénomène, une approche théorique est utilisée. Les interactions entre le sodium, l'eau et les groupements chargés négativement à la surface de la cellulose (carboxylate et sulfate) sont étudiées par méthodes de calculs de haut niveau (Théorie de la perturbation MP2 et de la fonctionnelle de la densité). Ces calculs permettent de mieux cerner le mécanisme d'auto assemblage de la nanocellulose cristalline et ainsi, comprendre comment peut-on mieux contrôler ses propriétés optiques.

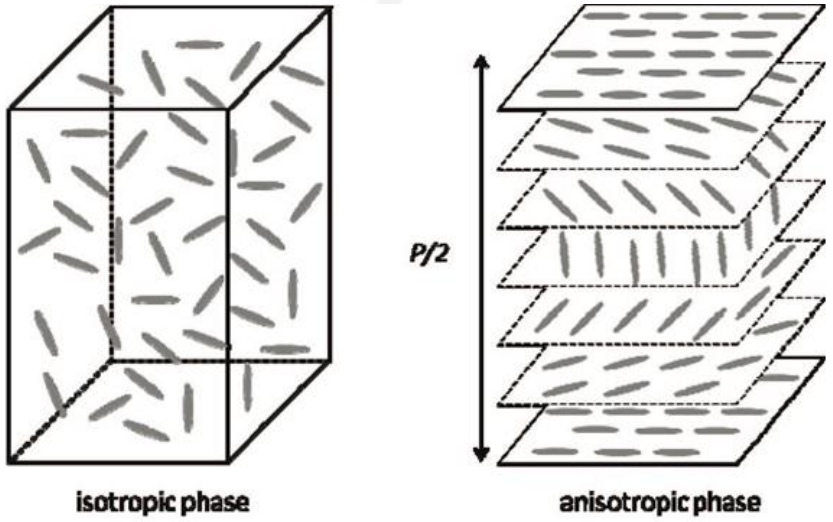

Figure 1 – Assemblage de nanoparticules de cellulose en phase anisotropique (cristaux liquides)

Références

[1] Y. Habibi, L. A. Lucia, O. J. Rojas, Chemical Reviews 110, 3479-3500 (2010).

Structural, energetic, and electronic properties of crystalline cellulose using molecular modeling

Ali Chamikhazraji

Université du Québec à Trois-Rivières, 3351, boul des Forges, Trois-Rivières, QC, Canada, G8Z 1V3

Cellulose is the most abundant chemical compound on earth and its natural affinity for self-adhesion has long been recognized. The ease of adhesion that occurs in cellulose has contributed to its use in paper and other fiber-based composite materials. We have studied the structural, energetic, and electronic properties of crystalline cellulose using molecular modeling Material Studio 5.5. We have found that cellulose has a strong affinity to itself and hydroxyl containing materials. Cellulose molecules are linear and are aggregated through van der Waals (vdW) dispersion forces and both intra- and intermolecular hydrogen bonds that are responsible for binding cellulose chains together.

On the one hand, cellulose has a strong affinity to itself and hydroxyl containing materials. Both hydrogen bonding and van der Waals (vdW) dispersion forces are responsible for bonding cellulose chains together. On the other hand, and based on the preponderance of hydroxyl functional groups, cellulose is very reactive with water. At common ambient environmental conditions, cellulose will have at least a monomolecular layer and up to several molecular layers of water associated with it. Besides that, the water molecules are able to penetrate into the cellulosic fibres network and then interacting. The formation of hydrogen bonds at the water/cellulose interface is shown to depend sensitively on the adsorption site, for example, above the equatorial hydroxyls or OH moieties pointing out the cellulose. The vdW dispersion interactions also contribute significantly to the adsorption energy.

Nouveaux matériaux

HYATT REGENCY, MONTRÉAL

www.nanoquébec.ca

Nanostructured Cu-Ni-Fe-O materials prepared by ball milling as inert anodes for Al electrolysis

S. Helle, G. Goupil, D. Guay, L. Roué*

INRS-EMT, 1650 bd. Lionel Boulet, Varennes, Canada, J3X 1S2

Mots clés : Al production, inert anode, nanostructured materials, mechanical alloying

The primary aluminum industry is a major producer of greenhouse gases. A significant fraction (3.7 tonnes CO_2-eq /tonne Al) comes from the use of consumable carbon anodes in the Al electrolysis process. In this context, a long-term objective of the aluminum industry is to substitute the consumable carbon anodes by inert materials, in order to release O_2 instead of CO_2 during the Al electrolysis process

Cu-Ni-Fe based alloys show promising properties as inert anodes due to their ability to form an adherent, electronically conducting nickel ferrite plus copper oxide scale during the operation of the electrolysis cell. However, Cu-Ni-Fe alloys present a two-phased microstructure (a Cu-rich phase and a Fe-Ni-rich phase), which decreases their corrosion resistance. We have recently shown that this limitation can be partially circumvented by the use of nanostructured and monophased Cu-Ni-Fe alloys synthesized by mechanical alloying [1,2]. However, their corrosion resistance still needs to be improved for long-term use in Al electrolysis cells.

In the present study, nanostructured Cu-Ni-Fe-O materials are prepared by ball milling under oxygen atmosphere. Their structural and chemical characteristics are studied at different stages of their preparation and after 20 h of electrolysis in low-temperature (700°C) KF-AlF_3 electrolyte. It will be shown that oxygen added in appropriate amount during the mechanical alloying process has a major positive effect on the electrode corrosion resistance and purity of produced Al (Fig. 1). The underlying mechanism responsible of this improvement will be discussed.

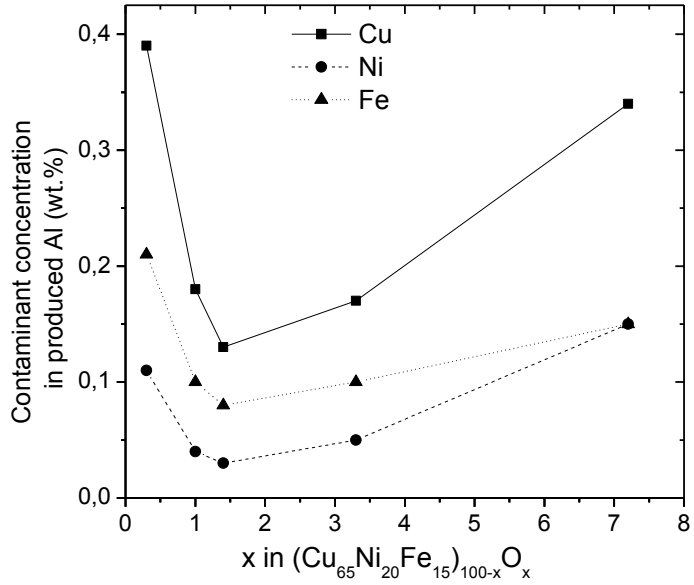

Figure 1 – Cu, Ni and Fe concentrations (wt.%) in the produced Al after 20 h of electrolysis as a function of the amount of oxygen *x* in the $(Cu_{65}Ni_{20}Fe_{15})_{100-x}O_x$ anodes

Références

[1] S. Helle, M. Pedron, B. Assouli, B. Davis, D. Guay and L. Roué, *Corros. Sci.,* 52 (2010) 3348.

[2] S. Helle, B. Brodu, B. Davis, D. Guay and L. Roué, *Corros. Sci.,* 53 (2011) 3248.

Nanoparticules de polymère dopées d'un complexe luminescent et de nanoparticules

J. Desbiens[1], B. Bergeron[1], M. Patry[1], A. Ritcey[1]

[1]CERMA, département de chimie, Université Laval, Québec, Canada, G1V 0A6

Mots clés : mini-émulsion, nanoparticules luminescentes, complexe d'europium, rehaussement de la luminescence, nanoparticules hybrides (organique-inorganique).

La polymérisation en mini-émulsion est maintenant bien connue et utilisée pour la préparation de nanoparticules (NPS) de polymère. L'objectif de nos travaux est de vérifier la possibilité d'intégrer un ou plusieurs dopants aux nanoparticules préparées par cette technique, dans le but de leur conférer des propriétés fonctionnelles additionnelles. La première génération de particules est constituée de polystyrène dopé d'un complexe d'europium choisi pour ses propriétés luminescentes intéressantes (figure 1). Les nanoparticules de polystyrène de la deuxième génération sont dopées simultanément du complexe d'europium et de nanoparticules d'argent (figure 2). Les propriétés de surface des nanoparticules d'argent sont reconnues pour modifier la fluorescence des fluorophores situés à proximité. Il est donc intéressant de connaître l'impact que les nanoparticules d'argent ont sur le comportement du complexe luminescent contenu dans une même nanoparticule de polymère. La polymérisation en mini-émulsion permet la synthèse de grandes quantités (de l'ordre de quelques grammes) de particules de polymère en milieux aqueux. En modifiant la proportion de tensio-actif, le diamètre des particules peut varier entre 40 et 200 nm. Nos travaux ont montré qu'il est possible d'obtenir un taux de dopage de 2% (g cpx Eu/100 g NPs) sans modifier les propriétés luminescentes du complexe d'Eu. De plus, bien que l'incorporation des nanoparticules d'argent ne soit pas complètement optimisée, des premières mesures montrent un impact sur le temps de vie de luminescence du complexe d'europium.

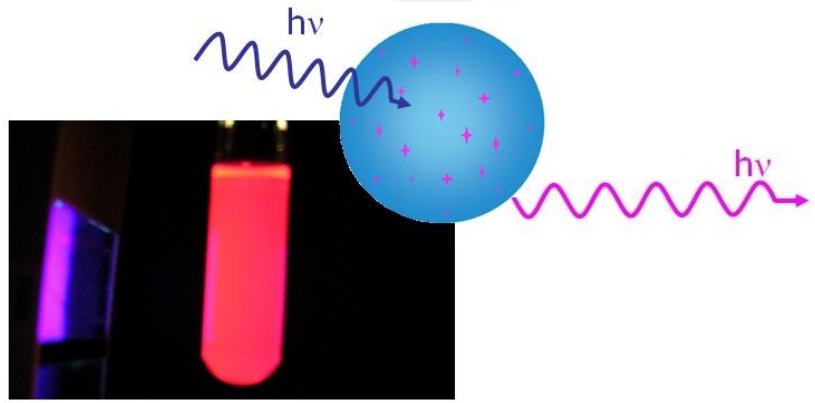

Figure 1 – Photographie d'un échantillon de nanoparticules de polystyrène dopées sous la lampe UV.

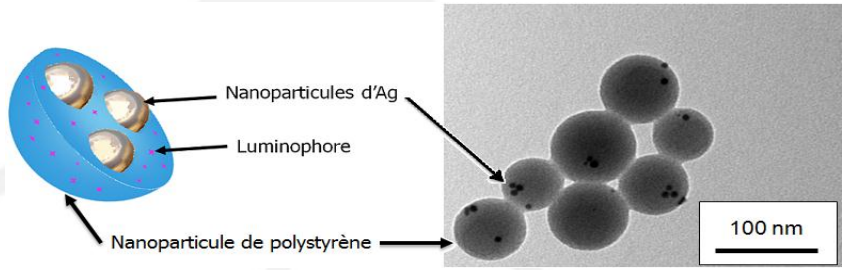

Figure 2 – Schéma et image de microscopie électronique à transmission de nanoparticules de polystyrène dopées simultanément par le luminophore et les nanoparticules d'argent.

Controlled 2D organization of gold nanoparticles in block copolymer monolayers

S. Lamarre, A. Ritcey

Département de chimie and CERMA, Université Laval, 1045 avenue de la Médecine, Pavillon Alexandre-Vachon, Québec, Canada, G1V 0A6

Mots clés : Gold nanoparticles, nanorings, surface organization, block copolymer

The organization of organic-capped gold nanoparticles in PS-*b*-PMMA monolayers is investigated. The preferred location of the particles within the block copolymer template is found to depend on both nanoparticle size and the length of the aliphatic capping agent. In the case of relatively short ligands, the particles behave as hard spheres and their incorporation in the polymer matrix is primarily determined by entropic considerations. Three distinct arrangements are observed. Particles that are small, relative to the radius of gyration of the host polymer, evenly disperse within the PS domains, whereas the largest particles considered form ordered, island-like aggregates. Particles of intermediate size exhibit the most striking arrangement, being relegated to the PS-PMMA interface to form organized ring structures. The tendency of these particles to assemble at the interface is sufficiently strong to force a modification of the polymer morphology to accommodate the particles at higher loadings. As the number of particles is increased, the circular PS-*b*-PMMA surface micelles elongate to form nanostrands.

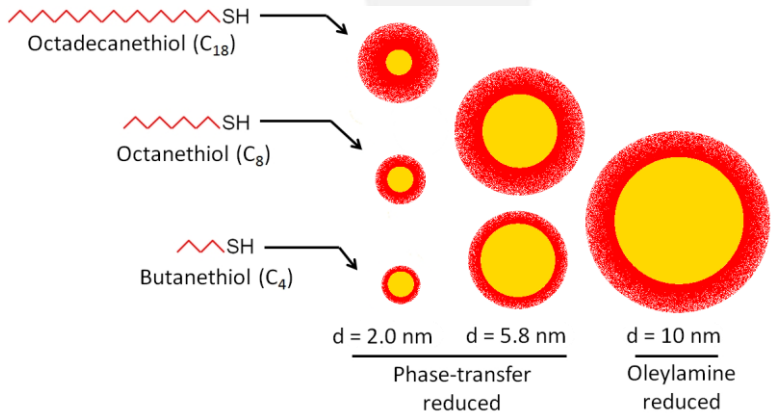

Figure 1 – Schematic representation of the six nanoparticle populations investigated in this work. Ligand contour lengths are drawn to scale relative to particle size.

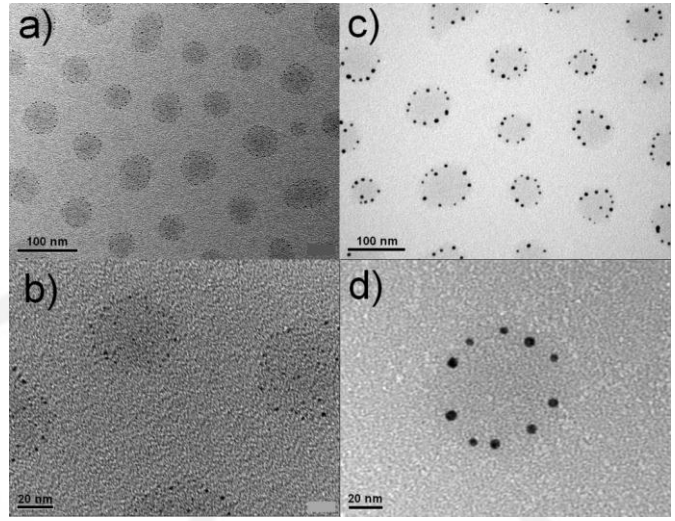

Figure 2 – TEM images of C_8SH stabilized gold NPs incorporated in PS-*b*-PMMA monolayer. Gold core diameter is 2.0 nm in a) and b) and 5.8 nm in c) and d).

Synthèse et caractérisation de nouveaux polymères poreux pour le stockage d'hydrogène

E. Gagnon-Thibault, R. Guillet-Nicolas, F. Kleitz, J.-F. Morin*

Université Laval, 1045 Avenue de la médecine, bureau 1407, Québec, Canada, G1V 0A6

Mots clés : hydrogène, polymère, adsorption

La dépendance aux combustibles fossiles que nous connaissons aujourd'hui créé des problèmes environnementaux majeurs. Une des solutions les plus prometteuses pour tenter de ralentir ceux-ci est sans équivoque l'utilisation de l'hydrogène dans les piles à combustibles pour les véhicules. Pour que ce système soit économiquement viable, son autonomie doit être comparable à celle des véhicules à essence, ce qui nécessite le stockage de plus de cinq kilogrammes d'hydrogène dans un seul véhicule. En ce sens, l'idée principale du projet porte sur le développement de nouveaux matériaux polymères mésoporeux à base de métaux, susceptibles de physisorber un gaz dans sa structure. Ainsi, il sera possible de maximiser les interactions entre les molécules de gaz et la structure, afin d'augmenter l'adsorption d'hydrogène. À ce jour, plus d'une dizaine de matériaux contenant des métaux ont fait leurs preuves, dont les MOFs (*Metal-Organic Frameworks*), les NOPNs (*Nanoporous Organic Polymer Networks*) et les PIMs (*Polymers with Intrinsic Micro-porosity*). Comme ceux-ci, nous exploitons le principe de cavités poreuses (<50 nm) ainsi que l'affinité de la molécule d'hydrogène avec certains types de structures, comme des groupements aromatiques.

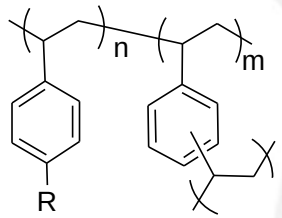

PFcSt-DVB: R = Fc
PSt-DVB: R = H

Figure 1 – Structure du poly(styrène-co-divinylbenzène)

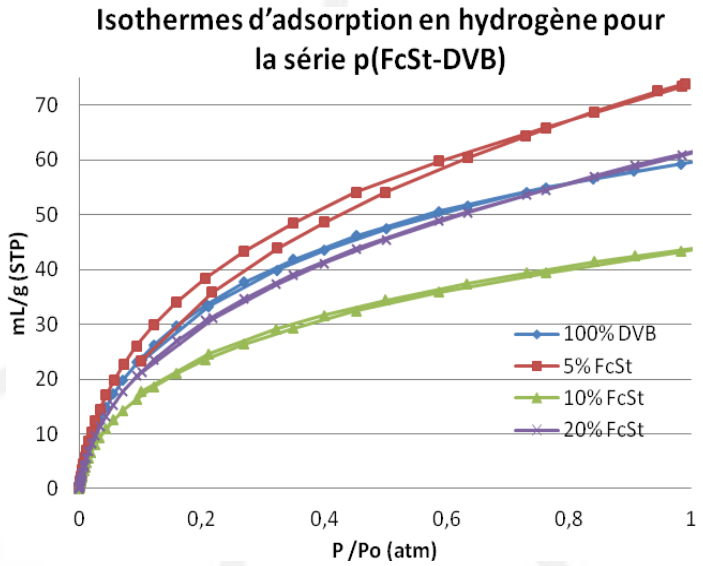

Figure 2 – Isothermes d'adsorption en hydrogènedu poly(ferrocenylstyrène-co-divinylbenzène)

Références
[1] J. Germain, J. M. J. Fréchet, F. Svec. Nanoporous Polymers for Hydrogen Storage, *Small*, **2009**, 5, 10, 1098-1111

Synthesis and Characterization of Core-Shell Quantum Dot-Polymer Nanohybrid Materials Prepared by RAFT-Assisted Emulsion Polymerization

Mitra Vasei[a], *Paramita Das*[a], *Jerome P. Claverie*[a*], *Jean-Philippe Masse*[b] and *Gilles L'Espérance*[b]

[a]NanoQAM, Department of Chemistry, University of Quebec at Montreal, Montreal, Quebec, Canada
[b]Centre de Caractérisation Microscopique des Matériaux, École Polytechnique de Montréal, Montreal, Quebec, Canada

Keywords: Core-shell, Dispersion, Emulsion polymerization, Encapsulation, Quantum dot.

Our recent works propose a simple approach for the synthesis of polymer encapsulated semiconductor quantum dots (QDs). The process involves two steps: dispersion of quantum dots (CdS and PbS) in water by a dispersant polymer and then further emulsion polymerization of dispersant-QDs assembly by a hydrophobic monomer in the presence of an initiator in order to form quantum dot-polymer latex particles. The dispersant is a random copolymer having an average of ten acrylic acid and five butyl acrylate units, synthesized by RAFT polymerization process. Absorption study shows the average size of the nanoparticle is in 4-5 nm range. The morphology of the core-shell nanoparticle is investigated by transmission electron microscopic (TEM) analysis. Depending on the amount of starting QDs, different morphologies of core-shell QDs are obtained. Multiple core to single core core-shell QDs are prepared in this process. The variation in pH suggests that neutral pH provides most significant encapsulation. Detailed mechanism of formation of core-shell QDs is also proposed.

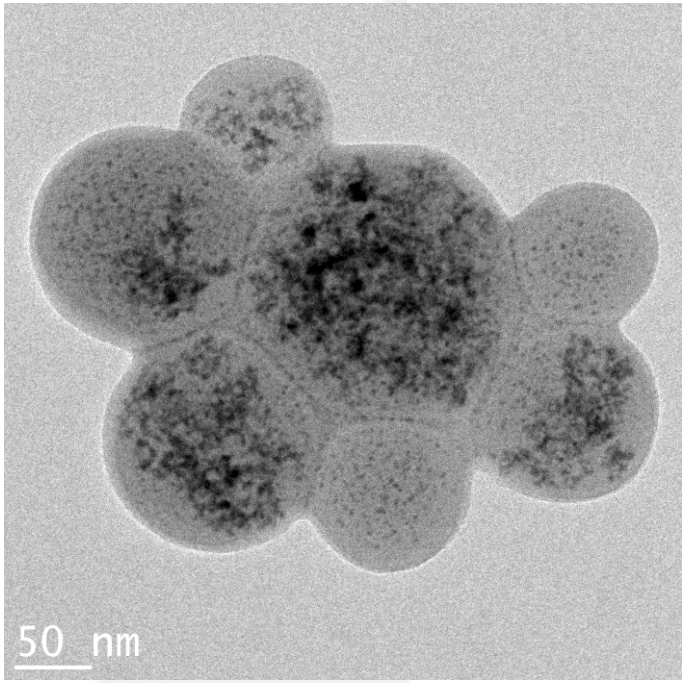

Figure Caption: TEM image of CdS QD-polymer latex particle.

References:
[1] P. Das, W. Zhong, J. P. Claverie, *Colloid Polym. Sci.*, **2011**, 289, 1519.
[2] J-C. Daigle, J. P. Claverie, *J. Nanomaterials*, **2008,** article ID 609184.
[3] Nguyen, H. S. Zondanos, J. M. Farrugia, A. K. Serelis, C.H. Such, B. S. Hawkett, *Langmuir*, **2008**, 24, 2140.
[4] W. Sheng, S. Kim, J. Lee, S-W. Kim, K. Jensen, M. G. Bawendi, *Langmuir*, **2006**, 22, 3782.

Sulfophenyl functionalities grafted on graphitic surfaces for Lithium-ion battery applications

Gul Zeb[1], X. T. Le[1], X. Xiao[2], T. Szkopek[3], M. Cerruti[1]

[1] Mining & Materials Engineering, McGill University, Montreal, QC, Canada
[2] General Motors Global R&D Center, Warren, MI, United States
[3] Electrical and Computer Engineering, McGill University, Montreal, QC, Canada

Mots clés : Lithium ion batteries, nanocomposite, graphene, diazonium chemistry

Sn is a promising anode material for high energy density lithium ion batteries. However, its large volume change during Li insertion and extraction leads to quick mechanical degradation. A promising solution is to use Sn nanoparticles (NPs) in combination with graphitic materials such as graphene to form a composite anode material. Previous studies showed that graphene can be functionalized through oxidation. Sn NPs can then be deposited on the functionalized graphene [1]. The efficiency of these methods is limited by either poor functionalization or low affinity of functional groups towards Sn.

We have investigated sulphophenyl functionalization for capturing Sn-containing NPs with controlled size. Here we have used highly oriented pyrolitic graphite (HOPG) as a model system for graphene. We grafted sulphophenyl groups on HOPG in an aqueous solution of sulfophenyl diazonium cations. Next, we immersed the functionalized HOPG in a stablized $SnCl_{2(aq)}$ and subsequently reduced to obtained Sn NPs. We compared the amount and size of Sn NPs deposited on sulfophenyl functionalized surfaces with HOPG surfaces oxidized by HNO_3. The quantity of Sn on sulfophenyl grafted surface was 2.5% with very small Sn particles size (< 50 nm) and homogeneous distribution. The Sn deposition on HNO_3 oxidized surface resulted in large, uncontrolled and inhomogenously distributed micrometer sized aggregates of Sn. The smaller particle size of Sn is suitable for Li battery applications as it minimizes stress in the Sn/SnO_2 particles upon Li insertion. The functionalization strategy presented therefore allows us to obtain small Sn particles on HOPG, which can be extended to graphene for the synthesis of graphene/Sn NP composite anode materials with the aim of enhancing Li ion battery capacity.

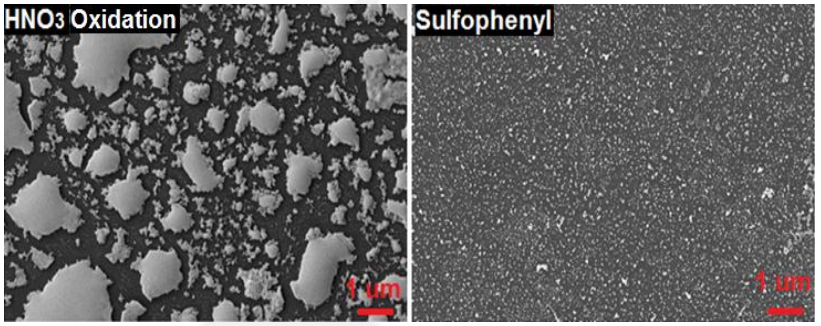

Figure 1 – The functionalization of HOPG through grafting of sulfophenyl groups helps to obtain smaller and homogenously distributed Sn nanoparticles in comparison with functionalization through oxidation.

Reference(s)
[1] G. Wang, B. Wang, X. Wang, J. Park, S. Dou, H. Ahn and K. Kim, *Journal of Materials Chemistry* **2009**, *19*, 8378-8384.

Silica Frustules of Marine Diatoms as Templates for the Growth and Patterning of Gold Nanoparticles

*Jonathan C. Hiltz[1], Ahmadreza Hajiaboli[1], R. Bruce Lennox[1], Mark P. Andrews[1]**

[1]McGill University, Chemistry Department, 801 Sherbrooke west, Montreal, Canada H3A 2K6
*Professor Mark P. Andrews, McGill University, Chemistry department, 801 Sherbrooke west, Montreal, Canada H3A 2K6

Key Words: Diatoms, dewetting, template, nanoplasmonic

The diatom, *Nitzschia Palea*, exhibits a complex silica shell (frustule) topography that resembles the warp and weft pattern of woven glass. The surface is perforated with a lattice of roughly oblong pores between periodically undulating transverse weft ridges. The frustules act as templates for dewetting of thin metal films, where they give rise to two hierarchies of particle sizes and patterned distributions of particles. The temperature dependence of dewetting films of varying thickness on the frustule at varying annealing times is examined. Films 5 nm thick give small particles randomly distributed over the surface, and multiple particles in the pores. Thicker films (10-15 nm) yield larger, faceted particles on the frustule surface and particles that exhibit shapes that are roughly conformal to the shape of the pore container. The pores and ridges (costae) are sources of curvature instabilities in the film that lead to mass transport of gold and selective accumulation in the weft valleys and pores. We suggest that, with respect to dewetting, the frustule comprises 2-dimensional sublattices of trapping sites. The pattern of dewetting is radically altered by inserting a self-assembled layer of mercaptopropyltrimethoxysilane between the Au film and the frustule. By adjusting the interfacial energy in this manner, semi-continuous Au islands are found to coexist with a periodic distribution of nanoparticles in the pores.

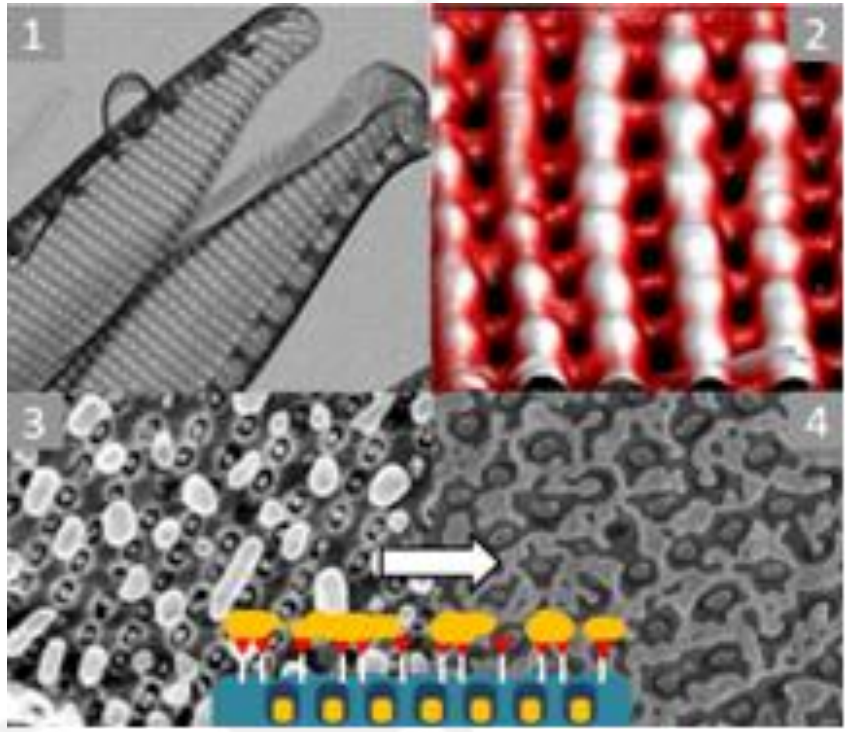

Figure 1 – TEM image of the cleaned frustule of the diatom *Nitzschia Palea* (1) and rendered 3-d image of contact mode AFM scan (2) of the surface, showing the complex topography of the frustule. This texture gives rise to curvature instabilities in deposited metal films, which give rise to two hierarchies of metal structures on the surface (3). Functionalization of the frustule surface modifies the surface energy and gives rise to new structures (4).

References:
[1] P. Das, W. Zhong, J. P. Claverie, *Colloid Polym. Sci.*, **2011**, 289, 1519.
[2] J-C. Daigle, J. P. Claverie, *J. Nanomaterials*, **2008,** article ID 609184.
[3] Nguyen, H. S. Zondanos, J. M. Farrugia, A. K. Serelis, C.H. Such, B. S. Hawkett, *Langmuir*, **2008**, 24, 2140.
[4] W. Sheng, S. Kim, J. Lee, S-W. Kim, K. Jensen, M. G. Bawendi, *Langmuir*, **2006**, 22, 3782.

The curious case of amorphous germanium laser induced crystallization revealed with high temporal resolution transmission electron microscopy

*L. Nikolova*1*, T. LaGrange*2*, M. Stern*3*, J. M. MacLeod*1*, B. W. Reed*2*, H. Ibrahim*1*, G. Campbell*2*, F. Rosei*1 *and B. J. Siwick*3

INRS Center EMT, 1650, Lionel-Boulet blvd, Varennes, QC, Canada, J3X 1S2
LLNL, 7000 East Ave., Livermore, CA, USA, 94550-9234
McGill University, 845 Sherbrooke St. W., Montreal, QC, Canada, H3A 2T5

Mots clés : a-Germanium, laser crystallisation, DTEM

Germanium, known for the significantly higher mobility of carriers in comparison with silicon, finds wide application in the fabrication of solar cells, infrared detectors and high efficiency transistors [1] with ongoing research on laser processing of thin amorphous germanium (a-Ge) films for control over the formed structure. Laser induced crystallisation in a-Ge has shown to be a complex process completing with growth of a unique microstructure with sizes of the crystalline features ranging from a few nanometers to several micrometers (Figure 1). The process evolves over long time interval after initiation of the amorphous to crystalline phase transition and the crystallization may occur at large distances beyond the limits of the laser beam spot. Earlier studies have showed the time for initiation and completion of the process but lack of the requisite spatio-temporal resolution has impeded the in situ observation of the crystallization leaving open questions on the thermodynamics leading to the observed structure. Owing to the newly developed Dynamic Transmission Electron Microscopy at Laurence Livermore National Laboratory [2] we succeeded in visualization of the growth front during its propagation and the events of nucleation and nanocrystallization (Figure 2). By tracking the number and size of the nanocrystals in time, we estimated the nucleation rate and the time for full crystallisation in a-Ge [3]. Based on the time resolved images we have developed a model to estimate the evolution of the temperature in time within the film and in radial direction.

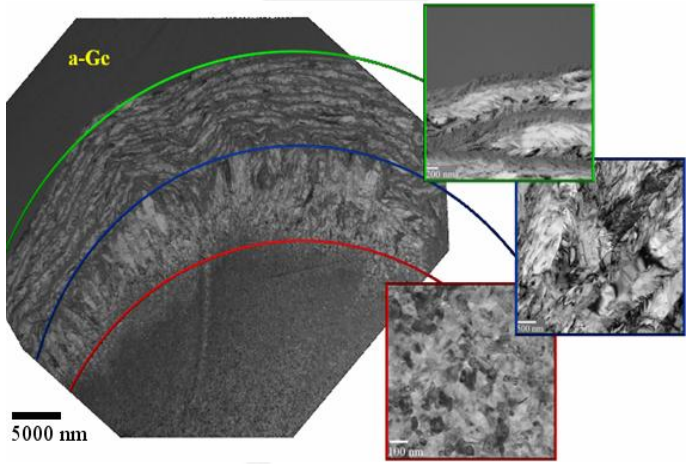

Figure 1: Conventional TEM image showing three qualitatively distinct morphological regions produced after single-shot nanosecond laser induced crystallization in a-Ge (insets – higher magnification view: central coarse nanocrystalline structure (block image framed in red), large raddially elongated crystals (in blue) and layered structure (in green)

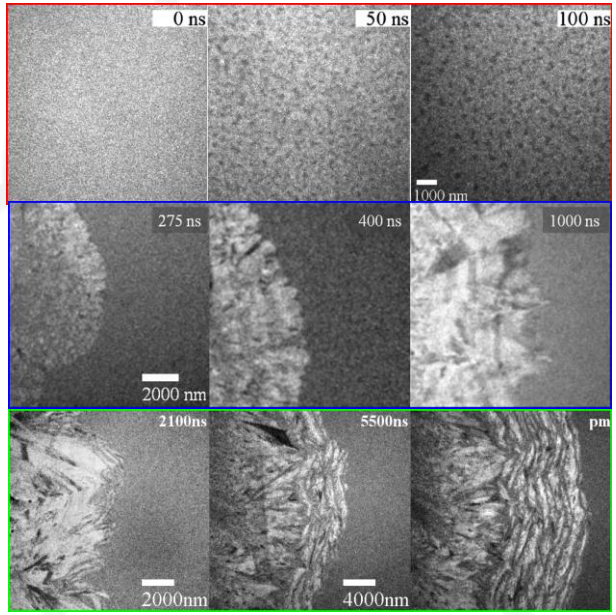

Figure 2: Time resolved images of the evolution of the structures (the same color coding is kept)

Références
[1] R. Pillarisetty, Nature **479**, 324 (2011)
[2] T. Lagrange, *et al.* Ultramicroscopy **108**, 1441 (2008)
[3] L. Nikolova, *et al.* Appl. Phys. Lett. **97**, 203102 (2010)

Reconnaissance chirale et organisation stéréosélective

V. Demers-Carpentier[1], J.-C. Lemay[*1], G. Goubert[1], P. H. McBreen[1]*

[1]Département de Chimie, Université Laval, Québec, Québec

La demande de produits énantiopurs, particulièrement par l'industrie pharmaceutique, conjugée au désir de réduire l'empreinte environnementale de l'industrie, fournit une importante motivation au développement de méthodes de catalyse asymétrique hétérogène.
Parmi les approches prometteuses, notons celles se basant sur la création de sites énantiosélectifs sur un catalyseur par la chimisorption d'un modificateur chiral. Ces réactions demeurent toutefois bien souvent mal comprises, et la rationalisation des assemblages entre les modificateurs chiraux et les substrats pro-chiraux est nécessaire aux développements futurs. Dans cette optique, nous avons étudié de tels assemblages avec la molécule pro-chirale céto-pantolactone (KPL) et le modificateur chiral (R)-1-(1-naphthyl)éthylamine ((R)-NEA) par microscopie à effet tunnel. Une étude statistique des assemblages formés par ces deux molécules révèle que le KPL interagit différemment avec chacun des deux conformères du (R)-NEA présent sur la surface. Il est possible d'obtenir des informations régio- et stéréospécifiques sur ces différents assemblages, qui peuvent être utilisées afin de procéder au développement rationnel de nouveaux chemins catalytiques, de même qu'à l'amélioration de ceux qui sont déjà connus.

Références

[1] Demers-Carpentier, V.; Goubert, G.; Masini, F.; LafleurLambert, R.; Dong, Y.; Lavoie, S.; Mahieu, G.; Boukouvalas, J.; Gao, H.; Havelund Rasmussen, A.; et al. Direct Observation of Molecular Preorganization for Chirality Transfer on a Catalyst Surface. *Science* **2011**, *334,* 776−780.

Highly conductive structural adhesives based on single wall carbon nanotubes for aerospace applications

I.D. Rosca[*1], S.V. Hoa*[1],

[1]Concordia University Mechanical and Industrial Engineering, 1455 Maisonneuve West, Montreal, Canada, H3G 1M8

Keywords : carbon nanotube, structural adhesive, electrical conductivity

Conductive structural adhesives will ensure electrical continuity of bonded aerospace structures and will eliminate the time consuming and weight adding silver brazing or strapping. Using high quality SWCNTs produced by Nikkiso Co (Fig. 1), Epon 862 epoxy resin, and optimized three-roll milling we have obtained homogeneous nanotube dispersions with an ultra-low percolation threshold (0.002 wt%) and conductivities several orders of magnitude higher than those reported in the literature for low nanotube loadings (Fig. 2). The aluminum 2024-T3 lap-joints displayed low electrical resistance (240 W) and higher shear strength (29.9 MPa) than that of the Hysol EA 9392 structural adhesive.

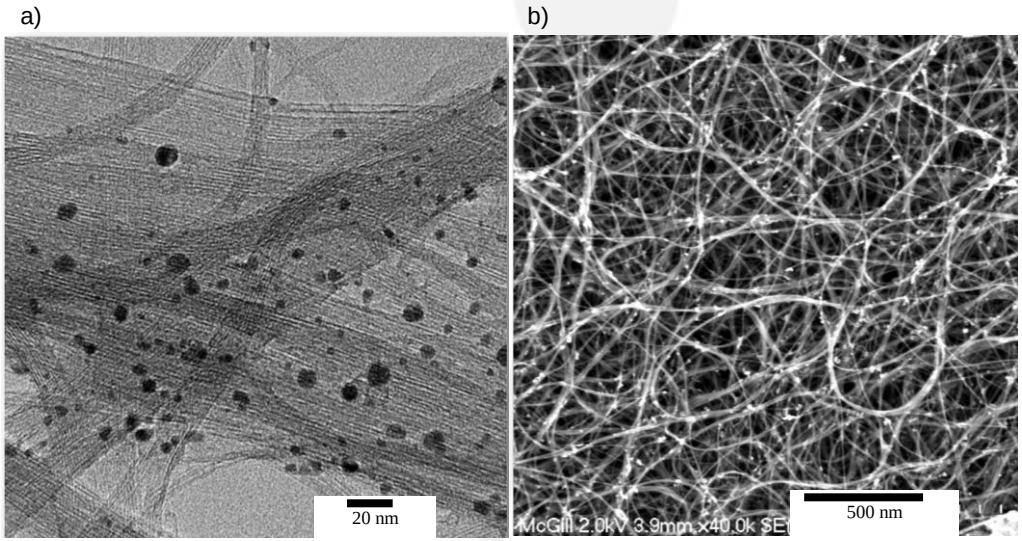

Figure 1 –TEM (a) and SEM (b) images of the as grown SWCNTs

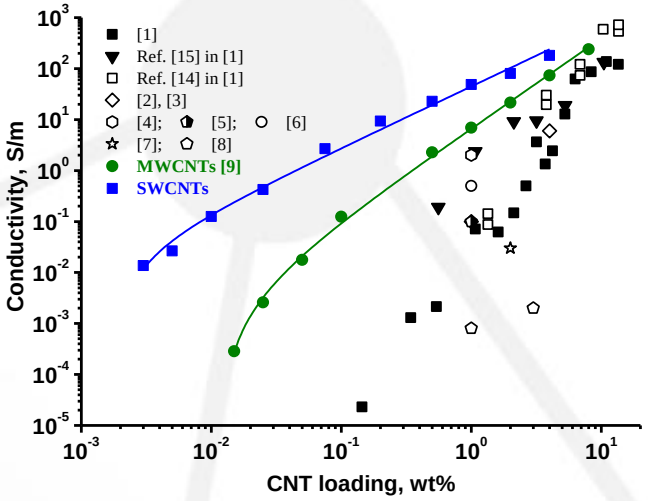

Figure 2 –Conductivity vs. nanotube loading of epoxy composites

References

[1] N. Hu, Z. Matsuda, G. Yamamoto, H. Fukunaga, et al. *Composites A,* **39,** 893, 2008.
[2] J.B. Bai, A. Allaoui, *Composites A,* **34,** 689, 2003.
[3] A. Allaoui, S. Bai, H. M. Cheng, J. B. Bai, *Compos Sci Technol,* **62,** 1993, 2002.
[4] J.K.W. Sandler, J.E. Kirk, I.A. Kinloch, M.S.P. Shaffer, et al. *Polymer,* **44,** 5893, 2003.
[5] J. Li, P.S. Wong, J.K. Kim, *Mater Sci Eng A,* **483–484,** 660, 2008.
[6] J.Li, P.C. Ma, W.S. Chow, C.K. To, et al. *Adv Funct Mater,* **17,** 3207, 2007.
[7] M.H.G Wichmann, J. Sumfleth, B. Fiedler, F.H. Gojny, et al. *Mech Comp Mat,* **42,** 395, 2006.
[8] S. Tian F. Cui, X. Wang, *Materials Letters* **62,** 3859, 2008.
[9] I.D. Rosca, S.V. Hoa, *Carbon*, **47,** 1958, 2009.

Effect of the hydrogen bubbles on the morphological features and optical properties of gold-polymer nanocomposites

Mohammed Alsawafta, Simona Badilescu, Muthukumaran Pakirisamy, and Vo-Van Truong

Concordia University, 1455 de Maisonneuve Blvd. W., Montreal, QC, Canada, H3G 1M8

Keywords : Gold nanoparticles, Nanocomposite material, Nanobubbles.

Gold-polymer nanocomposite is a hybrid material that consists of gold nanoparticles integrated into a polymer host material. Incorporating nano-sized inorganic fillers such as metallic nanoparticles in a polymer matrix, results in the formation of a novel material, with unique physico-chemical properties and interesting applications. The synthesis and properties of the gold-gelatin and gold-poly(vinyl alcohol) nanocomposites with embedded micro- and nanobubbles are investigated in this work [1]. A gold-gelatin nanocomposite is prepared by using sodium borohydride ($NaBH_4$) as a reducing agent for the gold anions and this system is used as a model. Upon adding the aqueous solution of the borohydride to the mixture of the gold precursor ($HAuCl_4$) and gelatin aqueous solution, the formation of a large amount of hydrogen bubbles is observed. During the drying of a thin nanocomposite film deposited on a glass substrate, hydrogen micro- and nanobubbles are entrapped in the material and a “foam”-like material is formed. The gold nanoparticles are coated by gelatin, its positive charged amino groups ($-NH_2$) interacting with the negative surface charges of Au particles. The entrapment of the gold nanoparticles in the traces left upon the explosion of hydrogen bubbles enhances their stability against the natural process of coalescence and agglomeration [2]. The optical response of the gold nanoparticles, controlled by the molar ratio of the BH_4^-/Au^{3+} and the effective refractive index of the surrounding medium is studied in both, solution and solid film. The micro- and nanobubbles entrapped in the nanocomposite are remarkably stable and their interaction with the polymer film, gives rise to very interesting morphological features which are studied in this work (Figure 1).

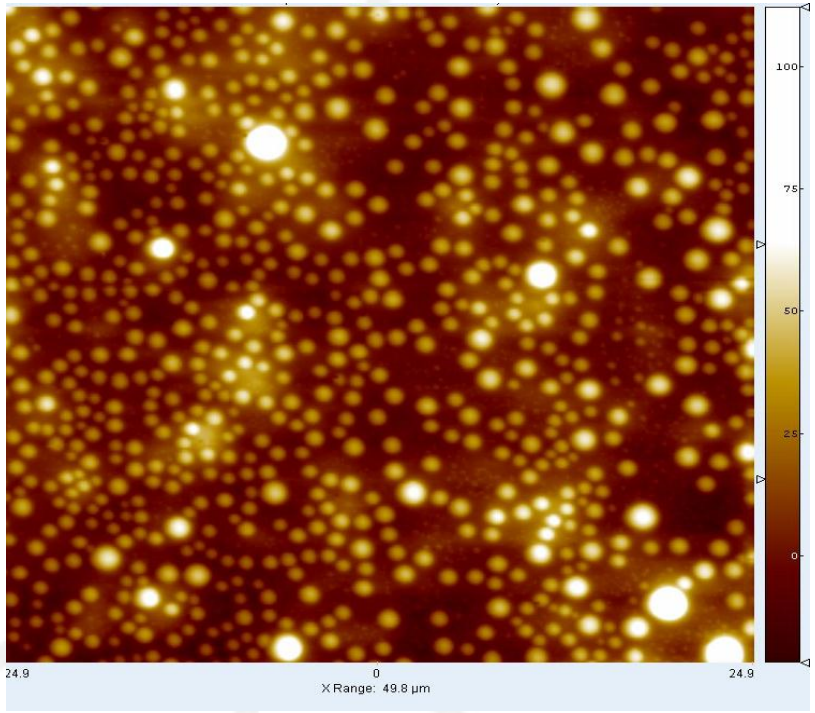

Figure 1 – AFM-height image of well distrusted bubbles.

References

[1] Gold-Poly(methyl methacrylate) Nanocomposite Films for Plasmonic Biosensing Applications, Mohammed Alsawafta , Simona Badilescu , Abhilash Paneri , Vo-Van Truong and Muthukumaram Packirisamy, *Polymers* , 2011, *3*, 1833-1848.

[2] The effect of hydrogen nanobubbles on the morphology of gold–gelatin bionanocomposite films and their optical properties, M Alsawafta, S Badilescu, Vo-Van Truong and M Packirisamy, IOP-Nanaotechnology,2012,23,065305.

Fluorescent, Thermoresponsive Oligo(ethylene glycol) Methacrylate- based Copolymers via Nitroxide Mediated Controlled Radical Polymerization

B. Lessard[1], *E. Ling*[1], *M. Marić**[1]

[1]McGill University, Dept. Chemical Engineering, 3610 University Streeet, Montréal, Canada, H3A 2B2

Keywords : thermo-responsive, nitroxide mediated polymerization (NMP), Controlled radical polymerization (CRP), fluorescent and tunable lower critical solution temperature (LCST)

Poly[oligo(ethylene glycol) methacrylate] (OEGMAs), are known to be non-toxic, biocompatible and thermo-responsive when dissolved in water, exhibiting a lower critical solution temperature (LCST). Consequently, OEGMA based materials have found application in next-generation drug delivery and bio-sensing applications. LCST tuning of POEGMAs is readily done by changing the length of the oligo(ethylene glycol) segment in the side chain or by copolymerizing OEGMAs of varying EG lengths.[1] We applied controlled radical copolymerization of OEGMAs with functional comonomers to allow not only LCST tuning but incorporation of a hole-transporting functionality, which is suitable as a fluorescent tag. Nitroxide mediated polymerization (NMP) using an alkoxyamine initiator (BlocBuilder^{TM}) and 9-(4-vinylbenzyl)-9H-carbazole (VBK) as a comonomer, resulted in a controlled copolymerization, exhibited by a linear increase in number average molecular weight (Mn) versus conversion ($X < 0.6$) and resulting in final copolymers with relatively narrow molecular weight distributions (M_w/M_n = 1.3-1.6). By modifying the copolymer composition, a tunable LCST library (81 °C < LCST < 31°C) for the poly(OEGMAs-*ran*-VBK) was obtained. The poly(OEGMAs-*ran*-VBK) were then used as macroinitiators for the polymerization of a second poly(OEGMAs-*ran*-VBK) segment with a different composition, resulting in block copolymers exhibiting two tunable and distinct LCSTs. VBK served not only as a controlling comonomer for the synthesis of poly(DMAEMA) and poly(OEGMAs), but also as a fluorescent tag, demonstrating that NMP can be used to synthesise fluorescent, thermo-responsive *"*smart*"* materials with controlled microstructures.

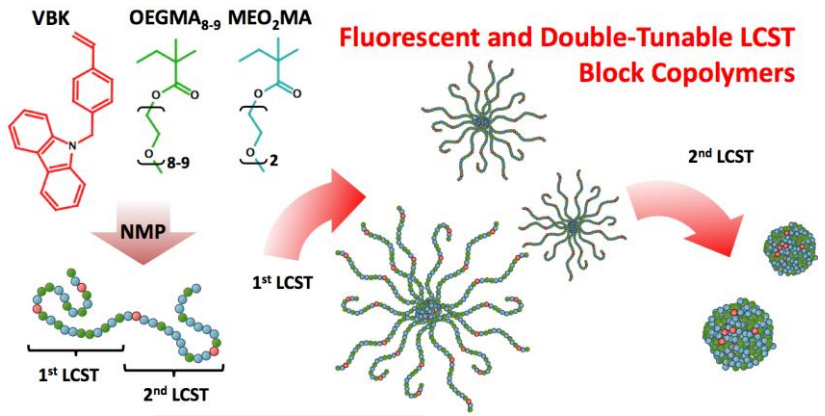

Figure 1 – Fluorescent and double-tunable lower critical solution temperature (LCST) block copolymers.

References
[1] Lutz, J.-F.; Hoth, A. *Macromolecules* **2006**, *39*, 893–896.

Layered Double Hydroxides for Alkaline Fuel Cells

M. J. Paulo[1], B. Matos[1,2], F.C.Fonseca[2] and A.C. Tavares[1]

[1] INRS-EMT, Institut National de la Scientifique Recherche – Enérgie, Matériaux et Télécommunications, Varennes, Qc, Canada
[2] CCCH, Instituto de Pesquisas Energéticas e Nucleares , S.Paulo, SP, Brazil

Keywords : Layered double hydroxides, monobutyletherethyleneglycol, anionic electrolyte, alkaline fuel cell.

Layered Double Hydroxides (LDH) are structurally composed by stacks of positively charged Mg^{2+} and Al^{3+} ions with a double hydroxide layer intercalated by anions in a hydrated gallery to maintain the overall charge neutrality. Hydrotalcite ($Mg_6Al_2(OH)_{16}(CO_3).4H_2O$) is the most representative compound of the LDH family. However, hydrotalcite has carbonate anions in the interlayer space which are characterized by a low mobility due to its size, bi-valence and strong interaction with the [Mg-Al-OH] layers [1]. The aim of the current work is to improve the electrical properties of hydrotalcite-like compounds in order to use this type of materials as electrolyte in alkaline fuel cells. In this work, Meixnerite ($Mg_6Al_2(OH)_{18}.4H_2O$), a LDH with OH^- anions in the gallery (HT-OH), was synthesized from hydrotalcite (HT) by reconstruction method, and was further modified with monobutyletherethyleneglycol (HT-MBEEG) a very hydrophilic molecule. These samples were characterized by X-ray Diffraction, X-ray Photoelectron spectroscopy, N_2 physisorption analysis, Dynamic Vapor Sorption, Transmission Electron Microscopy, Electrochemical Impedance Spectroscopy (EIS). EIS measurements revealed that the anion conductivity of HT-MBEEG is superior to the HT-OH by three orders of magnitude, Figure 1. The electrical properties of the materials are correlated to their morphology and water sorption properties. HT-MBEEG is a promising candidate to work as electrolyte in alkaline fuel cells.

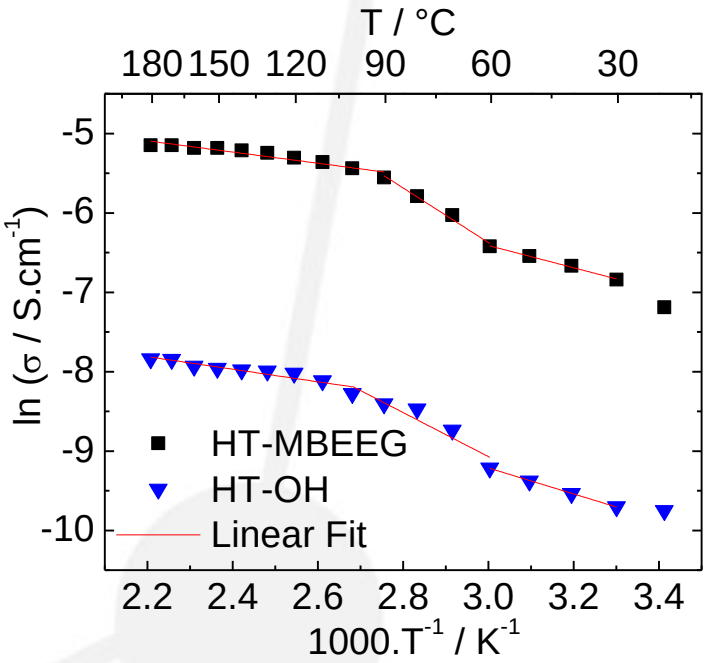

Figure 1– Arrhenius plot of Mexnerite intercalated with hydroxide anion (HT-OH) and modified with monobutyletherethyleneglycol (HT-MBEEG).

Références
[1] V. REEVES, In “Layered Double Hydroxides: Present and Future”, New York: Nova Science, 2001, pp. 140.

Synthesis of lanthanides fluorides nanoparticles for MRI and luminescent bimodal imaging.

M. Blanchette, A. Ritcey*[1]

[1]Université Laval et CERMA, 1045 ave de la Médecine, Québec, Canada, G1V 0A6

Mots clés : Nanoparticules, micelles inverses, lanthanides, gadolinium, imagerie

Présentation des avancées de la synthèse de nanoparticules cœur-coquille de fluorure de terres rares par microémulsion inverse[1]. La synthèse se déroule en deux étapes. En premier, il y a la synthèse des cœurs de fluorure d'yttrium (YF_3). Puis, dans le même milieu réactionnel, nous faisons l'ajout d'une coquille de fluorure de gadolinium (GdF_3). Le cœur de fluorure d'yttrium est un monocristal qui peut être dopé avec d'autres lanthanides afin de produire des nanoparticules fluorescentes. Dans notre laboratoire, nous avons démontré qu'il est possible de doper le cœur avec différents lanthanides sans en affecter la structure[2]. De plus, la matrice d'YF_3 est transparente aux longueurs d'ondes d'excitation et d'émission des lanthanides. L'ajout de la coquille de gadolinium a été démontré grâce à la microscopie électronique en transmission à haute résolution (HR-TEM) et par spectroscopie à dispersion d'énergie par rayons-X (EDXS); voir figure 1. Également, des mesures préliminaires démontrent que la coquille de gadolinium est en mesure de réduire le temps de relaxation longitudinale (T1) du cyclohexane et de l'eau, les deux solvants retrouvés dans le milieu de synthèse. Finalement, nous travaillons également sur l'ajout d'une coquille de silice afin de rendre les nanoparticules cœur-coquille dispersables en milieu aqueux et biocompatibles.

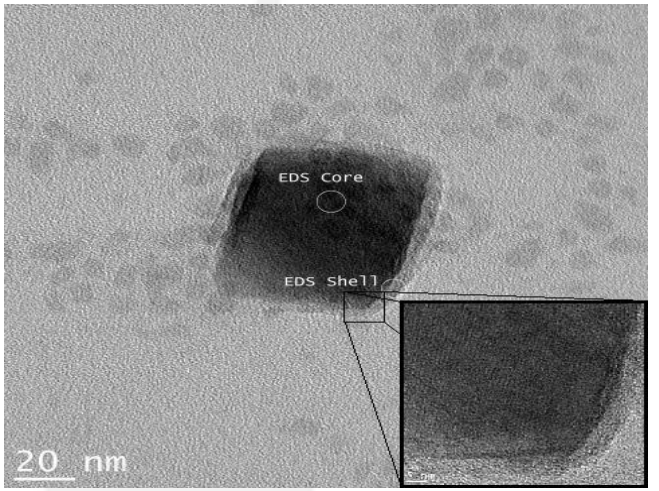

Figure 1 – Image HR-TEM d'une nanoparticule d'YF_3@GdF_3

Références

[1] Lemyre, J.-L., Lamarre, S. b., Beaupré, A., Ritcey, A. M., *Mechanism of YF_3 Nanoparticle Formation in Reverse Micelles*. Langmuir 2011, 27 (19), 11824-11834.

[2] Dorais, M.C. *Développement de nanoparticules inorganiques luminescentes dopées aux lanthanides, mémoire de maîtrise*, Université Laval, Québec, 2011.

Dispersion des nanotubes, science ou art?

W. Zhong, J. Claverie

NanoQAM, Département de Chimie, Université de Québec à Montréal, succ Centre Ville CP8888, Montréal, Canada, H3C 3P8

Mots clés : carbone nanotubes, dispersion, isotherme de Langmuir, seuil de percolation

Depuis leur découverte, les nanotubes de carbone (CNT) ont connu de nombreux succès dans le domaine de la nanotechnologie. Ses propriétés mécanique, électronique et thermique nous conduisent à de nouvelles gammes de matériaux nanocomposites fonctionnels. La performance de ces nanocomposites dépend grandement de la dispersion des CNT dans la matrice solide. L'avantage d'une dispersion stable permet d'éviter la modification chimique des CNT, qui d'une part peut être coûteuse et d'autre part risque de réduire leurs propriétés exceptionnelles. Les études de mécanisme d'adsorption nous permettront d'élaborer de meilleures stratégies de dispersion. Les isothermes de Langmuir sont tracées avec les nanotubes à parois simple (SWNT) et à parois multiples (MWNT) en présence des tensioactifs anioniques (SDS, SDBS), cationique (BzT) et non-ionique (Tx-100). Les résultats expérimentaux nous montrent que l'adsorption des tensioactifs dépend non seulement de la température et de la présence des électrolytes. Mais d'autres paramètres tels le diamètre des CNT, la structure et la taille du tensioactif peuvent conduire à la formation de monocouche, de double couche, ou d'hémi-micelles adsorbées. L'ensemble influence fortement la stabilité colloïdale des CNT en fonction du type de tensioactif. Avec l'optimisation de la méthode de dispersion, des films de CNT sont préparés en présence de nanoparticules polymériques. Des mesures de conductivités sur ces films permettent de déduire le seuil de percolation du réseau de CNT au sein d'une matrice solide. La connaissance de ce mécanisme d'adsorption nous permettra de sélectionner de meilleures stratégies de dispersion des CNT dans des matrices plus complexes en vue d'applications industrielles.

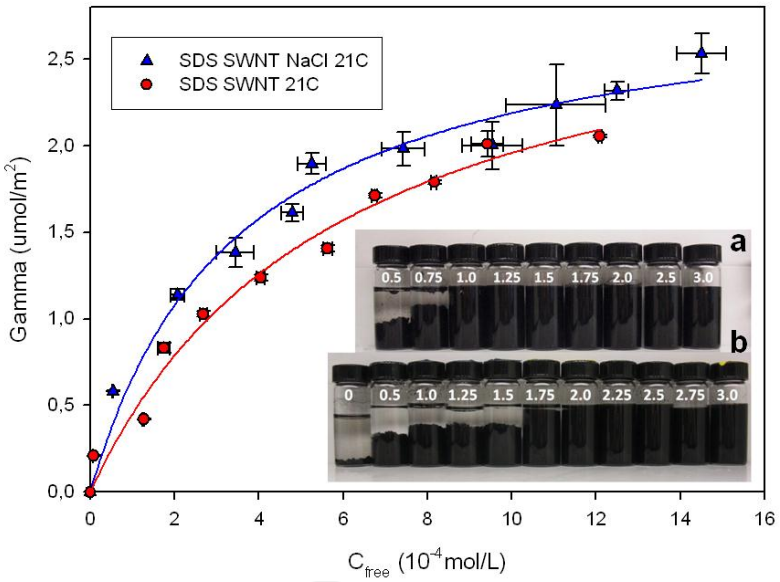

Figure 1 – Isotherme d'adsorption des nanotubes à parois simple (SWNT) par le SDS avec et sans présence d'électrolytes (NaCl) - Dispersion des SWNT (1g/L) dans l'eau (a) et dans une solution saline (NaCl = 0,5 mmol/L) avec différentes concentrations de SDS (g/L)

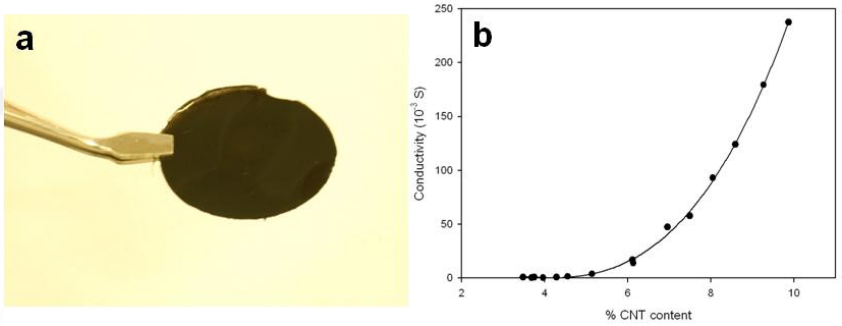

Figure 2 – (a) Film de nanotube de carbone, (b) Mesure de conductivité du film en fonction de l'incorporation de MWNT (% wt)

Références
[1] Lemyre, J.-L., Lamarre, S. b., Beaupré, A., Ritcey, A. M., *Mechanism of YF_3 Nanoparticle Formation in Reverse Micelles*. Langmuir 2011, 27 (19), 11824-11834.
[2] Dorais, M.C. *Développement de nanoparticules inorganiques luminescentes dopées aux lanthanides, mémoire de maîtrise*, Université Laval, Québec, 2011.

Procédé de co-extrusion pour la fabrication de microfilaments tubulaires en écriture directe

M. Arguin, D. Therriault

Laboratoire de Mécaniques Multi-échelles, École Polytechnique de Montréal, 2500 chemin de Polytechnique, Montréal, Canada, H3T 1J4

Mots clés : Co-extrusion, micro-tubes, procédé de fabrication, micro-fluidiques

La fabrication d'un micro-tube est un procédé complexe dû aux nombres importants d'étapes. Un montage de co-extrusion (figure 1) a été conçu de façon à fabriquer des microfilaments tubulaires. Ainsi, deux matériaux sont extrudés simultanément de façon à ce qu'ils soient coaxiaux. En utilisant un matériau sacrificiel au centre, il sera donc possible de créer un microtube. Des tests ont été faits pour vérifier s'il est possible d'utiliser la co-extrusion dans la fabrication de microfilaments en écriture directe. Pour les tests, deux encres fugitives composées de cire microcristalline et de vaseline ont été utilisées. Pour vérifier le fonctionnement du montage avec des matériaux de différentes viscosités, l'encre fugitive à l'extérieur et à l'intérieur étaient composées respectivement à 30% et 40% de cire microcristalline. Un colorant bleu a aussi été intégré dans l'une des encres de façon à les différencier. Ainsi, des filaments concentriques de 840µm et 510µm ont pu être fabriqués grâce à la co-extrusion (figure 2). Il est donc envisageable d'utiliser le montage de co-extrusion pour la fabrication de microfilaments avec différents matériaux. Dans les travaux futurs, des tests seront faits afin de fabriquer des microfilaments tubulaires à partir de deux matériaux différents. Aussi, le montage sera adapté pour permettre l'écriture directe assistée par rayonnement ultraviolet [1]. En utilisant un matériau sacrificiel au centre du filament, il sera possible de créer des microtubes ou une structure tubulaire. Plusieurs applications en microfluidique seraient alors envisageables comme pour les mélangeurs chaotiques. [2]

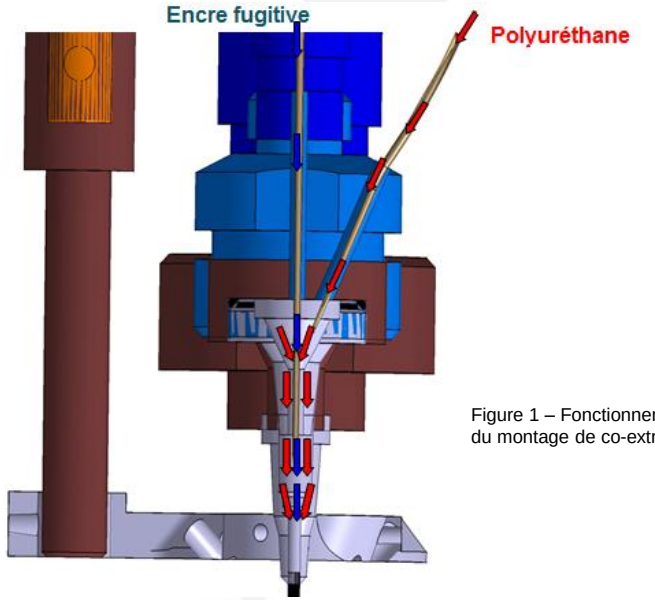

Figure 1 – Fonctionnement du montage de co-extrusion

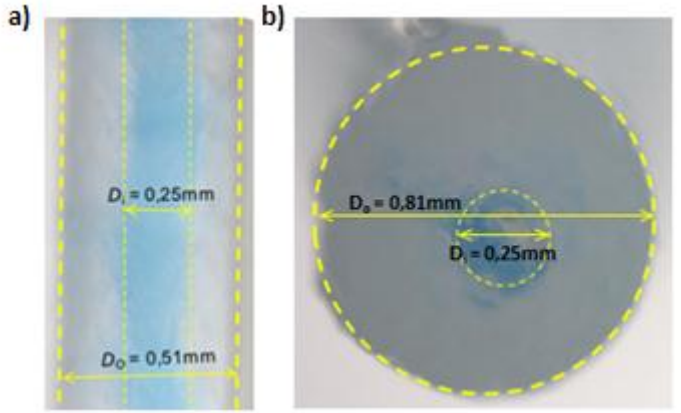

Figure 2 – a)Vue de profil d'un filament co-extrudé de 0,51mm de diamètre; b) Vue transversale d'un filament co-extrudé de 0,81mm de diamètre

Références
[1] L. Laberge Lebel et al. Ultraviolet-Assisted Direct-Write Fabrication of Carbon Nanotube/Polymer Nanocomposite Microcoils, Advance Materials, 2011.
[2] D. Therriault et al. Chaotic mixing in three-dimensional microvascular networks fabricated by direct-write assembly, Nature Materials, 2003

Optimisation de la dispersion de nanoparticules dans les revêtements à base aqueuse pour le bois.

Carmel Jolicoeur, Thi Cong To, Nathalie Otis, Patrick Ayotte, Thomas Gaudreault

Université de Sherbrooke

Mots clés : nanoparticules, oxydes métalliques, dispersants, DLS, UV, potentiel zêta, dispersion

L'utilisation de particules nanométriques d'oxydes métalliques dans des revêtements protecteurs pour le bois permet d'en bonifier les propriétés telles que la résistance à l'abrasion et la durabilité sous l'influence des rayons UV. Cependant, l'agglomération en suspension est favorisée par la petite taille des particules et davantage au pH d'application où le potentiel zêta est proche du point isoélectrique. Les principaux objectifs du projet consistent à comprendre les phénomènes d'agrégation des nanoparticules dans différents milieux et à développer des méthodes et des adjuvants pour assurer une dispersion optimale des nanoparticules dans les formulations à base aqueuse. La stabilité de suspensions nanométriques d'oxydes métalliques en milieu aqueux a été évaluée par des mesures de taille des agrégats (diffusion statique et dynamique de la lumière), du potentiel zêta et par l'observation de la sédimentation en fonction du temps. Les conditions de préparation (protocole de dispersion, milieu, pH, force ionique, température) influencent la stabilité des suspensions. La stabilité est améliorée par l'utilisation de dispersants moléculaires et polymériques de faibles masses, qui permettent de conserver en suspensions pendant plusieurs semaines des agglomérats d'environ 100 nm. Les travaux réalisés à date permettent d'identifier les caractéristiques d'un dispersant idéal pour les nanoparticules d'oxydes métalliques.

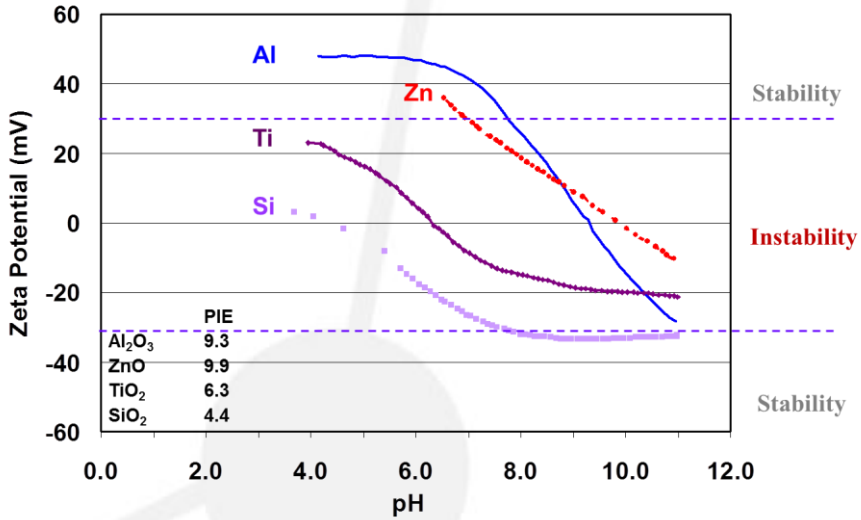

Collaborateurs : Véronic Landry, FPInnovations
Bernard Riedl, Université Laval
Monique Pagé, Handy Chemicals (Rutgers Polymères)
Stanislav Stoyanov, NINT-CNRC

Hydrogen Uptake in Palladium doped Electrospun Boron Nitride Nanofibers at Room Temperature

Samaneh Shahgaldi, Zahira Yaakob,Dariush Jafar Khadem, Wan Ramli Wan Daud

[1]Fuel Cell Institute, Universiti Kebangsaan Malaysia, 43600 UKM Bangi, Selangor, Malaysia

Keywords : Hydrogen storage, Boron nitride nanofibers, palladium, electrospinning

Undoubtedly, global warming is one of the main issues causing environmental degradation. Currently, the primary issue related to global warming is the combustion of fossil fuels. Hydrogen was introduced as an ideal energy source because it is abundant, renewable, highly efficient, and clean. Hydrogen also has a higher chemical energy than hydrocarbon fuels; however, the storage of hydrogen is the main barrier to the further improvement of hydrogen technology. Extensive study on different carbon nanostructures has led to the comparison with other carbonless nanomaterilas. In this study, pd-doped boron nitride nanofibers were synthesized via electrospinning for first time. Electrospinning method is often adopted for the synthesis of one-dimensional nanofibers due to high productivity, simplicity, and cost-effectiveness. In this work, boric oxide was coated on electrospun pd-doped polyacrylonitrile nanofibers. Pd-boron nitride nanofibers, with the diameter of less than 100-150 nm were produced after nitridation. The presence of palladium nanoparticles, and unique morphology of nanofibers were shown by Scanning electron microscopy (SEM), energy dispersive X-ray spectroscopy (EDX), and transmission electron microscopy (TEM). Hexagonal structure of boron nitride nanofibers and palladium peaks were studied by X-ray diffraction (XRD). The pressure composition isotherm shows that the presence of platinum and increasing pressure has a direct effect on the hydrogen absorption.

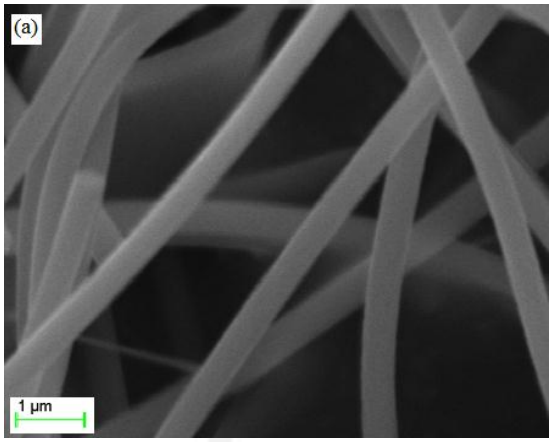

Fig.1 (a) SEM image of electrospun polyacrylonitrile (b) TEM image of Pd doped boron nitride nanofibers

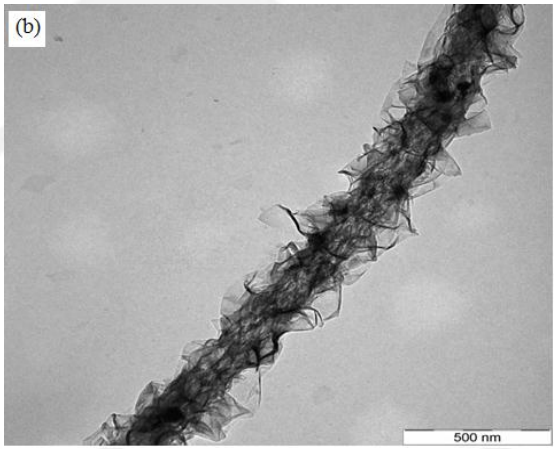

Références

[1] M. Niemann, S.Srinivasan, AR. Phani, A. Kumar, DY. Goswami, EK. Stefanakos. Nanomaterials for hydrogen storage applications: a review. J Nanomater; 2008:950967.

[2] D. Portehault, C. Giordano, C. Gervais, I. Senkovska, S. Kaskel, C. Sanchez, M. Antonietti, High-Surface-Area Nanoporous Boron Carbon Nitrides for Hydrogen Storage, Advanced Functional Materials (2010), Volume: 20, Issue: 11, Pages: 1827-1833.

.

Fabrication and Characterization of Electrospun $LaNi_5$ Nanofibers

Samaneh Shahgaldi, Zahira Yaakob,Dariush Jafar Khadem, Wan Ramli Wan Daud

[1]Fuel Cell Institute, Universiti Kebangsaan Malaysia, 43600 UKM Bangi, Selangor, Malaysia

Keywords: $LaNi_5$ nanofibers, Electrospinning, Surface area, Hydrogen Storage

One of the most obstacle for improving of hydrogen technology is the finding a safe, reliable and efficient method for hydrogen storage. AB5 type alloys have been intensively investigated due to the suitable hydrogenation properties and many application such as hydrogen storage, purification, Ni- metal hydrides batteries and chemical heat pumps. This work reports synthesize and characterization of LaNi5 nanofibers via electrospinning for first time. The sol-gel for electrospinning was prepared by dissolving proper amount of polyvinylpyrrolidone in ethanol with 10%wt ratio at 40°C and solution was stirred for 2h with a magnet and stirrer system to gain a homogenous solution. Lanthanum and nickel nitrate was mixed to polymer solution. The final homogeneous viscous solution was immediately drawn into the hypodermic syringe. Electrospun nanofibers were collected on aluminium collector and calcined in air. Calcined nanofibers were exposed to hydrogen gas with calcium hydride as a reduction agent. LaNi5 nanofibers with diameter of around 150nm-200 nm were successfully obtained for first time. The electrospun nanofibers were characterized by SEM, XRD, FT-IR, and BET. The result indicated a significant effect of calcination temperature on the morphology of nanofibers. Long and continuous $LaNi_5$ anofibers shows higher surface area in compare to the other $LaNi_5$ nanostructures.

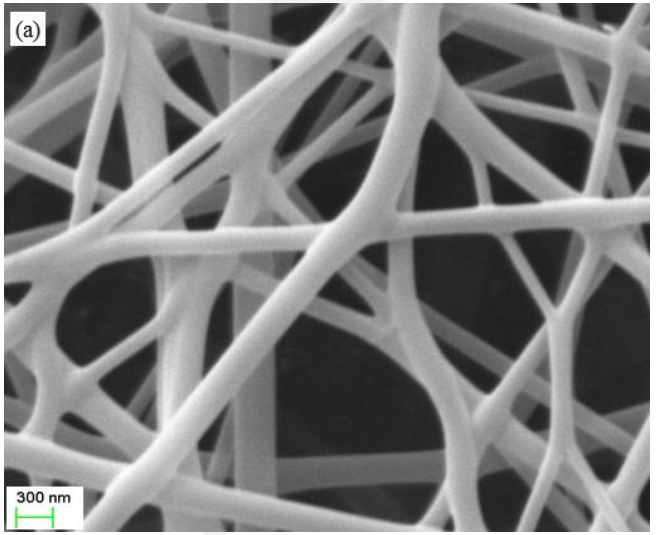

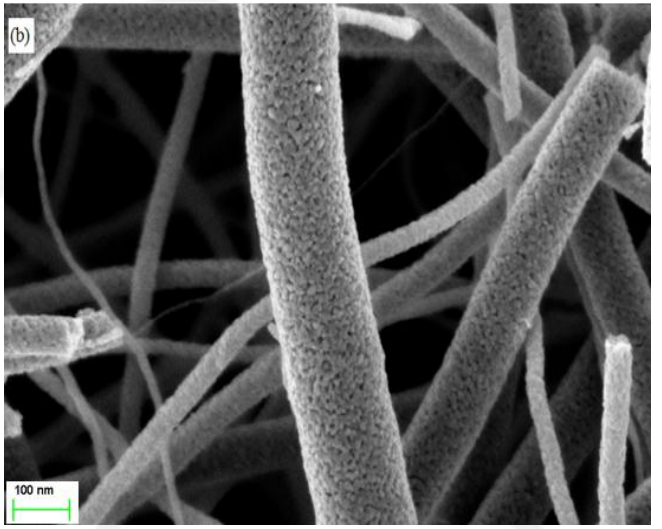

Références
[1] M. Niemann, S.Srinivasan, AR. Phani, A. Kumar, DY. Goswami, EK. Stefanakos. Nanomaterials for hydrogen storage applications: a review. J Nanomater; 2008:950967.
[2] D. Portehault, C. Giordano, C. Gervais, I. Senkovska, S. Kaskel, C. Sanchez, M. Antonietti, High-Surface-Area Nanoporous Boron Carbon Nitrides for Hydrogen Storage, Advanced Functional Materials (2010), Volume: 20, Issue: 11, Pages: 1827-1833.
.

Atomistic simulations of ultrashort pulse laser ablation of nancrystalline Al

M. Gill-Comeau[*1], *L. J. Lewis*[1]

[1]Département de physique et Regroupement Québécois sur les Matériaux de Pointe, Université de Montréal, C.P. 6128, Succ. Centre-Ville, Montréal, Québec, Canada, H3C 3J7

Mots clés : ablation laser, impulsions ultrabrèves, matériaux nanocristallins

En utilisant un modèle hybride de dynamique moléculaire et de simulation des milieux continus nous avons étudié l'ablation par impulsions laser ultrabrèves de cibles nanocristallines d'aluminium. Nos résultats indiquent que la technique serait applicable pour le micro- et le nano-usinage puisque les dommages thermiques sont relativement faibles. Notre étude montre d'ailleurs que l'énergie nécessaire pour causer l'ablation dans une cible nanocristalline est significativement plus faible que dans une cible polycristalline traditionnelle. Toutefois nous avons aussi observé que les cibles nanocristallines étaient plus susceptibles de subir des dommages mécaniques découlant de l'ablation. Ces résultats sont à la fois imputables aux propriétés électroniques et aux propriétés mécaniques du métal nanocristallin. Des cibles possédant des tailles de cristallites différentes ont été utilisées et il a été trouvé que les effets cités sont plus prononcés lorsque les cristallites sont plus petites. De même, l'impact de la porosité de la cible a été abordée et il a été montré que celle-ci tend à dissiper la pression se créant suite au chauffage rapide de la cible et donc à légèrement inhiber l'ablation.

Références

[1] M. Gill-Comeau et L.J. Lewis, Ultrashort-pulse laser ablation of nanocrystalline aluminum, *Physical Review B* **84**, 224110 (2011).

Ferroelectric properties of individual single-crystalline $BiFeO_3$ nanowires

S. Li[1], R. Nechache[1,2], C. Harnagea[1], A. Ruediger[1] and F. Rosei[1,3]

[1] Université du Québec, Institut national de la recherche scientifique, Énergie, Matériaux et Télécommunications, INRS, 1650, boulevard Lionel-Boulet, Varennes, Québec J3X 1S2, Canada
[2] NAST Center & Department of Chemical Science and Technology, University of Rome Tor Vergata Via della Ricerca Scientifica 1, 00133 Rome, Italy
[3] Centre for Self-Assembled Chemical Structures, McGill University, Montreal, QC, H3A 2K6, Canada

Mots clés : nanotechnologies, expertise, leadership

One-dimensional (1D) materials such as various kinds of nanowires and nanotubes have attracted considerable attention due to their potential application in electronic and energy conversion devices. To explore the rich physics of ferroelectricity, especially at low dimensionality and at nanoscale, perfectly structured polar oxide nanomaterials are the optimal samples for study. They are also potential building blocks for the realization of nanoscale actuators, sensors, nonlinear optics, and especially high density ferroelectric nonvolatile memory devices. With the recent advance in the synthesis of piezoelectric or ferroelectric nanomaterials, it is now possible to study 1D physics of ferroelectricity using such chemically and structurally well defined crystalline materials. We report piezoresponse force microscopy (PFM) investigations on the ferroelectric properties of individual single-crystalline bismuth ferrite ($BiFeO_3$) nanowires fabricated by a solution based hydrothermal method. Piezoelectric hysteresis loops were obtained from as-synthesized $BiFeO_3$ nanowires, thereby demonstrating that nanowires retain ferroelectricity. The effective remnant piezoelectric coefficient is about 40 pm/V and comparable with the values obtained from $BiFeO_3$ thin films. Furthermore, we show that nonvolatile electric polarization can be reproducibly induced and manipulated on these nanowires. These $BiFeO_3$ nanowires should provide promising materials for fundamental investigations on nanoscale ferroelectricity, and they may also be useful in nanoscale nonvolatile memory applications.

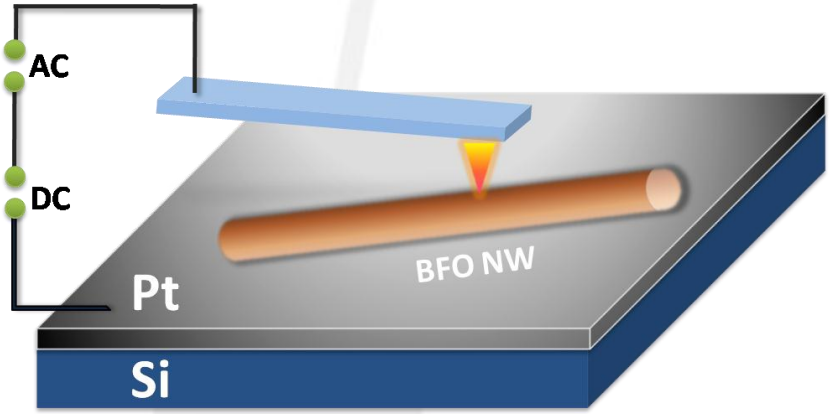

Figure 1 – Schematic illustration of the experimental setup of PFM for ferroelectric switching study of nanowire.

Références
[1] P. M. Rørvik , T. Grande, and M.-A. Einarsrud. Adv. Mater. 2011, 23, 4007–4034
[2] B. Liu, B. Hu and Z. Du. Chem. Commun., 2011, 47, 8166-8168

Effect of Surface Oxidation on the Interaction of 1-Methylaminopyrene with Gold Nanoparticles

*J.-M. Zhang, D. Riabinina, M. Chaker and D.-L. Ma**

Institut National de la Recherche Scientifique, INRS-Énergie, Matériaux et Télécommunications, 1650 Boulevard Lionel-Boulet, Varennes, QC, Canada, J3X 1S2

Keywords : gold nanoparticles, laser irradiation, amine adsorption, surface chemistry, gold oxide

The effect of the surface chemistry of gold nanoparticles (GNPs) on the GNP-amine (-NH_2) interaction was investigated by conjugating an amine probe ─ 1-methylaminopyrene (MAP) chromophore ─ with three Au colloidal samples of the same particle size yet different surface chemistry. The surface of laser-irradiated and ligand-exchanged-irradiated GNPs is covered with acetonedicarboxylic ligands (due to laser-introduced citrate oxidation) and citrate ligands, respectively. Both surfaces contain oxidized Au species that are essentially lacking in the case of citrate-capped GNPs prepared using the pure chemical approach. Laser irradiated GNPs show lower adsorption capacity of MAP as compared with the purely chemically prepared GNPs. Detailed investigations indicate that MAP molecules mainly complex directly with Au atoms via forming Au-NH_2R bonds. Moreover, the oxidization of GNP surface strongly influences the ratio of this direct bonding to the indirect bonding originating from the electrostatic interaction between protonated amine (-NH_3^+) and negatively charged surface ligands. The influence of the oxidized GNP surface prepared using a laser treatment is further confirmed by aging experiment on GNP-MAP conjugation systems, which straightforwardly verifies that the surface oxidation leads to the decrease in the MAP adsorption on GNPs.

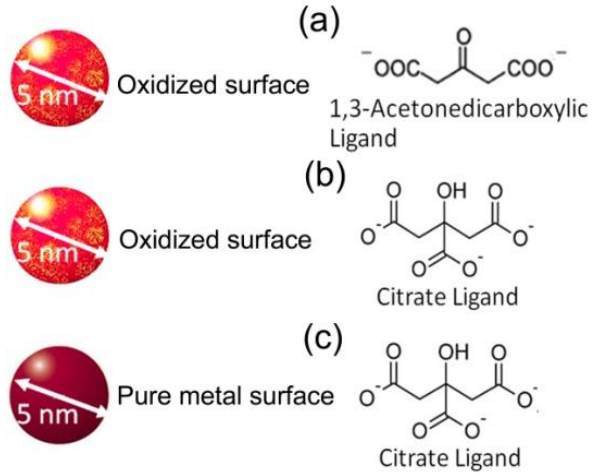

Figure 1. Surface characteristics of the GNPs prepared by laser-irradiation before (a) and after (b) ligand exchange using citrate, and by $NaBH_4$ reduction (c) for MAP conjugation.

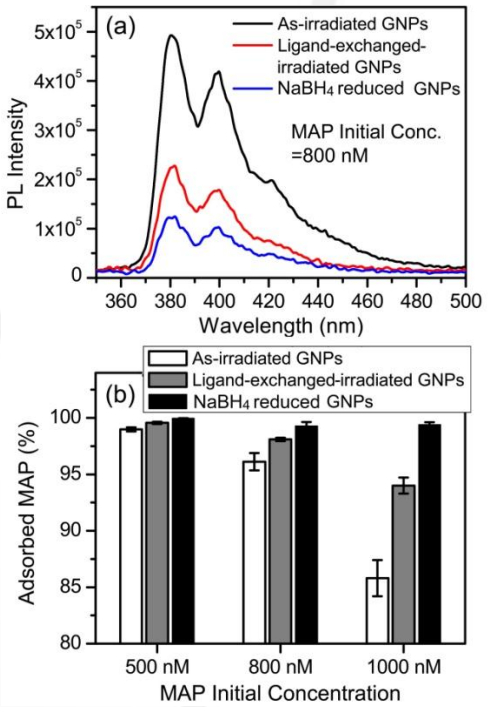

Figure 2. (a) Photoluminescence spectra of the filtrate solutions after 800 nM MAP conjugating with the laser-irradiated GNPs before and after ligand exchange with citrate, and the chemically prepared ones, respectively, at pH=5.5. (b) Adsorption of 500, 800 and 1000 nM of MAP to the three types of GNPs at pH=5.5.

References
[1] J.-M. Zhang, D. Riabinina, M. Chaker, D.-L. Ma, *Langmuir.* **2012**, *accepted*.
[2] J.-M. Zhang, D. Riabinina, M. Chaker, D.-L. Ma, *Adv. Sci. Lett.* **2011**, *4*, 59–64.

Purification de nanoparticules paramagnétiques par chromatographie d'exclusion de taille

M. Laprise-Pelletier[1,2,3,4], J.L. Bridot[1,2,3,4], L. Faucher[1,2,4], J. Lagueux[1], F. Kleitz[3,4] , M.A. Fortin[1,2,4]

[1]Centre Hospitalier Universitaire de Québec, Axe métabolisme, santé vasculaire et rénale (CRCHUQ-MSVR), Québec, Canada, G3L 1L5
[2]Département de génie des mines, de la métallurgie et des matériaux, Université Laval, Québec, Canada, G1V 0A6
[3]Département de chimie, Université Laval, Québec, Canada, G1V 0A6
[4]Centre de recherche sur les matériaux avancés (CERMA)

Mots clés : chromatographie, nanoparticules, imagerie IRM, imagerie TEP

Les nanoparticules paramagnétiques à base de l'élément gadolinium sont développées pour des applications d'imagerie cellulaire et moléculaire. L'élément chimique gadolinium permet de diminuer le temps de relaxation des protons d'hydrogène, se traduisant par une augmentation du signal dans les images de résonance magnétique (IRM). La préparation des particules paramagnétique nécessite une étape de purification qui, jusqu'à présent, était effectuée par dialyse. Cette procédure est relativement longue et utilise plusieurs litres de liquide de dialyse. Une des approches les plus prometteuses dans le domaine de l'imagerie moléculaire et cellulaire, est l'intégration de radio-isotopes dans les particules paramagnétiques, en vue de coupler l'excellente résolution de l'IRM, avec la très grande sensibilité de la tomographie par émission de positons (TEP). Or, les radio-isotopes métalliques d'intérêt pour la TEP ont une demi-vie relativement courte ($t_{1/2}$ (^{64}Cu) = 12.3 h), incompatible avec les temps de dialyse actuels. Afin d'accélérer l'élimination des ions paramagnétiques (Gd^{3+}) et radioactifs (^{64}Cu) des suspensions colloïdales, la chromatographie par exclusion de taille a été choisie afin de purifier des nanoparticules ultra-petites de Gd_2O_3 (~3nm), de même que des nanoparticules de silice mésoporeuses de plus forte taille (~150 nm). La purification des particules mésoporeuses a été réalisée au moyen de colonnes de chromatographie commerciales (NAP-25). Les particules ultra-petites de Gd2O3 nécessitent la conception d'une colonne adaptée et réutilisable, permettant une purification rapide et reproductible de ces produits. Ces techniques seront intégrées aux procédures de synthèse de traceurs bimodaux IRM/TEP.

Références

[1] Faucher, L. et al. Ultra-small PEGylated Gd2O3 nanoparticles (submitted Feb 2012).
[2] Guillet-Nicolas R, Bridot JL, Seo Y, Fortin MA, Kleitz F (2011) Enhanced relaxometric properties of MRI “positive” contrast agents confined in three-dimensional cubic mesoporous silica nanoparticles. *Advanced Functional Materials* (Wiley) (accepted)

Propriétés thermiques et nanostructure de revêtements de $Y_2Si_2O_7$: effet des paramètres de marche du procédé de projection thermique à partir de précurseurs liquides

Émilien Darthout[1], Guillaume Laduye[1], François Gitzhofer[1]

[1]CREPE, Université de Sherbrooke, Sherbrooke, Québec, CA, J1K 2R1

Mots clés : barrières environnementales, SPPS, projection plasma inductif, plan d'expérience, diffusivité thermique.

Le disilicate d'yttrium $Y_2Si_2O_7$ fait partie de la famille des silicates de terre rare et possède une excellence résistance à la corrosion humide [1-3]. Les revêtements de disilicate d'yttrium sont élaborés par projection plasma à partir de précurseurs liquides : le nitrate d'yttrium ($Y(NO_3)_3 \bullet 6H_2O$) et le TEOS ($Si(OC_2H_5)_4$), respectivement précurseurs d'yttrium et de silicium. Les précurseurs liquides sont injectés dans le plasma sous forme de goulettes micrométriques qui vont subir une pyrolyse à cause de haute température du plasma (>10 000 °C). En résulte la formation de nanoparticules d'oxydes d'yttrium et de silicium qui viendront de déposer à la surface du SiC pour former un revêtement protecteur. Le temps de vol entre le moment où sont injectées les goulettes dans la plasma et le dépôt de nanoparticules sur le substrat est de 100 ms. Les différents paramètres de marche du procédé de synthèse influent sur la structure du revêtement qui conditionne ses performances. Nous avons choisi la distance de projection (influe sur le temps de vol et la température du subtrat), la concentration des précurseurs en solution (influe sur le mécanisme de pyrolyse et le flux de matière), le débit de gaz d'atomisation (influe sur la taille et la vitesse d'injection des goulettes dans la plasma) et la pression de travail (influe sur la vitesse des particules en vol). Un plan d'expérience de type D-optimal a été réalisé afin d'évaluer l'influence de chacun des paramètres (qu'ils soient couplés ou non) sur l'épaisseur et la porosité des revêtements nanostructurés. L'observation de coupes polies au microscope électronique (*Figure 1*) à balayage permet l'évaluation de l'épaisseur moyenne des revêtements et par traitement de l'image la porosité peut être estimée. Des mesures de diffusivité thermique des différents échantillons jusqu'à 800 °C permettent de corréler les effets de l'épaisseur et de la porosité des revêtements avec des performances thermomécaniques.

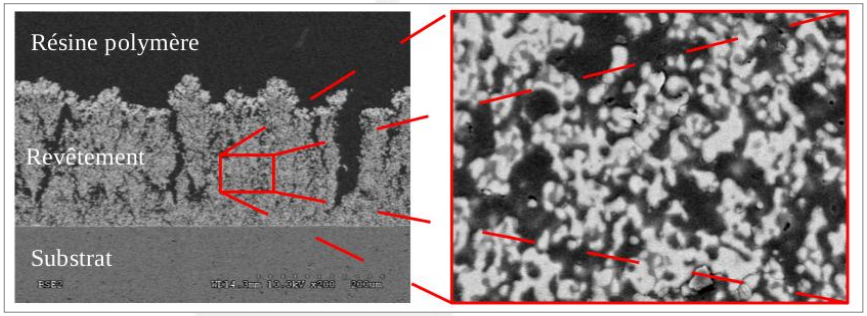

Figure 1: Clichés MEB de coupes polies (gauche, x200) pour mesure d'épaisseur et (droite, x6000) pour mesure de porosité

Références

[1] Accelerated oxidation of SiC CMC's by water vapor and protection via environmental barrier coating approach, Harry E. Eaton, Gary D. Linsey, Journal of the European Ceramic Society 22 (2002) 2741–2747

[2] Effects of high water-vapor pressure on oxidation of SiC at 1200°C, P. F. Tortorelli and K. L. More, Journal of the American Ceramic Society 83 (2003) 1249-1255

[3] Preparation and the hydro thermal corrosion resistance of silicon nitride with a Lu-Si-O EBC layer at high temperature, Ueno, S., Jayaseelan, D.D., Ohji, T., Kondo, N., Kanzaki, S., (2003) Journal of Ceramic Processing Research, 4 (4), pp. 214-216

Morphology and properties of proton conducting titanate - Nafion nanocomposites prepared by microwave-assisted hydrothermal *in situ* method

B.R. Matos[1,2], E.I. Santiago[2], M. Linardi[2], J.F.Q. Rey[3], A.C. Tavares[1]and F.C. Fonseca[2]*

[1]INRS-EMT, Institut National de la Recherche Scientifique – Enérgie, Matériaux et Télécommunications, Varennes, Qc, Canada, J3X 1S2.
[2]CCCH, Instituto de Pesquisas Energéticas e Nucleares , S.Paulo, SP, Brazil, 05508000.
[3]CECS, Universidade Federal de ABC, S.André, SP, Brazil,

Keywords: PEM fuel cell, Nafion®, titanate, proton conduction, hybrid electrolyte.

The synthesis *in-situ* of inorganic nanoparticles such as titania, silica and zirconium phosphate in ionomer films using the sol-gel route is a well-established method to prepare hybrid proton conducting membranes [1]. One disadvantage of such method is the restriction of producing nanoparticles with new architectures such as nanotubes, nanosheets or porous frameworks [2].
The purpose of the present work is to show that spherical titania nanoparticles incorporated in a ionomer matrix can be modified *in situ* to a new nanostructure with designed phase and morphology. Titania nanofillers were prepared *in situ* by the sol-gel method in a Nafion membrane. This precursor composite membrane was immersed in a concentrated basic solution and placed inside a Teflon covered inox reactor. A conventional hydrothermal process was carried out in an oven at 150 °C for 24h, while the microwave-assisted hydrothermal process was performed by placing the reactor in a microwave oven at 150 °C for 180 min. The composite membranes were characterized by Transmission Electron Microscopy, X-ray Diffraction (XRD), Small Angle X-ray Scattering (SAXS), Dynamic Vapor Sorption and Impedance Spectroscopy. The XRD measurements revealed that the anatase precursor phase was successfully modified into the proton conducting titanate phase ($H_2Ti_3O_7$). SAXS spectra confirmed the morphological change of the inorganic phase inside the polymer matrix (Figure 1). The Nafion proton conducting nanocomposites are envisioned as good candidates for electrolytes in proton exchange membrane fuel cells.

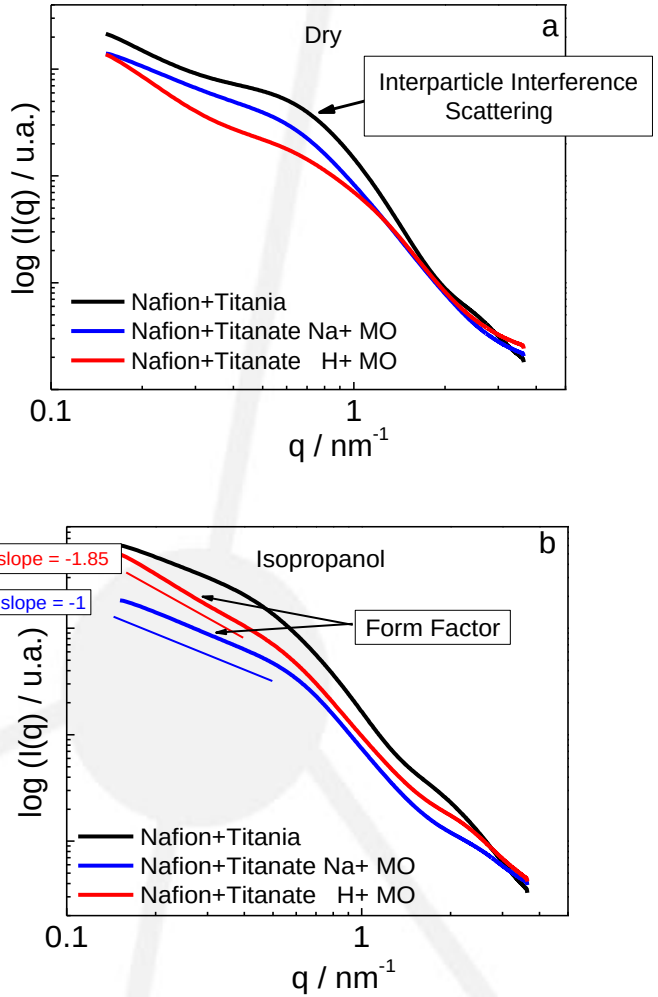

Figure 1 – Small Angle X-ray Scatering patterns of the *in situ* modified Nafion-Titanate composites in the dry (a) and saturated with isopropanol (b).

References
[1] G. Alberti, M. Casciola, Annu.Rev.Mater.Res. **33**, 129 (2003).
[2] G.J. Wilson, A.S. Matijasevich, D.R.G. Mitchell, J.C. Schulz, G.D Will, Langmuir **22**, 2016 (2006).

Acknowledgements
This work supported by the following agencies: *CAPES, CNPq, CNEN* and *FAPESP* from Brazil; *CFI* and *FQRNT* from Quebec, Canada.

Piezoelectric and ferroelectric properties of $Bi_4Ti_3O_{12}$ nanorods

M. Azodi[1], C. Harnagea[1], V. Buscaglia[2], M. T. Buscaglia[2], P. Nani[2], F. Rosei[1], A. Pignolet[1]

[1]Institut National de la Recherche Scientifique, Centre Énergie, Matériaux Télécommunications (INRS-EMT), 1650 Boulevard Lionel-Boulet, Varennes, Canada J3X 1S2
[2]Institute for Energetics and Interphases, National Research Council, Genoa, Italy, I-16149,

Mots clés : $Bi_4Ti_3O_{12}$, nanorods, piezoresponse force microscopy.

We report on the piezoelectric and ferroelectric properties of individual one-dimensional objects made of $Bi_4Ti_3O_{12}$ (BiT). The nanorods and nanowires investigated in this study were fabricated by a two-step process: (1) preparation of reactive templates using hydrothermal-like synthesis and colloidal chemistry and (2) transformation of the reactive templates in $Bi_4Ti_3O_{12}$ by solid-state reaction at 600-700°C, overcoming the morphological instability problem of 1D templates. The polarization switching behaviour of several individual nanorods, with different sizes, using a scanning probe microscopy, namely, piezoresponse force microscopy (PFM). PFM with both out-of-plane and in-plane detection capability showed that both types of objects exhibit a strong piezoelectric activity and a good ferroelectric switching behaviour. Remarkably, a careful analysis of the PFM hysteresis loops revealed that polarization switching can occur via rotation of polarization.

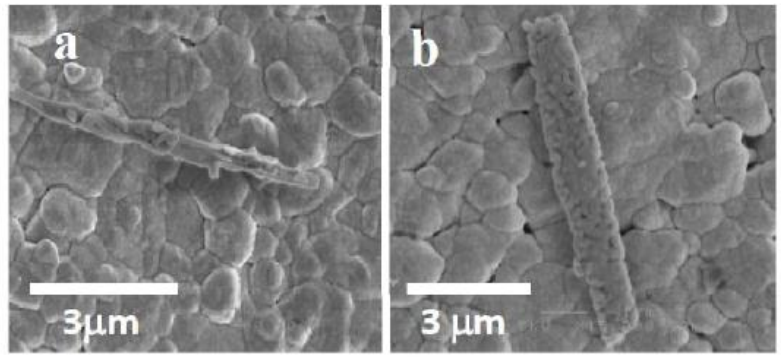

Fig. 1. SEM images of (a) BiT single crystalline nanorods, (b) BiTpolycrystalline nanorods.

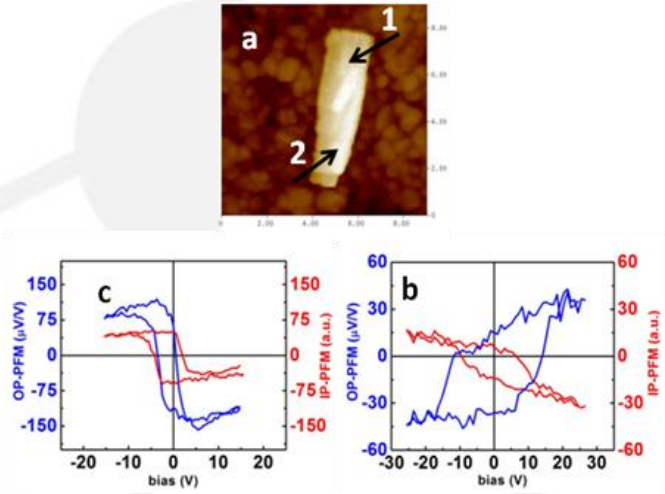

Fig. 2. PFM experiment on a polycrystalline BiT nanorod. (a) Topography, (b) and (c) Local PFM at locations marked “1” and “2”, respectively.

Références
[1] C. Harnagea, A. Pignolet, M. Alexe, D. Hesse, and U. Gösele, “Quantitative ferroelectric characterization of single submicron grains in Bi-layered perovskite thin films,” Appl. Phys. A, vol. 70, pp. 261267, Feb. 2000.
[2] M. T. Buscaglia, M. Sennour, V. Buscaglia, C. Bottino, V. Kalyani, and P. Nanni, “Formation of $Bi_4Ti_3O_{12}$ one-dimensional structures by solid-state reactive diffusion. From core-shell templates to nanorods and nanotubes,” Cryst. Growth Des., vol. 11(4), pp. 1394-1401, Feb. 2011.

Caractérisation du Chemin Réactionnel de la Télomérisation du Fluorure de Vinylidène avec des Radicaux Trichloromethane

F. Porzio[1], P. Laflamme[1], B. Ameduri[2], A.Soldera[1]

[1]Centre Québécois des Matériaux Fonctionnels (CQMF), Département de Chimie, Université de Sherbrooke, 2500 boulevard de l'Université, Sherbrooke, Québec, J1K2R1, Canada
[2]Institut Charles Gerhardt, Ingénierie et Architectures Macromoléculaires, UMR CNRS 5253, Ecole Nationale Supérieure de Chimie de Montpellier, 8 Rue de l'Ecole Normale, 34296 Montpellier, France

Mots clés : fluorure de vinylidène, radicaux trichlorométhane, telomère, polymère, *ab initio*

Les polymères fluorés constituent une classe unique de matériaux avec des propriétés remarquables telles qu'une faible énergie de surface, une grande stabilité thermique et un fort indice de réfraction [1]. Ils sont de ce fait mis à profit dans une grande variété d'applications : des revêtements aux piles à combustibles, en passant par les fibres optiques. La télomérisation radicalaire des alcènes fluorés sert de modèle dans l'étude de la polymérisation de ces composés. Ce domaine fait l'objet d'une recherche expérimentale active [2,3,4]. Afin de compléter les données expérimentales, l'étude par simulation du chemin réactionnel devient fortement appropriée [5]. Le chemin réactionnel du processus de télomérisation met en jeu une compétition entre les étapes de propagation et de transfert. L'issue de cette compétition est mise en valeur par la constante de transfert. Celle-ci dicte *in fine* le poids moléculaire du télomère obtenu. Nous proposons d'étudier cette compétition grâce à des calculs *ab initio*, en utilisant la théorie de la fonctionnelle de la densité (DFT). Trois agents de transfert Cl_3-Z (Z=H,Cl,Br) ont été considérés. Le chemin réactionnel le plus probable a ainsi été identifié en considérant le modèle d'Eyring. Les constantes de transfert ont été par la suite calculées selon différentes méthodes. Une corrélation linéaire entre les constantes de transfert expérimentales et simulées a été obtenue. Cette corrélation, présentée en Figure 1, souligne la pertinence de l'approche proposée.

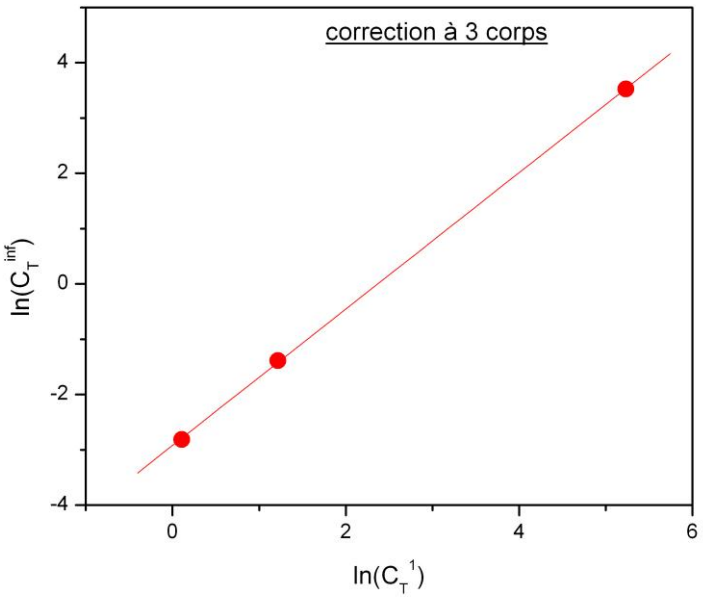

Figure 1 – Valeurs du logarithme népérien de la constante de transfert expérimentale [$\ln(C_T^{inf})$] en fonction des valeurs du logarithme népérien de la constante de transfert simulée [$\ln(C_T^1)$], obtenues par la méthode de correction à trois corps.

Références
[1] B. Améduri and B. Boutevin, *Well-architectured fluoropolymers : synthesis, properties and applications*, Elsevier, Amsterdam, 2004.B.
[2] M. Duc, B. Ameduri, G. David and B. Boutevin, *J. Fluor. Chem.*, 2007, **128**, 144-149.
[3] B. Boutevin, Y. Furet, L. Lemanach and F. Vial-Reveillon, *J. Fluor. Chem.*, 1990, **47**, 95-109.
[4] L. O. Moore, *J. Phys. Chem.*, 1971, **75**, 2075-2079.
[5] P. Laflamme, F. Porzio, B. Ameduri and A. Soldera, *Polym. Chem.*, 2011, DOI: 10.1039/c1py00467k, cover

Molecular Modeling of PVDF in Amorphous and Crystal Forms

N. Anousheh[1], A. Soldera[1]

[1]Centre Québécois des Matériaux Fonctionnels (CQMF), Département de Chimie, Université de Sherbrooke, 2500 boulevard de l'Université, Sherbrooke, Québec, J1K2R1, Canada

Mots clés : nano crystals, poly(vinylidene fluoride), molecular modeling, glass transition

Many theoretical and experimental works are devoted to study the problem of glass transition. In this project, the glass transition of poly (vinylidene fluoride), PVDF, has been investigated through atomistic simulations of short duration using an accurate force field, pcff. By using Kohlraush-Williams-Watt (KWW) equation, Tg is obtained in good agreement with experimental data. We also discuss the effects in glass transition of structural disorder due to the presence of inverted monomer units with 10 and 20 percent of structural defects, caused by "head to head" or "tail to tail" position. The mean squared deviations of PVDF polymer were analysed by means of another technique to find Tg. Vogel-Fulcher-Tammann (VFT) equation is used to describe the alpha-relaxation process that is the relaxation process of the cooperative segmental motions of the glass transition. Finally, the different crystal phases of PVDF are regarded. The focus is made on the two more usual crystalline structures: the alpha and beta forms. In this poster, the melting transition is more specifically investigated. The linear relationship of the melting temperature with the inverse sheet thickness is verified. A different slope can be obtained if the nano surface in nano crystals is modified. The influence of the defect on the final behaviour is thus regarded.

Design of Ti-Si-C nanocomposite coatings for wear, erosion and corrosion protection of aerospace alloys

Duanjie Li[1], Salim Hassani[1], Etienne Bousser[1], Jolanta E. Klemberg-Sapieha[1]

[1]Functional Coatings and Surface Engineering Laboratory – FCSEL
Department of Engineering Physics, École Polytechnique de Montreal,
2900 boul. Edouard-Montpetit, Quebec, H3C 3A7, Canada

Keywords : Ti-Si-C coating; microstructure; nanocomposite; corrosion resistance; tribological properties

Recent advances in the technological sectors of aerospace, automotive, biomedical and optical and optoelectronic applications as well as in energy and environment control stimulate research on high-performance functional coatings. In order to explore new film properties and open new opportunities, in the present work, we prepared and analyzed a series of Ti-Si-C nanocomposite coatings with tailored functional properties for the protection of aerospace alloys against wear, erosion and corrosion. We show that the silicon and carbon concentration of the Ti-Si-C coatings has a significant impact on the microstructure, and the mechanical, tribological and electrochemical properties. XRD and XPS analyses demonstrate that the Ti-Si-C coatings mainly consist of nanocrystalline nc- TiC embedded in amorphous a-SiC:H and a-C:H matrices. Ti-Si-C coatings with a high Si concentration possess enhanced mechanical properties (high hardness), while those with additional C exhibit superior tribological behaviors. The increase of Si and/or C concentrations leads to a grain size refinement of the TiC nanocrystals and to an expansion of the amorphous phase. This in turn substantially enhances their corrosion resistance. Ti-Si-C coatings with the highest Si or C contents exhibit the best corrosion performance among the tested samples by improving the corrosion resistance of the SS410 substrate by a factor of ~400. Erosion tests confirm superior performance of the novel Ti-Si-C coatings that allows one to reduce the erosion rate by more than a factor of 20, and hence significantly increase the lifespan of aerospace components.

Purity evaluation of induction thermal plasma grown single-walled carbon nanotubes using thermogravimetry

A. Shahverdi[1], G. Soucy[1]*

[1] Department of Chemical and Biotechnological Engineering, Université de Sherbrooke 2500, boul. de l'Université, Sherbrooke (Québec) CANADA J1K 2R1

Keywords: Single-walled carbon nanotubes, Induction thermal plasma, Thermogravimetric analysis

Since their discovery in 1993, thermogravimetry (TG) has become an important technique to characterize single-walled carbon nanotubes (SWCNTs). Up to now, no TG standard procedure has been suggested for these particular synthetic materials. In this study, a procedure for TG of carbonaceous materials including single walled carbon nanotubes was developed based on a statistical design to study the effect of three main parameters: temperature ramp (TR), initial mass of the sample (IM), and the rate of flowing gas (FR) on the TG results. Moreover, the effect of sampling: (1) sample morphology; (2) moisture content on TG were studied. The results of statistical design clearly showed that TG was affected particularly by TR and IM. The sample morphology and low moisture content had no noticeable effect on the TG results. This study also confirmed the potential of TG combined with high resolution scanning electron microscopy to be a simple and straightforward method for purity evaluation of SWCNT containing samples with a complex TG behavior such as those of induction thermal plasma grown. Additional study on nano-metric catalysts indicated that these types of materials enable to gain or loss mass in an oxidative ambient during TG. For pure nano-metric yttrium oxide, 6% of mass loss and for nickel, 23% mass gain were observed.

References

[1] A. Shahverdi, G.Soucy. Thermogravimetric analysis of single-walled carbon nanotubes synthesized by induction thermal plasma, Journal of Thermal Analysis and Calorimetry, p 1-7, 2011.

Improving the Mechanical Reliability of a Cryomilled Al 5356 Alloy using a Two-Stage SPS (TSS-SPS) Sintering Cycle

B. Akinrinlola, R. Gauvin and M. Brochu

McGill University, Materials Engineering Department, 3610 University street, Montreal, Canada, H3A 2B2

Mots clés : Spark Plasma Sintering, Cryomilling, Aluminum alloys, Mechanical reliability

Nanostructured materials possess many improved properties when compared to their conventional counterparts. This quality is especially of interest for high strength-to-weight ratio metals such as Aluminum alloys. With the bottom-up approach to nanostructuring, maintaining a nanocrystalline microstructure during consolidation and producing highly reliable materials is a challenge. Here, a bulk nanostructured Al 5356 alloy is successfully produced from cryomilled powders. Consolidation is obtained by a two-stage SPS (TSS-SPS) sintering cycle with $T_1 = 0.78T_m$ and $T_2 = 0.53T_m$, where T_m is the melting temperature of the alloy. Consolidation does not induce significant grain growth nor influence the hardness and flexural strength, but improves the reliability of the material by doubling the fracture strength distribution statistic (Weibull modulus *m*) from 13 to 25. The increased duration of the hold at T_2 (from 5 to 20 minutes) marginally increases the Weibull modulus, from 23 to 25.

Cryomilling and Spark Plasma Sintering of Al-12Si Alloy for Improved Wear Resistance Applications

J. Milligan, J. Shockley, R. Chromik and M. Brochu

McGill University, Materials Engineering Department, 3610 University street, Montreal, Canada, H3A 2B2

Mots clés : Spark Plasma Sintering, Cryomilling, Aluminum alloys, Wear resistance

Spark Plasma Sintering (SPS) has recently come in to view as a highly effective method for rapidly sintering nanostructured powders. SPS offers significant advantages and consistently produces a highly dense compact in a shorter sintering time than conventional methods. SPS was used to sinter cryomilled nanostructured aluminum silicon powder. The cryomilling serves to break up and disperse the eutectic phase in the powder to create a well-distributed Si throughout the matrix and to modify the morphology of the Si phase. The two-phase Al-Si alloy is ideal for wear applications due to the high hardness of the Si phase, which imparts excellent wear resistance to the alloy and can be increased with the refinement of the Si phase. The wear resistance of the SPS compacts was tested using stripe test under dry sliding conditions using a steel counterface. The wear track and debris was then characterized to observe the wear properties of the system after being cryomilled and sintered. The wear tracks and debris were characterized using Scanning Electron Microscopy (SEM), Energy Dispersive Spectroscopy (EDS) and X-Ray Photoelectron Spectroscopy (XPS).

Protection of metal and alloy surfaces using corrosion resistance nanostructured superhydrophobic coatings

Ying Huang[*1], D. K. Sarkar[1], X-Grant Chen[1]*

University Research Center on Aluminum (CURAL), University of Québec at Chicoutimi, Chicoutimi, QC, Canada, G7H 2B1

Mots clés : superhydrophobic copper and aluminum surfaces, micro-nanostructure, scanning electron microscope (SEM), X-ray diffraction (XRD), corrosion

The superhydrophobic copper surfaces were fabricated by immersing two copper plates in a dilute ethanolic stearic acid solution in the application of DC voltage. The surface of the anodic copper electrode transforms to superhydrophobic due to the formation of micro-nanofibres low surface energy follower-like copper stearate as confirmed by X-ray diffraction (XRD) and scanning electron microscope (SEM), respectively. The modification time of 1.5 h at 30 V DC voltage is found to be necessary to obtain superhydrophobicity on the anodic copper electrode, where the water contact angle is 155 °. The superhydrophobic aluminum alloy surfaces were fabricated by firstly coated with copper films followed by electrochemical modification with stearic acid solution. The number densities of copper microdots increase with the increase of the negative deposition potentials. The surface roughness and water contact angle of electrodeposited copper film followed by electrochemical modification in ethanolic stearic acid solution increase with the increase in negative copper deposition potentials. The stearic acid modified copper films deposited at -0.6 V provides a surface roughness of 6.2 μm with a water contact angle of 157 ° providing superhydrophobic properties of AA6061 aluminum alloy surfaces. The corrosion prevention property of the superhydrophobic copper surface was then analyzed by electrochemical experiment. The decrease of the corrosion current density as well as the increase of the polarization resistance in polarization curves shows that the superhydrophobic copper surface is more stable as compared to bare copper surface in the corrosion environment. Both superhydrophobic Cu and AA6061Al alloy surfaces show anti-corrosion properties.

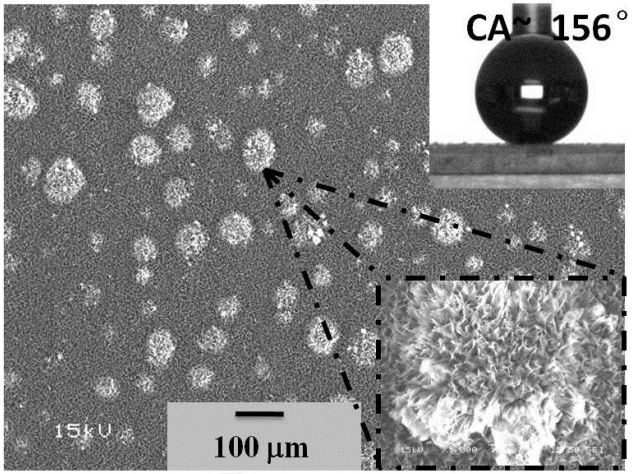

Fig. 1 SEM image of anodic copper surface coated with copper stearate for 3h at DC voltage of 30 V. Insets show the magnified image of one of the flower-like particles and the water drop images on the surface, respectively.

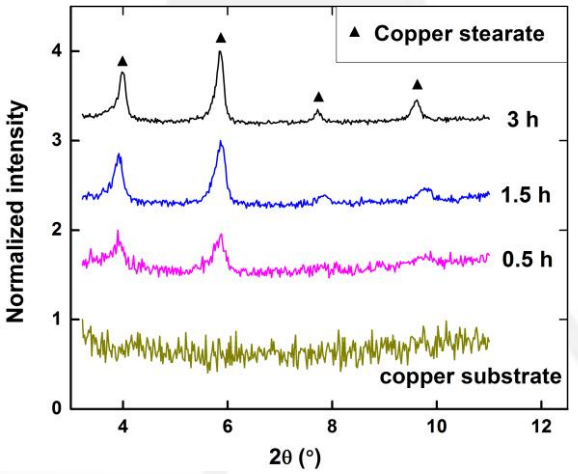

Fig. 2 XRD patterns of the anodic surface of the copper electrode after the application of 30 V DC voltage in an ethanolic stearic acid solution for (a) 0.5 h, (b) 1.5 h, (c) 3 h and (d) bare copper substrate.

Références
[1] Y. Huang, D.K. Sarkar and X.-Grant Chen, University Research Center on Aluminum (CURAL), University of Québec at Chicoutimi, Chicoutimi, QC, Canada, G7H 2B1

Mechanical and electrical properties of epitaxial Si nanowires grown by Pulsed Laser Deposition

D. Obi [1], R. Nechache [1,2], C. Harnagea [1] and F. Rosei [1]

[1]INRS-Énergie, Matériaux et Télécommunications, Université du Québec, Varennes, J3X 1S2, Canada.
[2] *NAST Center & Department of Chemical Science and Technology, University of Rome Tor Vergata, Via della Ricerca Sceintifica 1, 00133 Rome (Italy)*

Keywords: Silicon Nanowires, Young Modulus, Device Miniaturization, Nanoelectronics, electrical properties.

Silicon nanowires (NWs) have attracted significant attention from electronics and semiconductor Industries [1] as devices miniaturization gradually transit from 32 node (in 2009) to 22node (in 2011) [2]. Understanding Si NW deformability and strength is essential to the design and reliability of emerging nanodevices like nanosensors, nanoelectronics and nanostructured solar cells. This has made detailed research on mechanical properties of Si NWs very important. In this work, the young modulus and tensile strength of Si NWs with diameters 90-150nm and lengths between 468-653nm were investigated. The NWs were vertically and epitaxially grown on a Si [111] substrate by V-L-S process via pulsed laser deposition technique (PLD) (cf. Fig. 1). They were subjected to bending tests using an atomic force microscope (AFM) set up inside a scanning electron microscopy (SEM). The relationship between young modulus and size estimated for the PLD-grown SiNWs will be discussed and compared with those synthesized by other conventional techniques (i.e. molecular beam epitaxy and Chemical vapor deposition). The results on electrical properties of the Si NWs will also be presented.

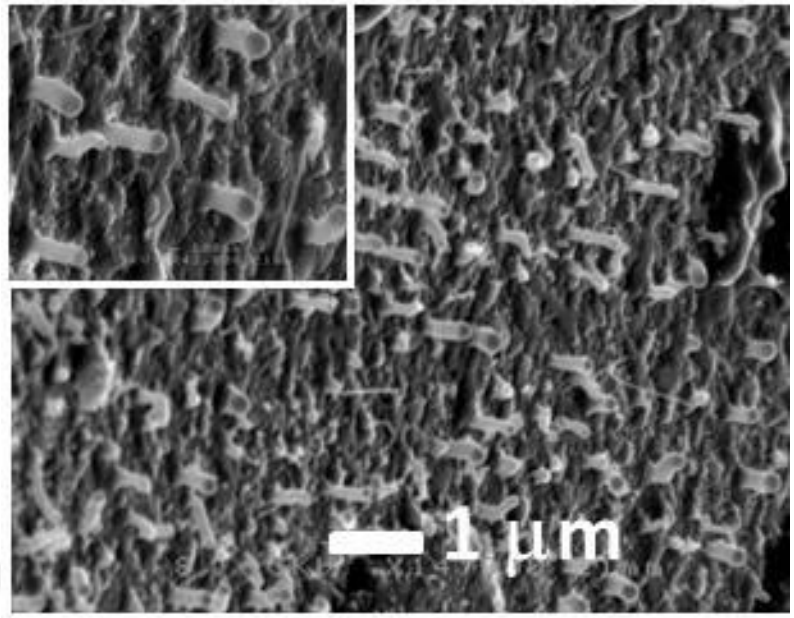

Figure 1 – Scanning electron microscopy (SEM) images of Si NWs epitaxially grown on Si(111) substrate by PLD.

[Références] Références
[1] Y.-S Sohn, J. Park, G. Yoon, J. Song, S.W.Jee, J-H. Lee, S Na, T. Kwon and K. Eom. Nanoscale Res Lett (2010) 5: 211 – 216.
[2] X. Wu, J. Kulkarni, G. Collins, N. Petkov, D. Almecija, J. Boland, D. Erts and J. Holmes. Chem. Mater. (2008), 20 : 5954 – 5967.

Chemical Vapor Doping of conductive and transparent films of carbon nanotubes

Hongjun Gao[1,3], Guillermo Mendoza-Suarez[2], Ricardo Izquierdo[3], Vo-Van Truong[1]*

[1]Department of Physics, Concordia University, 7141 Sherbrooke Ouest, Montréal, Québec H4B 1R6, Canada, [2]Revision Sparc, Pavillon des sciences biologiques, 141 Ave Président Kennedy, Suite SB 5541, Montréal, Québec, H2X 1Y4, [3]Département d'informatique, Université de Québec à Montreal (UQAM), Case postale 8888, succursale Centre-ville, Montréal, Québec H3C 3P8, Canada

Key words: chemical vapor doping (CVD), carbon nanotube (CNT), thin films, networks, acid treatment

Conductive films of carbon nanotubes (CNT) are very promising materials as transparent electrodes. In order to increase its conductivity, oxidizing acids such as HNO_3 are frequently used for doping the films. The traditional way of doping CNT with HNO_3 is by immersing the films in the acid solution. However, this method introduces limitations on the substrates for CNT films that can be used. In this poster we present an alternative Chemical Vapor Doping (CVD) method for CNT films. The differences between the solution and vapor doping methods are compared systematically and in detail by means of sheet resistance, SEM, Raman, UV-Vis-NIR and XPS. We show that the level of reduced sheet resistance is comparable for the two treatments and that the vapor-treated film showed better stability in air with the same initial sheet resistance. A doping mechanism is proposed. As this method avoids direct contact with strong nitric acid solution, it is suitable for post-treatment of the CNT films on some flexible plastic substrates with low chemical resistivity like polycarbonate and it could be very useful for the applications in flexible display, touch screen, eyeglass, etc.

References

[1] Wu, Z.C., et al. Science, 2004. 305(5688): p. 1273-1276.
[2] Hennrich, F., et al., Physical Chemistry Chemical Physics, 2003. 5(1): p. 178-183.
[3] Zhang, X.F., et al., Journal of Physical Chemistry B, 2004. 108(42): p. 16435-16440.
[4] Geng, H.Z., et al., Journal of the American Chemical Society, 2007. 129(25): p. 7758-7759.
[5] Kamaras, K., et al., Physica Status Solidi B-Basic Solid State Physics, 2010. 247(11-12): p. 2754-2757.
[6] Xu, G.H., et al., Applied Physics a-Materials Science & Processing, 2011. 103(2): p. 403-411.

Ultrafast microwave hydrothermal synthesis of BiFeO3 nanostructures

S. Li[1], R.Nechache[1,2], I. Alejandro Velasco Davalos [1], , L. Nikolova[1], A. Ruediger[1] and Federico Rosei[1,3]

[1]Université du Québec, Institut national de la recherche scientifique, Énergie, Matériaux et Télécommunications, INRS, 1650, boulevard Lionel-Boulet, Varennes, Québec J3X 1S2, Canada
[2]NAST Center & Department of Chemical Science and Technology, University of Rome Tor VergataViadella Ricerca Scientifica 1, 00133 Rome, Italy
[3]Centre for Self-Assembled Chemical Structures, McGill University, H3A 2K6, Montréal, QC, Canada

Keywords: Microwave hydrothermal synthesis; Nanoplates; Bismuth ferrite; Magnetism, oxides nanowires

Multiferroic materials, with electric and magnetic order parameters coupling in the same phase, have attracted increasing interest because of their potential applications in data storage, spintronics, sensors, quantum electromagnets, and electronics [1]. In particular, considerable attention has been attributed to multiferroic BFO nanomaterials (i.e. nanotubes, nanospindles), which show interesting magnetic and optical properties because of their nanosize effect [2,3].Therefore, the design of multiferroic BFO nanostructures with novel and well-defined morphologies is considered important for fundamental research as well as of relevance for designing new multifunctional materials combining magnetic, ferroelectric and optical properties. Recent developments on 2D crystalline nano-sheets/plates show promising properties for developing a new generation of optoelectronic devices and high performance catalysts [4]. However, so far only Lu *et al*. reported the synthesis of two-dimensional BFO plates using the surfactant of cetyltrimethylammonium bromide (CTAB) [5]. It is therefore essential to develop an alternative approach to synthesize planar BFO nanosheets or nanoplates without any surfactant. Here, we will present a rapid and simple solution based method of synthesizing BFO nanoplates and nanowires under Microwave-assisted hydrothermal (M-H) conditions within a very short reaction time (cf. Fig. 1). The final products were characterized by X-ray diffraction (XRD), scanning electron microscopy (SEM) and transmission electron microscopy (TEM). Various parameters influencing the final products such as reaction time, irradiation power and alkali concentration will be discussed in detail.

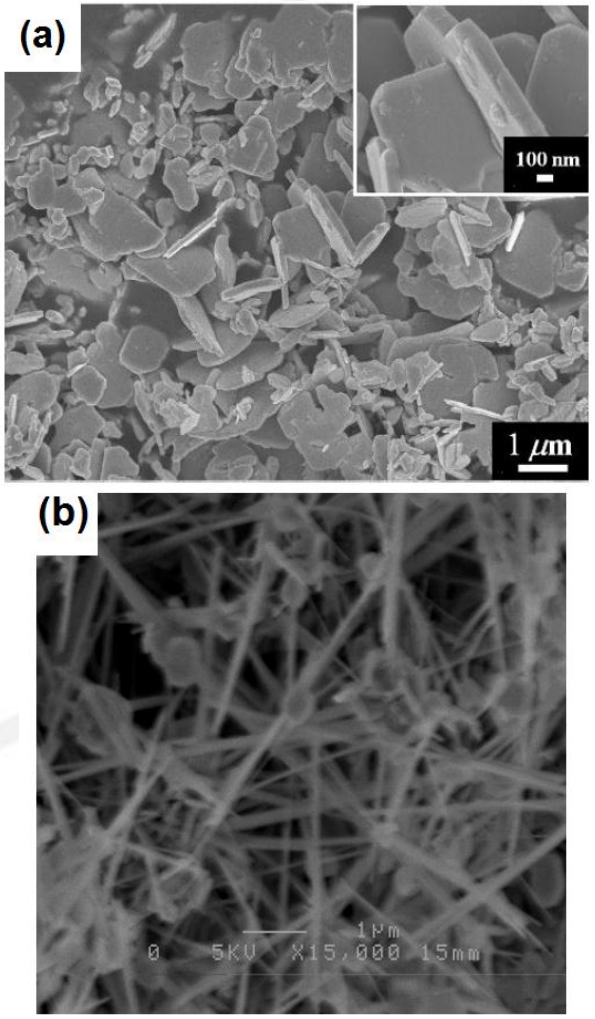

Figure 1 – Scanning electron microscopy images of the BFO products prepared by M-H method. **(a)** Nanoplates, **(b)** nanowires.

References
[1] Wang J et al. 2003 *Science* **299** 1719
[2] Wong S S et al. 2007 *Nano Lett.* **7** 766
[3] Ren W and Bellaiche L 2010 *Phys. Rev. B* **82** 113403
[4] Zhu Y F and Zhang C 2005 *Chem. Mater.***17** 353
[5] Xie J M, Lu X M, Song Y Z and Lin J M 2007 *J. Mater. Sci.***42** 6824

Biogenic precipitation of nano-gold particles using plant extracts

K. Krishnaswamy[*1], V. Orsat[1], H. Vali[2]*

[1]Dept. of Bioresource Engineering, McGill University, Ste-Anne-de-Bellevue, Canada, H9X 3V9.
[2]Facility for Electron Microscopy Research, McGill University, Montréal, Canada, H3A 2B2.

Keywords: Green chemistry, gold nanoparticles, grape byproducts, HR-TEM, FTIR

Green nanotechnology integrates the principles of green chemistry into nanotechnology to produce eco-friendly, safe and novel metal nanoparticles that do not use toxic chemicals in their synthesis protocol. The goal of green nanotechnology is to produce nanomaterials and products without harming the environment or human health. Over the last decade production of nanoparticles from bacteria, fungus and plants has gained considerable attention owing to the growing demand for environmentally benign, clean nontoxic materials that could be used in energy, food, health, and medicine as well as other applications. This would be a viable alternative to the conventional physical and chemical methods of nanoparticle synthesis [1]. Herein we report a simple and cost effective method for the synthesis of gold nanoparticles (AuNP) using grape by-products and pine needles which act as both a reducing and stabilizing agent. The synthesized AuNP were characterized using UV-Vis absorption spectrophotometry, FTIR and high-resolution transmission electron microscopy (HRTEM). The appearance of a pink-ruby red colour due to surface plasmon resonance was obtained between 534-550 nm (Fig. 1). Observation in TEM showed that the AuNP have mostly spherical shape and ranged in size from 12-44 nm (Fig. 2). Grape by-products and pine needles have similar polyphenolic profile, which might explain the bioreduction of gold nanoparticles and also act as a capping/stabilizing agent. The AuNP produced in this manner may find potential application as biocompatible AuNP for use in medical application, drug delivery, molecular imaging and cancer therapy.

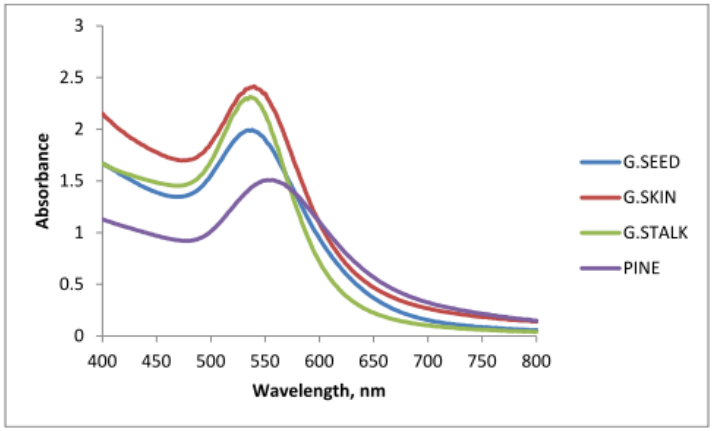

Figure. 1. UV-Vis spectra recorded for different plant extracts at 10 min of reaction time.

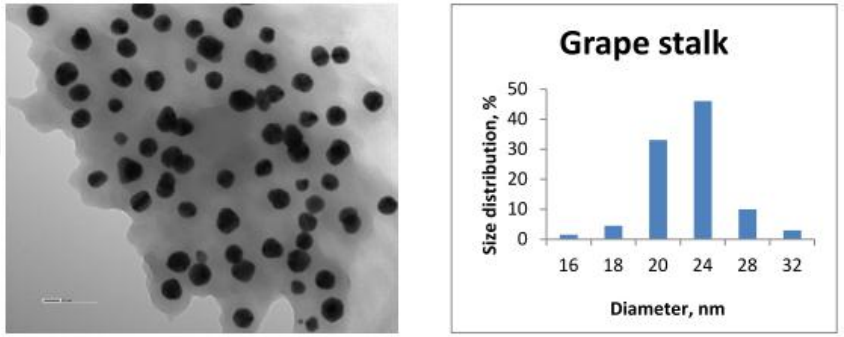

Figure. 2. TEM image of grape stalk extract reduced gold nanoparticles (scale bars = 20 nm) with size distribution graph.

References
[1] A.E. Schwarz, NanoEthics, 3 (2009) 109-118.

Structural profiling and electronic properties of pentacene on Ni(111) surface

Laurentiu Eugeniu Dinca[*1], *Csaba E. Szakacs*[1], *Jennifer MacLeod*[1], *Josh Lipton-Duffin*[1], *Rico Gutzler*[1,2], *Dongling Ma*[1] *and Federico Rosei*[1]

[1] Institut National de la Recherche Scientifique, 1650 boulevard Lionel-Boulet, Varennes, QC, J3X 1S2, Canada
[2] Department of Chemistry and Centre for Self-Assembled Chemical Structures, McGill University, 801, Sherbrooke Str. West, Montreal, QC, H3A 2K6, Canada

Keywords: pentacene, Ni(111), STM, molecular orbitals, DFT.

Tailoring the fabrication of organic/inorganic interfaces through control of the first layer growth may offer a way to concurrently control their electronic behavior. Therefore, we have investigated experimentally using scanning tunnelling microscopy (STM), the adsorption of pentacene on Ni(111) surface. A detailed insight into the degree of ordering and interaction mechanism of pentacene on the metal surface is revealed, backed up by theoretical simulations, based on density functional theory (DFT). At room temperature and at close to monolayer coverage a randomly tiled structure of pentacene emerges (Figure 1). Pentacene molecules are evenly distributed along the Ni(111) axes. This suggests that Ni(111)-substrate/molecular interaction is stronger than the intermolecular one leading to a complex behaviour. We find that the STM images of pentacene have extraordinarily fine resolution. Frontier orbitals have been previously imaged for the case of pentacene alone on passivated surfaces, which we complement with a better inter- and intra-molecular resolution. A peculiar molecular packing structure occurs at monolayer coverage after 220^0 C annealing (Figure 2a). We still investigate the new complex. It may be the result of two pentacene blocks covalently attached to each other accompanied by a strong and coherent electronic coupling between the two constituents (Figure 2b). Prolonged annealing of under monolayer coverage will conduce to a various degree of irreversible pentacene dissociation. This observation may sustain our hypothesis of pentacene-pentacene lateral bonding at high monolayer coverage and elevated temperature. We have also investigated the energetics of the adsorption sites of pentacene at monolayer coverage for different single molecule-substrate configurations using DFT.

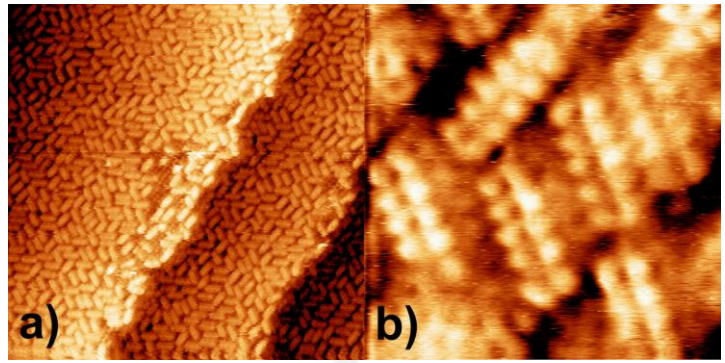

Figure 1. a). Room temperature (RT), 30nm x 30nm, STM image of pentacene molecules adsorbed on Ni(111) substrate. I = 1.36 nA, U = 1.83 mV; The observed carbide structures along the step-edges seem to passivate the nickel surface. No pentacene was identified on the top of carbide structure. In practice it could influence the mechanism of charge transport near the electrode of any electronic device. b). RT, 3nm x 3nm, band gap STM image of pentacene molecules adsorbed on Ni(111) substrate. I = 1.49 nA, U = 1.83 mV; The pinned molecules are oriented with their long axis along the Ni(111) directions, with no privileged trend.

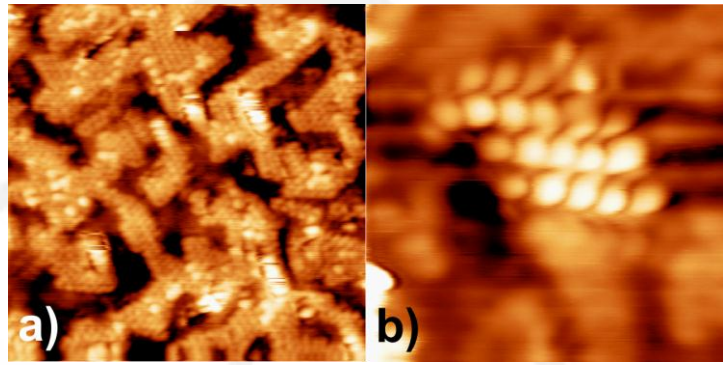

Figure 2. a). RT, 10nm x 10nm, STM image of pentacene packing structure on Ni(111) substrate. I = 1.47 nA, U = 10.68 mV; Following the molecular deposition and prior to imaging, the substrate was thermally treated to ~220^0 C for 15 minutes and subsequently slowly cooled to RT. b). RT, 3nm x 3nm, HOMO-like STM image of two isolated pentacene molecules on Ni(111) substrate. I = 1.51 nA, U = 45.47 mV; Direct STM imaging of the orbital hybridization upon bond formation provides insight into the energetic/charge flow, shifts and occupation of the molecular resonances inside the molecules and the molecular junction.

Nano-scale crystal structure analyses of novel biogenic magnetite

D. Schumann[1,2], U. Lücken[3], S.K. Sears[2], I. Rouiller[2,4], H. Vali[1,2,4]*

[1]Department of Earth and Planetary Sciences, McGill University, 3450 University Street, Montréal, Québec, H3A 2A7, Canada.; [2]Facility for Electron Microscopy Research, McGill University, 3640 University Street, Montréal, Québec, H3A 2B2, Canada.; [3]FEI Company, Nanobiology Marketing, Eindhoven, 5600KA Eindhoven, The Netherlands.; [4]Department of Anatomy and Cell Biology, McGill University, 3640 University Street, Montréal, Québec, H3A 2B2, Canada.

Keywords: biomineralization, PETM-clay, magnetofossils, biogenic magnetite, TEM

Clay-rich sediments of the Paleocene-Eocene boundary contain important evidence of a 100- to 200-ky interval of atmospheric and oceanic perturbations that resulted in 5-9ºC abrupt global warming known as Paleocene-Eocene Thermal Maximum (PETM). These sediments host novel, exceptionally large biogenic magnetite crystals in various locations of the Atlantic margin unlike any previously reported from living organisms or from sediments [1],[2]. Here we present new HRTEM and SEM data of these up to 4000nm large spearhead-like, spindel-like, and elongated hexaoctahedra magnetofossils which reveal their crystal structure. Similar to magnetite produced by magnetotactic bacteria, these single-crystal particles exhibit chemical composition and lattice perfection consistent with a biogenic origin. Spearheads were also observed in arrangements of tip-outward spherical assemblages while the elongated hexaoctahedras can be arranged like shingles in larger rod-shaped particles both possibly representing the preserved original biological crystal arrangement in a hitherto unknown magnetite producing organism. Electron holography indicates single-domain magnetization of the crystals and gives insights into the shape of the magnetic field around these crystals, which enables the interpretation of their physical arrangement in such spherical- and rod-shaped assemblages. The discovery of these crystals, which may represent the remains of micro-organisms that appeared and disappeared with the PETM, sheds some light upon the ecological response to the biogeochemical changes that occurred during this warming event.

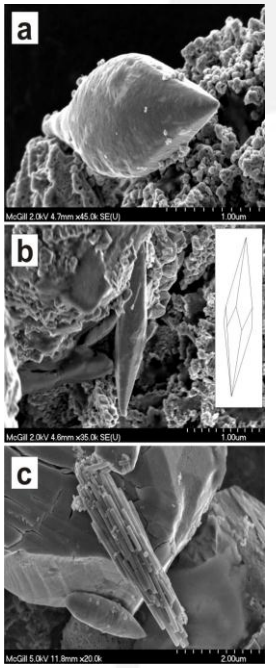

Figure 1 – SEM images of (a) spearhead-like, (b) spindel-like, and (c) elongated hexaoctahedral biogenic magnetite crystals.

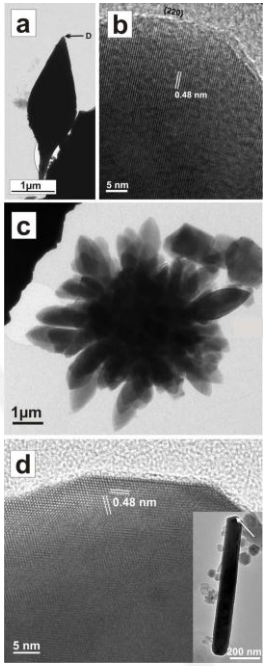

Figure 2 – (a) Low-resolution and (b) lattice-fringe TEM image of a spearhead-like magnetite crystals. (c) Spherical assemblage of spearhead-like particles. (d) Lattice-fringe image of an individual elongated hexaoctahedral particle.

References
[1] D. Schumann et al. (2008) PNAS **105**, 17648-17653, [2] R. Kopp et al. (2009) *Paleoceanography* **24**, doi: 10.1029/2009PA001783..

Synthesis of a Core@Shell Zeolitic Hydrocarbon Adsorbent to Control Cold-Start Emissions in Automotive Exhaust

N. Masoumifard[1, 2], F. Kleitz[1], S. Kaliaguine[2]*

1Departement of chemistry, Université Laval, Québec, Canada, G1V 0A6, Tel.: 1 418 656 7812, *
Freddy.Kleitz@chm.ulaval.ca
2Department of Chemical Engineering, Université Laval, Québec, Canada G1K 7P4

Keywords: Nanozeolites, Core@Shell, Cold-start emission, ZSM-12

Automotive emissions are known as significant sources of air pollution. Catalytic convertors are only able to eliminate the steady-state emissions. Therefore, all toxic emissions during the cold-start period are being released to the atmosphere. Common strategy to solve this problem is to employ hydrocarbon traps to keep emissions until the catalyst reaches its ideal working temperature. Recent studies in our group [1] demonstrated that ZSM-12(Ag^+) is the best choice among all conventional molecular sieves; however, still significant improvement is required. Modifying this conventional trap via synthesizing a novel zeolitic architecture, i.e. core@ZSM-12 and hollow ZSM-12 spheres, are the main focus of this study. We applied layer-by-layer technique to produce nanozeolites-coated cores along with secondary hydrothermal treatment to strengthen the zeolitic shell and make it uniform (Scheme 1). Different types of materials have been screened, in order to determine the best candidate as a core material, which could provide a variety of desirable features such as support for zeolitic shell and a porous or hollow core in the final product. Since the size and monodispersity of the nanozeolites are the most crucial parameters to permit a fine control of the zeolitic shell coverage, in terms of crystal phase, thickness and even micropores orientation, different techniques, e.g. clear-gel technique, confined-space synthesis and top-down centrifuge-assisted milling method, have been applied to synthesize colloidal nano-SM-12 with particle size smaller than 50 nm. The performance of all these materials are investigated using common characterization methods, e.g. XRD, TEM, SEM, N_2 Sorption, as well as TPD of probe molecules in conditions as close as possible to the real engine operational situations.

Scheme 1 – Schematic reperesentation of Core@ZSM-12 synthesis

Références
[1] Z. Sarshar, et. al., MTW zeolites for reducing cold-start emissions of automotive exhaust, Applied Catalysis B: Environmental, 2009. 87(1-2): p. 37-45.

Microfabrication assistée par instabilité de fibres tenaces bioinspirées de la soie d'araignée

F. P. Gosselin[*1], D. Therriault[1], M. Lévesque[1]*

[1]Laboratoire de Mécanique Multi-échelles, École Polytechnique de Montréal, C.P. 6079, succursale Centre-ville, Montréal (Québec) Canada, H3C 3A7

Mots clés : instabilité, microfabrication, matériau micro-structuré, biomimétique

La soie d'araignée surpasse la plupart des matériaux synthétiques en terme de ténacité spécifique. Nous développons une technique pour fabriquer des filaments tenaces dont la microstructure est inspirée de la structure moléculaire de la soie d'araignée. Pour fabriquer des fibres d'un diamètre de 30 à 100 microns avec différentes propriétés mécaniques, nous cédons le contrôle du design de leur géométrie à l'instabilité de la corde fluide. C'est cette même instabilité qui cause l'enroulement et la dance d'un fin filament de miel qui flambe lorsque versé sur une surface rigide. De façon analogue, nous injectons un filament de solution polymérique visqueuse vers un substrat qui se déplace perpendiculairement à une vitesse plus faible que la vitesse d'injection (Figure 1). Le filament flambe à répétition créant ainsi des patrons de méandres et de boucles. Exposé à l'air, le solvant s'évapore et le filament se solidifie en une fibre dont la géométrie lui est conférée par l'instabilité. Des tests de microtraction réalisés sur les fibres montrent des liens intéressant entre les propriétés mécaniques des fibres et les patrons d'instabilité (Figure 2). Certaines formes d'enroulement donnent lieu à une forte ténacité due à la création de liens sacrificiels lorsque le filament forme une boucle et se soude à lui-même. Les liens sacrificiels dans la microstructure des fibres jouent un rôle analogue à celui des liens hydrogène présents dans la structure moléculaire de la protéine de soie et qui donnent à celle-ci sa ténacité.

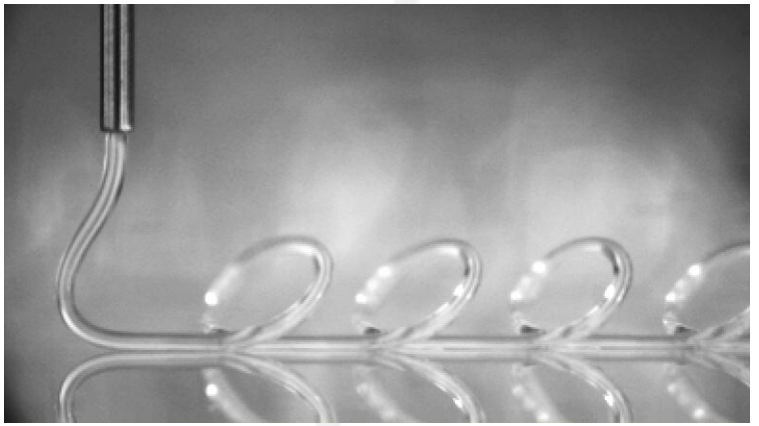

Figure 1 – Déposition d'un jet de diamètre de 100 microns d'une solution polymérique sur un substrat se déplaçant à vitesse constante. La vitesse du substrat est inférieure à la vitesse du jet ce qui cause le flambement du filament et donne lieu à un patron d'instabilité répétitif.

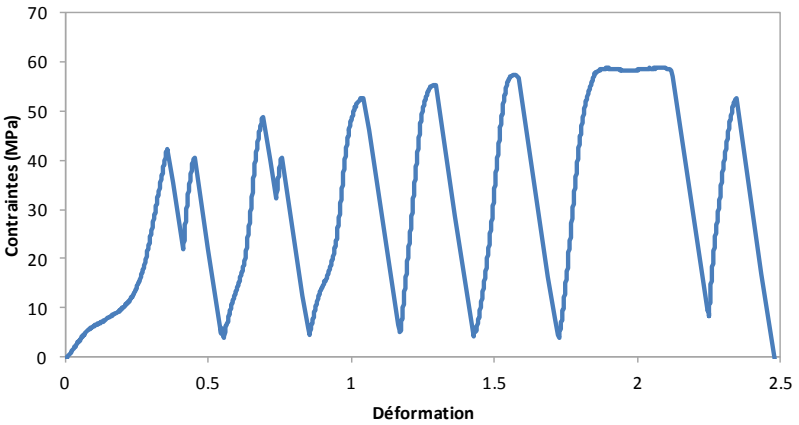

Figure 2 – Courbe de contraintes-déformation obtenue lors d'un test de traction simple d'un filament. Chaque sommet sur le graphique correspond à la rupture d'un lien sacrificiel créé lorsque le filament complète une boucle et se soude sur lui-même lors de la microfabrication.

Controlling adhesion and friction using nanostructured polymer layers: role of polymer conformation and ionization

Benoît Liberelle[1], Xavier Banquy[2], Béatrice Lego[1], Olga Borozenko[1], Éric Charrault[1], Suzanne Giasson[1,2,*]

[1]Department of Chemistry and [2]Faculty of Pharmacy, Université de Montréal, C.P. 6128, succursale Centre-Ville, Montréal, QC, Canada, H3C 3J7

Mots clés : polymers, surfaces, adhesion, thin films, friction

Experimental surface forces studies of different classes of polymer- bearing surfaces were carried out using the surface forces apparatus and similar molecular techniques in order to elucidate the role of the conformation and degree of dissociation of the polymer chains in controlling friction and adhesion between polymer-bearing surfaces. We used “grafting to” and grafting from” approaches to covalently attach the polymers onto modified mica and silica surfaces with a controlled surface density. Chemical grafting approaches prevent cleavage and/or slipping at the polymer/substrate interface. Such polymer detachment, which can occur with non-covalently attached (or physisorbed) polymers, explain some discrepancies observed between similar studies and the lack of clear understanding of the mechanism underlying polymer-mediated lubrication.

Using chemical grafting approaches, we investigated the role of electrostatic interactions and polymer conformation on adhesion and friction between two opposing polymer-coated surfaces without uncertainties in the slip plane, i.e., friction dissipation occurring at polymer/polymer interface. We measured high friction forces under high pressure (or applied load between the two surfaces) and high shear rates which are not associated with polymer cleavage or surface damage; problems which are frequently observed with physisorbed polymers. Moreover, our results suggest that the role of electrostatic interactions in controlling friction is to control the thickness of the mutual interpenetration zone (between opposing polymer layers) over which friction dissipation occurs. We have also showed that the brush conformation is not solely responsible for the extremely low friction measured between polymer-bearing surfaces. Rather, the fluidity of the hydration layers surrounding the rubbing polymer segments plays an important role in lubricating the polymer/polymer interfaces.

Synthèse de nanoparticules octaédriques d'oxyde de fer par co-précipitation

B. Bergeron, A.M. Ritcey

Université Laval, Département de Chimie, 1045 avenue de la Médecine, Pavillon Alexandre-Vachon, Québec (Québec), G1V 0A6.

Mots clés : nanoparticules magnétiques.

Connue depuis longtemps, la synthèse de nanoparticules par coprécipitation permet d'obtenir des particules magnétiques en grande quantité et à faible coût. Normalement limitée à la synthèse de petites nanoparticules (2 à 8 nm)[1], cette synthèse peut être modifiée pour obtenir des particules octaédriques de plus grandes dimensions (50 à 200 nm), tout en conservant leurs propriétés magnétiques[2]. La synthèse de nanoparticules par coprécipitation offre certains avantages. Bien que les particules soient plus polydisperses que celles issues des autres méthodes communes, la coprécipitation permet de produire de grande quantité de nanoparticules dans des conditions simples et sans danger. Dans cette synthèse, un des paramètres contrôlant la taille finale des nanoparticules est le rapport Fe2+ :Fe3+. Alors qu'un rapport de 1 :2 produit des nanoparticules quasi-sphériques d'une taille de 8 nm, l'augmentation du rapport permet l'obtention d'une deuxième population, composée de particules octaédriques et beaucoup plus grosses. Les quantités relatives des deux populations dépendent des paramètres de réaction, tels que l'ajout retardé de Fe2+ et le contrôle du pH de la solution. Il est ainsi possible de favoriser la formation de nanoparticules octaédriques. De plus, comme les grosses particules résistent bien au traitement à l'acide, il est possible de les isoler du mélange. Selon leurs propriétés physiques, plusieurs applications de ce type de nanoparticule sont envisageables, dont l'utilisation dans des matériaux à mémoire magnétique ou bien simplement dans des ferrofluides.

Référence :
[1] An-Hui Lu, E. L. Salabas, et Ferdi Schüth : Angew. Chem. Int. Ed. **2007**, *46*, 1222 – 1244
[2] Wenguang Yu, Tonglai Zhang, Jianguo Zhang, Xiaojing Qiao, Li Yang, Yanhong Liu : Materials Letters **2006,** *60,* 2998–3001

Simulation and Engineering of functionalized carbon nanostructures by thermal plasma

N. Mendoza[*1], D.Binny[1], J.L. Meunier, D. Berck[1]*

[1] Plasma Processing Laboratory, McGill University, Department of Chemical Engineering, Wong Building, 3610 University St., Montreal, Quebec, Canada H3A 2B2

Keywords : Thermal plasma modeling, nitrogen functionalization, catalysis, carbon nanoflakes.

The addition of specific nitrogen and iron functionalization on carbon nanostructures is presently allowing the use of this material for applications as non-noble catalysts in replacement of platinum-based catalyst. We are currently developing a process for the synthesis and functionalization of carbon nanoflakes (CNF) powders using thermal plasmas for PEM (polymer electrolyte membrane) fuel cells applications. This plasma method offers several advantages such as the possibility to use different carbon sources, a continuous process and more importantly an industrial scale production. Our latest work proved the potential and robustness of the production process [1]. However, functionalizing the surface of a powder by plasma is more challenging than treating a flat surface. This process involves fast and complex phenomena that need to be understood for optimization and control. Numerical simulation forms a useful tool to provide insight in those elements in the high temperature plasma reactors. This work presents the 2D axysimetrical simulation (20,000 cells) of a thermal plasma reactor including various physical processes such as the plasma generation, fluid dynamics and particle dynamics with nucleation. Based on our recent work [1], we consider here the presence of a central probe surface inserted counter current in the reactor and affecting the CNF functionalization based on local values of the flow/temperature/composition fields. Results show temperature , velocity, residence time, nucleation and particle growth at different probe positions. The analysis of the simulation results enables to tune the reactor design for the synthesis and functionalized of the CNF structures. Results indicate a strong stability of the various fields are obtained for the specific reactor design, meaning a very robust process leading to very stable and pure production even under strong fluctuations of the process parameters. A decoupling of the CNF nucleation fields and functionalization fields enables an independent control of the two processes.

References
[1] "Carbon Nanoparticles Production by Inductively Coupled Thermal Plasmas: Controlling the Thermal History of Particle Nucleation"., R. Pristavita, N.Y. Mendoza Gonzalez, J.L. Meunier and D. Berk.,Plasma Chemistry and Plasma Processing, Volume 31, Number 6, Pages 851-866, 2011

Studying the aspect ratio effect of randomly oriented carbon nanotubes in nanocomposites

*Hadi Moussaddy[1], Martin Lévesque[1], Daniel Therriault[1]**

Center for Applied Research on Polymers and Composites (CREPEC), Mechanical Engineering Department, École Polytechnique de Montréal, C.P. 6079, Succ. Centre-Ville, Montreal (QC), Canada H3C 3A7

Keywords : Carbon nanotubes, Nanocomposites, Mechanical properties, Homogenization, Finite element.

The objective of this work is to study the effect of the aspect ratio of randomly oriented carbon nanotubes (CNTs) on the overall mechanical properties of nanocomposites. The properties of randomly oriented CNTs reinforced nanocomposites studied in this work were obtained using two different approaches : i) using three-dimensional FE models of detailed CNTs nanocomposites microstructures and ii) using analytical homogenization models to estimate the resulting mechanical properties. In this study, the SWCNTs are assumed to be cylindrical fibers randomly distributed into the matrix. Isotropic properties are assumed for both the matrix and SWCNTs. A perfect bonding between the SWCNTs and the matrix was assumed. The 3D models are generated using a modified Random Sequential Adsorption algorithm. The representative volume element is found statistically using the method of Kanit et al.[1]. The two analytical homogenization methods studied are the self-consistent scheme and that of Mori-Tanaka. It is found that the Mori-Tanaka model slightly overestimates (~11%) the overall stiffness of the nanocomposite when compared to the FE results. The self-consistent scheme estimations were also stiffer than that of the FE simulations (47%). However, the best results were obtained when using a modified Mori-Tanaka model which takes into account the microstructure images information. An asymptotic behavior is observed when the aspect ratio of the CNTs reaches 100. These results are of significant interest since they allow the modeling of very high aspect ratio CNTs by modeling them using modified Mori-Tanaka and only at their effective length, hence considerably reducing needed computational resources.

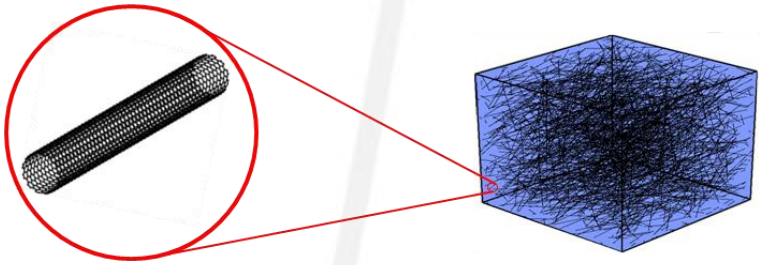

Figure 1 – Randomly oriented carbon nanotubes in a nanocomposite volume element.

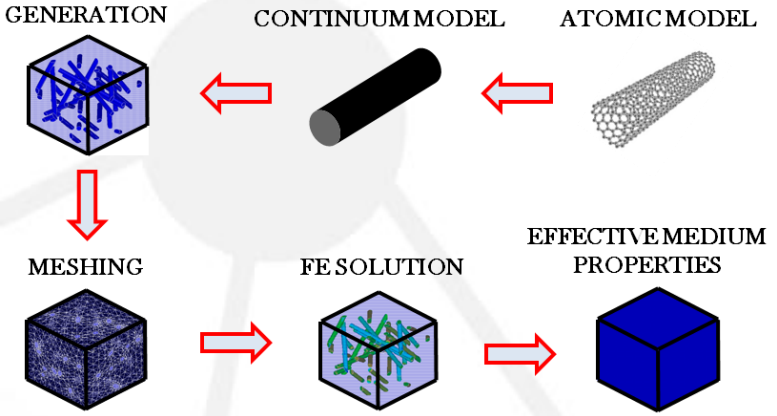

Figure 2 – Numerical modeling approach to estimate effective properties of carbon nanotube reinforced nanocomposites.

References
[1] T. Kanit, *et al.*, "Determination of the size of the representative volume element for random composites: Statistical and numerical approach," *International Journal of Solids and Structures,* vol. 40, pp. 3647-3679, 2003

Nitrogen functionalization of graphene nanoflakes by thermal plasma

Dustin Binny[1], Jean-Luc Meunier[1], Dimitrios Berk[1]*

[1]Plasma Processing Laboratory - PPL, McGill University, Department of Chemical Engineering, Wong Building, 3610 University St., Montréal, Québec, Canada H3A 2B2

Keywords: functionalization, nitrogen, n-doping, graphene, catalyst

Non-noble metal catalyst utilizing carbon nanostructures now begins to rival the activity of platinum catalyst currently used in the Proton Exchange Membrane (PEM) fuel cell [1]. However, stability and durability of these new catalysts remains an important issue preventing their commercialization. In the Plasma Processing Laboratory at McGill University, a highly stable functionalized graphene nanoflake powder was produced for PEM fuel cell operation [2]. Activities for the oxygen reduction reaction (ORR), however, are still low. This work demonstrates enhanced nitrogen functionalization, making closer the availability of an active and stable non-noble catalyst using these nanopowders. Macrocenters composed of atomic iron coordinated to nitrogen atoms that are functionalized onto the graphene matrix create the catalytic centers [1]. Nitrogen functionalization is therefore a key component. Using a thermal plasma and proper reactor design, nitrogen functionalization of the graphene nanoflakes up to 27 at.% has been demonstrated. Pyridinic nitrogen constitutes approximately 15-35% of this total nitrogen. To our knowledge, this is the largest amount of total and pyridinic nitrogen reported to date. Ionized and excited nitrogen species that react with the graphene leading to incorporation are created by manipulating key variables such as reactor design, pressure, power, axial position and nitrogen precursor selection/amount/location. The graphene nanoflakes are created and functionalized in the thermal plasma afterglow within the same reactor in a two-phase processing step. The resulting nanostructure has potential use in a variety of domains requiring catalitic activity and stability in various corroding environments, on top of the targeted PEM fuel cell application.

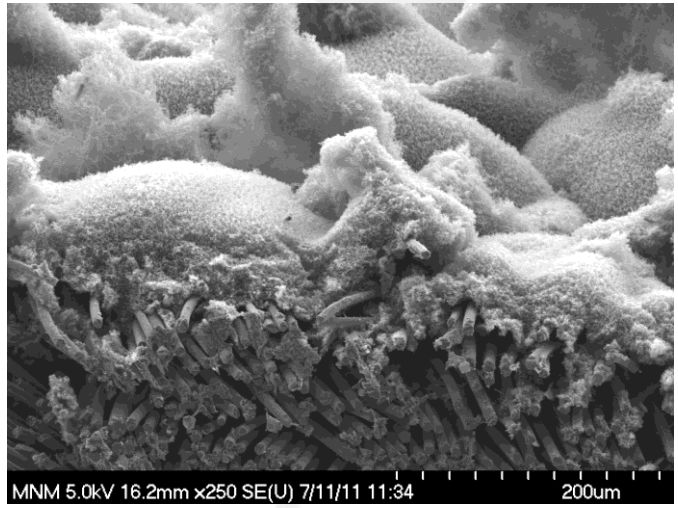

Figure 1 – Cross-section of graphene nanoflake film grown in-situ on top of the weaved carbon cloth fibers

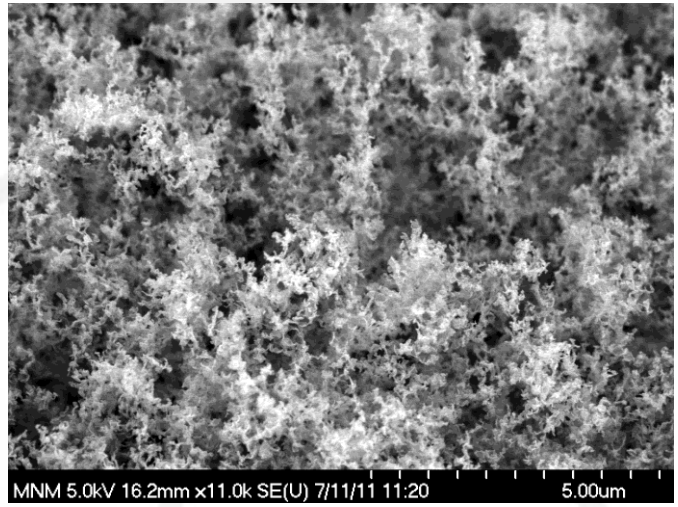

Figure 2 – Close-up of the graphene nanoflake matrix illustrating the high surface area and crystallinity

References

[1] E. Proietti, F. Jaouen, M. Lefevre, N. Larouche, J. Tian, J. Herranz, J.-P. Dodelet, Iron-based cathode catalyst with enhanced power density in polymer electrolyte membrane fuel cells, Nature communications 2 (2011) 416.

[2] R. Pristavita, N.Y. Mendoza-Gonzalez, J.L. Meunier, D. Berk, Carbon Blacks Produced by Thermal Plasma: the Influence of the Reactor Geometry on the Product Morphology, Plasma Chemistry and Plasma Processing 30 (2010) 267-279.

Nanofils de silicium : fabrication, manipulation et mesures térahertz.

J-F.Allard[1], T.Baron[2], A.Beaudoin[1], M.Bernier[1], D.Morris[1], B.Salem[2]

[1]Université de Sherbrooke, Département de Physique 2500, boul. de l'Université, Sherbrooke (Québec) CANADA J1K 2R1
[2]LTM CNRS, 17 avenue des Martyrs 28054 Grenoble, France

Mots clés : Nanofils, silicium, térahertz, microélectronique

Les nanofils sont des nanoparticules de forme cylindrique dont le diamètre atteint quelques dizaines à quelques centaines de nanomètres. La géométrie particulière des nanofils leur confère un grand potentiel applicatif tant en ce qui a trait à l'intégration des nanotechnologies à la microélectronique actuelle que comme composante première de dispositifs technologiques novateurs. La fabrication des nanofils peut se fait par approche *Bottom-Up*. Le principe de cette méthode est d'exploiter les propriétés d'auto-assemblage de la matière pour créer la structure désirée. Le dépôt chimique en phase vapeur dans le régime vapeur-liquide-solide est souvent utilisé pour synthétiser les nanofils à partir d'un catalyseur métallique. Les conditions de croissance déterminent principalement la longueur du nanofil tandis que la taille du catalyseur limite le diamètre de celui-ci. L'approche *Bottom-Up* présente l'avantage de fournir une grande quantité de nanofils sur substrat. Des méthodes chimiques et mécaniques permettent de détacher et de positionner les fils en fonction de l'utilisation envisagée. L'alignement de ceux-ci en un réseau de quelques millimètres permet, par exemple, une étude en spectroscopie térahertz. Dans ce travail nous avons réussi à obtenir des réseaux denses de nanofils de 100 à 300 nm de diamètre, de quelques microns en longueur et ce sur des surface de l'ordre du cm² (voir Fig.1). Des mesures de conductivité AC, obtenues par spectroscopie pompe visible sonde THz sont en cours afin d'évaluer la dynamique des photoporteurs dans ces nanofils. La spectroscopie d'absorption THz devrait également permettre d'obtenir des informations sur le niveau de dopage.

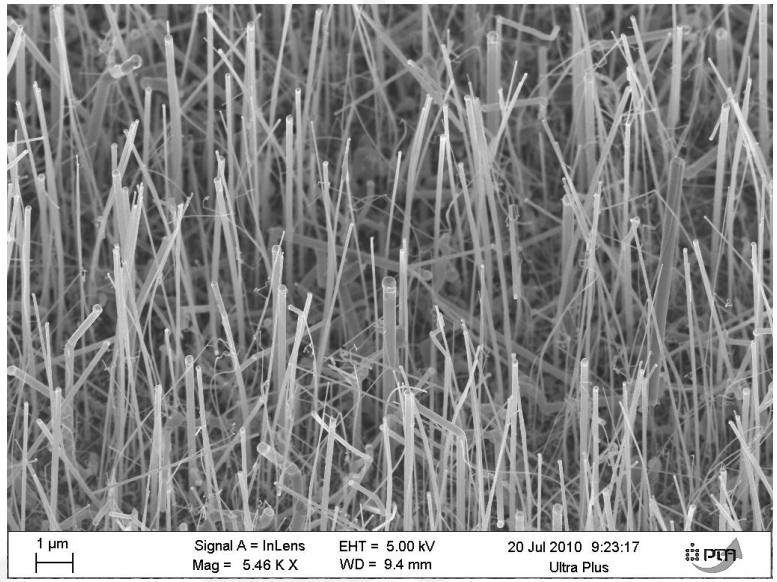

Fig.1 Nanofils de silicium dopés n sur substrat de silicium. Les catalyseurs d'or sont visibles à l'extrémité des fils. (Image prise par Guillaume Rosaz)

Synthèse hydrothermale de la couche mince de $BiFeO_3$ épitaxiale pour application photovoltaïque de volume

I. Velasco-Davalos[*1], M. Moretti[1], M. Nicklaus[1], C. Nauenheim[1,2], S. Li[1], R. Nechache[3,1], D. Drouin[2], A. Ruediger[1]*

1Centre Énergie, Matériaux et Télécommunications, INRS, 1650 boul. Lionel-Boulet, Varennes, Québec, J3X1S2, Canada.
23IT, Université de Sherbrooke, 2500 boul. de l'Université, Sherbrooke, Québec, J1K2R1, Canada.
3Department of Chemical Science and Technology and NAST Center, University of Rome, Tor Vergata Via della Ricerca Scientifica 1, 00133 Rome, Italy.
1Centre Énergie, Matériaux et Télécommunications, INRS, 1650 boul. Lionel-Boulet, Varennes, Québec, J3X1S2, Canada.
23IT, Université de Sherbrooke, 2500 boul. de l'Université, Sherbrooke, Québec, J1K2R1, Canada.
3Department of Chemical Science and Technology and NAST Center, University of Rome, Tor Vergata Via della Ricerca Scientifica 1, 00133 Rome, Italy.

Mots clés : BFO, hydrothermique, photovoltaïque.

Le ferrite de bismuth ($BiFeO_3$ ou BFO), un matériau multiferroïque de structure perovskite, possède un coefficient piézoélectrique remarquablement grand ainsi qu'une polarisation électrique et magnétique simultanée à température ambiante. Son intéressante propriété photovoltaïque de volume lui vaut un intérêt certain de la part de la communauté du photovoltaïque. On a réalisé la croissance d'une couche mince hétéroépitaxiale de BFO par la synthèse hydrothermale, une méthode que l'on présente dans ce projet comme étant une voie alternative réalisable et peu coûteuse. On a utilisé $Bi(NO_3)_3$ et $Fe(NO_3)_3$ comme précurseurs ainsi qu'une faible concentration de KOH comme minéralisateur dans le but de réduire les courants de fuite. La croissance et la cristallisation de la couche ont été réalisées dans un réacteur sous pression autogène qui correspond à la pression de vapeur de l'eau. La couche mince obtenue a été caractérisée par diffraction à rayon X (XRD), par microscopie à force atomique (AFM), par microscopie électronique à balayage (SEM), par microscopie à force piézoélectrique (PFM), et par microscopie à force atomique en mode photoconduction (PhAFM). Dans ce projet, on rapporte pour la première fois la démonstration d'une inversion de la polarisation électrique sur une couche mince de BFO synthétisée par la méthode hydrothermale, puisque l'on a réduit considérablement les fuites électroniques. Finalement, on a aussi effectué la première démonstration d'un effet photovoltaïque dans une couche mince de BFO synthétisée par cette méthode.

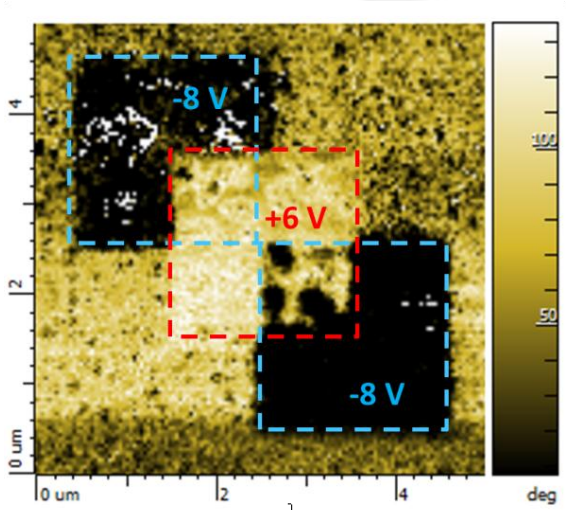

Figure 1. Inversion de polarization dans BFO

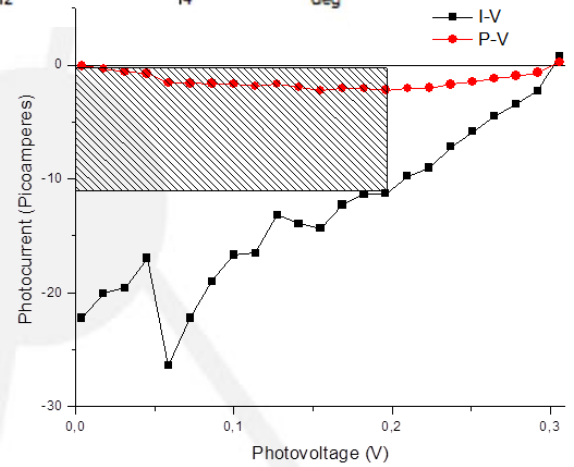

Figure 2. Courbe photocourant vs photovoltage ou l'efficience calculé η= 0.7%

Références
[1] B. Chen, et-al., Nanotechnlogy, 22 (2011) 195201 5pp.
[2] J. Seidel, et-al., Physical Review Letters, 107, 126805 (2011).
[3] M. Alexe, et-al., Nature Communications, DOI: 10.1038/1261 (2011).
[4] W. Ji, et-al., Advance Materials, 2010, 22, 1763-1766.
[5] S. Yang, et-al., Applied Physics Letters 95, 062909 (2009).
[6] A. Huang, et-al., CrystEngComm, 2010, 12, 3806-3814.
[7] D. Rout, et-al, Applied Physics Letters, 95, 122509, (2009).

The Carbon Nanotube Network in Multifunctional Polymer Composites

*C. Cattin *[1], M. Yourdkhani *[1], P. Hubert [1]*

1 Structures and Composite Materials Laboratory, Department of Mechanical Engineering, McGill University, Montréal QC, Canada

Keywords: carbon nanotube, CNT/polymer nanocomposite, CNT network, multifunctional polymer composites

Carbon nanotube (CNT) addition to polymers allows for the design of electro-conductive polymer nanocomposites [1]. With the formation of an electrically conducting network throughout the non-conducting polymer matrix, the CNTs enable electron flow through the material. Due to their outstanding electrical properties and high aspect ratio, small quantities of CNTs can induce a major improvement in electrical conductivity, without significant compromises on other material properties of the host polymer. CNT addition to polymers also allows for the design of polymer structures with improved mechanical properties [2]. Further, the electrical properties of CNT/polymer nanocomposites are coupled to the mechanical deformation of the material [3]. This makes CNT modified polymers an interesting candidate as a matrix material for multifunctional hierarchical polymer composites. Both the properties and the multifunctionality of the material are directly related to the structure of the CNT network. Against this background the motivation for this work is (i) to monitor CNT network formation during material manufacturing, and (ii) to analyze the relation between network structure and final material properties. Fist, CNT network formation prior to and during polymerization is monitored by means of simultaneous electrical and rheological characterization, and information about the network structure are obtained from the piezoresistive response of the material. Second, CNT dispersion stability is analyzed by means of microscopical observation during polymerization, and its influence on the mechanical performance of hierarchical CNT/carbon fibre polymer composites is investigated through mechanical testing and fractography.

Références

[1] J. N. Coleman, S. Curran, A. B. Dalton, A. P. Davey, B. McCarthy, W. Blau and R. C. Barklie, Phys Rev B **58** (12), R7492-R7495 (1998).
[2] J. N. Coleman, U. Khan, W. J. Blau and Y. K. Gun'ko, Carbon **44** (9), 1624-1652 (2006).
[3] M. H. G. Wichmann, S. T. Buschhorn, J. Gehrmann and K. Schulte, Phys Rev B **80** (24), - (2009).

Anisotropy in the Fermi Edge of Zinc Oxide Nanocrystals

C.D. Bain[1], D.S. Bohle[1]

[1]Department of Chemistry, McGill University, 801 Sherbrooke Street West, H3A 0B8

Mots clés : Zinc Oxide, nanoparticles, Fermi Edge

Zinc oxide is a widely used semiconductor and catalyst for whose photocatalytic and other properties may be fine-tuned by altering the size and shape of the particles, especially at the nano-scale. The special properties of ZnO nanoparticles originate from defects in the crystal structure and defects on their surface. The structure of the surface defects is intrinsic to the spectral behavior of the particles, however, the structure of these defects is poorly understood. The precursor counter ions, concentrations, and ripening times have been varied. The effect of these conditions on the observed size, shape, and the resulting effect on the optical and fluorescence properties of the particles has been explored.

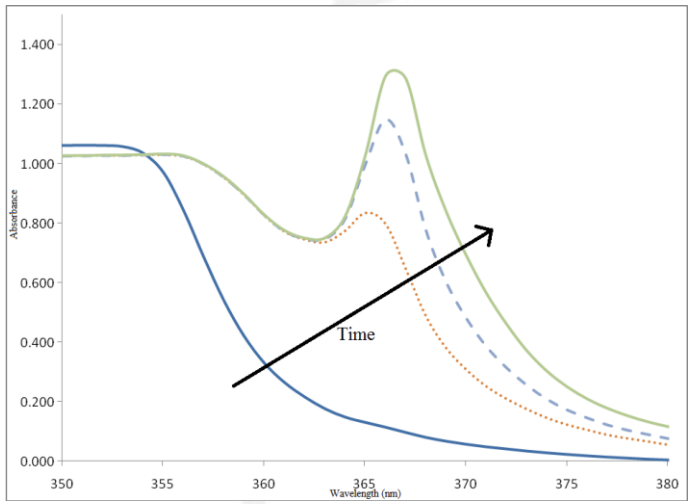

Figure 1 – Changes to the absorption spectrum of the ZnO over time

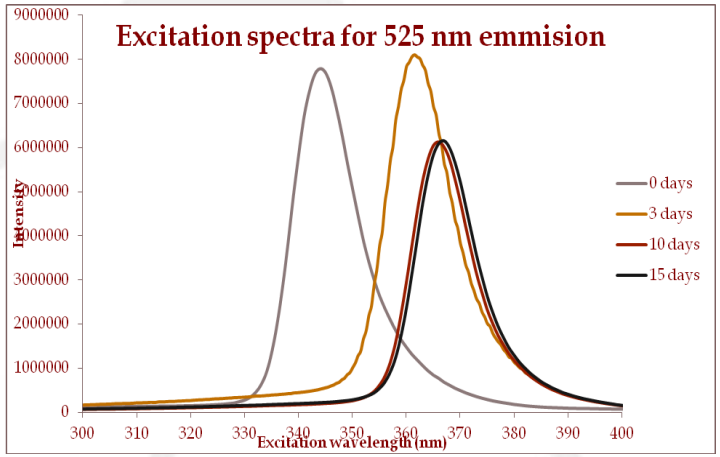

Figure 2 – Changes in the excitation spectra of ZnO sample over time

Encapsulation of α-Sexithiophene in Carbon Nanotubes: a Raman Study

N. Y-.W. Tang, E. Gaufrès, F. Lapointe, R. Martel

Regroupement Québécois sur les Matériaux de Pointe (RQMP) et Département de Chimie, Université de Montréal, Montréal, Canada, H3T 1J4

Key words : nanotechnology, carbon nanotubes, sexithiophene, Raman spectroscopy

In recent years, encapsulating organic molecules into carbon nanotubes has attracted much attention. It has been clearly shown that molecules inside the CNT are protected from degradation. In this study, we investigated using Raman spectroscopy the encapsulation of α-sexithophene (6T) into single-walled carbon nanotubes (SWNTs) via a liquid phase. Our results exhibit similar properties as 6T@SWNT obtained by sublimation. Raman performed on individual 6T@SWNTs, one metallic and one semi-conductor, and bromophenyl-functionalized 6T@SWNTs demonstrate that the Raman signal of the 6T is unaffected by the chemical modifications induced by the radical reaction on the surface of the nanotubes. The results also show that the Raman diffusion of the encapsulated molecules is a resonant process that shows no (or low) parasitic fluorescence emission.

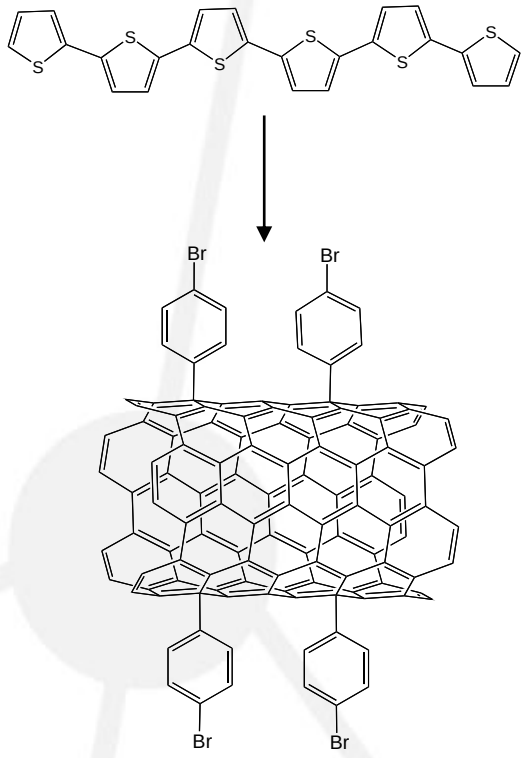

Figure 1 – Encapsulated a-sexithiophene in a bromophenyl functionalized carbon nanotube

Simulation de la fusion de nanocristaux de polyéthylène

S. Palato[1], N. Metatla[1], B. Commarieu[2], J. Claverie[2], A. Soldera[1]

[1]Centre Québécois des Matériaux Fonctionnels, Département de Chimie, Université de Sherbrooke, Sherbrooke, QC, Canada, J1K 2R1
[2]NanoQAM, Département de Chimie, UQAM, Succ. Centre Ville, Montréal, QC, Canada, H3C 3P8

Mots clés : nanotechnologies, polymères, fusion, cristaux.

Les nanocristaux de polymères attirent de plus en plus l'attention, à la fois par leurs applications technologiques potentielles et par leurs propriétés inédites qui diffèrent des propriétés du polymère massif. La simulation moléculaire montre alors toute sa pertinence en permettant l'analyse des propriétés nanoscopiques de ces composés. L'élaboration de modèles appropriés, bien que première étape du processus de simulation, s'avère riche en informations et esquisse les grandes lignes de réflexions que poursuivront les investigations à venir. Comme premier modèle, nous avons étudié le polyéthylène (PE). La finalité de ce travail fut de corréler les données émanant de la simulation aux températures de fusion expérimentales du PE nanocristallin. L'utilisation d'alcanes modèles montre l'évolution simultanée de la capacité calorifique, de l'énergie et de la conformation des molécules, révélant une température de fusion bien définie. Ces études nous ont permis de montrer que les températures de fusion relatives suivaient la même loi de Gibbs-Thomson (figure ci-dessous)[1]. La comparaison extensive entre deux systèmes, les nanocristaux d'alcanes et les nanofeuillets de PE fonctionnalisés, a permis de mettre en évidence le rôle prépondérant des interfaces sur les propriétés thermodynamiques des cristaux de dimensions nanométriques. Ces données soulignent pertinence de la dynamique moléculaire comme outil de choix pour l'exploration des propriétés de polymères nanostructurés.

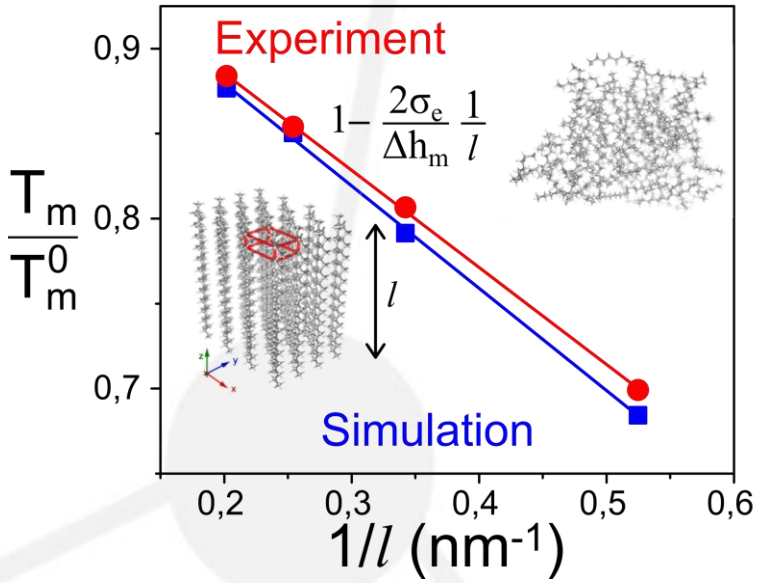

Figure 1 – La température de fusion de nanocristaux de polyéthylène révèle le rôle prépondérant des interfaces à l'échelle nanoscopique pour toutes les tailles étudiées.

Références
Metatla, N.; Palato, S.; Commarieu, B.; Claverie, J.; Soldera, A. *Soft Matter*, 2012, **8**, 347.

Propriétés de Photogénération de courant des nanotubes de carbone synthétisés par la méthode d'ablation laser-KrF

*V. Le Borgne, L.A. Gautier, M. A. El Khakani**

Institut National de la Recherche Scientifique, INRS-Énergie, Matériaux et Télécommunications, 1650 Lionel-Boulet, Varennes, Canada, J3X 1S2

Mots clés : Nanotubes de carbone; ablation laser; Photocourrant; Photovoltaïque; Énergie solaire.

Des nanotubes de carbone monoparoi (NTCs) ont été synthétisés en ablatant une cible de graphite et de catalyseur Co/Ni à l'aide d'un laser pulsé KrF. Les NTCs ainsi obtenus, à une température de synthèse de 1150°C, sont de haute qualité et possèdent une distribution étroite de diamètres centrée à 1.25 nm. Les caractérisations des NTCs ont été effectuées par différentes méthodes incluant la spectroscopie Raman et les microscopies électroniques.[1] Les NTCs ainsi produits ont été systématiquement purifiées par voie chimique. Ils ont été ensuite intégrés dans des dispositifs photovoltaïques hybrides constitués de n-Si recouvert d'un film de NTCs.[2] Nous présenterons les propriétés de génération de photocourant de ces dispositifs, soit l'efficacité quantique, qui atteint 50% dans le spectre visible, et des paramètres critiques pour la conversion de puissance (h), tels le courant à circuit fermé (I_{SC}) et la tension à circuit ouvert (V_{OC}). Le dopage approprié des nanotubes a permis de doubler leur capacité de conversion de puissance pour atteindre une valeur de h ~2 %. Il a également permis de mettre en évidence l'effet de saturation de la densité de charges et son atténuation. De plus, une étude systématique des propriétés électroniques et optiques des films de NTCs a permis d'établir des films de NTCs optimaux qui montrent une forte corrélation entre une figure de mérite et la photogénération.

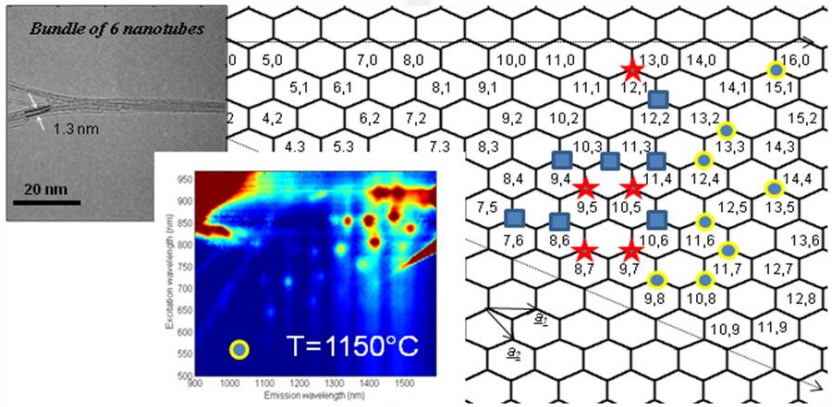

Figure 1 – Cartographie de photoluminescence (bas-milieu) des liasses de nanotubes de carbone (illustrés par l'image MET en-haut à gauche) synthétisés par laser à 1150 °C avec leurs chiralités respectives.

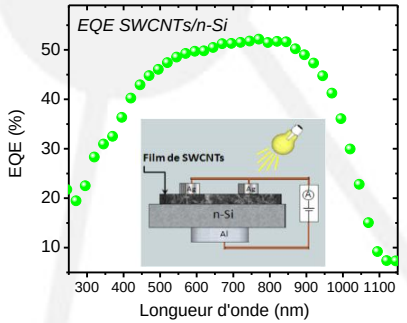

Figure 2 – Spectre EQE d'un dispositif SWCNT/n-Si fabriqué à l'aide de SWCNTs synthétisés à 1150°C. (encart) Diagramme des dispositifs SWCNTs/n-Si

References
[1] V. Le Borgne, B. Aïssa, M. Mohamedi, Y. Ahm Kim, M. Endo, M. A. El Khakani, J. Nanopart. Res., 13 (2011) 5759–5767.
[2] V. Le Borgne, M. A. El Khakani, + 5 others, Appl. Phys. Lett., 97 (2010) 193105

Points quantiques colloïdaux, de la recherche fondamentale à l'application

S. Lamarre[1,2], M.-A. Langevin[1,2], J. Tessier[1,2], M. Boivin[1] , V. Veilleux[1] , D. Lachance-Quirion[1], C. Nì. Allen [1]*

[1]Centre d'optique, photonique et laser (COPL), département de physique, de génie physique et d'optique, 2375 rue de la Terrasse, Université Laval, Canada
[2]Centre de recherche sur les matériaux avancés (CERMA), département de chimie, 1045 avenue de la Médecine, Université Laval, Canada

Mots clés : Points quantiques, cœur-coquille, pile solaire, fluorescence, spectroscopie cryogénique

Les points quantiques colloïdaux sont des nanocristaux semi-conducteurs dispersables dans un solvant et dont les propriétés optiques et électroniques dépendantes de leurs tailles. Notre laboratoire s'intéresse particulièrement aux structures cœur-coquille et au dopage de ZnSe par du Mn^{2+}. Des structures de types $CdSe/Cd_xZn_{1-x}S$ sont utilisées pour les applications dans le domaine du visible et celle de Ag_2Se/Ag_2S pour le domaine du proche infrarouge. Les nanocristaux non dopés émettent de la photoluminescence provenant de la recombinaison d'un exciton tandis que ceux dopés émettent par une transition interdite des états électroniques du Mn^{2+}, allongeant considérablement le temps de vie de photoluminescence. L'émission d'un nanocristal unique peut être détectée jusqu'à 8 K en utilisant un montage de micro photoluminescence muni d'un cryostat. Ainsi il est possible d'étudier les effets de la tension interfaciale de ces structures cœur-coquille et du couplage de l'exciton avec les phonons. Nous étudions aussi les effets de la structure de ces nanocristaux ainsi que de l'environnement sur la dynamique de l'intermittence de la photoluminescence [1]. Les nanocristaux avec un cœur de CdSe et une multicoque de $Cd_xZn_{1-x}S$ ont été étudiés pour des applications en imagerie biomédicale des neurones. Ils ont été fonctionnalisés pour leur dispersion dans l'eau ainsi que la reconnaissance d'une cible. Des cœurs de CdSe munis de ligands accepteurs d'électrons (4FTCNQ) ont été étudiés pour la fabrication de piles solaires plastiques comme accepteur de trous, augmentant l'efficacité de conversion par un facteur ~2,3 par rapport aux cœurs de CdSe seuls [2].

References
[1] Veilleux, V.; Lachance-Quirion, D.; Doré, K; Landry, D. B.; Charrette, P. G.; Allen, C. Nì. Strain-induced effects in colloidal quantum dots : lifetime measurements and blinking statistics. *Nanotechnol.*, **2010**, *21(13)*, 124024.
[2] Boivin, M.; Lamarre, S.; Tessier, J.; Lecavalier, M.-È.; Najari, A.; Dufour-Beauséjour, S.; Brown Dussault, E.; Collin, P.; Allen, C. Nì. Morphological control of hybrid polymer-quantum dot solar cells with electron acceptor ligands. *Appl. Phys. Lett.* **2012**, *100(3)*, 033302.

Control of block copolymer aggregate morphologies in poly(ethylene oxide)-block-polycaprolactone in an aqueous environment

G. Rizis[*1,2], *A. Eisenberg*[1,2], *T. van de Ven*[1,2]

[1]Department of Chemistry, McGill University, Pulp & Paper Research Centre, 3420 University Street, Montréal, Canada, H3A 2A7
[2]Centre for Self-Assembled Chemical Structures (CSACS)

Keywords : block copolymer, self-assembly, nanocrystals

This study documents an ordered series of morphological transformations induced by core crystallization within micelles of poly(ethylene oxide)-block-polycaprolactone (PEO-b-PCL), a promising biodegradable system for use in pharmaceutical applications. These transformations occurred in pure water starting with spherical core-shell micelles as precursors. Multiple aggregate morphologies were observed as a function of both time and composition of the diblock copolymers from which they were prepared. The aggregates contain nanocrystals of PCL in the hydrophobic core; heating the aggregates beyond the crystalline melting point makes it possible to restore the original micellar state, and reversibility is shown over multiple cycles. The crystallinity in the spherical precursors can be modified by incorporating PCL homopolymers into the micelles. The use of such additives offered control over transformation kinetics as well as the aggregate morphology. This example demonstrates how it is possible to engineer well-defined structures by manipulation of polymer crystallinity within nanoscopic objects.

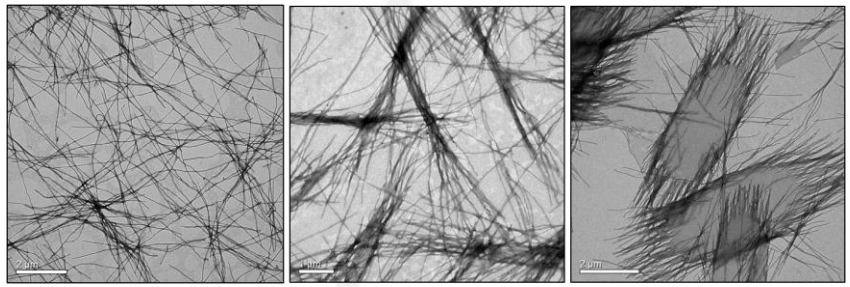

Figure 1 – Morphological phase transitions in binary mixtures of block copolymer PEO_{45}-b-PCL_{18} and homopolymer PCL_{10}.

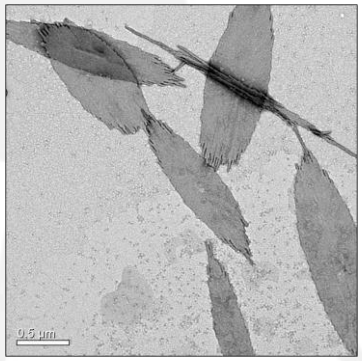

Figure 2 – Platelets of PEO_{45}-b-PCL_{27} in co-existence with spherical micelles.

References
[1] W. Reisner, N. B. Larsen, A. Silahtaroğlu, A. Kristensen, N. Tommerup, J. O. Tegenfeldt, and H. Flyvbjerg (2010) *Proc. Natl. Acad. Sci. U. S. A.* **107**, 13294–13299.
[2] M. F. Q. Kluytmans-VandenBergh and J. A. J. W. Kluytmans (2006) *Clin. Microbiol. Infect.* **12 (Suppl. 1)**, 9–15.
[3] M. Esteller (2007) *Nat. Rev. Genet.* **8**, 286–298.

High surface area mesoporous perovskites for oxidation of volatile organic compounds

Mahesh M Nair[1], Serge Kaliaguine[2] and Freddy Kleitz[1]*

[1]Department of Chemistry and Centre de Recherche sur les Matériaux Avancés (CERMA), Université Laval, Quebec City, G1V 0A6, Canada, [2]Department of Chemical Engineering, Université Laval, Quebec City, G1V 0A6, Canada

Keywords : mesoporous perovskites, high surface area, nanocasting, oxidation, kinetics

Total oxidation represents an effective tool to control the emission of volatile organic compounds (VOC) which are the major source of air pollution. Perovskite type mixed metal oxides (ABO_3), were found to replace the noble metal catalysts in a very effective way, especially with regard to their substantial thermal stability and low cost. However, high temperature treatments involved in the conventional synthesis methods for perovskite oxides, usually leads to low surface area materials. We have initiated a systematic study to optimize and generalize the synthesis of perovskite oxides with high surface area using the recently developed nanocasting method. The confined space available within the template pores controls the growth of the material favouring the formation of nanostrutures with enhanced surface area. Using this approach, a series of mesoporous $LaBO_3$ (B = Mn,Co and Fe) catalysts has been synthesized using ordered mesoporous silica (SBA-15 and KIT-6) as templates. Thus synthesized materials were characterized using powder X-ray diffraction, N_2 physisorption, transmission electron microscopy, X-ray photoelectron spectroscopy and temperature programmed reduction/desorption methods. All the catalysts thus synthesized, were found to exhibit extremely high values of surface areas. Higher conversion efficiencies for methanol oxidation were observed for nanocast $LaMnO_3$ catalysts compared to the same composition synthesized using other methods. Further, experimental conversion rates were found to depend on the partial pressure of methanol. The value of activation energy determined from the Arrhenius plot is found to be low. The calculated values of conversions were found to agree well with the experimental conversions obtained.

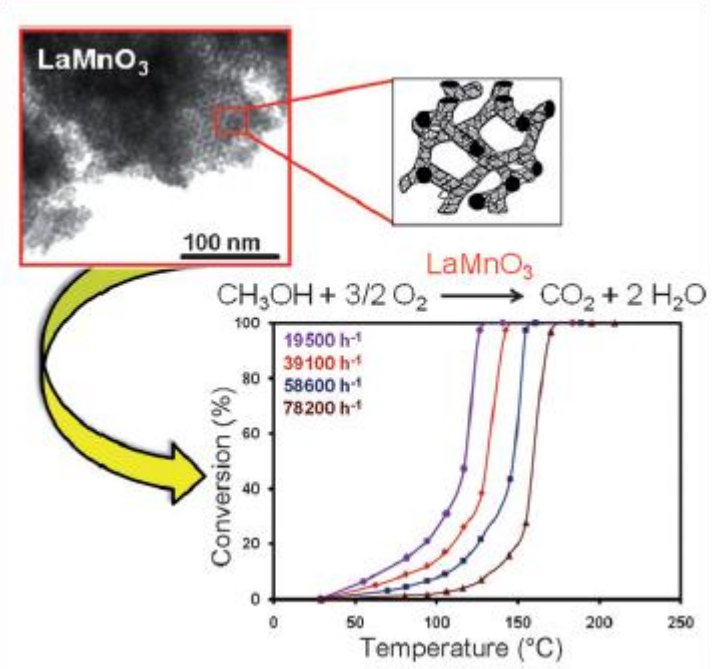

Figure 1 – Representative TEM image of nanocast mesoporous perovskite and the conversion curves obtained as a function of temperature, for the total oxidation of methanol.

References

[1] Lu, A. H.; Schüth, F. *Adv. Mater*. **2006**, 18, 1793-1805.
[2] Rumplecker, A.; Kleitz, F.; Salabas, E.; Schüth, F. *Chem. Mater.* **2007**, 19, 485- 496.
[3] Levasseur. B.; Kaliaguine, S. *Appl. Catal. A* **2008**, 343, 29-38.
[4] Nair, M. M.; Kleitz, F.; Kaliaguine, S. *Chemcatchem.* (in press).

Potential Pressure and Temperature Sensors using PEEK and CNT

M. Mohiuddin, S. V. Hoa

Concordia Centre for Composites, Department of Mechanical and Industrial Engineering, Concordia University, 1455 de Maisonneuve Blvd. W Montréal, QC, Canada H3G 1M8

Keywords: Pressure, Temperature, Carbon nanotubes (CNTs), Poly Ether Ether Ketone (PEEK), electrical conductivity.

Enhancement of electrical conductivity of polymer by mixing them with multi walled carbon nanotubes (MWCNTs) has found widespread applications as heating elements, self-regulating heaters, gas sensors, switching materials, over-current protectors etc. [1]. They can be used as sensing and actuating element in many engineering applications such as biomedical industry, automotive industry, food industry, environmental monitoring, agriculture and fishing industry, manufacturing industry, security and others where the ambient pressure and temperature are not constant [2]. Their dependence of electrical conductivity for conductive thermoplastic composites is now a day's an omnipresent phenomenon. In this article, the pressure and temperature dependent electrical conductivity of thermoplastic composites made of MWCNTs and Poly Ether Ether Ketone (PEEK) for different CNT loadings are presented. Different weight concentrations of carbon nanotubes were dispersed in PEEK through high shear melt mixing at Brabender at 100 rpm and 380°C for 20 minutes. The resulting nanocomposites were processed into round shaped pieces of 25.4 mm diameter and 1.4 mm thickness. The samples were then compressed by applying a pressure from zero to 40 MPa and heated from 20°C to 140°C. It was found that electrical conductivity increases significantly with increase of heat and pressure. Regardless of nanotube concentration, the samples were found highly sensitive at low pressure and low temperature as expected. Again, the samples were highly sensitive at lower nanotube content and less sensitive at higher nanotube content, but the range of sensitivity is higher for higher nanotube content. The samples also showed more temperature sensitivity than pressure sensitivity.

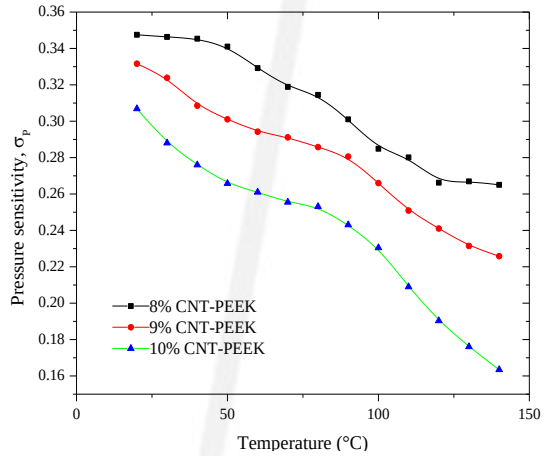

Figure 1 – Pressure sensitivity of CNT-PEEK samples at different temperatures

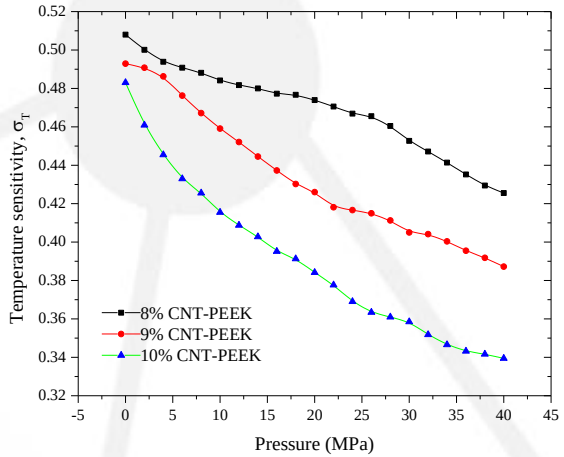

Figure 2 – Temperature sensitivity of CNT-PEEK samples at different pressures

References

[1] R. Strumpler. Polymer composite thermistors for temperature and current sensors. *Journal of Applied Physics,* vol. 80, Issue 11, pp. 6091-6096, 1996.

[2] N. Sinha, J. Ma & J.T.W. Yeow. Carbon nanotube-based sensors. *Journal of Nanoscience and Nanotechnology,* vol. 6, Issue 3, pp. 573-590, 2006.

Structural characterization of mesoporous materials using electron tomography

Yeoji Jane Kim, Karim Babak, Hojatollah Vali and Mihnea Bostina

Facility for Electron Microscopy Research, McGill University, 3450 University St, Montreal, Quebec, H3A 0C7

Mots clés : electron tomography, mesoporous carbon, nanoparticles

Electron tomography (ET) is a powerful tool for investigating the three-dimensional structure of nanomaterials. Starting with a series of projections recorded over a wide angular range, the internal morphology of the object can be reconstructed mathematically [1]. In the case of mesoporous materials, by using ET, it is possible to determine the distribution of nanoparticles in a supporting matrix, information which, otherwise, is lost in a single projection image. Of major interest in the characterization of porous nanosystems for their subsequent use, is to understand the structural details which provide the enhancement of their surface area with respect to their bulk volume and the relation between different components. In combination with electron energy loss spectroscopy, ET allows to map the chemical composition of the entire system and to correlate the position of various nano-structured objects with the inner morphology. A novel mesoporous carbon (IFMC) having nano-fibrous morphology (fig.1) was successfully prepared [2]. The material was then used to stabilize palladium nanoparticles and was shown to be an active catalyst for aerobic oxidation of alcohols with either molecular oxygen or air in water at low temperatures [3]. By using ET we show that the material has a monomodal distribution of Pd particles, with particle sizes typically between 2-4 nm. The nanoparticles are not only supported on the external surface of the carbon matrix but they are also well distributed inside the mesopores (fig. 2).

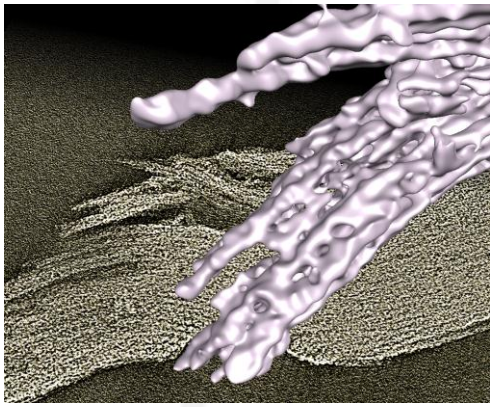

Figure 1. Electron tomography of the nano fibrillated mesoporous carbon IFMC. Surface rendering of a subregion of the reconstructed volume superimposed over a 200 nm central slice through the tomogram.

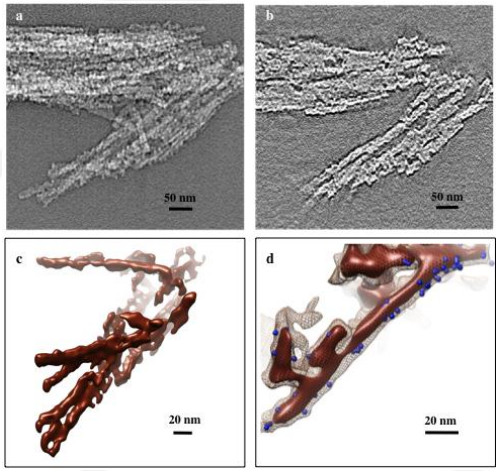

Figure 2. Electron tomography of Pd@IFMC. a) Projection of reconstructed volume. b) A 1 nm middle slice through the reconstruction. c) Surface representation of a portion of the tomogram presented in a) where individual fiber are clearly visible. d) Localization of Pd nano-particles (blue) at the exterior of individual fibers.

References

[1] Electron Tomography: Methods for Three-Dimensional Visualization of Structures in the Cell. Joachim Frank (Editor), 2006
[2] Electrochemical Performance of a Novel Ionic Liquid Derived Mesoporous Carbon. Babak Karimi, Hesam Behzadnia, Mohammad Rafiee and Hojatollah Vali Chem. Commun, 2012
[3] A Novel Nano Fibrillated Mesoporous Carbon as an Unique Support for Palladium Nanoparticles in Aerobic Oxidation of Alcohols in Pure Water. Babak Karimi, Hesam Behzadnia, Mihnea Bostina and Hojatollah Vali, *submitted*

Synthèse de nanoparticules de silice fluorées mono dispersées et leurs couches minces superhydrophobes

Jean-Denis Brassard†‡, D. K. Sarkar‡, and Jean Perron†

†Laboratoire international des matériaux anti-givre (LIMA) et ‡Centre Universitaire de Recherche sur l'Aluminium (CURAL), Université du Québec à Chicoutimi, 555 Boulevard de l'Université, Chicoutimi, Québec, Canada, G7H 2B1

Mots clés : superhydrophobe, silice, nanoparticules, fluore, angle de contact

Les surfaces superhydrophobes sont inspirées de la nature (1, 2). Dans le but d'obtenir ce type de surface, des nanoparticules de silice mono dispersées ont été obtenues via le procédé Stöber (3) et ont été fonctionnalisées en solution en y ajoutant des molécules fluorées (4). Ces molécules fluorées proviennent d'une solution de fluoroalkylsilane dans l'éthanol. Avec le procédé, six tailles de particules ont été obtenues, des diamètres entre 40 et 300nm tels que confirmé par microscopie électronique à balayage (MEB) . Ces différentes tailles de particules furent déposées en couches minces sur des substrats d'aluminium en utilisant l'enduction centrifuge (spin coating). La fonctionnalisation des nanoparticules de silice par le fluor a été confirmé par la présence de groupements –CF reliés à des liaisons Si-O-Si dans les minces couches tel que montrés par spectroscopie infra rouge à transformées de Fourrier (FTIR). Il a aussi été montré que les rugosités (RMS) de surface et l'angle de contact de l'eau (CA) se trouvent augmentés en fonction de l'augmentation de diamètre des particules. Les couches minces obtenues avec les nanoparticules de silice fluorées ayant un diamètre critique de 120 nm et ayant une rugosité de 0,697 µm permettent d'obtenir une surface superhydrophobe sur l'aluminium avec un angle de contact 151 °. Ces couches minces superhydrophobes sur l'aluminium proposent un très fort potentiel pour servir d'additif à des peintures et revêtements commerciaux pour l'application en grande échelle. L'utilisation de ces nanoparticules permet une application variée tel qu'en surfaces autonettoyantes, en surface anticorrosion mais encore en diminution de la traînée.

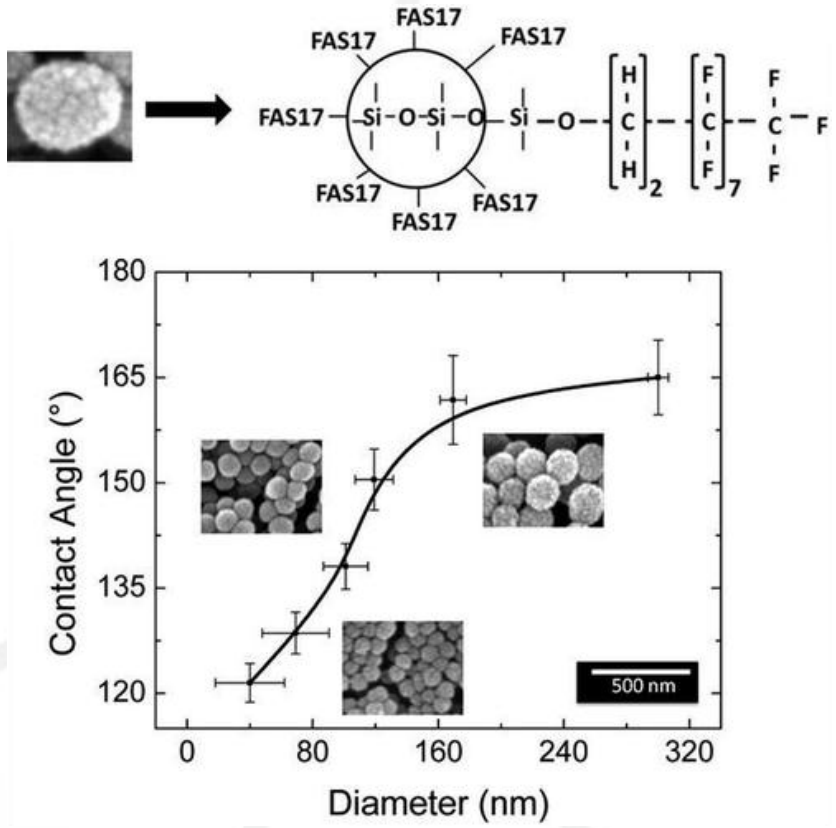

Figure 1 : Représentation schématique de la particule de silice fonctionnalisée par le fluoroalkylsilane (haut). Variation de l'angle de contact de l'eau en fonction du diamètre (BAS). Images MEB de nanoparticules de silice de différents diamètres.

References

(1) Cao, H., H. Zheng, K. Liu, and J.H. Warner, Bioinspired peony-like Î²-Ni(OH)₂ nanostructures with enhanced electrochemical activity and superhydrophobicity. *ChemPhysChem*, *11,* 489-494.

(2) Guo, Z., F. Zhou, J. Hao, and W. Liu, Stable Biomimetic Super-Hydrophobic Engineering Materials. *Journal of the American Chemical Society* **2005**, *127,* 15670-15671.

(3) Stöber, W., A. Fink, and E. Bohn, Controlled growth of monodisperse silica spheres in the micron size range. *J. Colloid Interface Sci.* **1968**, *26,* 62-69.

(4) Brassard, J.-D., D.K. Sarkar, and J. Perron, Synthesis of Monodisperse Fluorinated Silica Nanoparticles and Their Superhydrophobic Thin Films. *ACS App. Mater. Interfaces* **2011**, *3,* 3583-3588.

Phosphonate-functionalized nanoporous hybrid materials as highly efficient actinide extracting agent

*Pablo J. Lebed[1], Maëla Choimet[1], Jean-Daniel Savoie[1], François Bilodeau[2], Freddy Kleitz[*1]*

[1]Department of Chemistry, Université Laval, Centre de recherche sur les Matériaux Avancés (CERMA) and Centre de recherche sur les propriétés des interfaces et la catalyse (CERPIC) Québec, Canada; Fax: +1-418-656-7916; Tel: +1-418-656-7812/7250
[2] Hydro-Quebec Production, Gentilly-2 Nuclear Power Plant, Gentilly G9H3X3, QC, Canada

Key words: KIT-6, functionalization, radionuclides, actinides

The development of new sequestration materials for the nuclear industry is essential from a health and environmental protection point-of-view as they not only provide a solution to nuclear wastes, but also enable their detection if coupled with the appropriate analytical methods. [1] For on-line analysis of long-lived actinides, chromatographic resins will perform the chemical separation, pre-concentration, and purification required to achieve accurate detection. Extraction (EXC) chromatographic-based resins are commonly used for this purpose as they exhibit high selectivity for many analytes such as actinides, radiostrontium, and technetium. Nonetheless, EXC resins are plagued with issues, (lack of reusability, elution of organic extractant and stationary phase, and possibility of sample cross-contamination). Thus, developing new materials with excellent extraction properties and stability, achievable through chemical grafting of selective functionalities, is needed. [2, 3] This contribution highlights our findings regarding effective functionalization of large pore 2-D hexagonal (SBA-15) and 3-D cubic mesoporous (KIT-6)[4] silicas to produce new sorbent nanomaterials for radionuclides. Here, phosphonates groups are chemically-bonded onto the silica surface, providing selective and durable functions for the extraction of actinides. U and Th sequestration capability of the sorbents was investigated and adsorption equilibrium was achieved much faster (1 min) than commercial EXC U/TEVA resins (10 min). [5] The KIT-6-based nanoporous material showed excellent extraction properties, i.e. 40 times higher extractability compared to U/TEVA. Also, the unique spatial configuration of the 3-D cubic mesoporous hybrid has demonstrated much higher selectivity (affinity coefficients Kd > 104) than its 2-D counterpart and is applicable in a range of conditions relevant for real environmental analysis.

References
[1] D. Butler and L. Stricker, *Nature*, 2011, **472**, 274.
[2] A. Walcarius and L. Mercier, *J. Mater. Chem.*, 2010, **20**, 4478.
[3] Z. Wu and D. Zhao, *Chem. Commun.*, 2011, **47**, 3332.
[4] F. Kleitz, S. H. Choi and R. Ryoo, *Chem. Commun.*, 2003, 2136.
[5] P. J. Lebed, K. de Souza, F. Bilodeau, D. Larivière and F. Kleitz, *Chem. Commun.*, 2011, **47**, 11525.

Spectroscopy of quantum dots by force detection

A. Roy-Gobeil[1], *Y. Miyahara*[1], *L. Cockins*[1], *P. Grütter*[1]

[1] Department of Physics, McGill University, 3600 rue University, Montréal, Canada, H3A 2T8

Keywords : electrostatic force microscopy, quantum dots, nanoparticles, single electronics

Electrostatic force microscopy (EFM), a variant of atomic force microscopy (AFM) techniques, has been playing an essential role in characterizing nanoelectronic devices as well as their constituent materials. For example, local potentiometry experiments with EFM as well as Kelvin probe force microscopy (KPFM) have contributed to better understanding the microscopic nature of quantum Hall effects [1]. We have recently demonstrated that a high-sensitive EFM is capable of the local electrometry with single-electron charge resolution and it can be used for quantitative spectroscopy of individual quantum dots (QD) including coupled QDs [2, 3]. We present our recent experiments on chemically synthesized gold colloidal nanoparticles (Au NP). Au NPs are attached onto 1,16-hexadecanedithiol (C16S2) self-assembled monolayer (SAM) formed on a gold substrate (Fig. 1(a)). The charge state of an Au NP can be changed by the single-electron tunneling through C16S2 SAM. By controlling the tip-substrate bias voltage or the position of the tip, we can control and detect the electric charge stored in individual Au NPs. Figure 1(b) and (c) both show a set of concentric rings around 5nm Au NP. Each of the concentric rings corresponds to a change in electric charge in the Au NP by a single electron charge. By performing a voltage spectroscopy of frequency shift and dissipation signals, we can obtain the charging energy, discrete energy spectrum as well as tunneling rate, all quantitatively without patterned electrodes around the NPs. We will present how this new spectroscopic technique could be applied to other interesting entities such as self-assembled Au NPs using DNA.

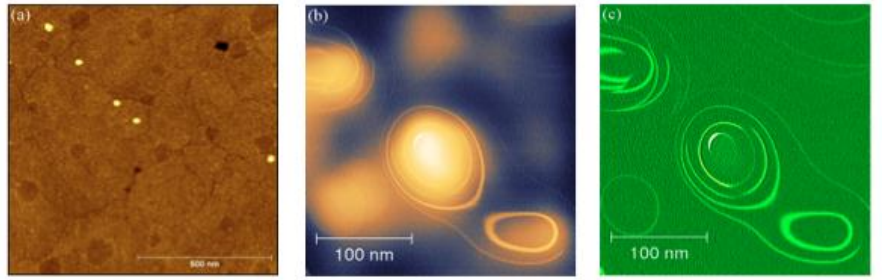

Figure 1 – (a) AFM topography image of 5 nm Au NPs on C16S2 SAM on Au substrate taken in air with amplitude modulation mode. (b) and (c) Frequency shift and dissipation images taken at 4.5 K at a constant tip height of about 15 nm. Au substrate bias voltage was 5 V.

References

[1] Y. Miyahara, L. Cockins and P. Grutter, “Electrostatic force microscopy characterization of low dimensional systems”, In *Kelving Probe Force Microscopy,* S. Sadewasser and T. Glatzel (eds.), Springer-Verlag, Chap. 9, (2011) and references therein.
[2] L. Cockins, Y. Miyahara, S. D. Bennett et al., PNAS, 107, 9496, (2010).
[3] S. D. Bennett, L. Cockins, Y. Miyahara et al, Phys. Rev. Lett., 104, 017203, (2010).

Bombardement ionique du *c*-Si : étude numérique par ART-cinétique

L.K. Béland[*1], *N. Mousseau*[1]

[1]Département de physique, Regroupement québécois sur les matériaux de pointe et Calcul Québec, Université de Montréal, C.P. 6128, Succursale Centre-Ville, Montréal, Québec, Canada, H3C 3J7

Mots clés : simulation, Monte Carlo cinétique, implantation ionique, semi-conducteur, nano-structures

La conception de modèles théoriques pour décrire la cinétique des nanostructures dans les semi-conducteurs est handicapée par le caractère élastique des interactions interatomiques en présence. De ce fait, les nanostructures dans le silicium cristallin (*c*-Si) sont principalement composées d'atomes dans des positions hors réseau. Les méthodes de simulation traditionnelles ne peuvent traiter ce type de configuration sur des échelles de temps comparables aux expériences.C'est dans ce contexte que nous avons développé la technique d'activation relaxation cinétique (ART-cinétique), une méthode de simulation atomistique autodidacte capable de gérer les déplacements hors-réseau.[1] Nous l'utilisons pour décrire la relaxation du *c*-Si suite à un bombardement ionique à 3 keV par Si^- sur des échelles de temps dépassant la microseconde. Nous montrons la nature des nanostructures créées par la cascade de défauts post implantation, étudions leur stabilité et déterminons les mécanismes atomistiques dominant lors du recuit de l'échantillon.

Référence

[1] L.K. Béland, P. Brommer, F. El-Mellouhi, J.-F. Joly et N. Mousseau, Phys. Rev. E 84, 046704 (2011)

Dusty Plasma Deposition of Zinc-Based Nano-structured Thin Films

M. Lennox[1], S. Coulombe*[1]

[1]Plasma Processing Laboratory, Department of Chemical Engineering, McGill University, 3610 University Street, Montréal, Canada, H3A 2B2

Keywords : dusty plasma, zinc oxide, nanoparticle, thin film, carbon nanotubes

Non-thermal plasma technologies are not only mature technologies complementing the field of nanotechnology, but drive continued research in nanoparticle synthesis, surface functionalization, and thin-film coatings. In the present work, the combination of aerosol flow condensation and a capacitively-coupled glow discharge plasma was used to rapidly deposit thin, nano-structured coatings of zinc-based nanoparticles that conformed to the topography of two types of substrates with decidedly different surface roughness: composites of multi-walled carbon nanotubes (MWCNTs) and stainless steel [1], and silicon wafers, as shown in Figures 1 and 2, respectively. Enhanced electron emission from CNT-ZnO nanoparticle composites [2] has been reported in the literature, and so the performance of the synthesized composites as cathode materials for sustaining electrical discharges was investigated. No immediate reduction in the voltage required to sustain the test glow discharge was observed in time-course studies and the composite cathode was degraded by ion bombardment. However, the heterojunctions present in this material may be of interest for other applications, such as dye-sensitized solar cells [3]. In order to investigate the effect of the plasma processing conditions on the synthesized films and to elucidate the composition and structure of the produced films, the silicon wafers were characterized using XPS, AFM, FE-SEM, and XRD. This poster will describe the results of the composites as cathode materials and detail the effects of the plasma composition and parameters on the produced coatings.

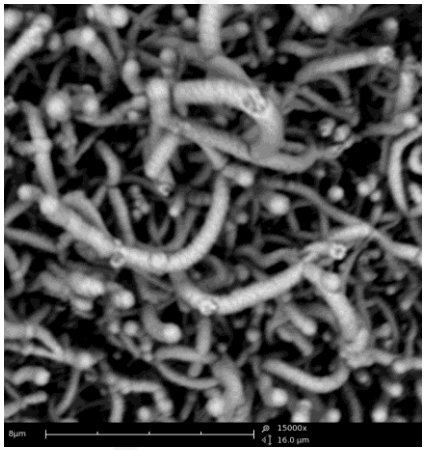

Figure 1 – After 6 min of deposition on MWCNTs with diameters of 20 nm – 50 nm, the coating of zinc nanoparticles can approach the micron scale.

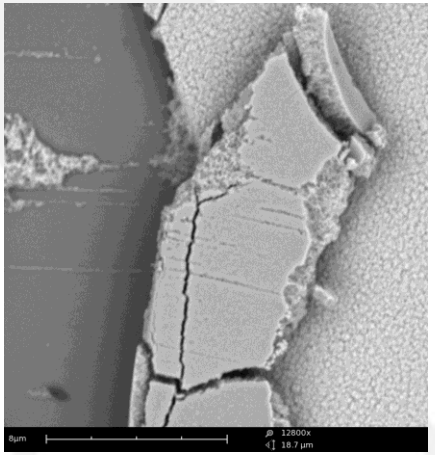

Figure 2 – By using elevated evaporation temperatures (650 °C), 90 s of deposition can produce similarly thick nanoparticle coatings on Si wafer substrates.

References
[1] C. E. Baddour, F. Fadlallah, D. Nasuhoglu, R. Mitra, L. Vandsburger, J.-L. Meunier. Carbon **47**, 313, 2009.
[2] J. M. Green, L. Dong, T. Gutu, J. Jiao, J. F. Conley, and Y. Ono. J. Appl. Phys. **99**, 094308, 2006.
[3] D. Wei, H. E. Unalan, D. Han, Q. Zhang, L. Niu, G. Amaratunga, and T. Ryhanen. Nanotechnology **19**, 424006, 2008.

Une mise à jour du procédé de synthèse de nanomatériaux (nanotubes de carbones monoparoi) par plasma inductif thermique

J.-F. Carrier1 et G. Soucy1

[1]Université de Sherbrooke, 2500 boul. de l'Université, Sherbrooke, Qc, J1K 2R1

Mots clés : nanotubes de carbone monoparoi, plasma inductif thermique

De nos jours, le préfixe nano est utilisée avec abondance dans le quotidien des scientifiques et de la population en générale. Bien que les matériaux nanométriques ne datent pas d'hier, le développement des technologies de caractérisations et de productions a fait en sorte que leur présence est de plus en plus abondante dans le quotidien des chercheurs.

Le corolaire de cette croissance des nanotechnologies est la préoccupation des effets sur la santé et l'environnement. Dans le but de réduire les risques reliés à l'utilisation de poudres nanométriques, un nouveau laboratoire a été mis en place par le groupe de recherche en nanomatériaux du Professeur Soucy, du département de génie chimique et génie biotechnologique, à l'Université de Sherbrooke.

De plus, la synthèse de nanomatériaux est souvent perçue comme une activité complexe et lourde en manipulations. Afin de faciliter le fonctionnement du laboratoire, sa nouvelle conception a également pris en ligne de compte l'opérabilité du procédé. Dorénavant, il est plus facile d'effectuer des essais de synthèse.

Par sa conception efficace et pratique, ces nouvelles installations permettent de poursuivre les activités de recherches en réduisant au maximum les différents risques, tout en facilitant les diverses manipulations requises pour la synthèse de nanomatériaux. De cette manière, le procédé est non seulement plus sécuritaire, mais également plus productif.

Les défis de la fabrication de nanostructures : à la limite des possibilités de gravure par plasma

Sébastien Delprat, Boris Le Drogoff, Étienne Charette, David Rocheleau, Amine Zitouni, Mohamed Chaker

Laboratoire de Micro et Nanofabrication, INRS-EMT, Varennes, Canada, J3X1S2

Mots clés : nanofabrication, lithographie par faisceau d'électrons, gravure plasma

Si la fameuse « Loi de Moore » a été suivie par l'industrie microélectronique depuis ses débuts, c'est surtout grâce à la réduction constante des dimensions de fabrication passées de 3 microns en 1980 à 32 nanomètres aujourd'hui. Non seulement pour la nanoélectronique, mais aussi pour une foule d'autres applications rendues possibles par ces développements, le défi est présentement de fabriquer des nanostructures de quelques atomes de résolution sur de grandes surfaces et au moindre coût dans des matériaux de plus en plus variés.
En approche « top-down » la fabrication de nanostructures repose sur deux grandes étapes : la définition de motifs nanométriques dans une résine et leur transfert dans un matériau. Pour étudier les limites de ces procédés, le Laboratoire de Micro et Nanofabrication (LMN) [1] de l'INRS a utilisé un des outils de lithographie électronique les plus performants du monde, combiné à des outils avancés de gravure par plasma. Dans un premier temps, des procédés de lithographie utilisant des résines commerciales ont été développés pour pouvoir réaliser sur de grandes surfaces des motifs allant jusqu'à 10nm (figure 1). Ces motifs de résine ont ensuite été utilisés pour étudier et mettre au point des recettes de gravure à l'échelle nanométrique sur de nombreux matériaux. La combinaison et l'optimisation de ces procédés a permis récemment de définir dans le silicium ou la silice des motifs sur une centaine de nanomètres de profondeur avec des dimensions latérales qui demeurent à ce jour parmi les plus petites jamais atteintes (figure 2).

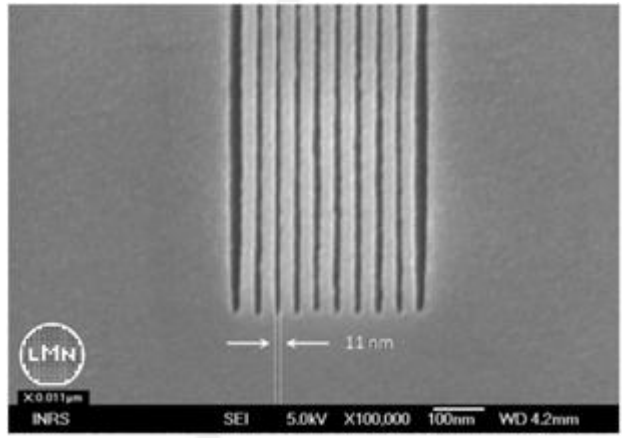

Figure 1 – Lignes de 11 nm espacées de 40nm (vues de dessus) obtenues dans de la résine ZEP520A par lithographie électronique

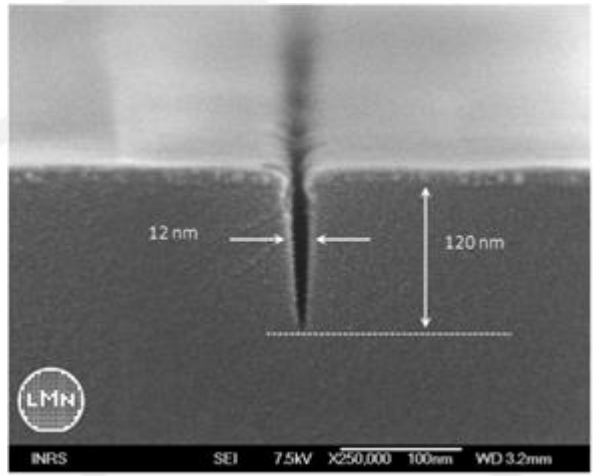

Figure 2 – Tranchée de 12 nm de large et 120 nm de profondeur (vue en coupe) gravée par plasma ICP dans la Silice

Références
[1] http://inf.emt.inrs.ca/FR/LMN.htm

Stabilisation of amorphous calcium carbonate with nanofibrillar biopolymers

D.C. Bassett[*1], *B. Marelli*[2], *S.N. Nazhat*[1,2] *and J.E. Barralet*[1]

[1]Faculty of Dentistry and [2]Department of Mining and Materials Engineering, McGill University, Montréal, QC, Canada, H3A 2B2

Key words : biomineralization, hydrogels, collagen, nanofibres, mineral.

Calcium carbonate is the most abundant biomineral that is biogenically formed with a vast array of nano and microscale features. Among the less stable polymorphs present in mineralised organisms, the most soluble, amorphous calcium carbonate (ACC), formed in chitin exoskeletons of crustacea is of particular interest since aqueous stability of isolated ACC is limited to a few hours in the absence of polyanions or magnesium. Here we investigated the influence of a selection of biopolymers on the mineralization and stability of calcium carbonate.

Mineralisation was achieved in all biopolymers tested, but was particularly abundant in collagen hydrogels (Figure 1), in which a significant proportion (~18%) was found to be amorphous. In dense collagen gels, this amorphous fraction did not crystallise for up to six weeks in deionised water at room temperature. The reason why collagen in particular should stabilise this phase remains obscure, although our results suggest that the fibre diameter, fibre spacing, and the amphoteric nature of collagen fibres were important.

Upon immersion in phosphate containing solutions, the calcium carbonate present within the collagen hydrogels was readily converted to carbonated hydroxyapatite, enabling the formation of a stiff bone-like composite containing 78 wt% mineral, essentially equivalent to cortical bone, , thereby demonstrating the potential of this approach for the formation of readily mineralisable hard tissue scaffold materials that could be applied through minimally invasive techniques. Our work points to the similarity in nanostructure of collagen and chitin being a key factor in their ability to stabilise amorphous calcium minerals.

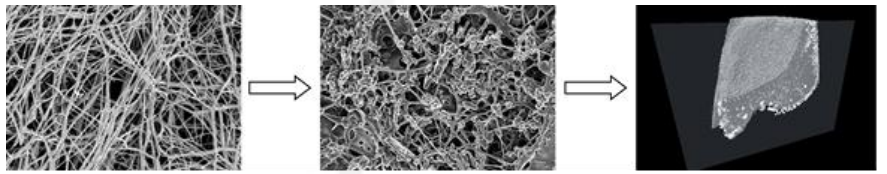

Figure 1 – SEM micrographs of as formed nanofibrillar collagen gel (A) and following mineralisation with calcium carbonate showing abundant mineral deposits throughout the hydrogel matrtix (B). C: MicroCT 3D reconstructions of the mineral phase within 0.2 wt % collagen gels confirmed abundant mineralisation throughout the material (highlighted in light grey) with areas of dense mineral deposits (highlighted in white)

Nanostructure de l'interface conductrice dans les composites polymères

Carmel Jolicoeur[1], Benjamin Duday[1], Jeff Sharman[1], Mathieu Savard[1], Jean Claude Mercier[2], Alexandre Beaudoin[2]

[1]Université de Sherbrooke et [2]American Biltrite (Canada)

Mots clés : interface, nanoparticules, noir de Carbone, composites polymères, couvre-planchers conducteurs

Le projet s'insère dans le développement et la commercialisation de nouveaux composites polymères pour remplacer les couvre-planchers à base de PVC, ces derniers présentant de fortes teneurs en chlore et en plastifiants qui peuvent constituer un risque pour la santé humaine. Les recherches portent spécifiquement sur la résolution d'un problème rencontré lors de l'incorporation de nanoparticules de carbone dans les matériaux proposés comme substituts au PVC. Le carbone assure la conductivité électrique des couvre-planchers, propriété essentielle dans certaines applications (e.g., salle blanche). S'appuyant sur une combinaison d'expertises académiques et un important savoir-faire industriel, les travaux en cours explorent plusieurs approches afin d'augmenter la rétention du carbone aux interfaces, tout en conservant la conductivité électrique requise pour ces matériaux : utilisation de différents types de nanoparticules de carbone; prétraitement des nanoparticules; incorporation d'agents de rétention pour stabiliser l'interface matrice/carbone; modification des propriétés de la matrice polymère; modification des agents de charge.

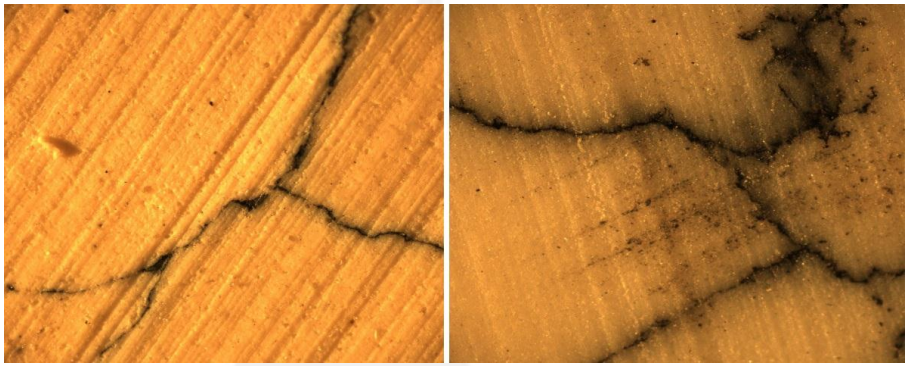

CONFÉRENCE NANOQUÉBEC 2012

Environnement Santé-Sécurité

HYATT REGENCY, MONTRÉAL

www.nanoquébec.ca

Évaluation de la toxicité des nanoparticules: un programme exploratoire chez le rat

M.C. Filion[*1], H. Slimani[1], M. Legaspi[1]*

[1]Centre National de Biologie Expérimentale, INRS, 531 boul. des Prairies, Laval, Qc, Canada, H7V 1B7

Mots clés : toxicité, effets secondaires, ingestion, administration intraveineuse, biodistribution

Il est essentiel de déterminer la toxicité des nanoparticules avant sa commercialisation et son usage chez l'humain. Les tests requis par les autorités règlementaires sont dispendieux. Il est donc important de déterminer tôt dans le développement l'innocuité de ceux-ci. Nous avons développé un modèle pour explorer la toxicité des nanoparticules à faible coût. Il repose sur la détermination de la dose létale 50 (LD50) sur un nombre limité de rats femelles Sprague-Dawley (3 par groupe par dose), suivi de l'évaluation des effets secondaires sur une autre cohorte de rats (4 par groupe) en utilisant 3 doses différentes de ces nanoparticules. Les voies d'administration pouvant être utilisées sont la voie orale (ingestion) ou la voie intraveineuse. Les nanoparticules sont administrées à raison d'une fois par jour pendant 5 jours. Les paramètres toxicologiques évalués sont : 1. la mortalité, 2. la détermination des signes cliniques au quotidien, 3. une biochimie clinique du sang (analyse de 22 composants), 4. une formule sanguine complète (comptage et différentiel) et 5. une histopathologie des principaux organes pouvant être affectée par les nanoparticules (poumons, cerveau, rate, reins, estomac/intestin et foie). Les résultats observés permettent de calculer un NOAEL et un NOEL («non-observable adverse effect limit » et «non-observable effect limit») et d'établir une marge de sécurité pour le produit testé. Ces données obtenues seront utiles afin de prendre rapidement une décision rationnelle sur une nanoparticule donnée avant d'investir temps et argent dans son développement (abandon, modification de la nanoparticule ou poursuite du développement).

Pollutant Emissions Control In the Machine Shops

A. Djebara[*1], W.N. Bernard[1], V. Songmene[1]*

[1]ÉTS, 1100 rue Notre-Dame Ouest, Montréal, Canada, H3C 1K3

Keywords: dry machining, aluminium alloys, ultrafine particles, fine particles.

Most manufacturing and especially metal working activities generate aerosols (dry or wet) that can be harmful or degrade the environment due to the use of new processes and advanced materials such as materials containing nanoparticles [1]. Dry machining is an environmentally conscious process, but under certain conditions, it can produce significant quantities of metallic particles [2]. New problematic appeared concerning the risk related to the exposure to metallic particles dispersed in the air. To limit the metallic particles generation, it is essential to know under what conditions they are formed as well as the mechanisms underlying their formation [31]. The main objective of this study was to evaluate the impact of machining conditions on metallic particles emission during dry machining. This work was carried out in order to minimize dust emission and thus preserve the environment and improve air quality in machine shops. Microscopy observations of ultrafine particles produced during dry machining show that there are a great heterogeneity in the particles shape and a large dispersion for the size (a few nanometers to a micrometer). It is also found that during machining the emission of ultrafine metallic particles decreases with the increase of cutting speed. This result is very encouraging from a practical standpoint. It is thus possible to machine parts at very high speeds, which ensures high productivity, good quality parts and limited metallic particles emission.

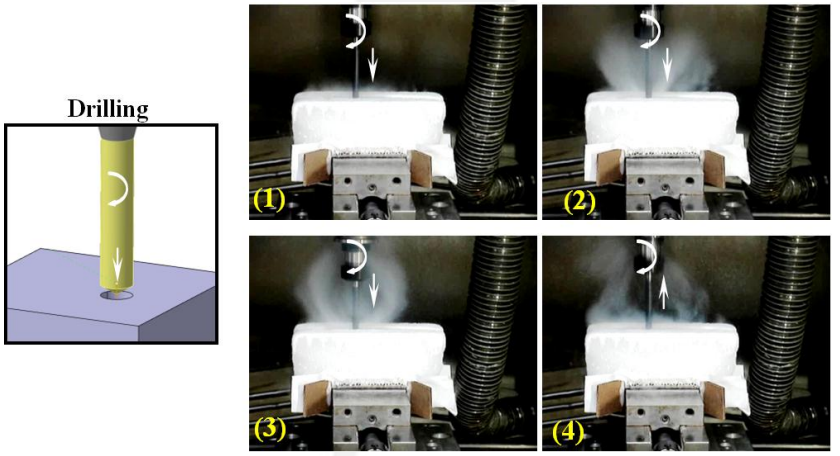

Figure 1 Direction taken by the particles emitted during machining

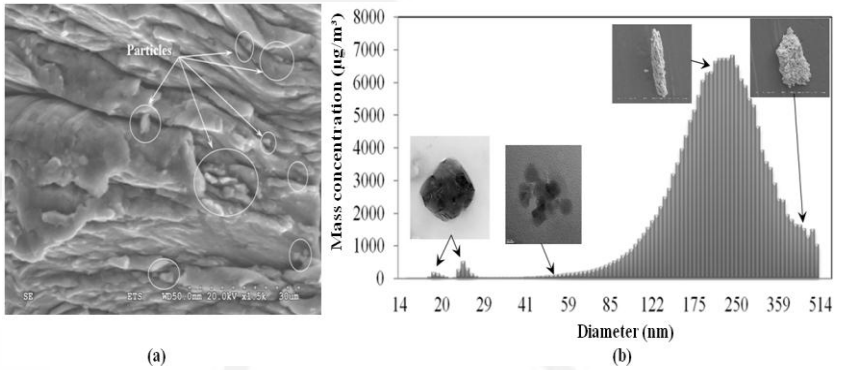

Figure 2 a) SEM image of particles emitted during machining b) Mass concentration from SMPS of 6061-T6 at cutting speed 300 m/min, feed 0,165 mm/rev

Références

[1] Sutherland JW, Kulur VN, N.C. King, (2000) An Experimental Investigation of Air Quality in Wet and Dry Turning. CIRP Ann Manufactur Technol 49(1):61-64

[2] Arumugam, P. U., Malshe, A. P., and Batzer, S. A., Bhat, D. G., (2002) Study of airborne dust emission and process performance during dry machining of aluminum-silicon alloy with PCD and CVD diamond coated tools NAMRC. Society of Manufacturing Engineers MR02-153, 1-8 p

[3] Djebara A, Songmene V, al. e, (2010) Experimental investigation on ultrafine particles emission during dry machining using statistical tools. Proceedings of the International Conference on Nanotechnology: Fundamentals and Applications 490(1):1-10

GIS-Based Multimedia Environmental Modeling for Fate and Transport of Nanoparticles

Amir M. Yadghar[1], Zhi Chen*[1]

[1]Building, Civil, and Environmental Engineering Department, Concordia University, 1515 St. Catherine W., Montréal, Canada, H3G 1M8

Mots clés: nanoparticles, fate and transport, multimedia environmental modelling, GIS

Environmental pollutions are crucial concerns of researchers and policy makers. Multimedia environmental modeling as a new tool for simulating the fate and transport of contaminants in all environmental media, is expanding fast. The motivation of this study is the absolute need for fate and transport models for nanoparticles in the environment with a spatial resolution and lack of these models. The current distribution models are developed for chemical substances. Since nanoparticles have unique characteristics compared to the bulk materials due to their nano size, it is necessary to develop a model especially for nanoparticles. The limitations in the current distribution models include: developed only for regular chemical substances, considering single media transport, lack of spatial resolution and temporal information, loose-coupled or not-coupled with GIS, and considering steady state flows in all media. Two multimedia environmental models for nanoparticles are applied and tested, which include an air dispersion module, a source module, an unsaturated, and a saturated zone module. This research aims to develop a multimedia model for nanoparticles with spatial resolution to assess their risks which allows estimation of the time- and spatial-varying chemical concentrations in air, water, soil, and groundwater media, and subsequently the characterization of the potential risk to human health and environment. This is the first time that an integrated multimedia environmental model is applied for nanoparticles. However, obtained results showed good match with the verified data got from the literature. The applied multimedia environmental model has been validated through a series of case analyses including real experimental data.

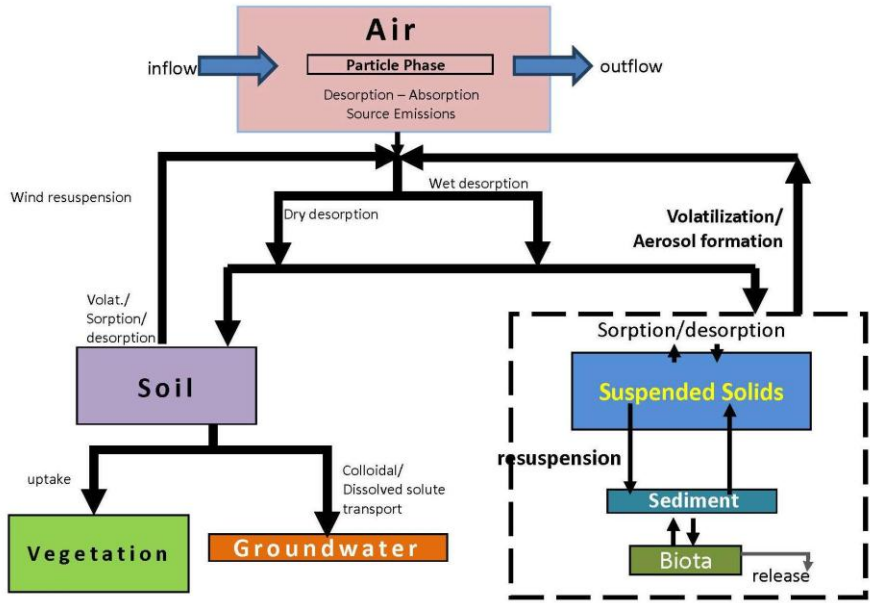

Figure 1 – Components of multimedia environmental model used for nanoparticles (obtained from Cohen & Cooter, 2002)

Références

[1] Cohen, Y., & Cooter, E. J. (2002). Multimedia environmental distribution of toxics (mend-tox). I: Hybrid compartmental-spatial modeling framework. Practice Periodical of Hazardous, Toxic, and Radioactive Waste Management, 6(2), 70-86.

[2] Mueller, N. C., & Nowack, B. (2008). Exposure modeling of engineered nanoparticles in the environment. Environmental Science & Technology, 42(12), 4447-4453.

[3] Zhang, R. R. (2006). Development of a fuzzy-set enhanced environmental multimedia modelling system. (Master of Applied Science, Concordia University).

Filtration of airborne particles through bimodal porous medium

Mathieu Gaudreault[*1], David Vidal[2], François Drolet[2] et François Bertrand[1,2]*

[1]Ecole Polytechnique de Montréal, Montréal, Québec, Canada, H3C 3A7
[2]FPInnovations – Paprican Division, Pointe-Claire, Québec, Canada, H9R 3J9

Keywords : Filtration, Porous material, Lattice Boltzmann method

Filtration of nano and submicron airborne particles through random networks of fibers is studied. Propagation of such particles through porous media composed of a single type of fiber is well understood [1]. In particular, the permeability is known to increase with the porosity. Furthermore, filtration efficiency exhibits a minimum around an airborne particle size of 0.2 µm, which is typical for air filters. However, it is not well understood if unimodal theory combined with an equivalent radius model can be applied to porous media composed of bimodal fibers. Transport of airborne particles through fiber networks is simulated numerically. Fibers are observed to have an elliptical cross-section experimentally and are modeled by cylinders with a bimodal distribution of radii and a fixed length. A three-dimensional filter is composed of these cylinders deposited in a box according to a Monte Carlo algorithm. The flow of air through the latter structure is computed using a Lattice Boltzmann method. The mechanical filtration efficiency is then calculated by simulating the propagation of airborne particles through the medium. We show that the porosity decreases with increasing volume fraction of large fibers, while the permeability stays constant. This contradicts prediction from unimodal theory used with an equivalent radius model. However, results on the filtration efficiency seem to agree with the unimodal theory, at least for the volume fractions of large fibers considered.

References

[1] M. Rebai, F. Drolet, D. Vidal, I. Vadeiko, and F. Bertrand. A Lattice Boltzmann approach for predicting the efficiency of random fibrous media. Asia-Pac. J. Chem. Eng. 2011: 6, 29, 2010.

Vers une gestion adaptative des risques de l'invisible…

J. Fatisson[1], S. Hallé[1], S. Nadeau[1]*

[1]École de Technologie Supérieure, 1100 rue Notre-Dame Ouest, Montréal, Canada, H3C 1K3

Mots clés : nanoparticules synthétiques, identification de risques, SST

La recherche scientifique démontre quotidiennement les bénéfices, mais aussi les problèmes liés aux nanotechnologies, et ce dans tous les secteurs. Malgré une importante activité scientifique dédiée à l'approfondissement des propriétés des nanoparticules, les incertitudes demeurent et limitent la compréhension de leurs interactions avec le corps humain et l'environnement [1]. D'après l'article 20 de la déclaration universelle sur la bioéthique et les droits de l'homme [2], il convient de promouvoir une gestion appropriée et une évaluation adéquate des risques relatifs aux technologies. Encore aujourd'hui, aucune règlementation n'est en vigueur, même si de multiples efforts sont faits en ce sens, dont en Europe très récemment [3]. Cependant, les entreprises doivent prendre des décisions particulièrement pour assurer la protection des travailleurs. L'objectif maître de ce projet est de concevoir et d'encadrer un outil adaptatif d'aide à la décision, destiné aux producteurs de nanoparticules synthétiques et aux intervenants en prévention au travail. Cet outil original, pourra ainsi être utilisé pour adapter des mesures de sécurité adéquates aux procédés manufacturiers et assurer pleinement la protection des travailleurs. Une revue exhaustive de littérature a permis d'identifier et de dresser la liste de tous les facteurs de risques liés à la production de nanoparticules synthétiques étudiés jusqu'ici. Les premières observations indiquent que ces paramètres sont interdépendants et mettent en évidence les liens entre les différents groupes de facteurs de risques. Ces résultats seront ultérieurement intégrés dans un modèle mathématique pour permettre une première priorisation des facteurs de risques à considérer.

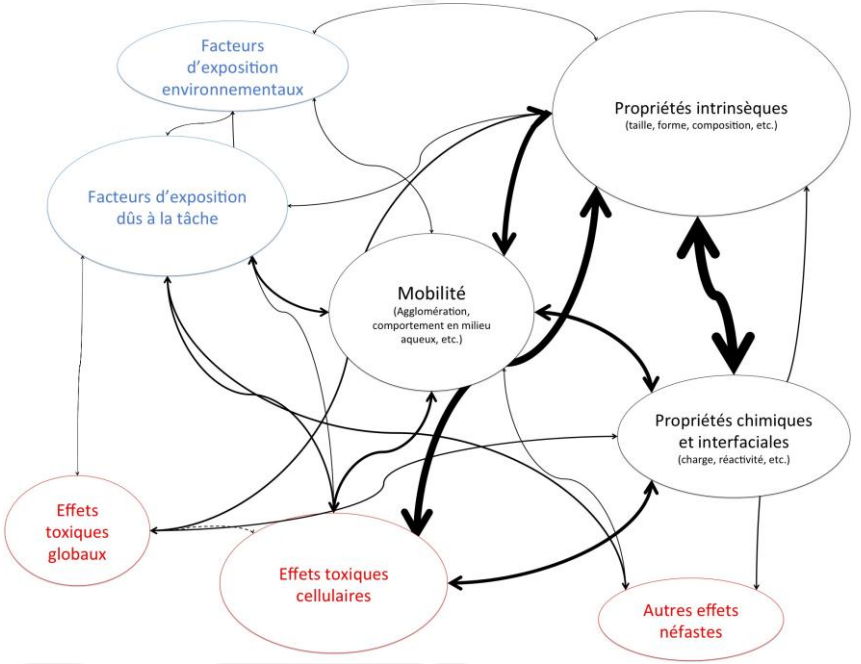

Figure 1 – Arbre de risques simplifié montrant les liens existants entre les principaux groupes de facteurs de risques à considérer

Références

[1] Ostiguy, C. et al. (2009). "A good practice guide for safe work with nanoparticles: the Quebec approach." J. Phys. Conf. Ser. **151**.

[2] Déclaration universelle sur la bioéthique et les droits de l'homme, http://portal.unesco.org/fr/ev.php-URL_ID=31058&URL_DO=DO_TOPIC&URL_SECTION=201.html

[3] Rapport de la Commission Européenne en vue d'une définition des nanomatériaux, http://eur-lex.europa.eu/LexUriServ/LexUriServ.do?uri=OJ:L:2011:275:0038:0040:EN:PDF,

Synthesis process affects the physicochemical properties and cytotoxicity of feedstock materials used for carbon nanotube production

Y. Alinejad [1,2], N. Faucheux [2], G. Soucy[1]*

[1.] Thermal plasma and nanomaterial synthesis laboratory, Department of Chemical and Biotechnological Engineering, Université de Sherbrooke, 2500 boul Université, J1K 2R1, Sherbrooke, QC, Canada
[2.] Cells-Biomaterials Biohybrid Systems laboratory, Department of Chemical and Biotechnological Engineering, Université de Sherbrooke, 2500 boul Université, J1K 2R1, Sherbrooke, QC, Canada

Keywords: Metallic catalysts, nanoparticle, cytotoxicity, apoptosis, synthesis process

With the increasing interest in nanomaterials such as carbon nanotubes in recent years, they are produced at large scale to be used in different fields of applications. Therefore, it has become inevitable to study the health effects of this promising industry. However, the effect of the synthesis process on the nanomaterial cytotoxicity is still poorly understood at the moment. So, in this study, a comparative cytotoxicity of the feedstock materials including Co, Ni, Y_2O_3, Mo and carbon black routinely used for carbon nanotube production is investigated on murine Swiss 3T3 fibroblasts. Effect of the synthesis process (radio frequency induction thermal plasma) was then investigated on the physicochemical properties and cytotoxicity of the particles using different characterization techniques and three *in vitro* assays. Cytotoxicity of the released ions from metallic particles was also assessed. Among feedstock materials tested, Co showed the strongest cytotoxicity causing dose-dependent reduction in cell viability and loss of cytoskeleton within 24 h. The thermal plasma process applied to produce nanoparticles affected the properties of the particles, even converted some of them such as Ni from non-toxic to strongly toxic. Comparing the properties and cytotoxicity of nanoparticles produced by thermal plasma process with commercial ones, it was shown that nanoparticles of Ni with the same size synthesized by different processes have different cytotoxicities. Overall, chemistry of the particle was found to be the most reliable property to predict cytotoxicity in fine-sized particles.

References

[1] A. Shahverdi, G.Soucy. Thermogravimetric analysis of single-walled carbon nanotubes synthesized by induction thermal plasma, Journal of Thermal Analysis and Calorimetry, p 1-7, 2011.

Investigation of the adhesion of diamond-like carbon coatings on stainless steel for the development of functionalized antibacterial surfaces.

M. Cloutier[1,3], O. Seddiki[2], C. Harnagea[2], S. Turgeon[1], A. Sarkissian[3], F. Rosei[2], D. Mantovani[1]

[1] Laboratoire de biomatériaux et bioingénierie, Département de génie des Min-Met-Matériaux, Université Laval & Centre de recherche du CHUQ, 10 rue de l'Espinay, Québec, Canada G1L 3L5
[2] Institut National de la Recherche Scientifique, Énergie, Matériaux et Télécommunications, Université du Québec, 1650 Boul. Lionel Boulet, Varennes, Canada, J3X 1S2
[3] Plasmionique Inc., 1650 boul. Lionel Boulet, Varennes, Canada, J3X 1S2

Mots clés : Diamond-Like Carbon, Antibacterial coatings, Plasma, Medical applications

Nosocomial infections (Nis) are a major issue in hospital or healthcare service unit treatment. According to the Centers for Disease Control and Prevention (USA), about 99 000 patients die each year due to Nis against 8 000 deaths in Canada and 25 000 in Europe, the contamination of medical devices and surgical tools by pathogenic bacteria being one of the main causes of Nis. To decrease the risk of contamination, the most common approach consists in a chemical treatment (alcohols, halogens, etc.) of hospital devices. Another strategy is the development of multifunctional materials not only with remarkable antibacterial activity, but, in addition, with outstanding mechanical (hardness, elasticity) as well as tribological properties, in addition to a good adhesion to the material underneath. Diamond-like carbon (DLC) coatings satisfy many of the requirements needed, also exhibiting a low surface energy, a low surface roughness and an excellent corrosion resistance thus being an ideal candidate for such applications. Furthermore, the antibacterial behaviour can be easily improved by doping the film with metallic ions (silver, copper, etc.). The goal is to demonstrate the antibacterial nature of doped DLC coatings and the possibility to deposit such coatings on materials typically used in hospitals, such as stainless steel. However, the adhesion of DLC films on metallic substrates is known to be poor, resulting in rapid delamination of the coating. To overcome this problem, we investigated different strategies to increase the adhesion: stress reduction, deposition of an interfacial layer and formation of a carbide interface. Surface science techniques and mechanical tests were carried out to assess the improvement achieved.

Risques et opportunités de collaboration dans les industries qui développent ou utilisent des nanotechnologies au Québec.

E. Garat, N. de Marcellis-Warin, T.Warin

CIRANO, Centre interuniversitaire de recherche en analyse des organisations
2020, rue University, Montréal *&* ***École Polytechnique de Montréal***, 2900, boul. Édouard-Montpetit Montréal.

Mots clés : Nanotechnologies, Collaborations, Risques, Stratégies

Les nanotechnologies forment un domaine axée sur la recherche scientifique fondamentale ayant des répercutions dans la plupart des secteurs économiques. Or, de nos jours, les droits de propriété intellectuelle et la lourdeur des investissements requis pour ces technologies de pointe freinent leurs développements et obligent les entreprises à collaborer entre elles ou avec les universités. Pour ces industries, la coopération semble aujourd'hui incontournable et nécessaire à leur survie. Toutefois, les entreprises peuvent aussi décider de ne pas collaborer. En effet, ces stratégies possèdent des risques, notamment relationnels et de performance[1], qui peuvent diminuer les chances de succès de la collaboration voir même d'entrainer les partenaires à leur perte.

L'objectif général de cette recherche est d'élaborer et de conseiller de nouvelles politiques technologiques favorisant le développement des industries de pointe auprès des acteurs clés des milieux de la recherche et de l'industrie. De surcroit, des pratiques de gestion qui permettront de favoriser le succès des alliances, partenariats et ententes de collaboration pourraient être proposés.

De manière plus spécifique, nous chercherons à déterminer comment se définit le domaine des nanotechnologies au Québec. Nous cherchons a identifier les acteurs principaux et les paramètres régissant leur environnement de collaboration en cherchant à comprendre si la décision d'effectuer une coopération est en lien avec le moment de l'entente, la localisation des partenaires[2], la protection de la propriété intellectuelle[3], etc.

Références

[1] Das, T. K. and Teng, B.-S. (1996), RISK TYPES AND INTER-FIRM ALLIANCE STRUCTURES. Journal of Management Studies, 33: 827–843. doi: 10.1111/j.1467-6486.1996.tb00174.x

[2] Gittelman, M. (2006). Does Geography Matter for Science-Based Firms? Epistemic Communities and the Geography of Research and Patenting in Biotechnology. DRUID Summer Conference on Knowledge, Innovation and Competitiveness: Dynamics of Firms, Networks, Regions and Institutions, Copenhagen, Denmark.

[3] HORSTMANN, I. MACDONALD, G. et SLIVINSKI, A. (1985) « Patents as information transfer mechanisms : to patent or (maybe) not to patent », Journal of Political Economy, vol. 93, n° 5.

CRAMPES, C. (1986) « Les inconvénients d'un dépôt de brevet pour une entreprise innovatrice», l'Actualité Économique, vol. 62, n° 4, décembre.

Instruments d'analyse interdisciplinaire des impacts et de l'acceptabilité sociale des nanotechnologies

J. Patenaude[1], J.P. Béland[2], L. Bernier[1], V. Chenel[1], C.E. Daniel[1], C. Fontaine[1], G.A. Legault1, J. Beauvais[1], P. Boissy[1], J. Genest[1], M. Parent[1], M.S. Poirier[1], D. Tapin[3]

[1]Université de Sherbrooke, [2]Université du Québec à Chicoutimi, [3]Université de Montréal

Mots clés : Analyse de risque, Acceptabilité sociale, Ne3LS, Nanotechnologies

La recherche, le développement et l'innovation impliquant les nanotechnologies peuvent soulever plusieurs enjeux éthiques, environnementaux, économiques, légaux et sociaux NE^{3}LS). Au cours des dernières années, plusieurs organismes nationaux [1] et internationaux [2,3] ont reconnu qu'une prise en compte précoce et intégrée de ces enjeux est devenue incontournable dans le cadre d'un développement responsable des nanotechnologies. Ainsi, une intégration des NE^{3}LS au processus de développement des nanotechnologies permettrait d'identifier et d'évaluer les impacts en temps réel et favoriserait la communication et les débats entre les différents acteurs (recherche, industrie, politique et citoyens) quant aux véritables choix de sociétés associés à un tel développement.
Cependant, comme il n'existe aucun instrument d'analyse interdisciplinaire d'identification et d'évaluation systématiques de ces enjeux à chaque stade du développement des nanotechnologies (produit, procédé, processus et usages), les contributions réelles que les NE^{3}LS peuvent apporter sont plutôt limitées.
Ainsi, ce travail s'inscrit dans un projet visant à développer un cadre interdisciplinaire d'accompagnement du développement des nanotechnologies [4]. Ce cadre passe entre autre par la co-construction d'instruments d'analyse interdisciplinaire susceptibles de favoriser l'identification et l'évaluation systématique des impacts ainsi que l'acceptabilité sociale liés à ces développements (figure 1).

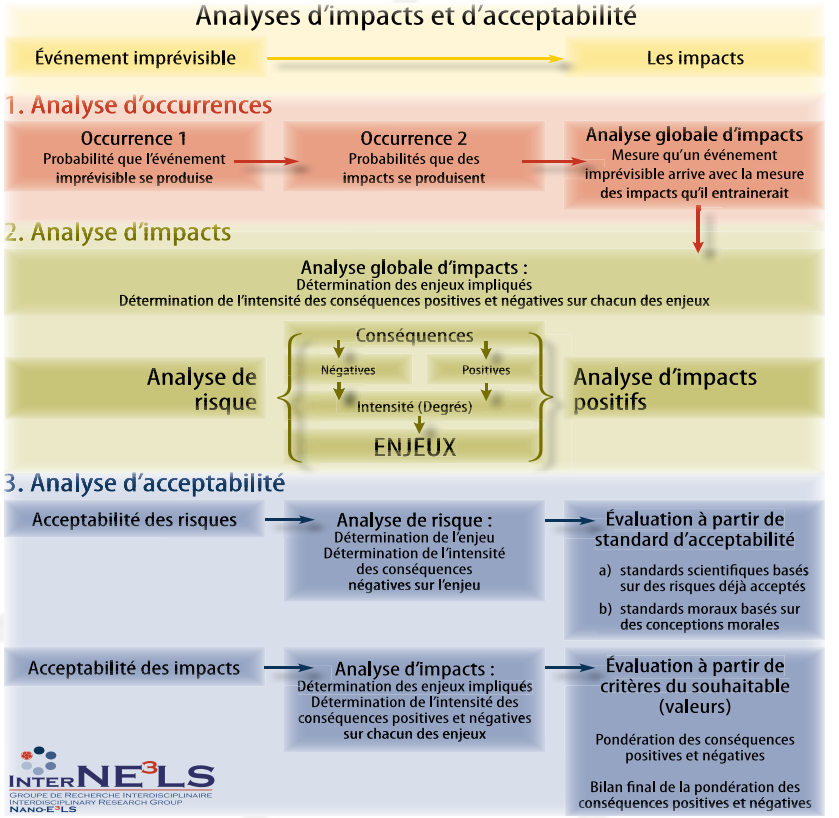

Figure 1 – Cadre interdisciplinaire d'analyse des impacts des nanotechnologies et de leur acceptabilité.

Références
[1] Conseil de la science et de la technologie, *Les nanotechnologies : la maîtrise de l'infiniment petit*, Gouvernement du Québec, juin 2006
[2] Ministère de l'écologie et du développement durable. Comité de la prévention et de la précaution. *Nanotechnologies, nanoparticules : Quels dangers, quels risques ?* Paris, mai 2006. 64 pages, p.37.
[3] International Risk Governance Council, *Survey on Nanotechnology Governance, Volume A. The Role of Government*, IRGC Working Group on Nanotechnology, december 2005.
[4] Béland, J.-P. et Patenaude J. (eds.), *Les nanotechnologies. Développement, enjeux sociaux et défis éthiques*. Québec: Presses de l'Université Laval. 2009.

Effectiveness of N95 Filters for Capturing Nano-Particles under cyclic and constant flow

A. Mahdavi[1,2], A. Bahloul[1], C. Ostiguy[1], F. Haghighat[2]

[1] Institut de recherche Robert-Sauvé en santé et en sécurité du travail, 505 boul. Maisonneuve West, Montreal, QC H3A 3C2
[2] Concordia University, BCEE, 1455 boul. Maisonneuve West, Montreal, QC H3G 1M8

Keywords: Nano-particles, N95, Penetration, Cyclic flow, MPPS.

Experimental studies indicate potential adverse effects of inhaling Nano-Particles (NPs) on human's health. In some workplace situations, respiratory protection plays a vital role to protect workers from NPs inhalation. Following the Quebec regulations, NIOSH-certified filters must be used and N95 is the most widely used. N95 filter is considered as an efficient device with capability of capturing over 95% of exposed particles under constant flow of 85 L/min at mono-disperse aerosols of 300 nm (known as the Most Penetrating Particle Size (MPPS) for mechanical filters). However, human breathing has a cyclic pattern and, in high workloads, respiratory peak flow may reach 400 L/min [1]; also, in some studies the MPPS was observed less than 100 nm with commercial filters [2]. Therefore in this research, the evaluation of N95 efficiency under various cyclic and constant flows is accomplished. Aerosol flow is dispersed through a chamber including the manikin with N95 connected to a breathing simulator (figure 1). Penetration of poly-disperse NaCl aerosols within 15-200 nm was measured under four sinusoidal flows with peaks of 360, 270, 200 and 135 L/min and their corresponding constant flows (Minute Volume, Mean Inhalation Flow (MIF) and Peak Inhalation Flow (PIF)) representing high to moderate workloads. Results indicate higher cyclic flows increased the penetration for all sizes. It is also found for high workloads the penetration under cyclic flow was less than PIF, but more than MIF and Minute Volume; showing the best corresponding constant flow to cyclic could be between MIF and PIF (figure 2).

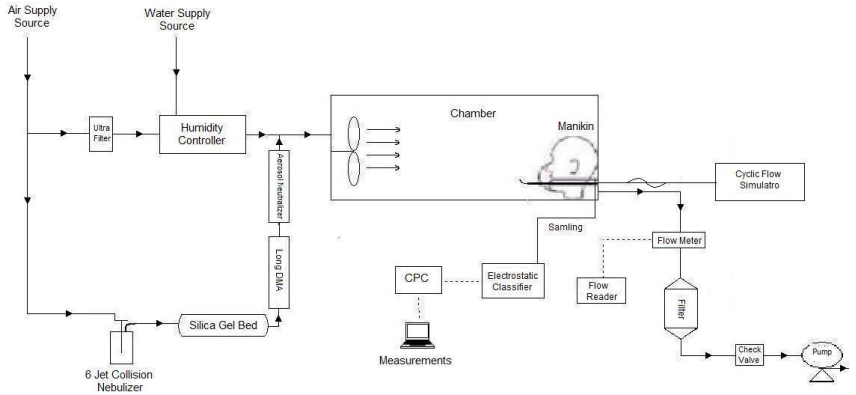

Figure 1 – Experimental set-up for measuring the effectiveness of N95 respirator

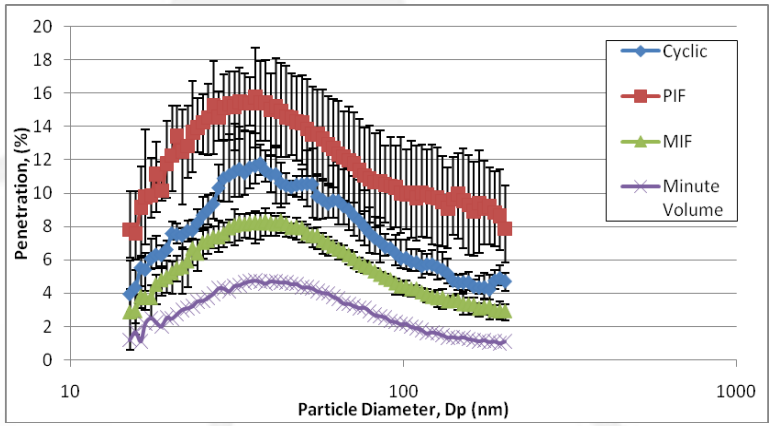

Figure 2 – Comparison of particle penetration under cyclic (40 BPM and 360 L/min as peak) and three corresponding constant flows (Minute Volume=115 L/min, MIF=230 L/min and PIF=360L/min)

Références
[1] D.M. Caretti, P.D. Gardner, K.M. Coyne. Workplace Breathing Rates: Defining Anticipated Values and Ranges for Respirator Certification Testing. U.S. Army ECBC – TR-316. 2004.
[2] R. Mostofi, A. Bahloul, J. Lara, B. Wang, Y. Cloutier, F. Haghighat. Investigation of potential affecting factors on performance of N95 respirator. J. of the Int. Soc. for Respiratory Protection. 28(1):26-39. 2010.

Transport of Bare and Polymer-coated Metal Oxide Nanoparticles in Natural and Artificial Groundwater Matrices

A. R. Petosa[1], C. Öhl[1], F. Rajput[1], S. J. Brennan[1], N. Tufenkji[1]*

[1] Department of Chemical Engineering, McGill University, 3610 University St., Montréal, Canada, H3A 2B2

Keywords: titanium dioxide, zinc oxide, cerium oxide, nanoparticle, transport

The increased production and use of metal oxide nanoparticles (NPs) will result in their heightened discharge into natural aquatic systems. To better understand the transport behaviour of various metal oxide NPs, deposition studies were performed with bare and polymer (polyacrylic acid)-coated cerium dioxide (*n*CeO_2), titanium dioxide (*n*TiO_2) and zinc oxide (*n*ZnO) NPs in natural and engineered water saturated granular systems. Laboratory-scale column experiments were conducted with packed beds consisting of pure quartz sand or loamy sand, and particles suspended in artificial or natural groundwater solutions. Suspended NP sizes were determined using dynamic light scattering and nanoparticle tracking analysis, while electrophoretic mobility was determined by laser Doppler velocimetry. Uncoated (bare) metal oxide NPs exhibited high retention and dynamic (time-dependent) deposition patterns within the water saturated granular matrices. At low ionic strength (IS), bare particle deposition was in qualitative agreement with the Derjaguin-Landau-Verwey-Overbeek (DLVO) theory of colloidal stability. At higher IS, enhanced NP aggregation resulted in physical straining within the granular matrix, completely altering particle deposition behaviour. Unlike the bare particles, polymer-coated NPs were highly stable in monovalent salt suspensions, demonstrating substantial transport potential. These same polymer-coated NPs exhibited limited mobility in divalent salt suspensions at high IS and in natural groundwater. Furthermore, for a given IS, enhanced particle retention was observed in loamy sand-packed columns when compared to the pure quartz sand-packed columns. The contrasting behaviours observed emphasize the need to consider NP surface modification, aquatic matrix composition and soil type when evaluating metal oxide contamination potential in granular aquatic environments.

References

[1] Petosa, A.R. *et al*., Water Res., 2012, 46, 1273-85.

Selected Organic Macromolecules Influence the Aggregation and Transport Behaviour of Palladized Nanosized Zero Valent Iron (PNZVI) Particles in Saturated Porous Media

Mohan Basnet[1], Subhasis Ghoshal*[2], and Nathalie Tufenkji[1]

[1]Department of Chemical Engineering, McGill University, Montreal, Quebec, Canada H3A 2B2
[2]Department of Civil Engineering, McGill University, Montreal, Quebec, Canada H3A 2K6

Keywords: Nanoparticle, DNAPL, PNZVI, Aggregation, Transport

Chlorinated solvents such as trichloroethylene are present as DNAPLs (denser than water non-aqueous phase liquids).These organic liquids when released in the environment can migrate deep into aquifers causing extensive contamination. Palladized nanosized zero valent iron (PNZVI) particles can contribute to the remediation of DNAPL source zones by degrading chlorinated organic compounds to innocuous products. To make PNZVI a good *in-situ* remediation agent, these particles need to be readily dispersible in water so that they can migrate through the subsurface to a targeted contaminated area. However, previous studies have reported very limited mobility of these particles and attributed it to rapid aggregation and subsequent pore plugging. Therefore, to reduce aggregation and make the particles more mobile in the groundwater environment, the surface of bare PNZVI can be modified with various stabilizing agents. In this study, we systematically investigated the influence of selected organic macromolecules on the aggregation and transport behavior of bare and coated (or stabilized) PNZVI. Aggregation behavior was investigated using dynamic light scattering (DLS) by monitoring the evolution of hydrodynamic diameter as a function of time whereas nanoparticle transport behavior was investigated by conducting saturated sand-packed column experiments.

Workplace Safety in Polymer Nanocomposites Research

C. Cattin [1], M. Debia [2], A. Dufresne [2], P. Hubert [1]*

[1]Structures and Composite Materials Laboratory, Department of Mechanical Engineering, McGill University, Montreal QC, Canada
[2]Département de santé environnementale et santé au travail, Université de Montréal, Montréal QC, Canada

Keywords: nanoparticle, carbon nanotube, polymer nanocomposite, exposure control, occupational safety

In recent years, research efforts to develop and advance nanoparticles (NPs) and NP based composite materials have been increasing rapidly. Well-known examples of such materials are carbon nanotubes (CNTs) and CNT modified polymers. Typically, research on CNT/polymer nanocomposites involves handling of dry CNTs. Although occupational and environmental health and safety practices are in place for the handling of most polymers and chemicals involved in such research, for the handling of dry CNTs this is often not the case. For a long time it was assumed that CNTs are not particularly hazardous and little effort was devoted to evaluating the toxicity of these NPs. A recent study, however, demonstrates that CNTs introduced into the abdominal cavity of mice show asbestos-like pathogenicity, and, hence, may pose a carcinogenic risk [1]. Overall, conclusions from studies exploring the toxicity of NPs vary considerably. Adequate knowledge does often not exist, but it has been shown that NPs, and CNTs in particular, can be highly toxic. The presented work addresses this problem and proposes a working practice to minimize/eliminate potential health, safety, and environmental risks associated with the handling of dry NPs in laboratory research. First the effectiveness of the proposed engineering control in minimizing occupational exposure to airborne NPs is analysed, and, second, the propensity of a widely used CNT sample to form airborne particles is measured. The combined results provide useful guidelines for both the selection and the use of an engineering control to minimize/eliminate exposure to airborne CNTs, and NPs in general.

Références

[1] C. A. Poland, R. Duffin, I. Kinloch, A. Maynard, W. A. H. Wallace, A. Seaton, V. Stone, S. Brown, W. MacNee and K. Donaldson, Nat Nanotechnol 3 (7), 423-428 (2008).

Détermination de la biosécurité des nanoparticules: Attention aux interférences!

L Tabet[1], L Barhoumi[1, 2 L Ben Taher 3, L Smiri 3], H Abdelmelek [2], K Maghni [1].

[1] Centre de recherche HSCM, Université de Montréal, Canada.
[3] Laboratoire de recherche 99/UR12-30, Université de Bizerte, Tunisie.
[2] Laboratoire de Physiologie Intégrée, Université de Bizerte, Tunisie.

Mots clés : Nanosécurité, Nanotoxicité, NSPM, Interférence, tétrazolium

Les nanoparticules (NP) superparamagnétiques (NSPM) possèdent des propriétés magnétiques intéressantes pour les applications biomédicales. Cependant, ces applications devraient exclure tout risque sur la santé humaine. Des études ont montré que les propriétés uniques des NP peuvent induire des interactions imprévisibles avec les composants d'essais de nanocytotoxicité. Ces interférences ont pour conséquence de conduire à une conclusion éronnée sur la biosécurité de ces NP. *Objectif:* Déterminer la possibilité, et selon le cas, le mécanisme d'interférence de trois NSPM (composition chimique différente) avec trois essais de nanocytotoxicité. *Méthodologie:* Les NSPM ont été incubées dans le milieu de culture sans cellules pour l'étude de l'interférence potentielle et son mécanisme avec les essais LDH, MTS et Prestoblue. La détermination de la nanotoxicité des NSPM a été réalisée chez les cellules A549 en utilisant ces mêmes essais.
Résultats: Les NSPM présentent une interaction avec les tests MTS et LDH attribuable à une activité catalytique de ces NP produisant une conversion non-enzymatique du tétrazolium. De plus, ces deux essais sont inadéquats pour la mesure de la nanocytotoxicité de ces NSPM, et cela malgré la correction pour ces interférences. En revanche, l'essai Prestoblue n'a indiqué aucune interférence avec ces NSPM, validant ainsi nos données indiquant une cytotoxicité des trois NSPM étudiées. *Conclusion:* Nous avons montré que les NSPM interfèrent avec les essais classiques de nanocytotoxicité questionnant ainsi les données des articles précédemment publiés (aucune détermination d'interférences). La détermination d'interférences potentielles est une étape essentielle qui devrait être incluse dans les études de biosécurité des NP.